THE FUNCTIONAL INVESTIGATION OF FORKHEAD FACTOR FOXQ1 IN HUMAN BREAST AND COLON CANCERS

QIAO YUANYUAN

NATIONAL UNIVERSITY OF SINGAPORE

2011

THE FUNCTIONAL INVESTIGATION OF FORKHEAD FACTOR FOXQ1 IN HUMAN BREAST AND COLON CANCERS

QIAO YUANYUAN

MRes, Newcastle University, UK

A THESIS SUBMITTED FOR

THE DEGREE OF DOCTOR OF PHILOSOPHY

DEPARTMENT OF PHYSIOLOGY

NATIONAL UNIVERSITY OF SINGAPORE

2011

Acknowledgements

First of all I would like to take this opportunity to express my sincere thankfulness to Dr. Yu Qiang, my supervisor, for his guidance and encouragement during these PhD years. This is also a great opportunity to express my thankfulness to A/Prof. Hooi Shing Chuan for being so supportive.

I would like to express my appreciation to National University of Singapore's Yong Loo Lin School of Medicine and Department of Physiology, especially to Department Head A/Prof. Soong Tuck Wah for providing the scholarship to pursue my PhD degree.

The Agency for Science, Research and Technology (A*STAR) has provided the right environment which allowed me to do my research work at the Genome Institute of Singapore (GIS).

I have made lasting friendship with my GIS colleagues at the laboratory of Cancer Biology and Pharmacology. They are Mr. Tan Jing, Ms. Jiang Xia, Ms. Lee Sheut Theng, Dr. Wu Zhenlong, Dr. Feng Min, Ms. Zhuang Li, Ms. Li Zhimei, Dr. Li Jingsong, Dr. Yang Xiaojing, Ms. Lee Puey Leng, Ms. Aau Mei Yee, Ms. Cheryl Lim, Mr. Eric Lee, Dr. Wong Chew Hooi and Mr. Adrian Wee.

And last but not least, my gratitude to my parents and fiancé for mentally supporting me during these difficult and challenging years in Singapore.

Table of Contents

Summary

The functional role of FOXQ1 in human cancers has recently and rapidly emerged a year ago, which was almost a decade after it was first identified. In this study, I have shown that FOXQ1 is closely associated with basal-like breast cancer subtype and colorectal cancers. Its clinical relevance as provided by Oncomine database suggest that FOXQ1 has potential therapeutic significance against breast cancer progression and invasion.

In this study, the functional role of FOXQ1 was investigated in both breast and colorectal cancers. During breast cancer progression, FOXQ1 was demonstrated to participate in the aggressive behaviour of metastatic breast cancer cell line MDA-MB-231. When ectopic FOXQ1 expression was introduced into immortalized human mammary epithelial cell line (HMLER), this triggered a transformation from epithelial morphology towards mesenchymal stage and the process is called 'Epithelial to Mesenchymal Transition' (EMT). FOXQ1 also generated breast cancer stem cell-like population as defined by cells with surface antigen CD44+/CD24- staining, and this enhanced the growth ability of mammospheres in vitro.

The induced EMT phenomenon by FOXQ1 was also observed in colorectal carcinoma cell line HCT116 which has a typical epithelial morphology. Hence, the resulting EMT by ectopic expression of FOXQ1 in HCT116 cells provided more evidence that FOXQ1 may have a broader role to play in regulating epithelial plasticity in human cancers. In HCT116 cells, FOXQ1 induced EMT also conferred resistance to a series of chemotherapeutic drug-induced apoptosis. In view of the anti-

apoptotic ability of FOXQ1 in colorectal cancer cells, I believe that FOXQ1 can be a potential therapeutic target. In addition, depletion of FOXQ1 expression by RNAi in aggressive breast cancer MDA-MB-231 cell line increased their sensitivity towards several DNA-damaging drug-induced apoptosis by more than fifty percent in terms of active Caspase 3 activity.

As a transcription factor, FOXQ1 regulates different targets in breast and colorectal cancers. In breast cancer, no significance changes to known EMT regulators that correlated with FOXQ1 were noticed in microarray gene expression analysis of FOXQ1 ectopic expression or knockdown systems. As reporter assay demonstrated that FOXQ1 was able to repress CDH1 promoter region of 450bp upstream and 193bp downstream in vitro, I therefore propose that FOXQ1 directly regulated CDH1 transcriptional activity. In colorectal cancer, FOXQ1 has significantly increased two well-known factors CTGF and Slug which were previously reported to regulate EMT. What's more, my reporter assay results showed that both CTGF and Slug promoters were activated by FOXQ1, and CTGF promoter responded much more intensively to FOXQ1 than Slug. Hence, CTGF promoter activity was used as an indicator in my study of the functional domains of FOXQ1 protein. By constructing various FOXQ1 deletion mutants, I have further identified the transactivation domain, nuclear localization signal (NLS) and inhibitory domain of FOXQ1 protein.

This thesis studied intensively the function of FOXQ1 in human cancer cells and further identified its downstream transcriptional targets. The evidence presented in this thesis showed that FOXQ1 is an important forkhead factor in cancer progression and demonstrated that it is worth further exploring.

List of Tables

List of Figures

List of Abbreviations

×g: times gravity

aa: amino acid

bp: base pair

BSA: bovine serum albumin

cDNA: complementary DNA

ChIP: chromatin immunoprecipitation

CSC: cancer stem cell

CTGF: connective tissue growth factor

DAPI: 4', 6-diamidino-2-phenylindole

DBD: DNA binding domain

DDFS: Distant disease–free survival

DMEM: Dulbecco's Modified Eagle's Medium

DMSO: dimenthysulfoxide

DNA: deoxyribonuclease

DOX: doxycycline

E.coli: Escherichia coli

EDTA: ethylenediamine tetra-acetic acid

EGFR: Epidermal growth factor recerptor

EMT: epithelial to mesenchymal transition

ER: estrogen receptor

FBS: fetal bovine serum

G: gram

GAPDH: glyceraldehyde-3-phosphate dehydrogenase

GFP: green fluorescence protein

HER2: human epidermal growth factor receptor 2

HR: hormone receptor

hr: hour

IHC: immunohostochemistry

LB: Lysogeny broth

LBX1: ladybird homeobox 1

MDCK: Madin-Darby canine kidney

mg: milligram

ml: millilitre

mM: mmilimolar

NaF: sodium fluoride

ng: nanogram

NLS: nuclear localization signal

nt: nucleotide

OS: overall survival

P: p-value

PAGE: polyacrylamide gel electrophoresis

PARP: poly(ADP-ribose) polymerase inhibitors

PARP: Poly(ADP-ribose)polymerase

PI: Protease Inhibitor

PMSF: phenylmethylsulfonyl fluoride

PR: progesterone receptor

PVDF: polyvinyllidene difluoride

qPCR: quantitative polymerase chain reaction

RNAi: RNA interference

rpm: revolutions per minute

RT-PCR: reverse-transcription polymerase chain reaction

SDS: sodium dodecyl sulphate

shRNA: short hairpin RNA

VEGF: vascular endothelial growth factor

CHAPTER 1:

INTRODUCTION

1.1 Overview of tumor

A tumor is a lesion resulting from autonomous or relatively autonomous abnormal growth of cells which persisted even after the initiating stimulus had been removed. Tumors can result from neoplastic transformation of any nucleated cell in the body, although some cell types are more prone to tumor formation than others. The term 'cancer' means malignant tumor and it develops in approximately 25% of human population with higher tendency in older people. The mortality rate associated with cancer is high and is therefore of great clinical significance (Underwood 2004).

1.1.1 Structure of tumor

Solid tumors consist of neoplastic cells and stroma. The neoplastic cell population reproduces to a variable extent depending on the growth pattern and synthesis activity of the parent cell of origin. There is a functional resemblance to the parent tissue. The neoplastic cell population is embedded in and supported by a connective tissue framework called the stroma. It provides mechanical support and nutrition to the neoplastic cells. Tumor stroma contains blood vessels which perfuse the tumor and provide nutrition. The growth of a tumor is dependent upon its ability to induce blood vessels to perfuse it, and this process is named angiogenesis. Histologically, a tumor has the appearance of lost differentiation, weakened cellular cohesion, enlarged nucleus and increased mitotic activity (Abell 1966; Smolak 1971; Folkman 1975).

1.1.2 Tumor classification

Tumors are classified according to their behavior and cell of origin. Depending on behavior, they are classified into two groups, namely benign and malignant. Benign tumors are relatively mild and remain localized within basement membrane. They are slow growing lesions that do not invade the surrounding tissues or spread to distant sites in the body. Malignant tumors on the other hand are rapidly growing and poorly circumscribed. They bear less resemblance to parent cell or tissue compared to benign tumor. Malignant tumor erodes into and destroys adjacent tissues, enabling neoplastic cells to penetrate the walls of blood vessels and lymphatic channels, thereby disseminating to distant sites. This important process is called metastasis and can result in development of secondary tumors which are called metastases. However, not all malignant tumors exhibit metastatic behavior. For example, basal cell carcinoma of the skin rarely forms metastases, yet is regarded as malignant because it is highly invasive and destructive (Zollinger 1968).

Tumors can arise from any part of the body. Depending on the cell of origin, malignant tumors can be divided into several groups. Malignant tumors arising from the epithelium are called carcinoma; from the mesenchyme or connective tissue are called sarcoma; teratoma has a mix of origin. Carcinoma is the most popular malignant tumor. Here, I will only focus on carcinomas, which arise in epithelial tissues. Normally, cells that form the epithelial sheets in tissues are tightly bound to neighboring cells as well as to the underlying basement membrane by adherens junctions which are tight junctions that effectively immobilize them in these sheets. These tight physical constraints are not only limited to normal epithelial cells, but also

those within many benign carcinomas. However, when a tumor progresses, the carcinoma cells liberate themselves from these associations and begin to migrate out on their own, first by dissolving underlying basement membranes and then invading adjacent stromal compartments. This invasiveness seems to empower carcinoma cells to both intravasate and subsequently extravasate (Thiery and Sleeman 2006).

1.1.3 Metastasis of cancer

Metastasis is responsible for as much as 90% of the great cancer-associated mortality. Yet, it remains the most poorly understood component of cancer pathogenesis. During metastatic dissemination, a cancer cell from a primary tumor executes a sequence of steps. First of all, it locally invades the surrounding tissue. Secondly, it enters the microvasculature of the lymph and blood systems (intravasation). Thirdly, it survives and translocates largely through the bloodstream to microvessels of distant tissues, then exits from the bloodstream (extravasation), survives in the microenvironment of distant tissues, and finally adapts to the foreign microenvironment of these tissues in ways that facilitate cell proliferation and the formation of a macroscopic secondary tumor (colonization) (Fidler 2003). This complex metastatic cascade can be conceptually broken down into two major phases: (i) physical translocation of a cancer cell from the primary tumor to the microenvironment of a distant tissue and then (ii) colonization (Figure 1.1). Presently, our knowledge of physical dissemination is becoming clearer, whereas the second phase, colonization, involves complicated interactions that may still require many years of research before we fully understand the mechanism. From the standpoint of treatment, knowing the mechanisms of physical translocation is likely to be important for preventing metastasis in patients

who are diagnosed with early tumor, whereas understanding the mechanisms leading to successful colonization may lead to effective therapies for patients with existing metastases (Chaffer and Weinberg 2011).

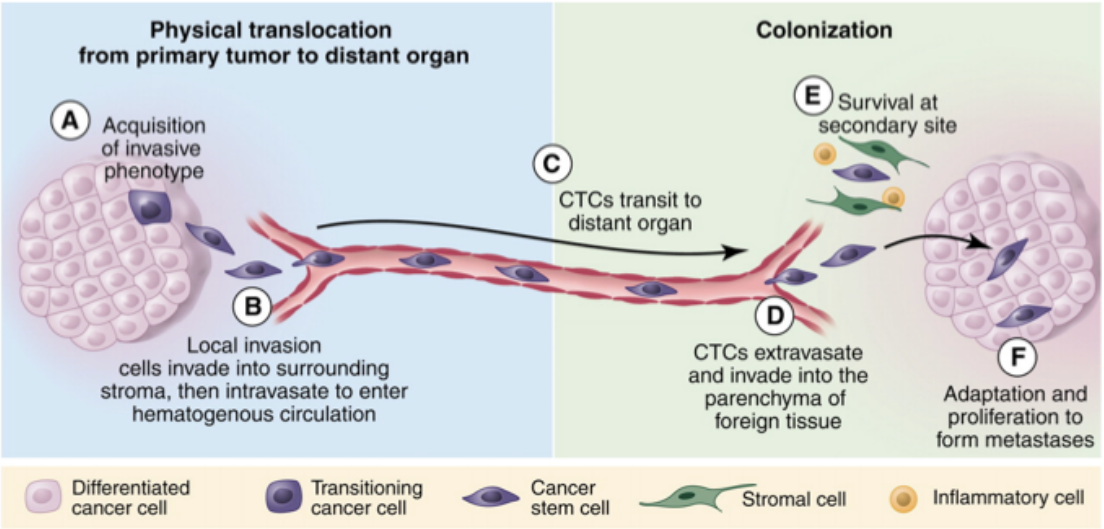

Figure 1.1 The metastatic cascade

Metastasis can be envisioned as a process that occurs in two major phases: (i) physical translocation of cancer cells from the primary tumor to a distant organ and (ii) colonization of the translocated cells within that organ. (A) To begin the metastatic cascade, cancer cells within the primary tumor acquire an invasive phenotype. (B) Cancer cells can then invade into the surrounding matrix and toward blood vessels, where they intravasate to enter the circulation, which serves as their primary means of passage to distant organs. (C) Cancer cells traveling through the circulation are circulating tumor cells (CTCs). They display properties of anchorage-independent survival. (D) At the distant organ, CTCs exit the circulation and invade into the microenvironment of the foreign tissue. (E) At that foreign site, cancer cells must be able to evade the innate immune response and also survive as a single cell (or as a small cluster of cells). (F) To develop into an active macrometastatic deposit, the cancer cell must be able to adapt to the microenvironment and initiate proliferation (Chaffer and Weinberg 2011).

1.2 Breast cancer

1.2.1 Epidemiology of breast cancer

Breast cancer is currently the most leading cancer among women with an estimated 1.38 million new cancer cases diagnosed in 2008 (23% of all cancers), and ranks second overall (10.9% of all cancers). It is now the most common cancer in both developed and developing regions with an estimated 690,000 new cases in each region. Incidence rates vary from 19.3 per 100,000 women in Eastern Africa to 89.7 per 100,000 women in Western Europe, and are high (greater than 80 per 100,000) in developed regions of the world (except Japan) but low (less than 40 per 100,000) in most of the developing regions. The range of mortality rates is however lower (approximately 6-19 per 100,000) because of the more favorable survival of breast cancer in (high-incidence) developed regions. As a result, breast cancer ranks as the fifth cause of death from cancer overall (458,000 deaths), but it is still the most frequent cause of cancer death in women in both developing (269,000 deaths, 12.7% of total) and developed regions, where the estimated 189,000 deaths is nearly equal to the estimated number of deaths from lung cancer (188,000 deaths) (Ferlay J, Shin HR et al. 2010).

1.2.2 Internal structure of mammary gland

Each mammary gland has 15-20 lobes arranged in a circular fashion, each of which has many smaller lobules. At the end of the lobules are tiny bulb-like glands, or sacs, where milk is produced. The lobes, lobules and glands are connected by thin ducts. These ducts channel milk to openings in the nipple. The lobules are secretory units of

breast, each lobule consists of a certain number of acini, or glands, embedded within loose connective tissue and connecting to the intralobule duct. Each acinus is composed of two types of cells, namely epithelial and myoepithelial cells. The epithelial cells form glandular lumens surrounded by myoepithelial cells which rest on the basement membrane (Figure 1.2). The most frequent type of breast cancer starts in the duct (ductal cancer), while other types begin in the lobes or lobules (lobular carcinoma). Less common is the inflammatory breast cancer where the breast becomes red and swollen (Debnath, Muthuswamy et al. 2003).

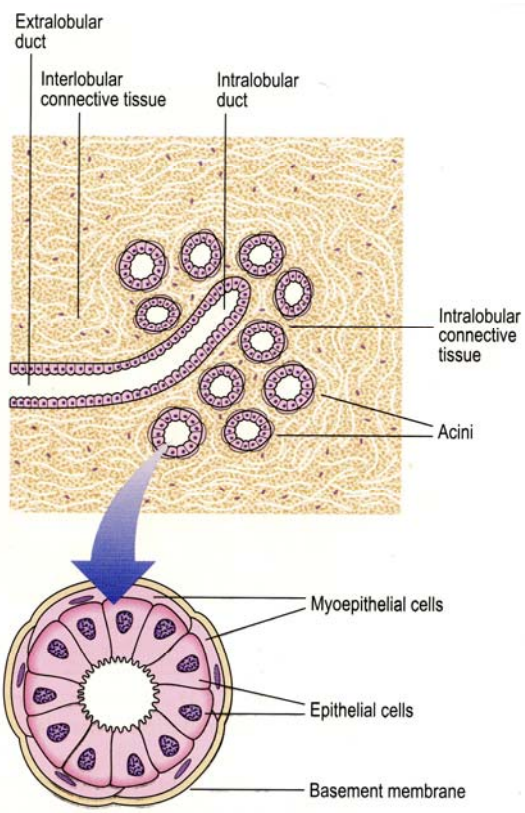

Figure 1.2 Internal structure of mammary gland

The acinus is lined by epithelial cells surrounded by myoepithelial cells and the basement membrane (Underwood 2004).

1.2.3 Subtypes of breast cancer

Breast cancer is a heterogeneous disease characterized by different gene expression patterns. Gene expression array analysis led to the identification of four major breast cancer subtypes. They are intrinsic subtypes including hormone receptor (HR)-positive Luminal A and B, human epidermal growth factor receptor 2 (HER2)-positive and basal-like breast cancer (Perou, Sorlie et al. 2000; Sorlie, Perou et al. 2001). These different subcategories of breast cancer have different prognoses. However, gene expression array is not practical for routine identification of breast cancer subtypes. A more common subtype classification clinically is to obtain by immunohistochemistry (IHC) analysis the degree of tumor expression of estrogen receptor (ER), progesterone receptor (PR) or HER2. By utilizing this simple analysis, it is possible to identify three major breast cancer subtypes: the ER/PR-positive, or hormone receptor-positive (HR) subtype, which basically includes the Luminal A and B intrinsic subtypes; the HER2-positive subtype; the triple-negative subtype, which lacks of the expression of all the three receptors (ER, PR and HER2) (Nielsen, Hsu et al. 2004; Arslan, Dizdar et al. 2009).

According to the classification of breast cancer, triple-negative subtype shares certain similarities with basal-like breast cancer in terms of genetic makeup and tumor behavior. Overall, triple-negative and basal-like breast cancer accounts for 12-17% of all types of breast cancer (Cleator, Heller et al. 2007). Histologically, they are poorly differentiated, show necrosis and are often accompanied by an aggressive clinical history. Both triple-negative and basal-like breast cancer occur more frequently in young women of black and hispanic ethnicity than in other ethnic groups. In addition,

BRCA1 mutation is common in both triple-negative and basal-like breast cancer. They have a mutual relationship with BRCA1 dysfunction. BRCA1 is an important breast cancer susceptibility gene; more than 75% of female tumors carry a mutation in this gene presents with a triple-negative phenotype, a basal-like phenotype, or both. BRCA1 plays a central role in repair of double-stranded DNA breaks and a lack of BRCA1 therefore results in genomic instability thereby increasing the chance of developing malignant diseases. Hereditary BRCA1-mutated breast cancer very frequently exhibits basal-like gene expression patterns and sporadic triple-negative breast cancers often have BRCA1 dysfunctions (Sorlie, Perou et al. 2001; Turner, Tutt et al. 2004).

Triple-negative breast cancer is highly though not exactly concordant with basal-like breast cancer as defined by gene expression analyses. Basal-like breast cancer is assumed to arise from the outer basal layer of breast ducts because its gene expressions can be found in the basal or myoepithelial cells of the human breast. Preparations of these tumors stain positively for basal cell cytokeratins (CK5, 6 and 17) and have the absence or low expression of ER, PR, and very low HER2 expression. For clinical purposes, after the term ‘triple-negative breast cancer’ was first mentioned in October 2005, large numbers of literature recognize the importance of this subtype of breast cancer. Triple-negative breast cancer has certain degree of overlay with basal-like breast cancer depending on the different criteria used for judging levels of ER, PR, and HER2 (Nielsen, Hsu et al. 2004; Foulkes, Smith et al. 2010).

Compared with HR-positive and HER2-positive patients, patients with triple-negative breast cancer have much higher likelihood of distant recurrence. The peak risk of recurrence occurs within the first three years after initial treatment of the disease with the majority of deaths occurring in the first 5 years. On the contrary, the risk for late recurrences declines by 50% over the next 5 years, compared with HR-positive disease (Dent, Trudeau et al. 2007). Triple-negative breast cancer tends to metastasize hematogenously instead of via the lymphatics and they are associated with more axillary lymph node metastasis than non-triple-negative breast cancers (Van Calster, Vanden Bempt et al. 2009). Both triple-negative and basal-like breast cancers are more likely than other subtypes of breast cancers to metastasize, particularly to the lungs and brain, but are less likely to metastasize to bone (Nam, Kim et al. 2008).

Breast cancer cell lines in-vitro displayed the same heterogeneity as the primary tumors. In hierarchical clustering of transcriptional profiles of 51 breast cell lines with published primary, Neve and team identified that luminal cluster was generally uniform across all samples, but basal-like cluster contained at least two major subsets including Basal A and B. Basal A cluster matched closely to the Perou's basal-like signature, but basal B showed a stem-cell like expression profile and may reflect the clinical 'triple-negative' tumor types (Neve, Chin et al. 2006).

1.2.4 Treatment of breast cancer

Luminal A and B breast cancers are potentially sensitive to hormonal treatment; the HER2-positive subtype is potentially sensitive to trastuzumab, lapatinib and other HER2-directed targeted drugs. However, the triple-negative breast cancer is

insensitive to the standard drugs used against breast cancer due to the lack of all three receptors (Rouzier, Perou et al. 2005). Therefore, the only systemic treatment option available for these patients is chemotherapy with standard cytotoxic agents. Neoadjuvant chemotherapy trials have shown that triple-negative breast cancers were more responsive to anthracyclines and taxanes than hormone-receptor-positive subtypes, as demonstrated with higher pathological complete response rates (Liedtke, Mazouni et al. 2008).

Nevertheless, triple-negative breast cancer still has ominous prognosis, especially in patients with poor response to chemotherapy. Novel therapeutic targets are urgently needed to improve the management of this subtype of breast cancer. It is not a single disease but instead encompasses a variety of diseases grouped together solely on the basis of absence of ER, PR, and HER2 expression, plus lacking a single common pathway of pathogenesis. Thus, multiple targeted therapies might be necessary in the management of these tumors (Carey, Dees et al. 2007). Besides chemotherapy, there are other inhibitors also designed to target triple-negative breast cancer. Poly (ADP-ribose) polymerases (PARPs) inhibitors specifically inhibit PARP-1 and, consequently of the DNA single strand break repair system. This PARP inhibitor could be used alone or combined with other DNA damaging agents to maximize DNA damage and destroy the repair system in cancer cells. Several PARP inhibitors are currently in clinical trials (Rottenberg, Jaspers et al. 2008). Epidermal growth factor receptor (EGFR) has been found to be 80% overexpressed in triple-negative breast cancer and this has been linked to poor outcome. Also, patients with triple-negative breast cancers have shown elevated levels of vascular endothelial growth factor (VEGF) (Linderholm, Hellborg et al. 2009). Angiogenesis is therefore regarded as a

key target for the development of new therapeutic strategies. Bevacizumab, a drug targeting angiogenesis, is now in phase II study and results in the neoadjuvant treatment of colorectal cancer and breast cancer are promising (Van Meter and Kim 2010).

1.3 Colorectal cancer

1.3.1 Epidemiology of colorectal cancer

Colorectal cancer is the third most common cancer in men (663,000 cases, 10.0% of the total) and second in women (571,000 cases, 9.4% of the total) worldwide. Almost 60% of the cases occur in developed regions. Incidence rates vary 10-fold in both sexes worldwide, the highest rates being estimated in Australia/New Zealand and Western Europe, the lowest in Africa (except Southern Africa) and South-Central Asia, and are intermediate in Latin America. Incidence rates are considerably higher in men than in women. About 608,000 deaths from colorectal cancer are estimated worldwide, accounting for 8% of all cancer deaths, thus making it the fourth most common cause of death from cancer. As observed for incidence, mortality rates are lower in women than in men, except in the Caribbean. There is less variability in mortality rates worldwide (6-fold in men, 5-fold in women), with the highest mortality rates in both sexes estimated in Central and Eastern Europe (20.1 per 100,000 for male, 12.2 per 100,000 for female), and the lowest in Middle Africa (3.5 and 2.7 respectively) (Ferlay J, Shin HR et al. 2010).

Every year in the United States, 160,000 cases of colorectal cancer are diagnosed, and 57,000 patients die of the disease, making it the second leading cause of death from cancer among adults (Jemal, Siegel et al. 2008). Worldwide, 655,000 death cases occur every year, and it ranks the third leading cause of cancer-related death in western countries. Colorectal cancer arises from adenomatous polyps in colon. Benign colorectal tumors are not deadly unless ignored for years after which it may develop into cancer and become invasive. About 73% of invasive colorectal cancers are curable when completely removed by surgery followed by chemotherapy. However, cancer that metastasized to distant sites are usually not curable, and chemotherapy can only help to delay death. Metastatic colorectal cancer often invade blood vessels and lymphatic channels first. It may then spread to lung, bone and/or brain. Chemotherapy for metastatic colorectal cancer can be administrated before/after surgery, or as primary therapy.

1.3.2 Molecular mechanism of colorectal cancer

The molecular etiology of colorectal cancers can be explained by genetic instability and epigenetic alteration which can occur either in inherited germ-line mutation or acquired somatic mutation. This can happen as a result of either inactivation of tumor suppressor or activation of oncogene.

1.3.2.1 Inactivation of tumor suppressor in colorectal cancer

In colorectal cancer, the initiating event is activation of Wnt signaling pathway. Wnt signaling occurs when the oncoprotein β-catenin bind to nuclear partners (member of the T-cell factor-lymphocyte enhancer factor family) to create a transcription factor

that regulates genes involved in cellular activation. The β-catenin degradation complex controls levels of β-catenin protein by proteolysis. A component of this complex APC, not only degrade β-catenin but also inhibits its nuclear localization. In colorectal cancer, the most common mutation is inactivation of gene encoding the APC protein. In the absence of functional APC, which serves as a brake to stop β-catenin, Wnt signaling is inappropriately and constitutively activated. Germ-line mutations of APC is responsible for close to 100% risk of familial adenomatous polyposis by the age of 40. Somatic mutations and deletions of APC are observed in most of sporadic colorectal adenoma and cancers (Goss and Groden 2000; Lynch, Lynch et al. 2008).

The second genetic step in colorectal cancer is the inactivation of p53 pathway by mutation of TP53, a well known tumor suppressor in a wide range of tumor. p53 pathway mediates cell-cycle arrest and as a cell-death checkpoint, it can be activated by multiple cellular stresses. In most tumors, the mutation of TP53 gene can inactivate the transcription activity of p53 and the inactivation of p53 coincides with transition of adenomas to invasive carcinomas. In addition, mutation of apoptotic effectors of wide type p53 pathway also contributes to colorectal cancer progression (Baker, Preisinger et al. 1990; Vazquez, Bond et al. 2008).

The third step during colorectal cancer progression is mutation of TGF-β pathway. During early tumor formation, this pathway is functional as a tumor suppressor that regulates cell growth arrest and apoptosis. In colorectal cancer, about one third of them carries somatic mutation of TGFBR2 (TGF-β receptor 2) which result in inactivation of TGF-β signaling. In addition, inactivation of downstream effectors of

TGF-β such as Smad2, Smad3 and Smad4 can also abolish TGF-β signaling (Markowitz, Wang et al. 1995; Parsons, Myeroff et al. 1995; Grady, Myeroff et al. 1999; Grady and Markowitz 2008).

1.3.2.2 Activation of oncogene pathway in colorectal cancer

During inactivation of tumor suppressor pathway, several oncogenes may in concomitant play key roles in promoting colorectal cancer. Oncogenic mutations of RAS and BRAF, which activate the mitogen-activated protein kinase (MAPK) signaling pathway occur in 37% and 13% of colorectal cancers respectively (Davies, Bignell et al. 2002; Rajagopalan, Bardelli et al. 2002). These mutations consistently result in activation of pro-survival and apoptosis suppression pathway in PI3K-PDK1-PKB and RAF-MEK-ERK1/2 (Bos, Fearon et al. 1987). The activation of somatic mutations in PI3KCA, which encodes the catalytic subunit of phosphatidylinositol 3-kinase (PI3K), also accounts for one third of colorectal cancer. This mutation results in loss of the inhibitor of PI3K (PTEN) and activation of an upstream activator (IRS2). Both signalings result in amplification of downstream effectors of PI3K signaling and colorectal cancer progression (Parsons, Wang et al. 2005; Parsons, Jones et al. 2008).

1.4 Cancer stem cell

Cancer stem cell (CSC) is also known as tumor-initiating cell (T-IC), which is responsible for initiating cancer. This idea was first introduced in hematopoietic system by Dr. John Dick and team. This identification has been accomplished in acute myeloid leukemia (AML), where it was demonstrated that a specific subpopulation of leukemic cells (that expressed CD34+/CD38- markers similar to normal

hematopoietic stem cells) was consistently enriched for clonogenic activity in non-obese diabetic/severe combined immunodeficient (NOD/SCID) immunocompromised mice, whereas other cancer cells were depleted of clonogenic activity (Lapidot, Sirard et al. 1994; Larochelle, Vormoor et al. 1996; Bonnet and Dick 1997). This concept emphasized the heterogeneity of a tumor and was soon followed by several tumor heterogeneity models with further identification of cancer stem cells in solid tumor. As more cancer stem cells were identified in different types of tumor, the biological and therapeutic values of cancer stem cell will be discussed in detail below.

1.4.1 Models of tumor heterogeneity

Cancer is a heterogeneous disease histologically and functionally. Currently, two mutually exclusive models are used to explain tumor heterogeneity, namely the stochastic and the hierarchy model.

The stochastic model predicts that the tumor is relatively homogeneous and the tumorigenic mechanisms (pathways, genetic programs) that underlie the malignancy are functional in all cells. Thus, key features of the tumor can be identified by studying the bulk of the cells that make up the tumor mass. The behavior of the cancer cells is affected by intrinsic (e.g., levels of transcription factors, signaling pathways) or extrinsic (e.g., host factors, microenvironment, immune response) factors. These influences are unpredictable as well as random and can result in heterogeneity in the expression of cell surface markers or other markers of maturation, in entry to cell cycle, or in tumor initiation capacity. A key tenet of this model is that all cells of the tumor are equally sensitive to such stochastic influences and also that tumor cells can

revert from one state to another because these influences do not induce permanent changes (Wang and Dick 2005).

In contrast, the hierarchy model predicts functional heterogeneity among the cells that make up the tumor and that the rare cancer stem cells are different from the vast majority of cells that constitute the tumor. Therefore, tumorigenic pathways may function differentially in distinct tumor subpopulations. This model also predicts that although eradication of the non-cancer stem cell may result in a remission, the disease will relapse if the tumor initiating cells are not destroyed. Resolution of the tumor initiating cell problem requires both purification of tumor cells into subfractions as well as a functional assay to detect cells with the capacity to initiate tumor growth in vivo (Figure 1.3) (Reya, Morrison et al. 2001; Dick 2008).

Thus, both the stochastic and hierarchy models accommodate the existence of cancer stem cell. The essential difference is that, in the stochastic model, cancer stem cells arise randomly and every tumor cell has the potential to behave like a cancer stem cell given the right conditions; whereas in the hierarchy model, there is only a distinct subset of cells that has the potential to behave like cancer stem cell. The stochastic model suggests that it will be impossible to predict which kind of cells become tumor initiating cell and that stochastic events will cause tumor initiating cells to be identified in any two sorted cell fractions with equal probabilities. By contrast, the hierarchy model predicts that it should be possible to separate tumor initiating cell from non-tumor initiating cell. Thus, theoretically it should be able to sort tumors into fractions with or without cancer stem cell activity if the hierarchy model is correct. In contrast, the stochastic model predicts that cancer stem cell activity may be observed

in any fraction and cannot be prospectively isolated because it assumes that all tumor cells have the same potential (even if it is low) for tumor initiation (Dick 2008).

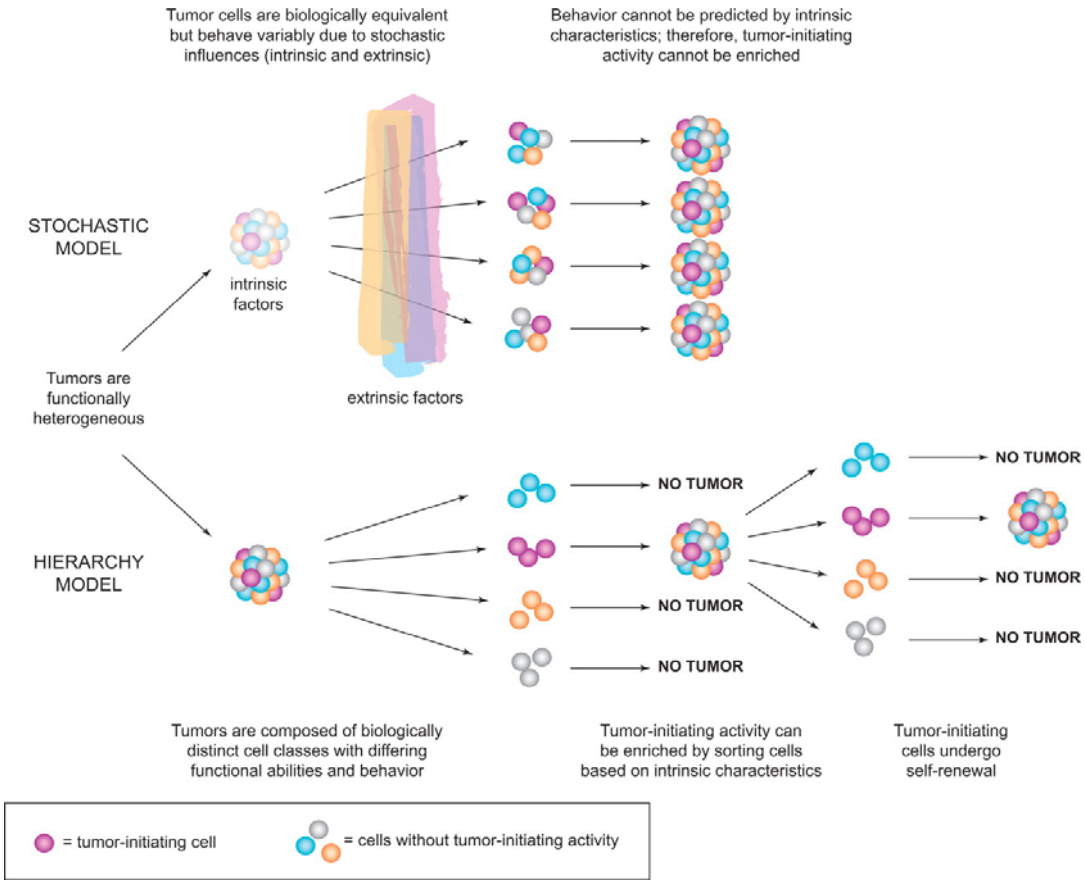

Figure 1.3 Models of tumor heterogeneity

Tumors are composed of phenotypically and functionally heterogeneous cells. There are 2 theories to explain how this heterogeneity arises. According to the stochastic model, tumor cells are biologically similar and their behavior is determined by internal and external factors. Thus, tumor-initiating activity cannot be enriched by sorting cells based on intrinsic characteristics. In contrast, the hierarchy model postulates the existence of biologically distinct classes of cells with differing functional abilities and behavior. Only a subset of cells can initiate tumor growth; these cancer stem cells possess self-renewal and give rise to nontumorigenic progeny that make up the bulk of the tumor. This model predicts that tumor-initiating cells can be identified and purified from the bulk nontumorigenic population based on intrinsic characteristics (Dick 2008).

1.4.2 Stem cell and cancer stem cell

Many human tissues undergo rapid and continuous cell turnover. In the colonic mucosa or in the peripheral blood, for example, the average life span of a mature, differentiated cell (e.g., a goblet cell in a crypt of the large intestine or a circulating granulocyte) can be measured in days or even hours. Despite the ephemeral nature of most of their individual cell components, human tissues maintain their mass and architecture over time through a tightly regulated process of reconstruction. Under physiological conditions, this process is sustained by a small minority of long-lived cells with extraordinary renewal potential, known as stem cells. Stem cells are defined by three main properties: 1. differentiation-the ability to give rise to a heterogeneous progeny of cells, which progressively diversify and specialize according to a hierarchical process, constantly replenishing the tissue of short-lived, mature elements; 2. self-renewal-the ability to form new stem cells with identical, intact potential for proliferation, expansion, and differentiation, thus maintaining the stem cell pool; 3. homeostatic control-the ability to modulate and balance differentiation and self-renewal according to environmental stimuli and genetic constraints (Reya, Morrison et al. 2001).

Like their normal tissue counterparts, tumors are composed of heterogeneous populations of cells that differ in their apparent state of differentiation. Indeed, the morphological and architectural differentiation features of a tumor are the key parameter used routinely by hospital pathologists to define a tumor's primary anatomical origin. This simple observation suggests that tumors are not mere monoclonal expansions of cells but might actually be akin to 'abnormal organs',

sustained by a population of diseased cancer stem cell which are endowed with the ability to self-renew and undergo aberrant differentiation (Reya, Morrison et al. 2001; Clarke and Fuller 2006). This hypothesis is further justified by the fact that cancer is known to result from accumulation of multiple genetic mutations in a single target cell, sometimes over a period of many years (Fearon and Vogelstein 1990). Because stem cells are the only long-lived cells in many tissues, they are the natural candidates in which early transforming mutations may accumulate. Currently limited knowledge of normal stem cells, partly due to the overall paucity of research on their functions has added a layer of smoke screen to the cancer stem cell theory. A new wave of studies, however, has recently began to probe this concept using an innovative, purely empirical approach, based on in vivo self-renewal assay (Clarke 2005). Starting from whole tumor tissues, cancer cells are purified into single-cell suspensions and subsequently fractioned in different subsets according to the expression of a specific repertoire of surface markers. Once isolated, individual cancer cell subsets are injected into suitable hosts (in most cases orthotopic tissues of immunodeficient mouse strains), and the tumorigenic capacity of different subsets compared. According to the cancer stem cell model, only a specific subset of the cancer cell population (i.e., the long-lived cancer stem cell subset) and not all other subsets should be able to sustain in vivo tumor growth. Indeed, this assumption has now been repeatedly confirmed in several tumor systems. Three key observations classically define the existence of a cancer stem cell population: 1. Only a small percentage of cancer cells within each tumor are usually endowed with tumorigenic potential when transplanted into immunodeficient mice. 2. Tumorigenic cancer cells are characterized by a distinctive profile of surface markers and can be differentially and reproducibly isolated from non-tumorigenic ones by using flow cytometry or other

immunoselection techniques. 3. Tumors grown from tumorigenic cells contain a mixture of tumorigenic and nontumorigenic cancer cells, thus recreating the full phenotypic heterogeneity found in the parent tumor (Reya, Morrison et al. 2001).

It is important to understand that, based on this approach, the term cancer stem cell represents a working definition with a purely operational significance. The term is used to indicate a subset of tumor-initiating cell population that can generate a heterogeneous progeny, similar in composition to its original parent tissue from which it was isolated. In most cases, it is currently not possible to define with certainty the 'genealogical' relationship between cancer stem cell and normal stem cells of the corresponding tissues (i.e., whether cancer stem cell originate directly from normal stem cells or the early stages of their progeny). Irregardless of the actual origins of cancer stem cell, the identification of a cancer stem cell population establishes a functional hierarchy within a tumor tissue and encompasses both the self-renewal and differentiation hallmarks of stem cells. First developed in human myeloid leukemias, the cancer stem cell working model is currently being progressively expanded to include several solid tumors, along with several biological and therapeutic implications (Dalerba, Cho et al. 2007).

1.4.3 CSCs in solid tumor

The cancer stem cell model was described for hematologic malignancies in 1997. John Dick's team provided evidence that leukemia growth and propagation were driven by a small population of leukemia cells that have the ability to perpetually self renew. They called this cell population cancer stem cells (CSCs) (Bonnet and Dick

1997). Since then, more evidence has emerged to support this hypothesis for many solid tumors as well. Importantly, these studies led to increasing depth of understanding of normal hematopoietic development over the past four decades. Functional assays in vitro and in vivo are available for all stem and progenitor cell types ranging from the primitive pluripotential stem cells to multipotential and unipotential progenitor (Weissman 2000). In addition, a rich collection of cell surface differentiation markers enabled detailed characterization of normal hematopoietic development, as well as providing insight into how normal differentiation becomes disrupted in human leukemia. It is clear that leukemic tissues, although abnormal, still retain remnants of normal differentiation and developmental programs (Appelbaum, Rowe et al. 2001). Following the knowledge and mature techniques on identification and isolation of hematopoietic stem cell, CSCs have been recognized in several solid tumors (Ailles and Weissman 2007).

1.4.3.1 CSCs in breast tumor

On the basis of these observations, Hajj and team undertook a new study to test whether a CSC model could be applied to the description of solid tumors, focusing on human breast cancer as a model system (Al-Hajj, Wicha et al. 2003). Their results showed that, in most human breast cancers, only a minority subpopulation of the tumor clone, defined as CD44+/CD24(-/low) and representing 11% to 35% of total cancer cells, is endowed with the capacity to sustain tumor growth when xenografted in NOD/SCID mice. Most importantly, tumors grown from CD44+/CD24(-/low) cells were shown to contain a mixed population of epithelial tumor cells, recreating the heterogeneous phenotype seen in parent tumors. This study demonstrated for the first

time the existence of a functional hierarchy reminiscent of stem cell systems in a solid human epithelial tumor. After that, putative CSCs have been isolated from many other tumors including brain, colon, pancreas, prostate, lung and head and neck tumors (Anton Aparicio, Garcia Campelo et al. 2007; Glinsky 2007; Li, Heidt et al. 2007; Prince, Sivanandan et al. 2007; Seo, Sung et al. 2007; Ceder, Jansson et al. 2008; Eramo, Lotti et al. 2008; Ferrandina, Bonanno et al. 2008).

Proponents of the 'breast cancer stem cell hypothesis' argue that cancer stem cells are ultimately responsible for the maintenance of a population of malignant cells with metastatic potential. Cancer cells from triple-negative and basal-like breast cancers display a profile of cell surface markers that is similar to that of breast cancer stem cells, characterized by the phenotype CD44+/CD24- (in which CD44 is expressed at high levels but levels of CD24 are low or undetectable) and also the expression of aldehyde dehydrogenase 1 (ALDH1). Although the population of cells expressing these markers is enriched with tumorigenic potential, not every cancer cell with this profile has the properties of cancer stem cells. Cancer stem cells do not necessarily originate from tissue stem cells. They may originate from a differentiated cancer cell that has acquired the ability to self-renew; the phenotypic plasticity of cancer cells is a well-documented phenomenon. Notably, breast-cancer cells that undergo epithelial to mesenchymal transition display characteristics that can be all but indistinguishable from those of breast-cancer stem cells. Basal-like breast cancers often display gene-expression patterns that are consistent with those of cells undergoing epithelial to mesenchymal transition. Basal-like breast cancer frequently express an 'embryonic stem-cell signature', exhibit well-established characteristics of epithelial to mesenchymal transition, and commonly express a CD44+/CD24- phenotype which

has been linked to ‘stem-cell’ phenotype (Ben-Porath, Thomson et al. 2008; Honeth, Bendahl et al. 2008; Sarrio, Rodriguez-Pinilla et al. 2008).

1.4.3.2 CSCs in brain tumor

The CSC working model has also been successfully applied to brain tumors. Studies performed on glioblastoma multiforme and medulloblastoma have shown that tumorigenic cells are confined to the CD133+ subpopulation, which usually represents about 5% to 30% of total tumor cells. As expected from the CSC model, tumors resulting from orthotopic, intracerebral injection of CD133+ cells reproduced the phenotypic diversity and differentiation pattern of the parent tumors. In the study of brain tumors, the availability of a well-characterized cell culture system for normal neural stem cells (the ‘neurosphere’ assay) provided a robust tool for the in vitro study of their candidate pathological counterparts. Based on this method, Galli et al. succeeded in the isolation and serial propagation from human glioblastoma multiforme of ‘cancer neurospheres’, which are highly enriched in long-term self-renewing, multilineage-differentiating, and tumor initiating cells. Notwithstanding the unclear relationship between CD133+ cells and cancer neurospheres which required further exploration, it is safe to assume that ex vivo purification of brain tumor CSCs based on CD133 coupled with in vitro functional studies using neurosphere assays will provide one of the most effective probes for the study of solid tumor CSCs in the near future (Galli, Binda et al. 2004).

1.4.3.3 CSCs in colorectal tumor

Amongst all the malignant tumor, colorectal cancer has the highest heterogeneity with varying degrees of differentiation. This heterogeneity suggest that the tumor mass within colorectal cancer may have diverse functions. In colorectal cancer, the tumorigenic cells within included a high-density of CD133+ subpopulation and these subpopulations of cells comprised 2.5% of total tumor cells. When CD133+ cell subpopulation is injected into immunodeficient mice subcutaneously, it can reproduce the original tumor, whereas CD133- population failed to generate any tumor. In addition, CD133+ subpopulation of colorectal cancer can maintain its tumorigeneity after a series of transplantation into animals. CD133+ cells can grow exponentially in vitro for a very long time in the undifferentiated form, yet reproduce the original tumor under favourable conditions. Hence, CD133+ subpopulation play an active role and is a useful marker in colorectal cancer propagation and maintenance (Ricci-Vitiani, Lombardi et al. 2007).

This model proposes that certain cells within the tumor mass are pluripotent, capable of self-renewal, and possessed enhanced ability to initiate distant metastasis. The cancer stem cell model has important implications for cancer treatment, since most current therapies target actively proliferating cells and may not be effective against cancer stem cells which are the culprits responsible for recurrence. In recent years, great progress has been made in identifying markers of both normal and malignant colon stem cells. Proposed markers of colon cancer stem cell include CD133, CD44, CD166, ALDH1, Lgr5, and several others (Kemper, Grandela et al. 2010; Sanders and Majumdar 2011; Takahashi, Ishii et al. 2011)**.**

In vitro expansion of colon CSCs isolated from clinical specimens can be maintained in culture enabling the identification of CSC cell surface-associated proteins. From primary colon tumor, isolation of enriched CD133+ population gave rise to long-term tumor sphere cultures carrying CD133 expression. These tumor sphere cells were able to self-renew and differentiate into adherent epithelial lineages and recapitulate the phenotype of the original tumor. Relative to their differentiated progeny, tumor sphere cells were more resistant to the chemotherapeutic agent irinotecan. Other surface markers such as CD44, CD166, CD29, CEACAM5, cadherin 17, and biglycan were also identified by mass spectrometry and found to be enriched in CD133+ tumor spheroid cells in vitro (Fang, Kim et al. 2010).

1.4.4 CSCs and biology of cancer metastases

CSC is believed to participate in tumor generation and propagation. The critical step for tumor propagation is cancer metastasis and during this process, the role of CSC is obvious. Tumor initiation by implanted cells under experimental condition is theoretically analogous to dissemination of cancer cells in a patient. Both processes depend on the ability of cancer cells to function as parent cells that spawn essentially unlimited numbers of descendants. Hence, the very traits that are used to define CSCs-self-renewal and tumor-initiating ability-would seem to be inextricable elements of successful metastasis formation. Hence, the concept of CSC model sheds new light on the biology of metastases and explains why is it that comparison of paired samples of primary tumors and autologous lymph node and/or distant-site metastases usually reveals striking similarities over a wide range of parameters despite extensive intra-tumor heterogeneity. These parameters included tissue

morphology, repertoire of somatic genetic mutations, expression of tumor-suppressor and immunomodulatory proteins, expression of epigenetically controlled genes, and overall transcriptional profile as defined by gene expression arrays.

These observations are in contrast to predictions from traditional cancer models, where metastases are considered to originate from monoclonal expansions of very specific, individual tumor subclones endowed with specific genotypic and phenotypic features, and therefore are postulated to be substantially different from primary tumors. However, if we take into account the CSC model and we assume that, in each individual tumor, the differentiation pattern is controlled by its specific repertoire of genetic mutations, then we can predict that, if two lesions share identical genetic backgrounds and similar genetic abnormalities, they will also undergo similar differentiation programs and display similar patterns of intratumor heterogeneity in the expression of differentiation antigens (Dalerba, Cho et al. 2007).

1.4.5 Implication of CSCs for cancer therapy

The CSC model has important implication for cancer therapy. Currently, most of chemotherapeutic drugs target rapidly dividing cells, which represent the majority of the tumor mass. However, conventional cancer therapy frequently fail to eliminate the CSC population and can result in relapses, and more importantly, inadvertently led to generation of therapy-resistant and more aggressive cancer cells. Several features of CSCs possibly make them hard to eliminate. CSCs are relatively quiescent and this allows them to escape from chemotherapeutic regimens that typically target actively dividing cells. Moreover, as shown in their normal counterparts, CSCs have been

proposed to exhibit high expression level of multidrug transporter family genes leading to more efficient efflux of chemotherapeutic drugs as well as innate multidrug resistance. In order to develop an efficient therapeutic approach, we must first identify distinctive molecular pathways active in CSCs. Next is the identification of agents that can either block CSC proliferation or induce CSC differentiation so as to enhance sensitivity to chemotherapeutic drugs (Ricci-Vitiani, Fabrizi et al. 2009; Fabrizi, di Martino et al. 2010). CSCs can be generated through EMT process. Hence, targeting molecules which are involved in generation of EMT should be a logical strategy in drug development. Gupta and colleague found that salinomycin treatment can selectively kill CSCs using EMT model (Gupta, Onder et al. 2009).

1.5 Epithelial to mesenchymal transition

Epithelial to mesenchymal transition (EMT) is a biological process whereby epithelial cells detach from surrounding to acquire mesenchymal phenotype. This process is governed by multiple biochemical processes and eventually results in the acquisition of enhanced migratory ability, invasiveness, elevated resistance to apoptosis, and greatly increased production of ECM components (Kalluri and Neilson 2003). Depending on the different functional consequences and the various origins of this transition process, EMT is parsed into three distinct biological settings. In a 2007 meeting in Poland and a 2008 meeting in Cold Spring Harbor Laboratory, the suggestion of EMT subtypes were well discussed and divided into three types based on context. Type 1 EMT is associated with implantation, embryo formation, and organ development processes. In these processes they share a common mesenchymal phenotype despite belonging to different cell types. Type 1 EMT generates

messenchymal cells (primary mesenchyme) from primitive epithelial cells as part of gastrulation and primitive neuroepithelial cells generating migrating neural crest cells. In such situations, some of the cells generated by EMT have the potential to subsequently undergo a mesenchymal to epithelial transition (MET) to create secondary epithelia. Type 2 EMT is associated with would healing, tissue regeneration, and organ fibrosis. In this type of EMT, secondary epithelial or endothelial cells transit into resident tissue fibroblasts in response to a repair-initiated trigger. During this event, fibroblasts are generated to reconstruct tissue after trauma, inflammation or other injuries. Type 2 EMT stops when the triggering event is attenuated after wound healing and/or tissue regeneration. In organ fibrosis, type 2 EMT is continuous in response to ongoing inflammation and eventually results in organ destruction. Type 3 EMT occurs in neoplastic cells that harbor genetic and epigenetic changes which give rise to tumors, and these are the changes that distinguishes type 3 EMT from the other two types. Epithelial carcinoma cells can metastasize by undergoing type 3 EMT transit to mesenchymal cancer cells. During metastatic cascade, type 3 EMT enabled cancer cells to migrate into blood stream and travel to distant sites in which some revert back to epithelial identity while others become fully mesenchymal. In this study, I will focus on the investigation of type 3 EMT (Kalluri 2009; Kalluri and Weinberg 2009; Zeisberg and Neilson 2009).

EMT not only occurs in gastrulation during early embryo development and generation of new fibrosis during wound healing and tissue inflammation, but also plays a role in cancer progression and metastases under definition of type 3 EMT. Type 3 EMT is exclusive to cancer and is linked to morbid consequences. Excessive epithelial cell proliferation and angiogenesis are hallmarks of initiation and early growth of primary

epithelial cancer also known as carcinoma. The subsequent invasiveness and metastatic dissemination is initiated by breaking through the basement membrane. The molecular mechanism governing the acquisition of invasive ability is frequently linked to type 3 EMT lately. Accumulating evidence suggest that type 3 EMT is triggered by certain signals to activate the malignant behavior of epithelial cancer cells. The full spectrum of signals that contribute to EMT of carcinoma cells remains unclear. One possibility is tumor-associated stroma of primary tumor that undergoes genetic and epigenetic alterations to provide specific EMT-inducing signal (Kalluri 2009).

Type 3 EMT is illustrated in Figure 1.4 (Thiery 2002). Under normal conditions, epithelial cells line the walls of cavities. Excessive epithelial cell proliferation and angiogenesis led to formation of carcinoma in situ which can remain benign if the epithelial boundary remained intact. This benign tumor can be successfully removed surgically. However, benign tumors can develop into malignant tumors before full diagnosis. During the development of malignancy, the immature epithelial cells within benign carcinoma shade their epithelial morphology, digest the basement membrane to enter the surrounding stroma, and in turn gain access to vascular channels to travel through the blood vassels to distant sites to become secondary tumors at these sites. The start of this malignant process is triggered by EMT signals. Epithelial cells induced by EMT signals gain mesenchymal morphology, and erode the basement membrane to enter blood vassels because of increased motility. When they arrive at the new site, the invading mesenchymal cells would shed their mesenchymal morphology, revert to epithelial and settle down to grow into a new

secondary tumor. This process is known as MET. Several inducers are known to regulate type 3 EMT directly or indirectly (Kalluri and Weinberg 2009).

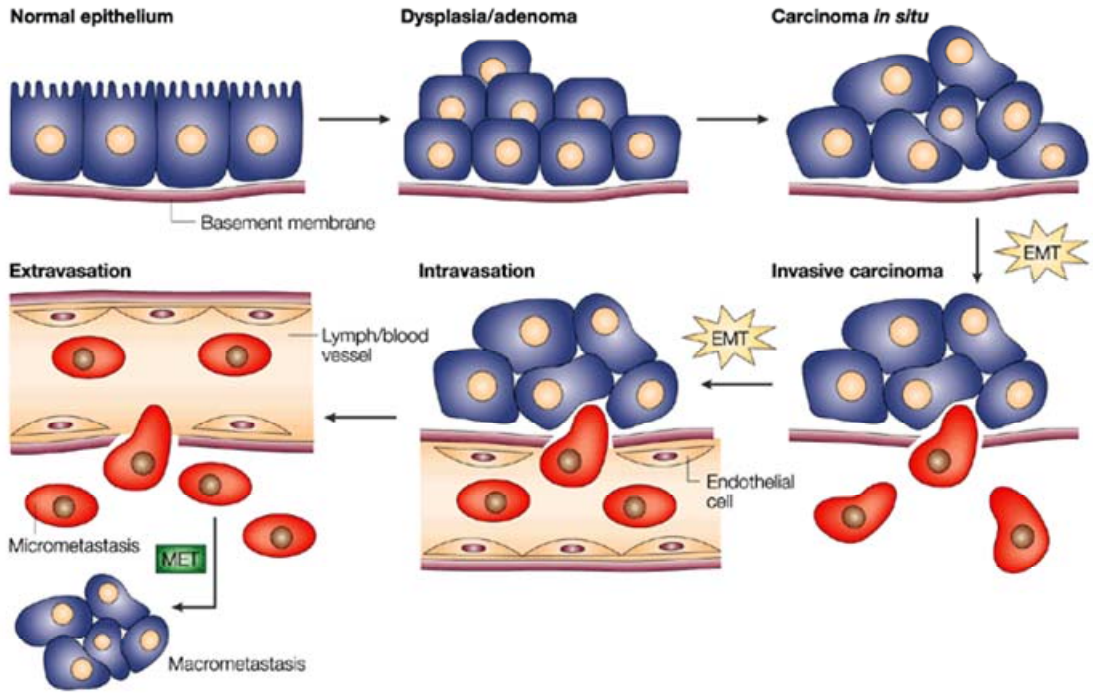

Figure 1.4 Epithelial to mesenchymal transition in cancer progression (Thiery 2002).

1.6 E-cadherin as a downstream effector in epithelial to mesenchymal transition

It is unavoidable to notice the protein E-cadherin if one mentions EMT. E-cadherin is a central adhesion molecule located at cell-cell junctions and is essential for formation and maintenance of epithelium phenotype. Loss of E-cadherin expression is considered a crucial step in the progression from benign to invasive carcinoma (Perl, Wilgenbus et al. 1998). This is a fundamental event in EMT. The reduction of cell adhesion between carcinoma cells facilitates their ability to migrate individually and invade their surroundings. Much effort has been devoted to understanding how E-cadherin is regulated during cancer progression. The E-cadherin promoter is frequently regulated by two ways: direct or indirect repression by transcription factors. Transcription factors such as Snail, Zeb, E47, and KLF8 physically bind to and repress E-cadherin promoter activity, whereas Twist, Goosecoid and FOXC2 inhibit E-cadherin transcription activity indirectly (Kang and Massague 2004; Hartwell, Muir et al. 2006; Mani, Yang et al. 2007; Peinado, Olmeda et al. 2007; Ray, Wang et al. 2010). I will proceed to discuss how E-cadherin is regulated by these individual factors.

1.6.1 TGF-β signaling

TGF-β is a regulatory cytokine whose members regulate organism development. TGF-β evolved to regulate the expanding systems of epithelial and neural tissues, the immune system, and wound repair. The consequence of malfunction of TGF-β signaling pathway can result in tumorigenesis.

TGF-β signaling regulates tumorigenesis and in human cancer its signaling pathways are often altered during tumor progression. Prior to initiation and in the early stages of cancer progression, TGF-β acts upon the epithelium as a tumor suppressor. However, at later stages, it is often a tumor promoter. In normal and premalignant cells, TGF-β enforces homeostasis and suppresses tumor progression directly through cell-autonomous tumor-suppressive effects (cytostasis, differentiation, apoptosis) or indirectly through effects on the stroma (suppression of inflammation and stroma-derived mitogens). However, when cancer cells lose TGF-β tumor-suppressive responses, they can use TGF-β to their advantage to initiate immune evasion, growth factor production, differentiation into an invasive phenotype, and metastatic dissemination or to establish and expand metastatic colonies. There are two major ways that TGF-β can lose its suppressive function: one is mutation of TGF-β receptors such as TGFBRII mutation in colorectal, ovarian, and head and neck cancers; two is downstream alteration of suppressive arms such as defective cytostatic responses in breast cancer and glioma (Pasche, Knobloch et al. 2005; Antony, Nair et al. 2010; Bellam and Pasche 2010; Moore-Smith and Pasche 2011).

The TGF-β ligands (TGF-β1, TGF-β2 and TGF-β3), receptors and downstream signaling components have been the subject of a large number of studies involving cancer over the past two decades. In cancer, TGF-β1 is upregulated to a greater extent than either TGF-β2 or TGF-β3, and as a result TGF-β1 has been the focus for most of the cancer related studies to date. TGF-β1 is a pleiotropic factor that plays a physiological role in regulating proliferation, differentiation, development, wound

healing, and angiogenesis. In early neoplasia, TGF-β1 can be a potent suppressor of proliferation (Roberts and Wakefield 2003). Conversely, TGF-β1 can promote the migration and proliferation of tumor cells in late-stage metastatic cancer (Gold 1999; Lu, Reh et al. 2004). TGF-β1 signals by first binding to TGF-β1 type II receptor (TGFBR2), which then recruits the TGF-β1 type I receptor (TGFBR1) to form a heterodimer serine/threonine kinase complex. This activated heterodimeric complex transphosphorylates TGFBR1 and enables TGFBR1 to directly phosphorylate 2 carboxyterminal serines on Smad2 and Smad3, leading to activation of these transcription factors (Derynck and Zhang 2003). Smad2 or Smad3 dimerizes with Smad4 and translocate to the nucleus, where the activated complexes associate with Smad-binding elements in promoters of numerous genes (Lagna, Hata et al. 1996; Heldin, Miyazono et al. 1997; Liu, Pouponnot et al. 1997). In human cancer, TGFBR2 is often mutated and these conserved mutations in a large percentage of cases led to pathway inactivation (Grady, Myeroff et al. 1999). TGFBR2 mutations occur frequently in colon cancer, gastric, glioma, non-small cell lung cancer and pancreatic cancer (Akhurst and Derynck 2001).

Colon cancer develops as a result of uncontrolled cellular proliferation and dysregulation of cell death mechanisms. Inactivation of TGF superfamily signaling appears to play a key role too. Inactivation of TGF signaling occurs in about 80% of colon cancer (Grady, Rajput et al. 1998). HCT116 cells are deficient in DNA mismatch repair and TGFBR2 (Veigl, Kasturi et al. 1998). In response to TGF-β1, the biochemistry of cancer cells can change and transit towards a metastatic phenotype (Muraoka, Dumont et al. 2002). Some epithelial cells may adopt a mesenchymal phenotype, which is termed EMT (Zavadil and Bottinger 2005).

1.6.2 The Snail family of gene repressors

Snail family members encode zinc-finger transcription factors that are essential for mesoderm formation in several organisms, from flies to mammals (Nieto 2002). The Snail family has emerged in recent years as an important regulator of EMT, a process that occurs at defined stages of embryonic development and during cancer progression. In vertebrate, the Snail family contains two important members namely Snail and Slug. They have now been firmly established as repressors of E-cadherin, one of the key molecules in the EMT process, both in early development and in different murine and human carcinoma and melanoma cell lines and tumors (Batlle, Sancho et al. 2000; Cano, Perez-Moreno et al. 2000; Hajra, Chen et al. 2002; Thiery 2002; Bolos, Peinado et al. 2003). The transcriptional repression of Snail and Slug occurs through binding to the consensus gene sequence of six bases CAGGTG to E-box to exert the transcriptional repressor function. The importance of Snail in triggering EMT in mammals is its ability to convert normal epithelial cells into mesenchymal cells through direct repression of E-cadherin expression by binding to the E-box of the E-cadherin gene promoter region (Cano, Perez-Moreno et al. 2000). During cancer development, however, additional target genes are most likely required to assist the role of Snail in cell migration and cancer development, such as the recently identified mucin-1, collagen IIa1 or MMP-2 (matrix metalloproteinase-2) genes (Guaita, Puig et al. 2002; Seki, Fujimori et al. 2003; Yokoyama, Kamata et al. 2003). Recently, it has also been shown that Snail is able to repress the expression of the tight junction proteins Claudin-3, -4, -7 and Occludin (Ikenouchi, Matsuda et al. 2003).

1.6.3 Twist family

Twist family belong to the larger family of basic Helix-Loop-Helix (bHLH) transcription factors originally found to modulate the expression of various target genes through canonical E-box responsive elements of consensus sequence NCANNTGN (Ellenberger, Fass et al. 1994; Lee, Park et al. 1997; Yin, Xu et al. 1997). In vertebrates, two Twist genes exist, namely Twist1 and Twist2. The Twist proteins display a high degree of sequence similarity in their C-terminal half, including the bHLH domain and a 'TWIST-box' protein interaction surface but are more divergent in their N-terminus (Li, Cserjesi et al. 1995; Bialek, Kern et al. 2004). Twist proteins can behave either as transcriptional repressors, recruiting histone deacetylases or inhibiting acetyl-transferases, or as transcriptional activators (Hamamori, Sartorelli et al. 1999; Gong and Li 2002; Pan, Fujimoto et al. 2009). Both Twist genes were found to be overexpressed in a large set of human and murine tumors including a variety of carcinoma as well as sarcomas, melanomas, gliomas and neuroblastomas (Puisieux, Valsesia-Wittmann et al. 2006; Ansieau, Bastid et al. 2008). Twist1 expression was found to correlate with metastatic potential in murine cell lines. In lung cancer progression, Twist1 depletion prevents metastasis without affecting primary tumor formation, hence suggesting that Twist1 specifically contributes to late cancer cell dissemination (Yang, Mani et al. 2004). This potential was suggested to depend on the ability of Twist1 to induce EMT and thereby promote motility, reminiscent of its embryonic biological properties. E-cadherin, encoded by the CDH1 gene, is generally defined as a guardian of the epithelium phenotype and loss of its expression is associated with tumor invasiveness, metastatic dissemination and poor patient prognosis (Schipper, Frixen et al. 1991; Oka, Shiozaki et al. 1993; Umbas,

Isaacs et al. 1994). Repression of CDH1 gene by Twist is directly through transcriptional repression which may require Twist stabilization through heterodimmerization, potentially in response to environmental signals. This gives a rational to the detection of Twist-positive, E-cadherin-negative cells at the invading fronts of malignant parathyroid tumor (Fendrich, Waldmann et al. 2009). Interestingly, Twist was found to be activated following loss of E-cadherin expression (Onder, Gupta et al. 2008), raising the possibility that Twist contributed to EMT induction by inducing the expression of mesenchymal genes rather than repressing CDH1. Accordingly, a correlation between VIM, CDH2 and TWIST gene expressions was also observed in breast cancer cell lines (Lombaerts, van Wezel et al. 2006).

In addition, Twist protein can override oncogene-induced senescence and apoptosis which are the natural barriers activated to constrain cell growth in pre-malignant lesions (Braig, Lee et al. 2005; Collado, Gil et al. 2005). By inhibiting both senescence and apoptotic programs, Twist proteins are suggested to promote malignant conversion and to provide cell with a growth advantage at the primary site. Accordingly, several studies reported the induction of Twist1 expression during the progression towards malignant stage in several cancer types including ovary, prostate, bladder, pancreas and hepatic carcinoma as well as melanomas and pheochromocytomas (Kwok, Ling et al. 2007; Ansieau, Bastid et al. 2008; Waldmann, Slater et al. 2009; Yoshida, Horiuchi et al. 2009). Associated-EMT might also contribute to Twist-induced chemoresistance. Growing evidence indeed support the assumption that EMT is as a transient state providing cells with higher stress tolerance threshold and could thereby constitute an escape route away from apoptosis. In vitro, oxaliplatin-resistant colorectal cancer cells, tamoxifen-resistant breast cancer cells,

gefintinib-resistant lung cancer cells as well as gemcitabine-resistant pancreatic cancer cells have all been shown to have undergone EMT (Hiscox, Jiang et al. 2006; Yang, Fan et al. 2006; Rho, Choi et al. 2009; Franco, Casasnovas et al. 2010). Twist acts upstream of Snail, Zeb1 acts downstream of Twist and Snail (Guaita, Puig et al. 2002).

1.6.4 Zeb1 and Zeb2

Zeb1 (also known as TCF8 and δEF1) and Zeb2 (also known as ZFXH1B and SMAD interacting protein 1), are two members of the ZEB family. Zeb factors (Zeb1 and Zeb2, encoded by the ZFHX1a and ZFHX1b genes) are transcriptional repressors that comprise two widely separated clusters of C_2H_2-type zinc fingers binding to paired CAGGTA/G E-box-like promoter elements. They induce EMT by suppressing the expression of many epithelial genes, including E-cadherin (Vandewalle, Van Roy et al. 2009). Zeb1 expression has mainly been studied in colorectal tumors and uterine cancers, where it was associated with aggressive behavior. Zeb2 has higher expression pattern in ovarian carcinoma effusions than in solid metastases (Aigner, Dampier et al. 2007; Spaderna, Schmalhofer et al. 2008; Yoshihara, Tajima et al. 2009).

1.6.5 Goosecoid

Goosecoid (Gsc) gene, which encodes a well conserved transcription factor that was first identified as the most highly expressed homeobox gene in the Spemann organizer. Gsc can recapitulate many of the properties of the organizer when ectopically

expressed in the amphibian embryo and is known to promote cell migration in xenopus laevis. Moreover, elements of the TGF-β superfamily and Wnt/β-catenin signaling pathways, which are known to be involved in tumor invasion and metastasis, can induce Gsc expression in embryonic cells and are required for Spemann organizer formation (Nakaya, Murakami et al. 2008).

Recently, Hartwell and team extend Gsc functional study in human breasts (Hartwell, Muir et al. 2006). They found that Gsc expression was elevated in three prevalent pathological types of human breast tumors which are atypical ductal hyperplasia (ADH), ductal carcinoma in situ (DCIS), and invasion ductal carcinoma (IDC). Ectopic expression of Gsc in immortalized human mammary epithelial cells (HMECs) and in Madin-Darby canine kidney (MDCK) epithelial cells induced epithelial to mesenchymal transition and enhanced cell motility. In addition, Gsc is induced in TGF-β signaling pathway in adult breast epithelial cells. Ectopic expression of Gsc in MDA-MB-231 human breast cancer cells enhance the lung metastatic ability of these cells.

1.6.6 Other molecules promoting EMT

Recently, a large amount of research articles identified several novel molecules in regulating EMT. In breast carcinoma, forkhead factor FOXC1 and FOXC2 were shown to positively regulate EMT in human mammary epithelial cells, and also participated in the metastatic process of aggressive breast cancer (Mani, Yang et al. 2007; Ray, Wang et al. 2010). In mammary epithelial cells, overexpression of LBX1 (Ladybird homeobox 1), a developmentally regulated homeobox gene, led to EMT

with morphological transformation, expression of mesenchymal markers, enhanced cell migration, increased CD44+/CD24- progenitor cell population, and tumorigenic cooperation with known oncogenes. In human breast cancer, LBX1 upregulation is associated with basal-like subtype (Yu, Smolen et al. 2009).

1.7 Forkhead box transcription factor family

Forkhead box transcription factor family is evolutionary conserved and share a common 110-amino acid DNA-binding domain (DBD) termed forkhead or winged helix domain. The forkhead gene was first identified in Drosophila melanogaster where mutation in this gene gave rise to two spiked-head structures in the embryos of Drosophila. Results of this mutation led to a defect in the formation of the anterior and posterior gut. In addition, the forkhead DNA-binding domain was previously referred to as hepatocyte nuclear factor 3 α (HNF3α) in mammals (Weigel, Jurgens et al. 1989; Lai, Prezioso et al. 1990; Clark, Halay et al. 1993).

After the first forkhead box member was discovered more than 20 years ago, a large number of forkhead gene families were subsequently identified. In order to streamline the nomenclature for the forkhead transcription factor family, an international conference was held in California, and a forkhead nomenclature committee was set up to standardize the nomenclature for these forkhead proteins. The name of 'Fox' which was adapted from 'forkhead box' was agreed upon and used to unify these proteins. Finally in the year 2000, Kaestner and colleagues finished the nomenclature of forkhead transcription factors. It provided an comprehensive and convenient classification for subsequent research in this area (Kaestner, Knochel et al. 2000).

They established a Fox nomenclature web site that provided the latest nomenclature for forkhead box family (http://www.biology.pomona.edu/fox.html).

As more and more forkhead factors were identified, some of them show functions in tumorigenesis, epithelial to mesenchymal transition, angiogenesis and apoptosis. In spite of the highly conserved DNA-binding domain, biological functions amongst this family display a large diversity. I shall be introducing several well-studied forkhead members especially relating to their functions in cancer.

1.7.1 FOXC1 and FOXC2

FOXC1 shares 85% homology with FOXC2, and similar functional roles in breast cancer progression. In particular, FOXC2 expression is necessary for metastasis of murine mammary carcinoma cells to the lung. Also, FOXC2 expression is upregulated following trigger by EMT signaling, and FOXC2 expression levels correlated positively with aggression levels of basal-like human breast cancers, hence suggesting that FOXC2 could be a specific molecular marker for this type of cancer (Mani, Yang et al. 2007). Moreover, in aggressive basal-like breast cancer subtype, FOXC1 was shown to be consistently overexpressed and its overexpression correlated with poorer overall survival, higher incidence of brain metastasis and shorter brain metastasis-free survival in lymph node-negative patients. Biologically, FOXC1 promotes cancer cell proliferation, migration and invasion. Clinically, FOXC1 maybe useful as a potential prognostic marker and a molecular therapeutic target in the treatment of patients with basal-like breast cancers (Ray, Wang et al. 2010).

However, FOXC2 is not always coupled with promoting epithelial to mesenchymal transition. Endogenous FOXC2 expression in injured renal tubular cells was increased in the cytoplasm rather than in the nucleus, and elevated FOXC2 further activated epithelial cell differentiation during tissue repair. These findings suggested that FOXC2 may have novel functions besides nuclear transcriptional activity (Hader, Marlier et al. 2009). Both FOXC1 and FOXC2 have overlapping expression patterns and similar regulatory functions in mesoderm and neural crest derivatives during development. Other studies indicated that FOXC1 and FOXC2 were involved in cardiovascular development particularly arterial cell specification, lymphatic vessel formation, angiogenesis and cardiac outflow tract development (Seo, Fujita et al. 2006; Hayashi and Kume 2008; Kume 2009).

1.7.2 FOXM1

FOXM1 has a very important role in cellular development pathway including the maintenance of homeostasis between cell proliferation and apoptosis. Deregulated FOXM1 inhibits differentiation and finally lead undifferentiated cells towards malignant transformation. In many human malignancies, FOXM1 expression level is upregulated and is often linked to malfunction of this transcription factor. These malignancies include prostate cancer, basal cell carcinoma, hepatocellular carcinoma, lung cancer, glioblastoma, primary breast cancer, and pancreatic cancer. In molecular basis, FOXM1 is associated with multiple oncogenic pathways including PI3K/Akt signalling, NF-κB signalling, EGFR signalling, Raf/MEK/MAPK, ERK, sonic hedgehog signalling, estrogen receptor signalling, cyclooxygenase (COX2) pathway, MMP, reactive oxygen species (ROS), vascular endothelial growth factor, c-Myc, p53,

HIF-1, and proteasome pathway. Generally, FOXM1 participate in many oncogenic pathways in cancer cells with poor outcome. Hence, inactivation of FOXM1 as a novel therapeutic approach would have a significant impact for cancer therapy (Wang, Ahmad et al. 2009).

FOXM1 has been reported to contribute to acute myeloid leukaemia (AML) cell proliferation. Aberrant FOXM1 expression results in AML cell proliferation through cell cycle progression while reduce FOXM1 expression in AML inhibits cell proliferation and colony formation. These findings suggested that FOXM1 could be a therapeutic target for AML treatment (Nakamura, Hirano et al. 2010). FOXM1 overexpression in majority of human cancers suggested that FOXM1 may have functions in initiation of human tumorigenesis. Recently, this hypothesis was supported by observations that FOXM1 participated in early oncogenic pathways by expanding the number of stem/progenitor cells in the epithelial compartment, and inhibiting keratinocyte terminal differentiation. These findings may provide the basis for designing therapy to target tumorigenesis at its initiation stage (Gemenetzidis, Elena-Costea et al. 2010). FOXM1 regulates normal lung morphogenesis as well as development of lung cancer, and increased FOXM1 activity resulted in altered lung sacculation, and increased proliferation in the respiratory epithelium and accelerated lung tumor growth (Wang, Zhang et al. 2010).

FOXM1 is involved in maintenance of stem cell pluripotency. In P19 cells (embryonal carcinoma cell line), FOXM1 was found to regulate Oct4 and knockdown of FOXM1 caused P19 cells to differentiate into mesodermal derivatives, such as muscle and adipose tissues. Maintaining FOXM1 expression in P19 cells prevented

down-regulation of pluripotency-related transcription factors such as Oct4 and Nanog during cell differentiation. Ectopic expression of FOXM1 in retinoic acid-differentiated P19 cells reinstated the expression of Oct4, Nanog and Sox2. These results suggested that FOXM1 plays a critical role in maintenance of stem cell pluripotency (Xie, Tan et al. 2010). FOXM1 is essential for endothelial proliferation after vascular injury and it regulates endothelial barrier reformation through direct regulation of β-catenin transcription. These findings represented a new therapeutic idea for treatment of inflammatory vascular disease associated with persistent vascular barrier leakiness, such as acute lung injury (Mirza, Sun et al. 2010). In breast cancer cells, overexpression of FOXM1 resulted in resistance to Herceptin (human epidermal growth factor receptor 2 monoclonal antibody) and paclitaxel. Inhibition of FOXM1 expression may relieve therapeutic resistance in breast cancer and should be seen as a target for cancer therapy (Carr, Park et al. 2010).

1.7.3 FOXF1

FOXF1 expression is up-regulated in tumors with a constitutively activated Hedgehog signaling pathway (Wendling, Luck et al. 2008). In the study of expression profile of normal prostate and diseased prostate, FOXF1 and FOXF2 were highly expressed in the normal prostate transition zone and benign prostatic hyperplasis (BPH), but decreased in prostate cancer (van der Heul-Nieuwenhuijsen, Dits et al. 2009).

In breast cancer, the transcription factor nuclear factor 1-C2 (NF1-C2) is a negative regulator of EMT, motility, invasiveness and tumor growth. NF1-C2 directly represses FOXF1, its downstream target. Hence, FOXF1 positively regulates to

promote mesenchymal phenotype, invasion and metastasis in breast cancer (Nilsson, Helou et al. 2010). However in some breast cancer, FOXF1 is epigenetically silenced by promoter methylation. Pharmacologic approach can restore FOXF1 expression and result in cell growth arrest in vitro and in vivo. This suggests that FOXF1 is a potential tumor suppressor in breast cancer (Lo, Lee et al. 2010). In lung cancer FOXF1 regulates tumor-promoting properties of cancer-associated fibroblasts (Saito, Micke et al. 2010).

1.7.4 FOXO family

Among the different subclasses of FOX genes, FOXO subfamily is one of the largest. This subfamily contains four members (FOXO1, FOXO3, FOXO4 and FOXO6). Functions include activation or repression of multiple genes such as Bim and FasL in apoptosis process, $p27^{kip}$ and cyclin D in cell cycle regression, DADD45a in DNA damage repair, response to superoxide induced stress and glucose-6-phosphatase in metabolism (Weidinger, Krause et al. 2008; Yang and Hung 2009).

FOXO activity is controlled at both the transcriptional and posttranscriptional levels. FOXO1 and FOXO3a were reported lately to be transcriptionally controlled by E2F1 through binding to FOXO1 and FOXO3a promoter. In human glioblastoma cells, E2F1 promotes the transcription of FOXO1 and FOXO3a in vitro. The activity of FOXO is also controlled by posttranscriptional regulation including phosphorylation, acethylation and uniquitination, which provides evidence that forkhead members can be regulated through posttranscriptional modification (Nowak, Killmer et al. 2007).

The ability of FOXO to control cell survival and cell death suggests that FOXO may function as tumor suppressors, and loss of FOXO function has been observed in a number of human cancers. The loss of function maybe due to genetic defects and altered posttranslational modification. Several genetic defects were observed in human cancers. In human alveolar rhabdomyo-sarcoma FOXO1 C-terminal domain is fused with the N-terminal domain of PAX3 or PAX7. This resulted in activation of transcription function to promote cell proliferation. The function of FOXO can also be lost. In PI3K/Akt cascade, tumor suppressor phosphatase PTEN could become lost due to genetic mutation. The decreased expression can lead to perpetual Akt activation. As a result, FOXO1 and FOXO3a are phoshorylated and translocate from nucleus into cytosol to abolish their inhibition of cell proliferation. Functionally impaired FOXO in cancer also can be found in other signaling pathways including NF-κB and RAS/ERK pathways. Again, FOXO can be a potential therapeutic target for cancer treatment (Weidinger, Krause et al. 2008; Yang and Hung 2009).

1.7.5 FOXA1 and FOXA2

FOXA1 is identified in breast, prostate and aggressive thyroid cancer (Nakshatri and Badve 2007; Nucera, Eeckhoute et al. 2009; Hu and Mackenzie 2010). FOXA1 is a marker of luminal cells in mammary gland and is associated with luminal type A (ER+) breast cancers. FOXA1 is a lineage-specific oncogene in proliferation of mammary cancer cells and could be a good candidate for prognosis (Badve, Turbin et al. 2007; Habashy, Powe et al. 2008; Thorat, Marchio et al. 2008; Yamaguchi, Ito et al. 2008; Albergaria, Paredes et al. 2009; Bernardo, Lozada et al. 2010; Liu, Niu et al. 2010). FOXA1 is expressed in epithelia of the prostate gland and regulates the

transcription of prostate-specific genes. FOXA1 negatively regulates androgen receptor by physical interaction with the receptor (Yu, Gupta et al. 2005; Mirosevich, Gao et al. 2006; Sun, Yu et al. 2009).

FOXA2 is expressed in many types of lung tumors including typical/atypical carcinoid, large cell NE carcinoma, small cell carcinoma, and adenocarcinoma, but not squamous cell carcinoma and (non-NE) large cell carcinoma (Khoor, Stahlman et al. 2004). In aggressive prostate cancer, FOXA2 forms a transcriptional complex with ubiquitin ligase Siah2 and HIF-1α to promote a transcriptional program to induce Hes6, Sox9 and Jmjd1a to facilitate the formation of aggressive prostate tumors (Qi, Nakayama et al. 2010). In human lung cancer cell lines, FOXA2 negatively regulate epithelial to mensenchymal transition through inhibition of slug expression by direct binding to slug promoter (Tang, Shu et al. 2010). In human pancreatic ductal adenocarcinoma, FOXA1 and FOXA2 expression occurred specifically in epithelial and well-differentiated cancer cells, but expression were lost in undifferentiated cancer cells. Ectopic expression of FOXA1 and FOXA2 is sufficient to reverse EMT phenotype by reactivating E-cadherin expression. In pancreatic ductal adenocarcinoma, suppression of FOXA1 and FOXA2 expression contributed to malignant progression (Song, Washington et al. 2010). In epithelial ovarian carcinoma, FOXA2 is downregulated in chemoresistant tumors (Ju, Yoo et al. 2009). In human embryonic stem cells overexpression of FOXA2 induced differentiation into pancreatic cells (Lavon, Yanuka et al. 2006).

1.7.6 FOXP1 and FOXP3

FOXP1 is widely expressed in cardiac, lung and lymphocytic cells. FOXP1 may function as an oncogene or a tumor suppressor depending on the cell type. FOXP1 locates on 3p14 where many tumor suppressor genes are also found to be localised in various cancers. Loss of FOXP1 in breast cancers is associated with worse outcome, and hence, FOXP1 was suggested to function as a tumor suppressor. FOXP1 possibly serve as a tumor suppressor in gastrointestinal, lung, head, breast and neck cancers, and also genitourinary malignancies. However, FOXP1 function as oncogene in diffuse large B-cell lymphoma and mucosal associated lymphoid tissue lymphoma (Koon, Ippolito et al. 2007).

FOXP3 expression is not only restricted to the lymphocyte lineage but also expressed in non-hematopoietic cells and cancer cells of a non-hematopietic origin. It seems that FOXP3 has roles in carcinogenesis and immune response in these different cell types. In prostate and breast cancers, downregulation of FOXP3 is associated with HER2 and SKP2 (S-phase kinase-associated protein 2) or c-MYC overexpression. This suggest that FOXP3 may act as a tumor suppressor in prostate and breast cancers (Martin, Ladoire et al. 2010).

1.7.7 FOXG1

FOXG1 acts as an oncoprotein inhibiting TGF-β-mediated anti-proliferative responses in ovarian cancer cells through suppression of $p21^{(WAF1/CIP1)}$ transcription (Chan, Liu et al. 2009). In addition, FOXG1 has oncogenic potential through modulating FOXO1 expression by acting as a transcriptional repressor (Kim, Jo et al.

2009). In cells of hepatoblastoma, FOXG1 overexpression may contribute to the maintenance of the undifferentiated state and could be a potential target for molecular therapeutics (Adesina, Nguyen et al. 2007).

1.7.8 FOXQ1

FOXQ1 (Forkhead box, subclass q, member 1) was previously known as hepatocyte nuclear factor 3 forkhead homolog 1 (HFH1) before the unified nomenclature. FOXQ1 was first mapped in murine autosome (Avraham, Fletcher et al. 1995). Murine FOXQ1 is a 2.7kb transcript in the adult kidney and stomach and was later revealed that it was most likely intronless and located within chromosome 13. The gene expression pattern was examined and results suggested that FOXQ1 gene is involved in the development of kidney in mice (Frank and Zoll 1998). Other laboratories reported that FOXQ1 mRNA expression is highest in stomach and bladder, especially in epithelial cells. The expression of FOXQ1 strongly repressed telokin promoter activity in A10 vascular smooth muscle cells by binding to the forkhead consensus sequence located within an AT-rich region of telokin promoter. Also FOXQ1 is able to repress other smooth muscle-specific promoter such as SM22α promoter (Hoggatt, Kriegel et al. 2000). FOXQ1 is involved in hair differentiation in Satin mice. Satin (Sa) homozygous mice carry a silky coat with high sheen because of the structurally abnormal medulla cells and defects in differentiation of hair shaft. This phenotype arises from FOXQ1 mutation in Sa mice, which suggested that FOXQ1 displayed a function in differentiation and development of hair shaft (Hong, Noveroske et al. 2001). Further study demonstrated that mice carrying a homozygous deletion of FOXQ1 developed a silky shiny coat and a defect in gastric

acid secretion even when exposed to secretagogue stimuli (Goering, Adham et al. 2008). FOXQ1 has been suggested to be a downstream mediator of Hoxa1 in embryonic stem cells and shown to be regulated by Hoxc13 during hair follicle development (Martinez-Ceballos, Chambon et al. 2005; Potter, Peterson et al. 2006).

FOXQ1 is predominantly expressed in the abundant mucin-producing cells called fovelar or pit cells that line the stomach's mucosal surface. Defective FOXQ1 in the stomach resulted in lose of mRNA and protein expression of gastric MUC5AC synthesis. These findings suggested that a function of FOXQ1 is in promoting major stomach mucin MUC5AC formation (Verzi, Khan et al. 2008). The functions of FOXQ1 in mouse mammary gland cell line NMuMG was lately revealed. In this heterogeneous epithelial cell line, FOXQ1 was found to be transcriptionally up-regulated in response to TGF-β1 signalling. They further utilized the morphological homologous subclone of NMuMG cell line (NM18) to demonstrate that FOXQ1 has a functional impact on epithelial differentiation (Feuerborn, Srivastava et al. 2011).

The human FOXQ1 gene was finally isolated and characterized by Bieller in 2001. They found that the human FOXQ1 gene is located on chromosome 6p23-25 and encodes a protein of 403 amino acids. The human FOXQ1 gene was expressed predominantly in the stomach, trachea, bladder and salivary gland. Additionally, the expression status of FOXQ1 in colorectal adenocarcinoma and lung carcinoma cell lines were very high. There is 82% homology between mouse and human FOXQ1 with an updated rat FOXQ1 gene. The DNA-binding motif is extremely conserved whether in humans, mice or rats. The putative trans-activation domain of human

FOXQ1 shares a high degree of similarity in amino acid sequences with murine in matching domains (Bieller, Pasche et al. 2001).

In addition to its role in development, FOXQ1 was identified to be expressed in 36% (5 out of 14) of pancreatic cancer cell lines via bioinformatic analysis of microarray assays using expressed sequence tags. These findings suggested that FOXQ1 might contribute to pancreatic cancer development (Cao, Hustinx et al. 2004). Recently, FOXQ1 was reported to be overexpressed in human colorectal cancer which is similar to my own observations. In their study, they have identified that p21 is one of the downstream targets of FOXQ1, and overexpression of FOXQ1 in lung carcinoma cell line H1299 have increased tumorigenicity. Furthermore, the increased tumorigenicity is independent of p21 levels. In addition, they found that overexpression of FOXQ1 in H1299 cells resulted in reduced apoptotic signal in response to adriamycin (doxorubicin) treatment. They also showed that FOXQ1 promoted angiogenesis in tumor growth. The above results are quite consistent and in parallel with my own findings (Kaneda, Arao et al. 2010).

1.8 Study objectives and rationale

My aim in this study is to discover new biological roles of FOXQ1 in human cancers (breast and colorectal cancers), and to delineate underlying molecular mechanism associated with observed phenotypes. Before this study, FOXQ1 was a novel member of the forkhead family and not linked to any published functional reports relating to cancer. In view of the expressed status of FOXQ1 in basal-like breast cancer and most of colorectal cancers discovered at the start of this project, my starting hypothesis is FOXQ1 has an oncogenic role to play. Other forkhead members such as FOXC1 and FOXC2 were recently reported to influence basal-like breast cancer progression through promotion of EMT during invasion and metastasis. In this study, my hypothesis is FOXQ1 may have similar function roles in cancer progression. The principle strategy in this project uses an ectopic expression system and RNAi knockdown system to study FOXQ1 in human cancer cells and immortalized epithelial cell lines. Furthermore, the transcriptional network modulated by FOXQ1 will be dissected in both breast and colorectal cancer cells.

CHAPTER 2:

MATERIALS AND METHODS

2.1 Cell lines

The cell lines used in this study were purchased from American Type Culture Collection (Manassas, VA) unless otherwise stated. Colorectal cancer cell lines include HCT116, SW480, SW620, HT29, HT15 and DLD1; breast cancer cell lines include MCF7, T47D, MDA-MB-361, MDA-MB-415, BT549, BT474, SKBR3, MDA-MB-468, MDA-MB-436 and MDA-MB-231; other epithelial-like cell lines include SAOS2, U2OS, and A549. Non-cancerous human mammary epithelial cell lines include MCF10A, HMEC (human mammary epithelial cell immortalized with hTERT), and HMLER (HMEC cells further transfected with SV40 LT and H-Ras). HMLER cells were a generous gift from Dr. W.C. Hahn of Dana-Farber Cancer Institute.

2.2 Cell culture conditions

MCF10A, HMEC and HMLER were cultured in DMEM/F12 medium supplemented with 5% horse serum, 1% penicillin and streptomycin (PS), 20 ng/ml epidermal growth factor (EGF) (PeproTech, NJ), 0.5 mg/ml hydrocortisone (cat#H0888, Sigma-Aldrich), 100 ng/ml cholera toxin (cat#C8052, Sigma-Aldrich), and 10 μg/ml insulin (cat#I1882, Sigma-Aldrich). All other cell lines were maintained in DMEM supplemented with 10% fetal bovine serum (FBS) and 1% PS. In Tet-on inducible system, Tet system approved FBS was used (Clontech, Mountain View, CA) to replace normal FBS. All cell lines were maintained in logarithmic growth as a monolayer in 75 cm^2 flask at 37ºC in a humidified atmosphere containing 5% CO_2. Cell lines were regularly subcultured when cell density reached 80-90% confluence. Subculture procedure began with aspiration of existing culture medium followed by

rinsing with phosphate buffer saline (PBS) once, and then incubated with 0.25% trypsin in PBS with 0.02% (w/v) EDTA. After incubation at 37ºC for 5-10 minutes, the cells will detach from the flask. The detached cells were transferred into a fresh 15 ml tube with 5 ml culture medium. Cells were collected by centrifuge at 1000 rpm for 4 minutes, and then cell pellets were suspended in 10 ml fresh culture medium. 30% of the cell suspension was seeded into 75 cm^2 flask. All cell culture process and materials were carried out under sterile conditions. All cell culture materials were purchased from Invitrogen (Carlsbad, CA) unless otherwise stated.

2.3 Cryogenic preservation

All experiments have been done using cell lines that were passaged less than 20 times. Hence, the cell lines were frozen down regularly. The freezing progress is described below. Cells were harvested as usual, and then suspended in specific medium containing 90% culture medium and 10% DMSO for MCF10A, HMEC, and HMLER cell lines. The rest of cell lines were frozen down using 90% FBS together with 10% DMSO. The density of frozen cells was about 1×10^6 cells/ml, and cryovials were placed into Mr. Frosty freezing container (NALGENE, NUNC) at -80ºC overnight, and then transferred to liquid nitrogen for longer storage. To thaw frozen cells from cryo-preservated condition, cryovial was removed from liquid nitrogen and quickly thawed in 37ºC water bath. The cell suspensions were then neutralized by adding pre-warmed culture medium and centrifuged at 1000 rpm for 4 minutes. Cells were finally re-suspended in fresh medium and seeded into 25 cm^2 flask.

2.4 Drugs

5-Flurouracil (5FU), paclitaxel (Taxol), camptothecin (CPT), adriamycin (ADR), 4-hydroxytamoxifen (OHT) and doxycycline (DOX) were purchased from Sigma-Aldrich (St. Louis, MO). HDAC inhibitor suberoylanilide hydroxamic acid (SAHA) was purchased from Enzo Life Science. 5FU, Taxol, ADR, and SAHA were dissolved in DMSO in concentrations of 375 mM, 10 mM, 10 mM, and 10 mM, respectively. CPT and DOX were dissolved in MilliQ water filtered by Millipore and sterilized by passage through 0.2 μm filter unit (Millipore, Singapore). Concentrations were 10 mM and 1 mg/ml respectively. CPT was freshly prepared every two weeks. All drugs were stored at -20ºC in 50 μl aliquots.

2.5 Expression plasmid construction and molecular cloning procedure

Full-length FOXQ1 coding region containing 1212 base pairs (bp) was downloaded from NCBI database (http://www.ncbi.nlm.nih.gov). The forward and reverse primers were designed by Vector NTI advance 10.3.0 software (Invitrogen) with Kpn I and EcoR I restriction enzyme sites at 5' and 3' respectively. Normal colon tissue cDNA was used as the template, and FOXQ1 fragment was isolated by PCR program based on the manufacturer's instruction of FailSafe^{TM} PCR system (EPICENTRE Biotechnologies). The size of PCR product was subsequently verified using DNA agarose gel electrophoresis. The DNA fragment was viewed under ultra-violet light, and the correct band was excised and then subjected to gel extraction and the DNA fragment was eluted into 30 μl RNAse-free water.

TOPO TA cloning was carried out to ligate gel purified FOXQ1 fragment into the TOPO2.1 vector (Figure 2.1). In detail, 4 µl FOXQ1 fragment was mixed with 1 µl TOPO2.1 vector and 1 µl salt solution and the mixture was incubated for 15 minutes at room temperature. Volume ranging from 2 to 3 µl of ligated product was used in transformation into One Shot® TOP10 chemically competent *E. coli* cells according to manufacturer's instruction (Invitrogen). The cultured bacteria were spread and incubated overnight at 37ºC on the LB agar plate containing 100 µg/ml ampicillin and 80 µl of 20 mg/ml X-gal (cat#R0941, Fermentas) for growing single colonies. Positive clones appeared white while negative clones appeared blue. Positive clones were amplified and plasmid DNA was eluted into 30 µl RNAse-free water using QIAGEN Miniprep kit followed by Kpn I and EcoR I double restriction enzyme digestion. In digestion process, 10 µl of Miniprep products was mixed with 1 µl Kpn I and EcoR I enzyme each, 0.2 µl 100× BSA, NEB buffer 2 and incubated for 1 hour at 37ºC. Digested products were separated by 1.2% agarose DNA gel electrophoresis. According to weight separation, the correct inserts were identified, excised, purified and finally ligated into pcDNA4.0/myc-His-B expression vector (Figure 2.2) with myc-tag at the C-terminus of FOXQ1. A mixture comprising of 4 µl DNA fragment, 2 µl pcDNA4.0/myc-His-B pre-digested by Kpn I and EcoR I enzyme, 1 µl T4 ligase and 1 µl T4 ligation buffer were prepared and incubated at room temperature for 1 hour for use in ligation. The resulting ligation product was transformed into One Shot® TOP10 chemically competent *E. coli* as described in section 2.10 and spreaded onto ampicillin LB agar plate and incubated at 37ºC overnight for growing single colonies. The content of the resulting plasmids was verified by DNA sequencing. Next, the plasmid with the correct DNA sequence was amplified using QIAGEN Midiprep kit. FOXQ1 deletions (D1-D8) were cloned into pcDNA4.0/myc-His-B

expression vector using full-length FOXQ1 as the template with the same experimental procedures but using different designated forward and reverse primers. For the Tet-on inducible expression system, FOXQ1 fragment was obtained from pcDNA4.0/myc-FOXQ1 after double digestion by Kpn I and EcoR I restriction enzymes, and then ligated into pcDNA4.0/TO/myc-His-B inducible vector (Figure 2.4) within the same restriction enzyme sites using T4 ligase. For the retroviral expression system, myc-tagged FOXQ1 was cloned into pMN GFP/IRES retroviral vector (Figure 2.5) (a gift from Dr Linda Penn's lab). Primers used for expression plasmid and deletion mutant were shown in Table 2.2.

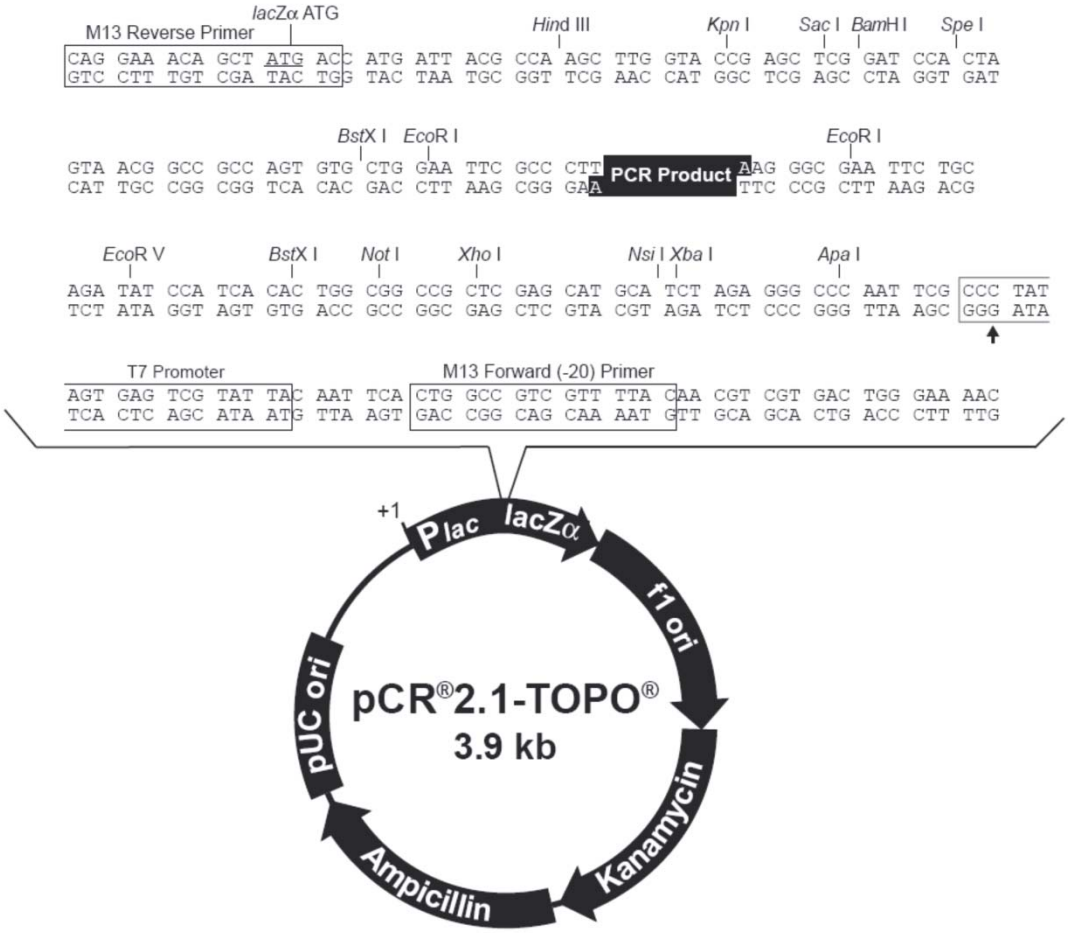

Figure 2.1 Map of TA cloning vector pCR® 2.1-TOPO®.

PCR product was ligated into this vector, and correct sequence was verified by sequencing using M13 reverse primer and T7 promoter.

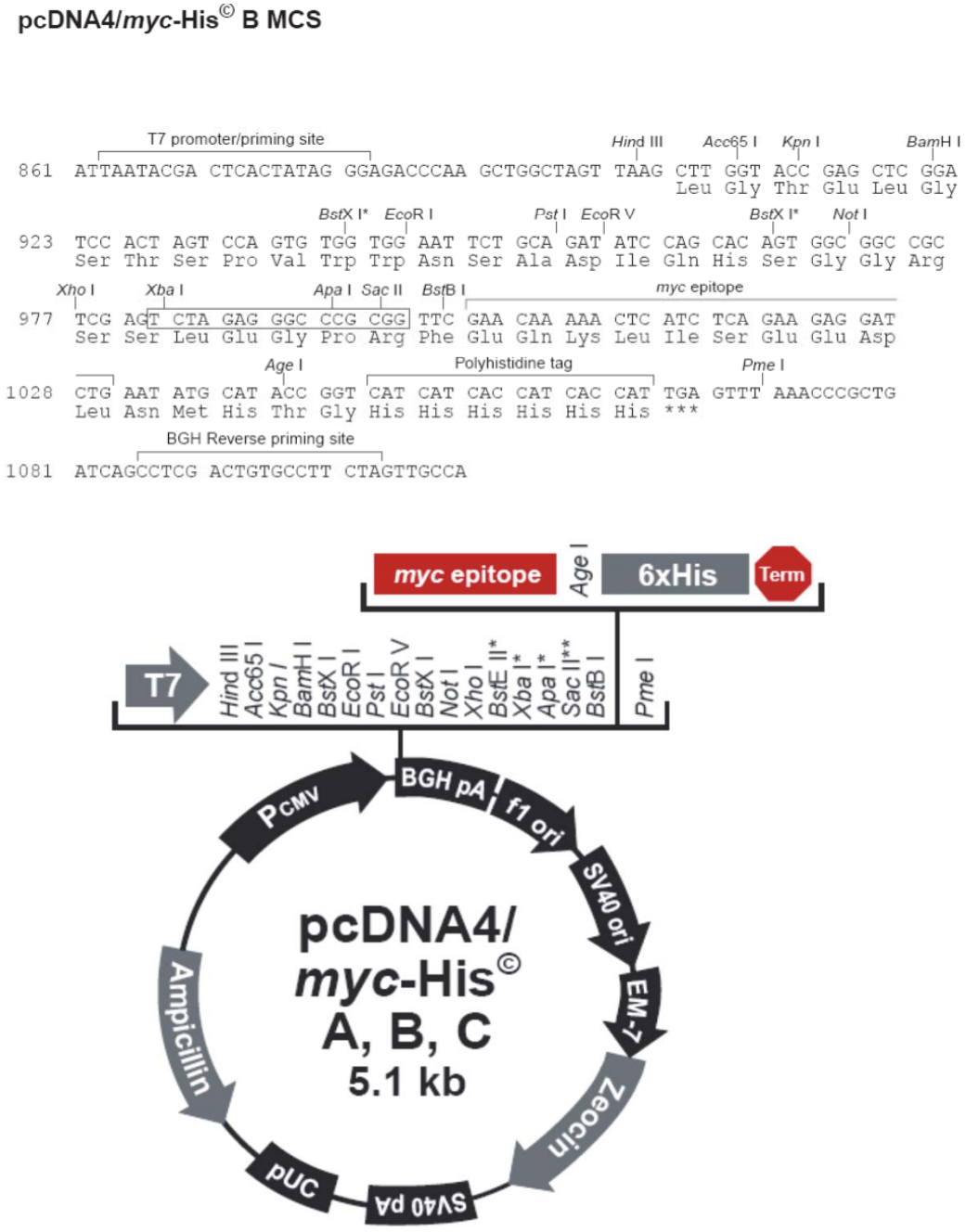

Figure 2.2 Map of mammalian expression vector pcDNA4/myc-His®.

Type B was used in this thesis. Gene of interest was ligated into multicloning sites (MCS) before myc-tag.

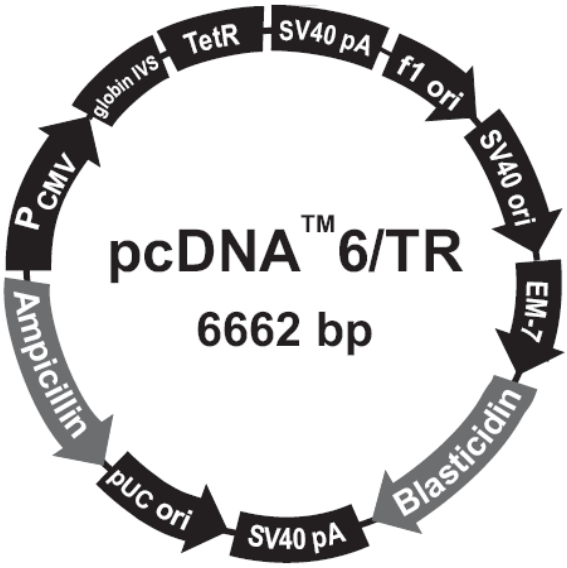

Figure 2.3 Map of pcDNA6^{TM}/TR vector of Tet-on inducible system.

It expresses Tet repressor which will bind to the Tet operator in pcDNA4^{TM}/TO/myc-His B. The mammalian antibiotic selection marker is blasticidin.

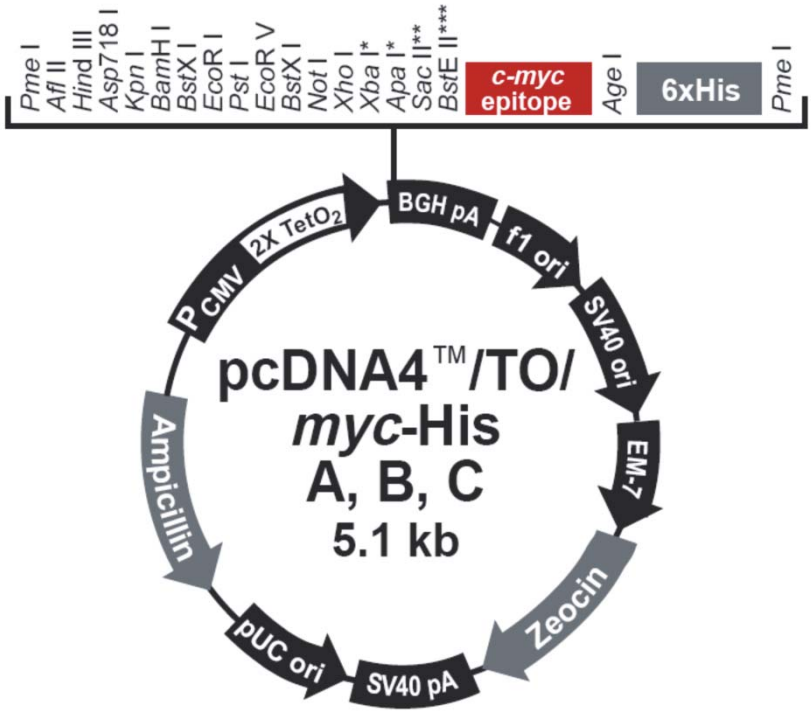

Figure 2.4 Map of pcDNA4™/TO/myc-His B expression vector in Tet-on inducible system.

This vector shares the same MCS with vector pcDNA4/myc-His®. The mammalian antibiotic selection marker is zeocin.

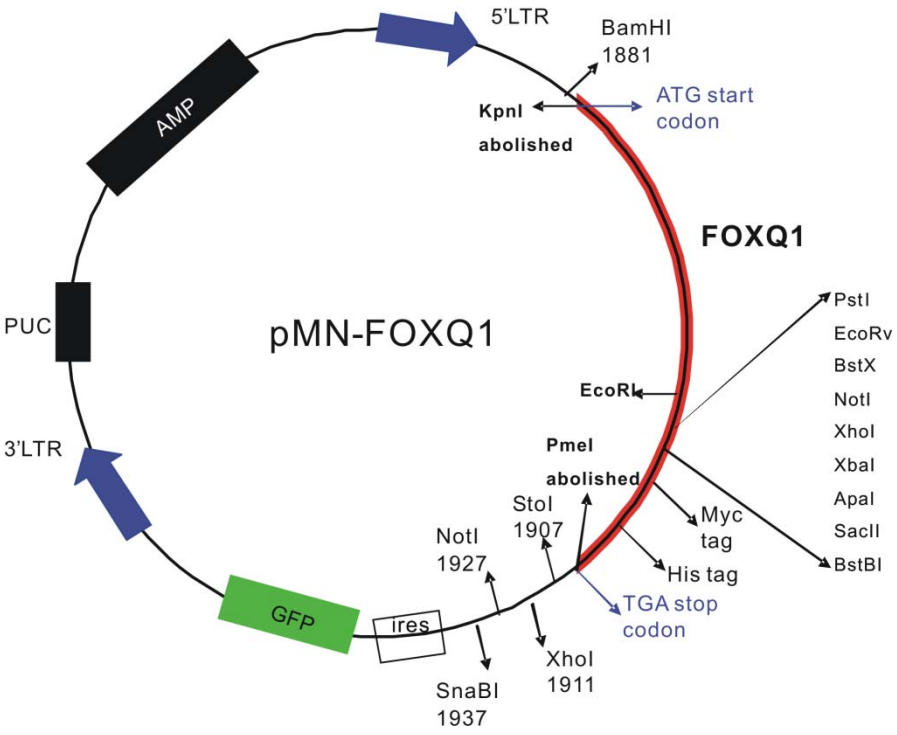

Figure 2.5 Schematic view of retroviral expression system ligated to FOXQ1 gene with myc-tag.

2.6 Site-directed mutagenesis

Site-directed mutagenesis was performed using QuikChange® Multi Site-Directed Mutagenesis Kit (Stratagene). Primers for designated site mutation were designed by the QuikChange® primer design program provided online by Agilent Technologies (Table 2.6). pcDNA4.0/myc-FOXQ1 plasmid DNA was used as template and diluted into 100 ng/μl and 1 μl of it was mixed with 2.5 μl of 10× QuikChange buffer, 0.75 μl QuikSolution, 1 μl of 100 ng/μl primer, 1 μl dNTP mix, 1 μl QuikChange enzyme blend and it was topped up with water to final volume of 25 μl. The mixture was next incubated in thermal cycler with following program. Step one is 95ºC for 1 minute, step two is 95ºC for 1 minute, step three is 55ºC for 1 minute, and step four is 68ºC for 13 minutes. Step two to step four were then repeated for 30 cycles, and after that, step five operated at 37ºC for 2 minutes. The resulting 25 μl PCR product was mixed with 1 μl Dpn I restriction enzyme and incubated at 37ºC for one hour for digesting unmethylated parental single strand plasmid DNA. The 26 μl digested product containing single-stranded site-mutated plasmid DNA was then precipitated with 74 μl isopropanol and centrifuged at 14680 rpm for 15 minutes at room temperature. Pellet was washed with 100 μl of 70% ethanol, and centrifuged at 14680 rpm for 15 minutes at room temperature. Pellet containing plasmid DNA was air-dried, then dissolved in 5 μl of water, and finally ready for transformation into bacteria. XLGold-ultracompetent cell was used for this transformation and in that single-stranded site-mutated plasmid DNA was converted into double-stranded DNA. 45 μl competent cell was mixed with 2 μl β-BE and incubated on ice for 10 minutes with swirl every 2 minutes. 5 μl plasmid DNA was then added into the previous mixture and incubated on ice for 30 minutes. After that, the mixture was heat-shocked at 42ºC for 30 seconds,

and incubated with 500 µl pre-warmed LB medium containing 100 µg/ml ampicillin at 37ºC shaker for one hour. The resulting product was spreaded onto LB agar plate containing 100 µg/ml ampicillin and incubated at 37ºC overnight. Positive clones were verified by double restriction enzyme digestion with EcoR I and Kpn I, and correct sequences were confirmed by sequencing.

2.7 Construction of RNAi-Ready pSIREN-RetroQ vector expressing FOXQ1 shRNA

2.7.1 shRNA oligonucleotide design

FOXQ1 siRNA sequence containing 19bp nucleotides were input into online shRNA sequence designer provided by Clontech (Mountain View, CA) (http://bioinfo.clontech.com/rnaidesigner/oligoDesigner.do). Restriction enzyme sites 5' BamH I and 3' EcoR I overhangs were added to the insert fragment for directional cloning into RNAi-Ready pSIREN vector (Figure 2.6). Additional Mlu I site was added to verify the positive clone. The designed end products contain 65bp nucleotides. shRNA sequences are listed in Table 2.5.

2.7.2 Annealing the oligonucleotides

PAGE-purified oligonucleotides were synthesized by 1st Base (Singapore) and diluted in TE buffer at a concentration of 100 µM. Top and bottom strands were mixed in a ratio of 1:1 to give a final concentration of 50 µM. The mixture were heated at 95ºC for 30 seconds, 72ºC for 2 minutes, 37ºC for 2 minutes and finally 25ºC for 2 minutes to generate annealed double stranded oligonucleotide.

2.7.3 Ligation of double stranded oligonucleotide into RNAi-Ready pRIREN vector

The annealed oligos were first diluted into TE buffer at a concentration of 0.5 μM. After that, 1 μl of 0.5 μM annealed oligos and 2 μl of 25 ng/μl linearized pSIREN vector were mixed with 1.5 μl 10× T4 DNA ligase buffer, 0.5 μl BSA (10mg/ml), 9.5 μl nuclease-free water, and 0.5 μl T4 DNA ligase (400 unit/μl). The mixture was incubated at room temperature for 3 hours for ligation to take place. For transformation, 5 μl of the ligated products were inserted into One Shot® TOP10 competent *E. coli* as described in section 2.10. Positive clones were selected by single restriction enzyme digestion at Mlu I.

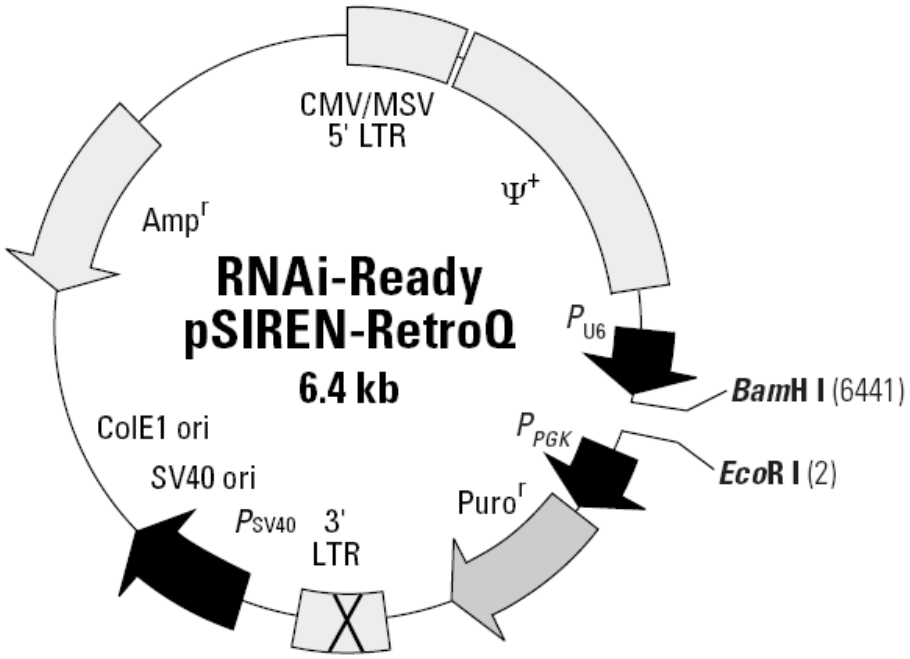

Figure 2.6 Map of RNAi-Ready pSIREN-RetroQ vector.

shRNA sequence was ligated between BamH I and EcoR I sites. The antibiotic selection for this vector is puromycin.

2.8 DNA agarose gel electrophoresis

Fermentas 6× loading dye was added into DNA to obtain a final concentration of 1× mixture. The mixture was loaded onto solidified agarose gel dissolved in TAE buffer with 0.5 μg/ml ethidium bromide and electrophoresed at constant voltage of 120V in 1× TAE buffer for 30 minutes at room temperature. After the electrophoresis was completed, the migrated DNA bands can then be viewed under ultra-violet light (GeneGenius Gel Imaging System from Syngene).

2.9 DNA gel extraction

DNA gel extraction was performed using QIAquick® Gel Extraction Kit. In detail, DNA fragments were excised under ultra-violet light and weighed. 3 volumes of QG buffer were added into the weighed gel slice and the mixture were incubated on a heat block at 50ºC for 10 minutes until the agarose gel is completely melted into the QG buffer. 1 volume of isopropanol was next added and mixed properly. The mixture was then transferred into a filter column and centrifuged at 13000 rpm for 30 seconds to allow the DNA materials to bind to the filter. 750 μl of PE buffer was used to wash the filter column once and DNA fragments were eluted into 30 μl RNAse-free water.

2.10 One Shot® TOP10 chemically competent *E. coli* transformation

Volume ranging from 2 to 6 μl of plasmid DNA product was mixed into one vial of One Shot® TOP10 chemically competent *E. coli* cells (Invitrogen) and incubated on ice for 30 minutes. The mixture was then subjected to heat shock at 42ºC in a water bath for 30 seconds and then transferred onto ice for 2 minutes. 150 μl SOC medium

was added to the mixture and cultured at 37ºC on a shaker operating at 280 rpm for 1 hour. 100 µl of cultured product was spreaded onto LB agar plate containing 100 µg/ml of ampicillin and incubate at 37ºC overnight for growing single colonies.

2.11 Plasmid amplification and preparation

Plasmids were extracted from bacteria (E.coli) through Mini- and Midi-prep method. Single bacterial colony was amplified into 2 ml LB medium containing 100 µg/ml ampicillin with shaking at 280 rpm for overnight at 37ºC. The next day, 1 ml of the cultured bacteria was used for plasmid purification using QIAprep® spin Miniprep kit. Firstly, bacteria were spun down by centrifuge at 3000 rpm for 3 minute at room temperature. The pellet was resuspended in solution using 250 µl of Buffer 1, and lysed by 250 µl of Buffer 2 followed by neutralization with 350 µl of Buffer 3. The neutralized mixture was centrifuged at 13000 rpm for 10 minutes. After that, 800 µl of supernatant was transferred into a filter column and further centrifuged at 13000 rpm for 30 seconds followed by one wash with 750 µl of PE buffer. The Miniprep products were finally eluted into 30 µl of RNAse-free water.

Midiprep was carried out using 50 ml bacterial culture material and QIAprep® spin Midiprep kit. Bacteria were first spun down by centrifuge at 4000 rpm for 15 minutes at 4ºC. The pellet was then resuspended with 4 ml of buffer P1, and lysed for 5 minutes with 4 ml of buffer P2 followed by neutralization with 4 ml of chilled buffer P3. The neutralized bacterial lysate was transferred into a filtered cartridge and incubated for 10 minutes at room temperature. Meanwhile, QIAGEN-tip was equilibrated with 10 ml QBT buffer. After 10 minutes, the bacterial lysate was filtered

through the cartridge into the QIAGEN-tip, and the clear lysate was allowed to go through the QIAGEN-tip by gravity flow. Next, the QIAGEN-tip was washed twice with 10 ml of QC buffer, and the plasmid DNA was eluted with 5 ml of QF buffer. The 5 ml of elution which contained DNA was precipitated with 3.5 ml of isopropanol by centrifuged at 13200 rpm for 30 minutes at 4ºC. The precipitated DNA was washed once with 2 ml of 70% ethanol and then centrifuged at 13200 rpm for 10 minutes at 4ºC. The DNA pellet was air-dried and reconstituted with 100 µl of RNAse-free water. The quality and concentration of DNA was measured by Nanodrop.

2.12 Sequences and plasmids for RNA interference

siRNA FOXQ1 sequences was designed and synthesized by 1st Base (Singapore), (#2 siRNA: AGATCAACGAGTACCTCAT). Another siRNA FOXQ1 oligos which contain three different siRNA oligos targeting human FOXQ1 were purchased from Santa Cruz. In addition, the FOXQ1 shRNA and negative control lentiviral particles with the same targeting site were purchased as well. PLKO.1-E-cadherin shRNA and PLKO.1-control plasmid, psPAX2 packaging plasmid and pMD2.G envelope plasmid were purchased from Addgene (Cambridge, MA).

2.13 Transient transfection

Target cell lines were seeded into 6-well plate at a density of 3 to 4 × 10^5 cells/well at 18 hours before transfection. Transfection mixture was prepared in 100 µl DMEM only medium at the ratio of 1 µg plasmid DNA to 3 µl Fugene 6, Fugene 6 HD

(Roche) or Lipofactamine 2000 (Invitrogen) for each well respectively. The mixture was incubated at room temperature for 20 minutes prior to adding into the cell culture plate which contained 1 ml PS-free DMEM. The DMEM was used without PS because PS can adversely affect the transfection efficiency.

To deliver siRNA sequence efficiently and firmly, Lipofectamine™ RNAiMAX reagent was used and siRNA was transfected twice. 5 µl of 20 nM siRNA oligos and 6 µl Lipofectamine™ RNAiMAX reagent were added into 100 µl OPTI-MEM® medium separately and incubated at room temperature for 5 minutes before mixing together. 20 µl mixtures were evenly dropped into cell culture well containing 800 µl OPTI-MEM® medium. After 6 hours incubation, OPTI-MEM® medium was changed to 2 ml PS-free DMEM to reduce the toxicity of the transfection reagent. The following day, transfected cells were trypsinized and reseeded into 6-well plate in preparation for the second transfection. The siRNA transfection procedure was repeated 18 hours later. The transfected cells were incubated for 48 hours prior to harvesting.

2.14 Generation of stable cell lines

2.14.1 Tet-on inducible expression system

To generate stable HCT116 Tet-on expression system, HCT116 epithelial colorectal cancer cell line was first transfected with pcDNA6.0/TR, followed by selection using 10 µg/ml blasticidin antibiotic. After selection for two weeks, the surviving colonies were pooled together and sequentially transfected with pcDNA4.0/TO/myc-FOXQ1

or empty vectors. Successfully transfected cells were selected, this time using 100 μg/ml zeocin antibiotic. After selection for two weeks, single colonies were picked and first seeded into 96-well plate after which the populations were further expanded. To examine for FOXQ1 expression, 2 μg/ml doxycycline (DOX) was introduced into the culturing medium. After 48 hours of treatment, the cellular proteins were harvested and immunoblotting for myc-tagged FOXQ1 were carried out using anti-myc antibody. Positively identified clones with myc-tagged FOXQ1 expression were expanded and maintained under conditions of 10 μg/ml blasticidin and 100 μg/ml zeocin which were added into the culturing medium.

2.14.2 Retroviral expression system

To generate retroviral expression system, platinum-A retroviral packaging cell line (CELL BIOLAB, INC., San Diego, CA) was seeded into collagen I coated 6-well plates (BD, BIOCOAT) at a density of 7×10^5 cells/well for 18 hours prior to transfection. At the start of the transfection process, 4 μg pMN-FOXQ1 or pMN empty plasmids were added into each well with 10 μl Lipofectamine 2000 (Invitrogen) transfection reagent. After 6 hours, transfection mixtures were replaced by DMEM cell culture medium with 10% FBS and 1% PS, and left aside for 48 hours to allow the packaging cells to express FOXQ1 or control retroviral particles. Target cell lines were seeded into 6-well plates at a density of 3×10^5 cells/well for 24 hours prior to introduction of the retroviral particles. At the start of the infection process, supernatants of retroviral packaging cells containing FOXQ1 or control retroviral particles were filtered through 0.45 μm filter unit to get rid of cell debris, and the resulting 1 ml of filtered retroviral supernatant were then added into each well of

target cells contained 1 ml of culturing medium. The 6-well plate, each well containing 2 ml mixture of retroviral supernatant plus culture medium and 8 μg/ml polybrene, was then centrifuged at 1800 rpm for 45 minutes to strengthen the efficiency of infection. Another 1 ml retroviral supernatant was sequentially added and the 6-well plate again centrifuged at 1800 rpm for another 45 minutes. The plates were then incubated at 37ºC for 48 hours after which the target cells were sorted for GFP expression. The retroviral expression system was generated in cells of HCT116, A549, SAOS2, MCF7, MCF10A, HMEC, and HMLER.

2.14.3 Stable RNA interference system

To generate FOXQ1 RNA interference system, cells were seeded into 6-well plate at a density of 3×10^5 cells/well. After 18 hours, either 10 μl shFOXQ1 or negative control lentiviral particles were added into the culture medium of each well with 8 μg/ml polybrene followed by 1800 rpm centrifuge for 45 minutes. After infection for 48 hours, positive cells were selected by exposure to 2 μg/ml puromycin for 2 weeks, following which single colonies were picked for knockdown efficiency validation by means of RT-PCR.

To generate E-cadherin RNA interference system, the human embryonic kidney (HEK) 293T cells were used for production of lentivirus. HEK 293T cells were seeded into collagen I coated 6-well plate at a density of 7×10^5 cells/well. After 18 hours, either 4 μg of PLKO.1-E-cadherin or PLKO.1-control was transfected into the cells along with 3 μg psPAX2 packaging plasmid, 1 μg pMD2.G envelope plasmid and 20 μl Lipofectemin 2000. The transfection medium was changed after 6 hours,

and then the 6-well plate incubated at 37ºC for 48 hours to allow for generation of lentiviral particles in the supernatant. Target cells were seeded at 24 hours before introduction of the lentiviral particles. The procedure for infection is the same as previously mentioned. After infection for 48 hours, selection for HMLER cells was carried out using 4 μg/ml puromycin for 2 weeks. The selected colonies were then pooled together and verified by immunoblotting with E-cadherin antibody.

2.15 Western blot analysis

Cells were harvested using trypsin and washed twice with cold PBS. The cell pellet was lysed using 30 μl of radioimmunoprecipitation assay lysis buffer [50 mmol/L Tris-HCl (pH7.4), 1 mmol/L EDTA, 150 mmol/L NaCl, 1% Nonidet P-40, 0.5% sodium deoxycholate, and proteinase inhibitors] for 60 minutes on ice. During the lysis process, the sample was vortexed for 15 seconds at 10 minutes interval. Subsequently, the cell lysate was sonicated 3 times at 5 seconds interval. After centrifuge at 132000 rpm for 15 minutes at 4ºC, the resulting supernatant was collected. Protein concentrations in the supernatant were determined with the Bradford protein assay kit (Bio-Rad, Hercules, CA). Protein samples (20-30 μg) were separated by 10% SDS-PAGE, transferred onto a PVDF immobilon membrane (Millipore), and blotted with specific primary antibodies followed by HRP-labelled secondary antibodies. The following primary antibodies were used in this study: E-cadherin (cat#610182, BD Biosciences), Vimentin (cat#6260, Santa Cruz), Myc-tag (9E10, Roche), CD44 (cat#550392, BD Biosciences), CD24 (cat#555426, BD Biosciences), FOXQ1 (AV39755, Sigma-Alrich), cleaved-PARP (cat#D214, Cell Signalling, Danvers, MA) and actin (Roche). ECL anti-rabbit (NA934V, GE

Healthcare) and ECL anti-mouse (NA931V, GE Healthcare) horseradish peroxidise-linked whole antibodies were used as secondary antibodies.

2.16 Immunofluorescence confocal microscopy

Stable cell lines were seeded at a density of 1.5×10^5 cells/well on 8 mm coverslips in 12-well plates under conditions with or without 2 μg/ml doxycycline treatments for 48 hours. For transient transfection, target cells were seeded under the same condition, which is with or without doxycycline treatment for 18 hours prior to transfection, and 2 μg plasmid DNA was transfected into each well with the experimental procedure previously mentioned. After 48 hours, cell coated coverslips were rinsed once with PBS and then fixed by ice-cold methanol for 5 minutes at -20ºC. After that, it was rehydrated with 3 washes of PBS at 10 minutes interval at room temperature. Fixed cells were permeabilized with 0.2% Triton-X-100 for 15 minutes at room temperature. After blocking with 10% FBS for 1 hour at room temperature, cell coated coverslips were probed with primary anti-myc-tag (9E10, Roche), E-cadherin (cat#610182, BD Biosciences) or Vimentin (cat#6260, Cell Signalling) antibodies in a 1/1000 dilution at room temperature for 1 hour followed by 3 washes with PBS. Next, the coverslips were probed with florescent-labelled secondary antibodies (Alexa Fluor®546 or Alexa Fluor®488) (Invitrogen, Molecular Probes, Eugene, Oregon) in a 1/2000 dilution at room temperature for 1 hour followed by 3 washes with PBS in subdued light. Finally, nuclei were stained with DAPI and coverslips were mounted with FluorSave™ reagent (CALBIOCHEM®). Flurorescence images were taken using Zeiss Meta upright microscope (LSM510 DUO system, Carl Zeiss) under 63×/1.40 oil DIC immersion objective with 488 nm (Argon) and 633 nm (Hene) wavelength lasers.

2.17 Promoter construction

The upstream promoter region for genes of interest was downloaded from UCSC database (http://genome.ucsc.edu/), and consensus transcription binding motifs were predicted by online software Genomatix MatInspector (http://www.genomatix.de). In this study, luciferase promoter activity assay was performed on three selected genes (CDH1, SLUG and CTGF) and tested genomic regions were shown in Table 2.1. Each gene was constructed in various fragments into the pGL3 reporter system depending on the consensus transcription binding motifs prediction. Primers used for promoter construction are listed in Table 2.4.

The procedure of promoter construct is described as follows. Human genomic DNA was used as the template for PCR amplification of specific promoter region, and PCR programme was run according to manufacturer's instruction for HotStarTaq (cat#203445, QIAGEN). In particular, the PCR master mix included 100 ng genomix DNA, 10 μM forward and reverse primer mix, 10 μl HotStarTaq master mix and it was topped up with water to final volume of 20 μl. PCR amplification was performed on peltier thermal cycler machine (DNA engine DYAD^{TM}). The machine operated in the following programme: step one is 95ºC for 15 minutes, step two is 94ºC for 30 seconds, step three is 68ºC for 30 seconds, and step four is 72ºC for 1 minute. Step two to step four were then repeated for 35 cycles, and after that, step five operated at 72ºC for 10 minutes. Finally, the samples were incubated at 4ºC for short-term storage. The remaining steps are the same as molecular cloning procedure previously mentioned.

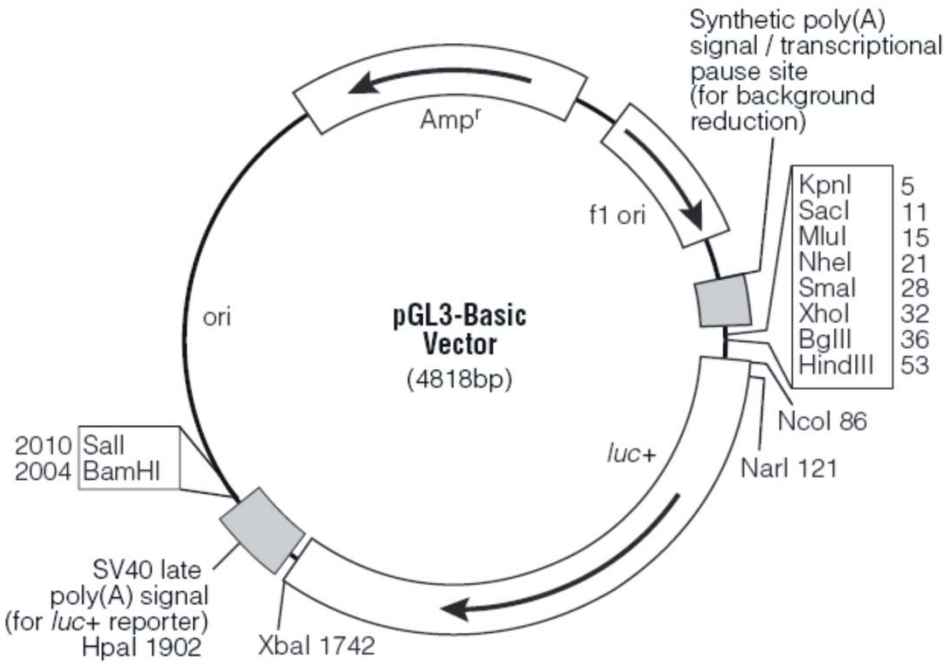

Figure 2.7 Map of luciferase vector pGL3-Basic.

2.18 Luciferase reporter assay

To perform luciferase reporter assay, desired target cell lines were seeded onto 12-well plates at a density of 1×10^5 cells/well. The target cells were transfected with various promoter or control plasmids according to procedures described for transient transfection. In particular, (i) the ratio of pGL3-basic promoter plasmid (firefly signal) to PRL-null (renilla signal) is 100/1, (ii) 500ng of pGL3-basic promoter plasmid was added to each well, and (iii) duplicates were carried out. Forty-eight hours after transfection, the luciferase activities were analyzed using the Dual Luciferase system according to manufacturers' instruction (Promega). Luciferase signals were measured by TriStar LB941 machine (BERTHOLD TECHNOLOGIES). Three independent experiments were performed.

2.19 Cell viability

Cell viability was measured using CellTiter-Glo® Luminescent Cell Viability Assay (Promega, Madison, WI). This assay is a homogeneous method of determining the number of viable cells in culture based on quantification of the ATP present, which signals the presence of metabolically active cells. This assay procedure involves addition of a single reagent named CellTiter-Glo® reagent which is a mixture of CellTiter-Glo® substrate and CellTiter-Glo® buffer. Adding CellTiter-Glo® reagent to cell culture medium result in cell lysis and generation of luminescent signal. This signal is proportional to the amount of ATP present, and the amount of ATP is directly proportional to the number of cells (Crouch, Kozlowski et al. 1993). In detail, cells were seeded at a density of 500-1000 cells/well in 96-well optical bottom plates with 100 µl medium. After indicated days, cells were lysed by 100µl of CellTiter-

Glo® reagent for 10 minutes with gentle shaking, and then incubated another 5 minutes to allow luminescence signal to stabilize. These luminescence signals generated were measured by MicroLumat Plus LB96V system (BERTHOLD TECHNOLOGIES). Six replicas were performed for each sample.

2.20 Anchorage-independent growth by soft agar colony formation assay

Soft agar colony formation assay was used to measure the ability of anchorage independent growth in vitro. It consists two layers of agar (base layer and top layer) with different agar concentrations. Base layer does not contain cells, but it has higher percentage of agar. Top layer is the cell layer, and contains lower percentage of agar. This assay was performed as follow: mixture comprising 3% agar in sterilized PBS was heated up in a microwave oven to dissolve the mixture homogenously. 6-well plates were pre-coated with 2 ml of 0.6% agar diluted with pre-warmed medium from 3% agar stock for each well as the base layer. Approximately 1000-3000 single cells were seeded into 0.3% agar for each well as the upper layer. After two weeks, formed colonies were stained with 4 μg/ml p-Iodonitrotetrazolium Violet (INT) overnight and photographed to produce phase contrast images. Duplicates were carried out for each sample, and three independent experiments were performed.

2.21 Flow Cytometry/PI staining and active Caspase-3 activity through FACS analysis

Cells were seeded into 6-well plate at a density of 3×10^5 cells/well, and treated with indicated drugs for various time durations. At the end of the drug treatment, cells were harvested by trypsin, washed once by 1 ml cold PBS, and then fixed by 70% ethanol for 1 hour at 4ºC. After fixing, the cells were washed twice with cold PBS, treated by 100 ng/μl RNase for 5 minutes, and stained with 400 μl of 50 mg/ml propidium iodide (PI) for 30 minutes in subdued light. The DNA contents were measured by FACS analysis (Becton Dickson), and 10000 cells were analyzed for each sample.

Active Caspase-3 activities were measured by FACS analysis using BD cytofix/cytoperm fixation/permeabilization kit with FITC rabbit anti-active Caspase-3 antibody (cat#559341, BD Biosciences) based on the manufacturer's instruction. In particular, cells were harvested by trypsin, washed once by 1 ml cold PBS, fixed and permeabilized by 800 μl Cytofix buffer for 20 minutes at room temperature, and washed twice using 1ml 1× Cytoperm buffer. 20 μl FITC rabbit anti-active Caspase-3 antibody was used for each sample and cells were incubated for 1 hour at room temperature in subdued light. Stained cells were washed once with 1 ml 1× Cytoperm buffer, and resuspended in 300 μl of the same buffer for FACS analysis.

2.22 Invasion and migration assay

Analysis of cell invasion and migration was performed using 24-well BD Falcon FluoroBlok^{TM} transwell insert (cat#351152, BD Biosciences) with 8 μm pore size and

special 24-well plates (cat#353504, BD Biosciences). For the purpose of invasion assay, inserts were prepared by coating the upper surface with 80 µl of 250 ng/ml growth factor reduced matrigel (cat#356231, BD Biosciences). The coatings were then incubated for 4 to 6 hours at 37ºC in a cell culture incubator prior to seeding of cells. For migration assay, the inserts remained un-coated. Cells (approximately 2.5 to 5×10^4) were seeded into the upper compartment of each insert with 200 µl DMEM containing 0.25% FBS. A chemoattractant consisting of 750 µl DMEM with 10% FBS were deposited into the bottom wells to allow the invading and migrating cells to penetrate through the insert. After 24 hours incubation at 37ºC, inserts were fixed with 3.7% formaldehyde for 20 minutes, and stained with 25 µg/ml propidium iodide for 30 minutes at room temperature in subdued light. Invaded and migrated cells beneath the inserts were scanned and counted using high content screening machine Cellomics ArrayScan V^{TI} (Thermo Scientific Inc.). 10 individual fields were scanned for each insert and the result was presented as the sum of 10 fields. Triplicates were carried out for each sample, and at least three independent experiments were repeated.

2.23 Three-dimensional matrigel culture

The three-dimensional culture of mammary epithelial cells on a reconstituted basement membrane (matrigel) has been widely accepted to recapitulate various features of breast epithelium in vivo. Unlike monolayer culture, mammary epithelial cells grown in three-dimension display the formation of acini-like spheroids with a hollow lumen and these acini were made up of apicobasal polarized cells. This structure mimics glandular epithelium in vivo. In the presence of oncogenes, the morphogenesis of glandular architecture by mammary epithelium became disrupted.

Thus, three-dimensional epithelial culture provides the appropriate structural and functional context fundamental for examining the biological activities of cancer genes (Debnath, Muthuswamy et al. 2003).

For three-dimensional culture of cells on matrigel, 8-well chamber slide (cat#384118, BD Biosciences) was used, and 7.6 mg/ml growth factor reduced matrigel (cat#356231, BD Biosciences) was thawed on ice and 50 µl matrigel was spread out evenly in each well. The matrigel coated culture slide was placed in 37ºC incubator to solidify the matrigel layer. The matrigel layer measured approximately 1-2 mm in thickness. MDA-MB-231 FOXQ1 knockdown and control cells were plated (5000 cells/well) in 8-well chamber slide on a solidified layer of matrigel. Each well was filled with 400 µl DMEM containing 2% FBS and 2-4% matrigel. For MCF10A cells, special assay medium was used for three-dimensional matrigel growth. The medium contained DMEM/F12 supplemented with 2% horse serum, 1% PS, 5 ng/ml EGF, 0.5 mg/ml hydrocortisone, 100 ng/ml cholera toxin, 10 µg/ml insulin and 2% matrigel. The medium in wells were replaced with fresh medium every four days. Phase contrast images of the three-dimensional structure were taken on indicated days.

2.24 Mammosphere formation assay

Mammosphere formation assay was developed by Dontu and Wicha to allow in vitro culture of undifferentiated human mammary epithelial cells in suspension. When cultured on non-adherent surfaces in the presence of growth factors, human mammary epithelial cells form spherical colonies termed ‘non-adherent mammospheres’. They have demonstrated that these non-adherent mammospheres are enriched in cells with

functional traits of stem/progenitor cells. This in vitro assay is suitable for testing self-renewal and differentiation of all three lineages present in the mammary gland, and it also facilitates the isolation and characterization of human mammary stem cells and the related pathway (Dontu, Abdallah et al. 2003).

To perform mammosphere formation assay, single cell suspension of target cells were plated at a density of 5000 cells/well in 6-well ultra-low attachment plates (Corning) containing 2 ml MammoCult medium with hydrocortisone and heparin (STEMCELL technologies) and cultured for a period of 7 days. For mammosphere numbers calculation, single cell suspension (100 cells/well) was plated in 96-well ultra-low attachment plates under the same conditions. Mammosphere sizes more than 100 μm were counted under microscope (Nikon ECLIPSE TS100). The data calculated for the number and size of mammosphere is the average of three independent experiments.

2.25 Total RNA extraction

Total RNA was isolated using Trizol (Invitrogen) and purified with the RNeasy Mini Kit (QIAGEN). First, 10^6 cells were lysed with 1 ml Trizol and 200 μl chloroform. The RNA layer was separated by centrifuge at 12000 rpm for 15 minutes at 4ºC. The upper layer containing RNA was transferred to a fresh RNAse-free tube and neutralized with equal volume of 70% ethanol. The mixtures were purified through filter column provided in the kit and washed once with 750 μl RW1 buffer followed twice with 500 μl RPE buffer based on manufacture's instruction. Finally, the RNAs were eluted into 30 μl RNAse-free water. The RNA quantity and concentration were determined using Nanodrop ND-1000.

2.26 RT-PCR

To perform RT-PCR, total RNA was diluted to a concentration of 125 ng/µl based on TITANIUM One-Step RT-PCR Kit (Clontech). 1 µl of the diluted total RNA was used for each reaction together with 1× one step buffer, 1× dNTP mix, 0.4 unit RNAse inhibitor, 0.5× thermostabilizing reagent, 0.2× GC-melt, 0.4 µM oligo(dT) primer, 1× RT-titanium Taq enzyme mix, 0.9 µM specific PCR primer mix and finally topped up with RNAse-free water to 25 µl volume. The PCR mixture was amplified in the PCR machine (DNA Engine DYAD^{TM,} MJ Research) programmed to run step one at 50ºC for 1 minute, step two at 94ºC for 5 minutes, step three at 94ºC for 30 seconds, step four at 60ºC for 30 seconds, and step five at 68ºC for 30 seconds. Steps three to five were then repeated for indicated cycles. Step six ran at 68ºC for 2 minutes, and finally the mixture was incubated at 4ºC. GAPDH was used as internal control. The RT-PCR results were visualized by 2% DNA agarose gel electrophoresis. RT-PCR primers are listed in Table 2.3.

2.27 Semi-quantitative RT-PCR

In order to carry out semi-quantitative real-time PCR, total RNAs were converted into cDNA first. In this converting experiment, 1-2 µg of total RNA was diluted into 25 µl RNAse-free water for preparing cDNA according to protocols of the High-Capacity cDNA Reverse Transcription Kits (Applied Biosystems). In detail, 25 µl of diluted RNA was mixed with PCR master mix comprising 5 µl 10X reverse transcription buffer, 2 µl 25X dNTPs, 5 µl 10× random primers, and 2.5 µl MultiScribe^{TM} reverse transcriptase. This mixture was finally topped up with RNAse-free water to 50µl. This

50 µl mixture was fed into the PCR machine which was ran using the programme of 25ºC for 10 minutes, 37ºC for 2 hours, and the sample finally incubated at 4ºC.

Semi-quantitative real-time PCR was performed using PRISM 7900 Sequence Detection System (Applied Biosystems). 2 to 4 ng cDNA were amplified using FOXQ1, E-cadherin, Vimentin, CD44, CD24 and GAPDH Taqman probes (Applied Biosystems) with Taqman fast universal PCR master mix (cat#4352042, Ambion, Applied Biosystems). Three independent experiments were performed for quantitative real-time PCR. Results were normalized to reflect fold changes of target genes with respect to internal control GAPDH.

2.28 Microarray gene expression profiling

Gene expression profiling was performed on the platform of Illumina Gene Expression Sentrix® BeadChip HumanRef-8_V2 and V3 (San Diego, CA). The procedure is described as follows.

2.28.1 RNA amplification and labeling

Total RNA was extracted using method as described in section 2.25. Illumina® TotalPrep™-96 RNA Amplification Kit was used for RNA amplification and labeling. For each sample, 500 ng RNA was diluted in 11 µl nuclease-free water, and 9 µl reverse transcription master mix [2 µl 10× first strand buffer, 4 µl dNTP mix, 1 µl T7 oligo(dT) primer, 1 µl RNAse inhibitor, and 1 µl ArrayScript™ reverse transcriptase]. This mixture was incubated at 42ºC for 2 hours in thermocyclers (DNA Engine

DYAD™, MJ Research) to synthesize first strand cDNA. In order to generate second strand cDNA, 80 µl second strand master mix (63 µl nuclease-free water, 10 µl second strand buffer, 4 µl dNTP mix, 2 µl DNA polymerase and 1 µl RNase H) was combined with the previous product, and incubated at 16ºC for 2 hours. To eliminate excess primers, salt and enzymes, 100 µl cDNA product was purified by adding 180 µl cDNAPure first. The cDNA became bound to the magnetic beads in the cDNA Pure buffer. cDNA binding beads were captured by magnetic stand, and these beads were washed twice with 150 µl cDNA wash buffer. cDNA was eluted with 20 µl preheated Nuclease-free water, and 17.5 µl eluted cDNA was transferred to a fresh PCR plate for labeling. In order to produce biotin-labeled cRNA, 7.5 µl IVT master mix (2.5 µl biotin-NTP mix, 2.5 µl T7 10× reaction buffer, and 2.5 µl T7 enzyme mix) was added into 17.5 µl purified cDNA and incubated at 37ºC for 14 hours. The mixture was then used to transcript biotin-labeled cRNA in vitro. On the next day, transcripted cRNA was added into 70 µl cRNA binding buffer that contained magnetic beads and further mixed with 95 µl 100% ethanol. cRNA binding beads were captured by magnetic stand, and washed twice with 100 µl cRNA wash solution. Finally, purified cRNA was eluted with 40 µl preheated cRNA elution buffer. cRNA concentration was measured with NanoDrop spectrophotometer. The biotin-labeled and purified cRNA was stored at -20ºC for further hybridization.

2.28.2 Hybridization

Illumina 8-sample Sentrix® BeadChip was used for hybridization. Before the samples were hybridized, buffer GEX-HYB and GEX-HCB were pre-warmed in 58ºC Illumina hybridization oven (San Diego, CA) until all salts were dissolved. For each

sample, 750 ng cRNA was diluted in 5 µl RNase-free water and 10 µl GEX-HYB, and incubated at 65ºC for 5 minutes. Illuminal Hyb camber gasket was placed into BeadChip Hyb chamber, and 200 µl GEX-HCB was added into each of the two humidifying buffer reservoirs in each Hyb chamber. BeadChip was placed into the Hyb chamber insert, and barcode was oriented to match the symbol on the insert. 15 µl of each pre-heated cRNA samples were loaded into BeadChip. The Hyb chamber insert containing samples was loaded into BeadChip Hyb chamber, and chamber was sealed with lid. The sealed Hyb chamber was baked in Illumina Hybridization oven at 58ºC for 18 hours to complete hybridization.

2.28.3 Wash and imaging BeadChip

After hybridization, on the next day, Hyb chamber was removed from oven and disassembled. The coverseal on top of the BeadChip was peeled off, and BeadChip was transferred to sliding rack submerged in diluted E1BC wash buffer for staining. The sliding rack with BeadChip was next transferred into the Hybex waterbath insert containing High-Temp wash buffer and incubated for 10 minutes at 55ºC. The BeadChip was washed at room temperature with 250 ml E1BC for 100 minutes followed by a 10 minutes wash with 100% ethanol. A second wash at room temperature with another 250 ml E1BC buffer, and BeadChip was then incubated with 4 ml E1 buffer for blocking. After blocking, BeadChip was detected with 2 ml buffer E1 at 1/1000 dilution of steptavidin-Cy3 for 10 minutes. The BeadChip was finally washed with 250 ml E1BC buffer. After wash, BeadChip was dried immediately by centrifuge at 100×g for 4 minutes at 25ºC. The dried BeadChip was

scanned using Illumina BeadArray Reader, and images were stored with indicated barcodes for further analysis.

2.28.4 Gene expression profiling and Gene ontology analysis

The scanned BeadChip images were processed through Illumina GenomeStudio™ first and the generated data were imported into GeneSpringGX™ (Agilent Technologies) software for further analysis. To do GeneSpringGX analysis, Illumina single color was selected for experimental type and signals were normalized to median of all samples in the same BeadChip. To achieve a meaningful gene expression profile, samples were numbered and grouped with experimental design. Fold changes were calculated by comparison of paired samples. Cluster heat map was generated by hierarchical analysis and the distance metric was set to Pearson centered. The analyzed gene sets by GeneSpring were next subjected to Ingenuity Pathway Analysis (IPA) (www.ingenuity.com) for gene ontology analysis. Gene name and fold changes were imported into IPA, and analyzed results showed the potential signalling pathways involved and related biological functions.

2.29 Clinical relevance and survival analysis

To get the information of gene expression pattern on published databases, I examined FOXQ1 expression in web-based cancer microarray database i.e. Oncomine (www.oncomine.org). Oncomine provides cancer microarray data in a variety of cancer subtypes and clinical-based as well as pathology-based analyses (Rhodes, Yu et al. 2004).

In the breast cancer data set of Vande Vijver, the expression of probes for each FOXQ1 gene was averaged and transformed to z-score. The positive z-score was treated as higher expression and the negative z-score was treated as lower expression. Kaplan-Meier survival analysis was used for the analysis of clinical outcome.

2.30 Statistical analysis

Statistical analysis was done using Prism (GraphPad software Inc., San Diego, CA) for three independent experiments. T-test was carried out for p-value calculation. Error bar was plotted with SEM (standard error of mean).

Table 2.1 Genomic region of CTGF, SLUG, and CDH1 promoters

Promoter name	Genomic region	Product length (bp)	Restriction enzyme site
CTGF-P1	(-2000 to -797bp)	1205	KpnI and BglII
CTGF-P2	(-874 to +195 bp)	1069	KpnI and BglII
SLUG-P1	(-2000 to -800 bp)	1200	KpnI and XhoI
SLUG-P2	(-900 to +100 bp)	1000	KpnI and XhoI
SLUG-P3	(-400 to -50 bp)	350	KpnI and XhoI
SLUG-P4	(- 400 to +100 bp)	500	KpnI and XhoI
SLUG-P5	(-900 to -400 bp)	500	KpnI and XhoI
CDH1-P2	(-1000 to +200 bp)	1200	MluI and BglII
CDH1-P3	(-450 to +193 bp)	643	MluI and BglII

Table 2.2 Oligonucleotide primers for expression vector construction

Name	Direction	Sequence
Full length-FOXQ1	forward	5' GGTACCCCACCATGAAGTTGGAGGTGTTCGTCC 3'
	reverse	5' GAATTCCAGGCTAGGAGCGTCTCCAC 3'
D1-FOXQ1	forward	5' AGGTACCACCATGAAGTTGGAGGTGTTCGTC 3'
	reverse	5' AGAATTCTTCTTGCGCAGGATGCTG 3'
D2-FOXQ1	forward	5' AGGTACCACCATGAAGTTGGAGGTGTTCGTC 3'
	reverse	5' AGAATTCATGCTGTCGATGGCG 3'
D3-FOXQ1	forward	5' GGTACCACCATGAAGTTGGAGGTGTTC 3'
	reverse	5' GAATTCCCGTCGGCGAAGGTGTAC 3'
D4-FOXQ1	forward	5' GGTACCCCACCATGCTCAACCCCAACAGCGAG 3'
	reverse	5' GAATTCCAGGCTAGGAGCGTCTCCAC 3'
D5-FOXQ1	forward	5' GGTACCATGAAGCGCCTCAGCCAC 3'
	reverse	5' GAATTCCAGGCTAGGAGCGTCTCCAC 3'
D6-FOXQ1	forward	5' GGTACCACCATGAAGTTGGAGGTGTTC 3'
	reverse	5' GAATTCCGCGTATATGGCTTGCT 3'
D7-FOXQ1	forward	5' GGTACCACCATGAAGTTGGAGGTGTTCGTCCCT 3'
	reverse	5' GAATTCCGCTTGCGGCGGCGGCGGAAGACCCC 3'
D7/NLS mut-FOXQ1	forward	5' GGTACCACCATGAAGTTGGAGGTGTTCGTCCCT 3'
	reverse	5' GAATTCCGGGCGCGGGCGCGGGCGAAGACCCC 3'
D8-FOXQ1	forward	5' GGTACCACCATGCGCCGCCGCCGCAAG 3'
	reverse	5' GAATTCCAGGCTAGGAGCGTCTCCAC 3'
FOXQ1/pMN	forward	5' TCCCGCACTCTGTTCGCCGTCGCC 3'
	reverse	5' CCCGGCGGCGGCCCCCGCCAAGCC 3'

Table 2.3 Oligonucleotide primers for RT-PCR

Name	Direction	Sequence
CTGF	forward	5' GCACAAGGGCCTCTTCTGTGA 3'
	reverse	5' TGTCTTCCAGTCGGTAAGCCG 3'
FOXQ1	forward	5' ATGAAGTTGGAGGTGTTCGT 3'
	reverse	5' TGAGCGCGATGTACGAGTAG 3'
GAPDH	forward	5' ATGGGGAAGGTGAAGGTCGG 3'
	reverse	5' AAGACGCCAGTGGACTCCACGA 3'
ACTIN	forward	5' GTGGGGCGCCCCAGGCACCA 3'
	reverse	5' CTCCTTAATGTCACGCACGATTTC 3'
VIM	forward	5' ATGTCCACCAGGTCCGTGTC 3'
	reverse	5'GCGGGTGTTCTTGAACTCGG3'
CDH1	forward	5' CTGCTGCTGCTGCAGGTCTCCTCTT 3'
	reverse	5' TTCTGAGGCCAGGAGAGGAGTTGGG 3'
SLUG	forward	5' CGCGCTCCTTCCTGGTCAAGAA 3'
	reverse	5' GGCATGGGGGTCTGAAAGCT 3'
SNAIL	forward	5' ATGCCGCGCTCTTTCCTCGT 3'
	reverse	5' AAGGACGAAGGAGCCGGTGA 3'
TWIST	forward	5' ATGATGCAGGACGTGTCCAG 3'
	reverse	5' TCGTAAGACTGCGGACTCCC3'

Table 2.4 Oligonucleotide primers for promoter construction

Name	Direction	Sequence
CDH1-P1	forward	5' ACGCGTTGGCTCATGCCTGTAAT 3'
	reverse	5' AGATCTCCCTCGCAAGTCAGGGG 3'
CDH1-P2	forward	5' ACGCGTATTAGGCCGCTCGAG 3'
	reverse	5' AGATCTCCCTCGCAAGTCAGGGG 3'
SLUG-P1	forward	5' GGTACCGATCTGTGCAGTGCACC 3'
	reverse	5' CTCGAGTCTCTCACACTTTTGACAAGAGAT 3'
SLUG-P2	forward	5' GGTACCATAATTGTCTCTAAAGACCCATACAACC 3'
	reverse	5' CTCGAGCTACAGCATCGCGGC 3'
SLUG-P3	forward	5' GTACCTAACACCAGAGGCTGGCCT 3'
	reverse	5' CTCGAGATCCAATCACAGCTGAGAGG 3'
SLUG-P4	forward	5' GGTACCTAACACCAGAGGCTGGCCT 3'
	reverse	5' CTCGAGCTACAGCATCGCGGC 3'
SLUG-P5	forward	5' GGTACCATAATTGTCTCTAAAGACCCATACAACC 3'
	reverse	5' CTCGAGATGAGAGCCTATATTTGGAAGTGG 3'
CTGF-P1	forward	5' GGGGTACCTCTTGAAAGGTTTCACTGTGG 3'
	reverse	5' GAAGATCTGTGGCCATCAATGTTTCCAG 3'
CTGF-P2	forward	5' GGGGTACCAGCCCCTACCTACCCAACACA 3'
	reverse	5' GAAGATCTAGGAGGACCACGAAGGCGAC 3'

Table 2.5 Oligonucleotide for FOXQ1 shRNA construction

Name	Target sequence	Direction	Sequence	Oligo length
FOXQ1 shRNA #1	GCCACAACCTTTCGCTCAA	Top Strand	5'gatccGCCACAACCTTTCGCTCA ATTCAAGAGATTGAGCGAAAG GTTGTGGCTTTTTTACGCGTg3'	65bp
		Bottom Strand	5'aattcACGCGTAAAAAAGCCACA ACCTTTCGCTCAATCTCTTGAAT TGAGCGAAAGGTTGTGGCg3'	65bp
FOXQ1 shRNA #2	AGATCAACGAGTACCTCAT	Top Strand	5'gatccAGATCAACGAGTACCTCA TTTCAAGAGAATGAGGTACTCG TTGATCTTTTTTTACGCGTg3'	65bp
		Bottom Strand	5'aattcACGCGTAAAAAAAGATCA ACGAGTACCTCATTCTCTTGAA ATGAGGTACTCGTTGATCTg3'	65bp

Table 2.6 Oligonucleotide primers for site-directed mutation vector construction

Name	Sequence
S18A	5' GGACAAGCAGGGCGCTGACCTGGAGGGC 3'
S217A	5' CGCAAGCGCCTCGCCCACCGCGCGCC 3'
T115A	5' CACGCAGCAAGCCATATGCGCGGCGGC 3'
S166A	5' GCTGGCGCAACGCCGTGCGCCAC 3'

CHAPTER 3:

FUNCTIONAL CHARACTERIZATION OF FOXQ1 IN BREAST CANCER

Recent evidence has shown that forkhead transcription factor family members such as FOXC1 and FOXC2 are associated with EMT and tumor progression in aggressive basal-like breast cancer (Mani, Yang et al. 2007; Ray, Wang et al. 2010). However, it is not clear whether other forkhead family members also have roles in breast cancer progression. FOXQ1 is the only member that has been identified so far in the 'Q' subgroup of the forkhead family, and its biological functions in breast cancer have not been previously studied. In this study, I investigated the functional role of FOXQ1 in breast cancer, in particular with respect to EMT.

3.1 FOXQ1 expression is associated with aggressive breast cancer phenotypes

In order to identify additional EMT regulators within the forkhead transcription factor family**,** microarray gene expression analysis was performed to compare the expression levels of forkhead transcription factor members between the highly invasive mesenchymal-like breast cancer MDA-MB-231 and non-invasive epithelial-like breast cancer MCF7 cells using Illumina Beadchip gene expression array. The results showed that among all 49 array detectable forkhead genes, FOXQ1 was identified as the most highly overexpressed in MDA-MB-231 cells relative to MCF-7 cells (Figure 3.1A). Notably, the differential expression of other established forkhead EMT inducers including FOXC1 and FOXC2 were less prominent. This finding was further confirmed by quantitative RT-PCR in a panel of breast cancer cell lines including luminal and basal-like subtypes and non-cancerous breast cell lines. The results showed the higher levels of FOXQ1 mRNA in basal-like breast cancer cell lines MDA-MB-231, MDA-MB-468, MDA-MB-436, and BT549 subtype as compared to luminal cell lines (MCF-7, T47D, SKBR-3, BT474, MDA-MB-361, and MDA-MB-

415) as well as non-cancerous mammary epithelial MCF10A and HMLER cells (Figure 3.1B). The endogenous protein levels of FOXQ1 in the above breast cancer cell lines were examined as well. Except for MDA-MB-468, all other basal-like breast cancer cell lines BT549, MDA-MB-436 and MDA-MB-231 expressed high levels of FOXQ1 protein (Figure 3.1C). Interestingly, MDA-MB-468 cell which is characterized as basal A, while the others (BT549, MDA-MB-436 and MDA-MB-231) are defined as basal B breast cancer. Clinically, basal B breast cancers are more representative of triple-negative breast cancer subtype, and displayed stem cell gene expression profile as shown by microarray analysis (Neve, Chin et al. 2006). The discrepancy between FOXQ1 protein level and mRNA level in MDA-MB-468 cells could be caused by posttranslational modification. In general, FOXQ1 expression seems to correlate with basal B (also known as triple-negative) breast cancer which exhibit aggressive phenotype and poor clinical outcome.

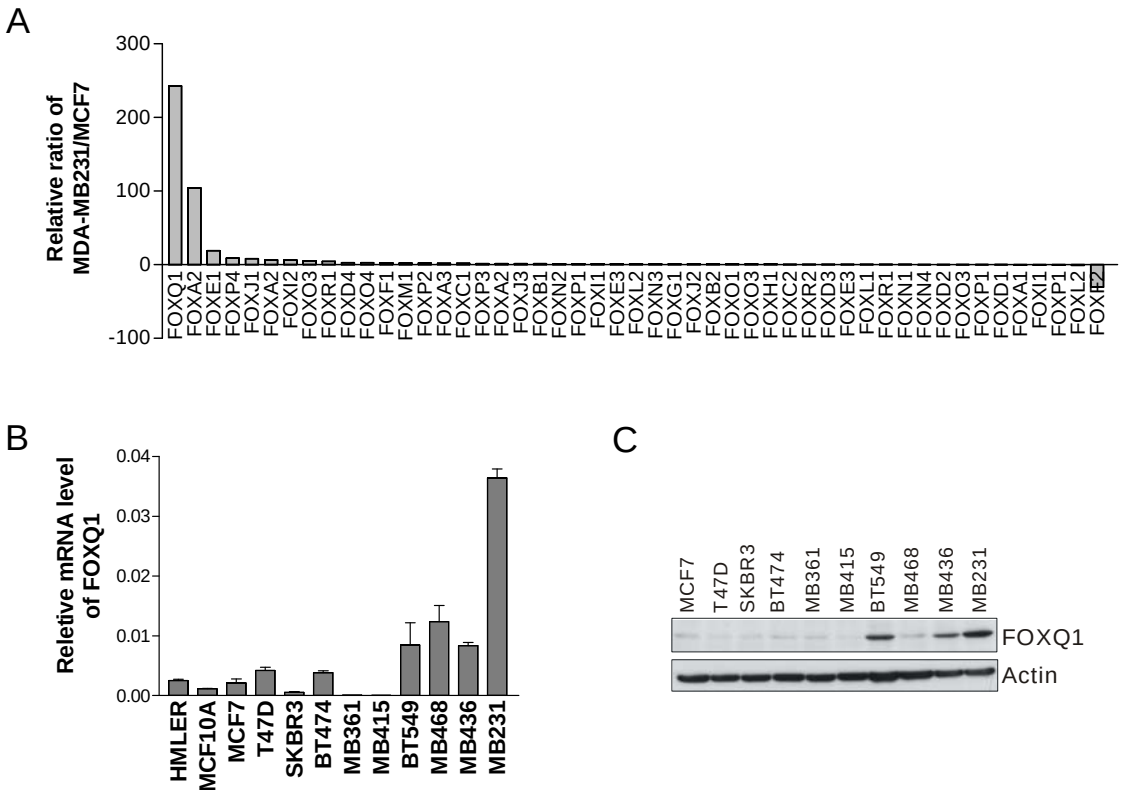

Figure 3.1 FOXQ1 is highly expressed in invasive breast cancer cells.

A, Relative gene expression levels of forkhead family members in MDA-MB-231 compared to MCF7 cells, based on Illumina gene expression array data from the respective two cell lines.
B, Quantitative RT-PCR analysis of FOXQ1 mRNA in indicated cell lines.
C, Endogenous FOXQ1 protein expression levels were measured among indicated cell lines.

To seek clinical evidence linking FOXQ1 expression to breast cancer, the FOXQ1 expression was examined in Oncomine data sets (www.oncomine.com). The data from various breast cancer cohorts showed that the FOXQ1 expression correlated with not only a higher tumor grade (P=0.0007) in VantVeer database (Figure 3.2A), but also metastasis (P=0.003) in VandeVijver database (Figure 3.2B). Especially FOXQ1 is highly enriched in unfavorable estrogen receptor (ER)/progesterone (PR)/HER2 triple-negative basal-like subtype (P=0.008) revealed in Richardson database (Figure 3.2C). Moreover, higher FOXQ1 expression is also associated with poor clinical outcomes (P=0.002) in VandeVijver database (Figure 3.2D). The patients with high FOXQ1 expression have less overall survival. These results from both in vitro and clinical data suggested a potential oncogenic role of FOXQ1 in a fraction of aggressive triple-negative breast cancers.

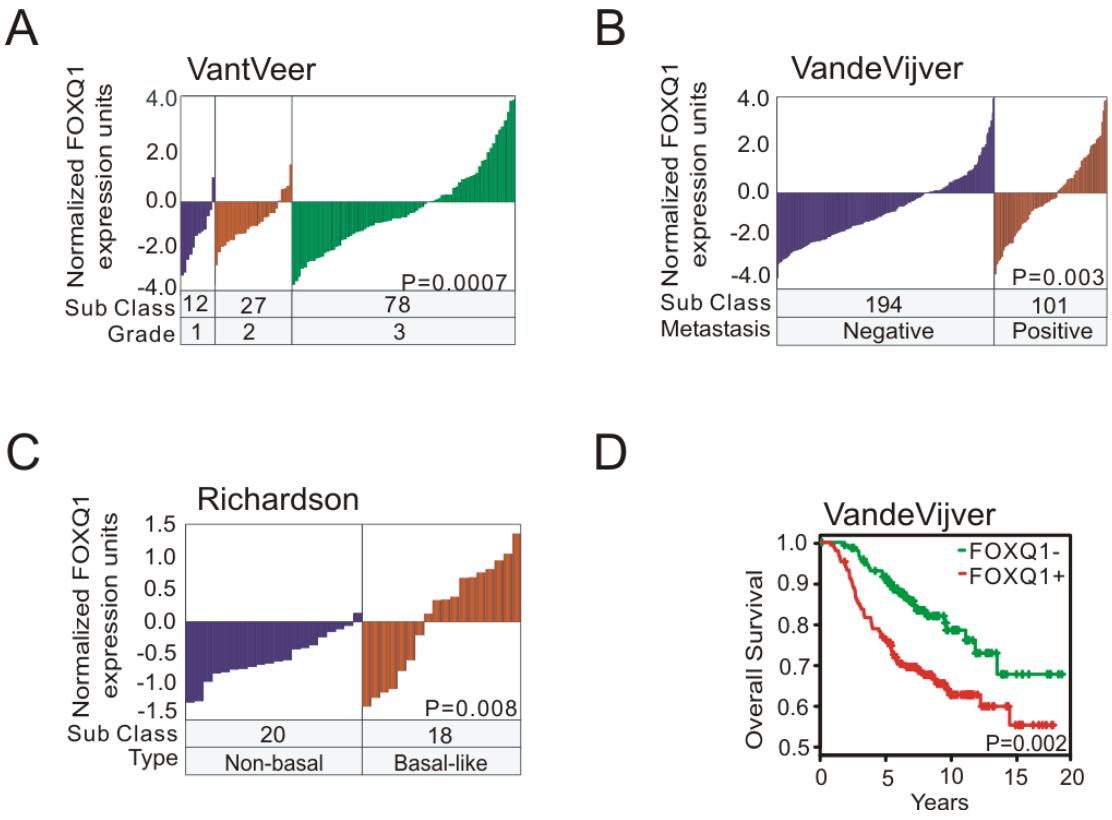

Figure 3.2 FOXQ1 expression is associated with aggressive breast cancers in clinical databases.

A, FOXQ1 expression level in breast cancer is associated with high grade in the Vant Veer cohort.
B, FOXQ1 expression level in breast cancer is associated with metastatic status in the Vande Vijver cohort.
C, FOXQ1 expression level in breast cancer is associated with basal-like disease type in the Richardson cohort.
D, Higher level of FOXQ1 expression is associated with poorer survival. Kaplan-Meier survival plots of overall survival from the Vande Vijver cohort. Patients with higher levels of FOXQ1 are highlighted in red, while patients with lower levels of FOXQ1 expression are highlighted in green.

3.2 FOXQ1 depletion reduces mesenchymal phenotype and invasive ability of MDA-MB-231 cells in vitro

To functionally validate the role of FOXQ1 in regulating aggressive breast cancer phenotype, triple-negative breast cancer cell line MDA-MB-231 was used. MDA-MB-231 is a mesenchymal-like aggressive breast cancer cell line and is often used to study breast cancer invasion and metastasIs. In order to investigate the role of FOXQ1 in MDA-MB-231 cells, several FOXQ1 shRNA sequences were introduced into MDA-MB-231 cells to establish stable FOXQ1 knockdown cell lines. A total of three FOXQ1 depletion clones were generated in MDA-MB-231 cells. One stable cell line was generated to express a pool of three individual FOXQ1 shRNA sequences which was purchased from Santa Cruz (designated as shFOXQ1-SC). Another two clones were derived from the same single FOXQ1 shRNA sequence with different single clones (designated as shFOXQ1 #2-9, #2-12). These stable FOXQ1-depleted MDA-MB-231 cell lines and their respective control cells were maintained under puromycin containing medium.

Typically, the morphology of MDA-MB-231 cells displays an elongated and spindle-like phenotype associated with invasive ability. Notably, FOXQ1 ablation induced a change from spindle-like mesenchymal morphology of MDA-MB-231 cells into epithelial-like morphology by manifesting an increased cell-to-cell adhesion in all three FOXQ1-depleted cell lines (Figure 3.3).

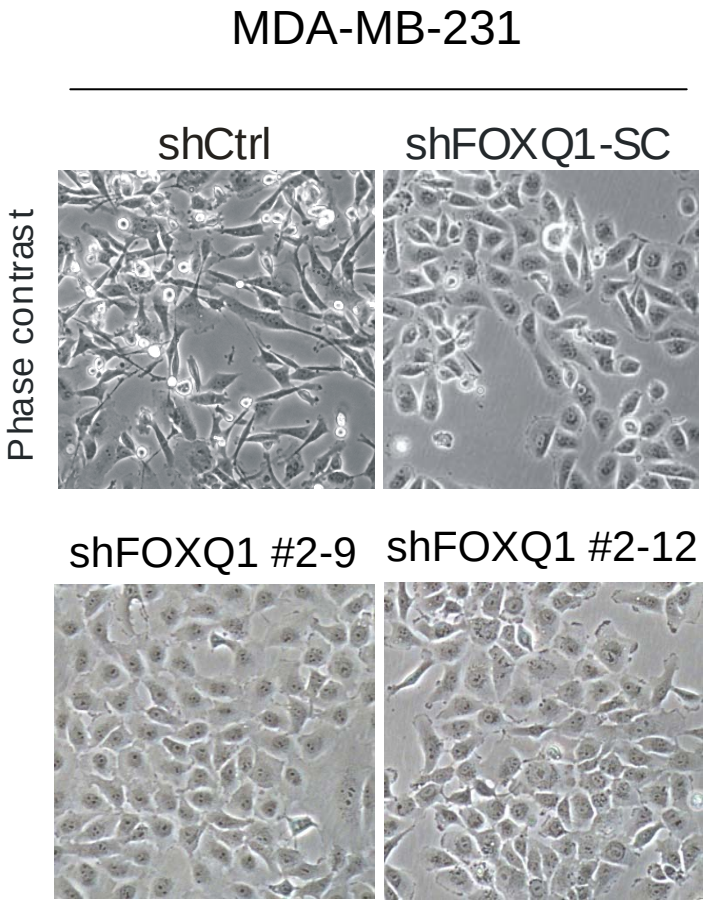

Figure 3.3 Morphological change of MDA-MB-231 cells after depletion of FOXQ1 with various short hairpin RNA sequences and clones.

Coupled with the loss of spindle-like phenotype and acquired pronounced cell-cell interaction and adhesion, related EMT markers E-cadherin and vimentin were then examined in protein and mRNA levels. E-cadherin serves as an epithelial marker which strengthens the bond between cells much like a glue. On the other hand, vimentin is a mesenchymal marker which indicates whether epithelial cells have acquired mesenchymal features. The mRNA level and protein level of these EMT markers were examined in three different FOXQ1 shRNA MDA-MB-231 cell lines. Consistent with the phenotypic change associated with FOXQ1-depletion was an increased expression of epithelial marker E-cadherin (CDH1) and a concomitant down regulation of mesenchymal marker vimentin (Vim) in all three FOXQ1 depletion cell lines (Figure 3.4). However, depending on the levels of FOXQ1 knockdown in the various established cell lines, changes to the EMT markers can be different. Cells expressing shFOXQ1-SC have greater knockdown efficiency than the other two cell lines and also, shFOXQ1-SC cells have more pronounced CDH1 mRNA and protein expression than others. Consistent with E-cadherin changes observed in these three cell lines, vimentin decreased largely in shFOXQ1-SC cells when compared to other cell lines. These E-cadherin and vimentin changes correlated with the degree of FOXQ1 knockdown in MDA-MB-231 cells. Therefore, FOXQ1 depletion could have resulted in a reversal of EMT in MDA-MB-231 cells. In addition, immunofluorescent confocal imaging shown in Figure 3.5 indicated similar alterations in the EMT markers at the level of single cells.

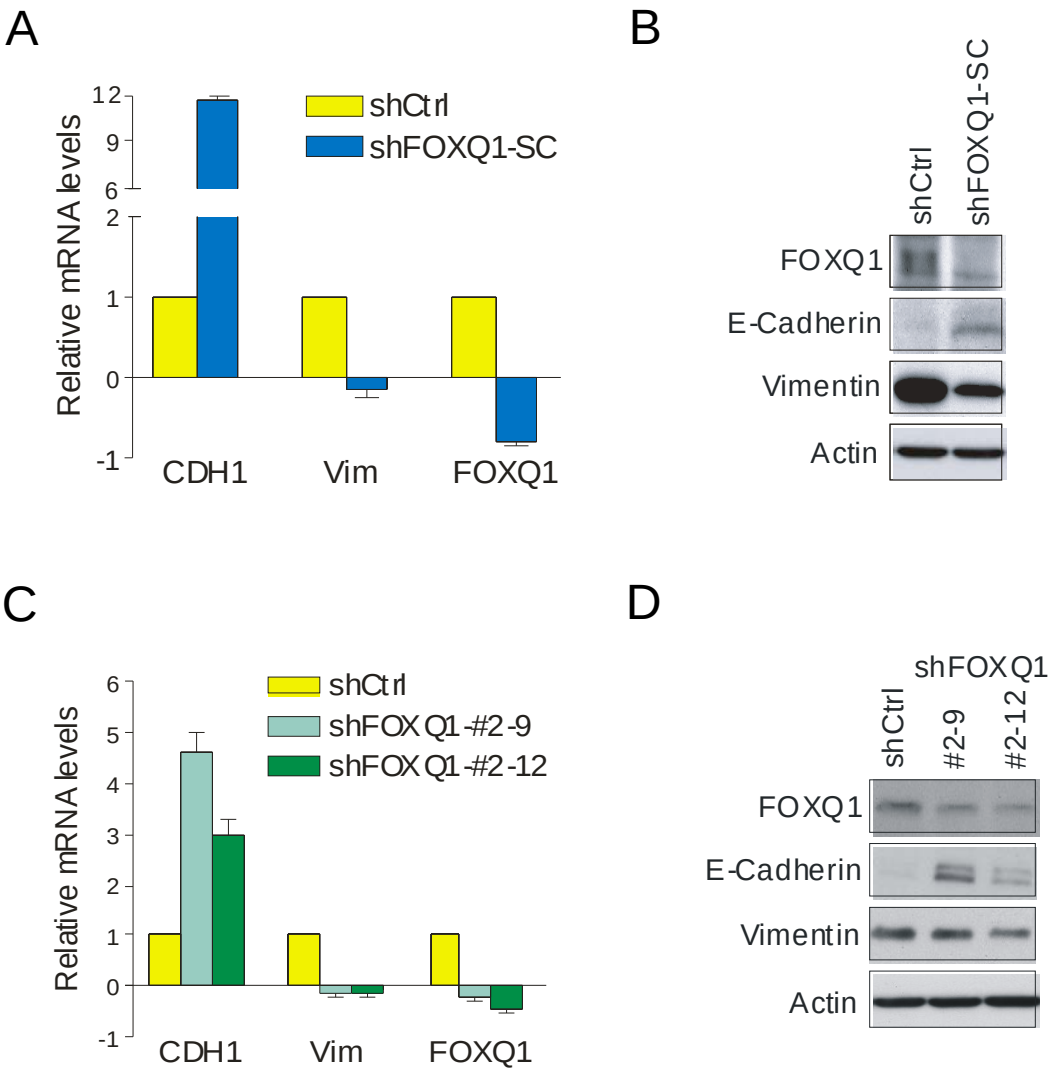

Figure 3.4 mRNA and protein levels of EMT markers and FOXQ1 in MDA-MB-231 FOXQ1 depleted cell lines.

A, Quantitative RT-PCR of CDH1 (E-cadherin), Vim (vimentin), and FOXQ1 mRNA levels in MDA-MB-231 FOXQ1-SC depleted cells.
B, Levels of the indicated proteins in MDA-MB-231 FOXQ1-SC depleted cells.
C, Quantitative RT-PCR of CDH1 (E-cadherin), Vim (vimentin), and FOXQ1 mRNA levels in two other clones of MDA-MB-231 FOXQ1 depleted cells.
D, Levels of the indicated proteins in two other clones of MDA-MB-231 FOXQ1 depleted cells.

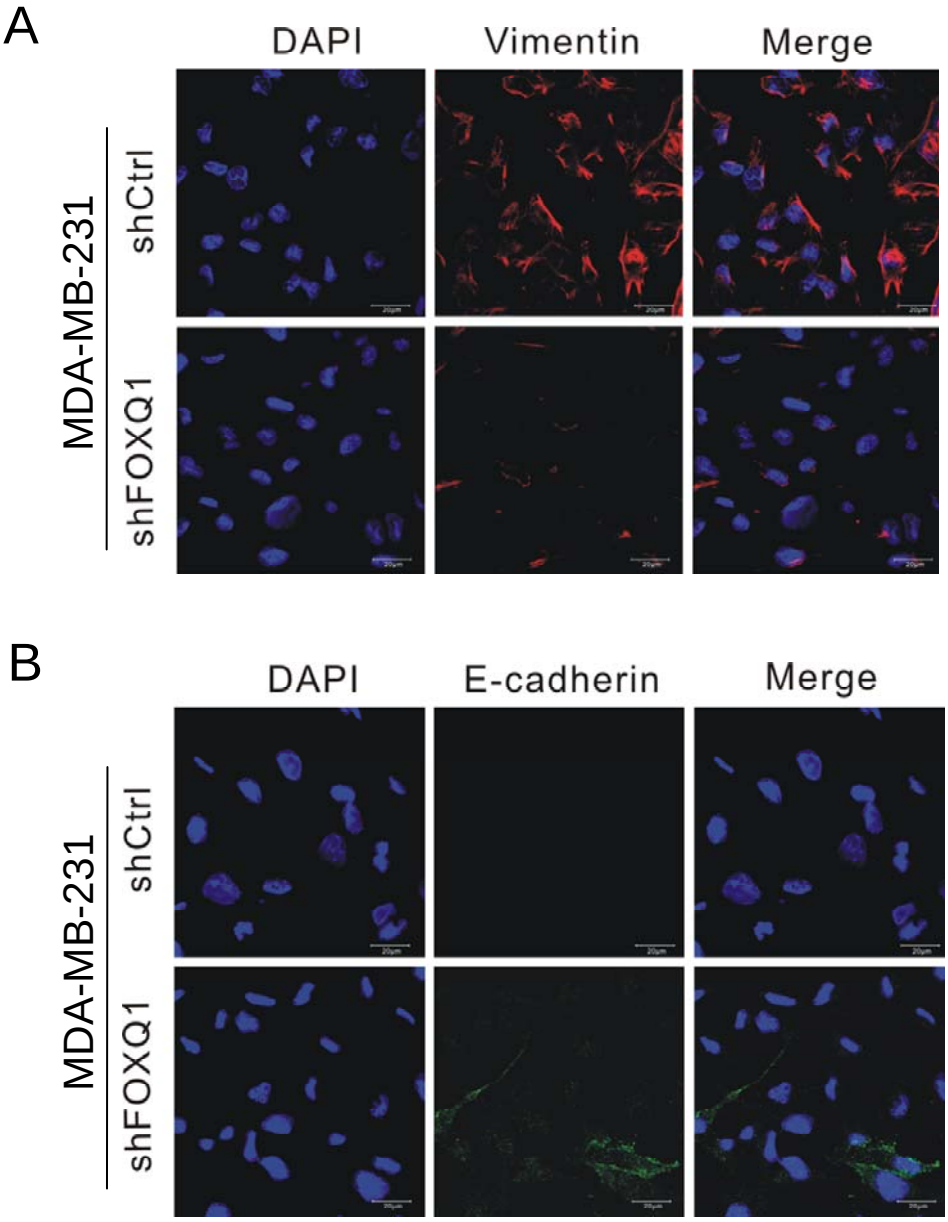

Figure 3.5 Immunofluorescent confocal images of E-cadherin and vimentin in MDA-MB-231 FOXQ1-SC depleted cells.

A, Vimentin (red) is detected by Alexa Fluor 546 and nucleus (blue) is detected by DAPI.
B, E-cadherin (green) is detected by Alexa Fluor 488 and nucleus (blue) is detected by DAPI.

In addition to loss of epithelial marker E-cadherin and gain of mesenchymal marker vimentin upon depletion of FOXQ1 in MDA-MB-231 cells, there is also a functional impact associated with FOXQ1 depletion upon analysis of these cells. In order to assess the invasion ability of MDA-MB-231 cells after FOXQ1 depletion, I used the in vitro transwell invasion assay technique. The representative images in Figure 3.6A indicated that FOXQ1 depletion markedly reduced the invasive ability of MDA-MB-231 cells in terms of number of cells which have crossed through the matrigel-coated membrane. The quantitative result showed that depletion of FOXQ1 in MDA-MB-231 cells attenuated its invasion ability by more than 50% in shFOXQ1-SC cells (Figure 3.6B), as well as two other FOXQ1 shRNA #2-9 and #2-12 expressing cell lines (Figure 3.6C). This reduction of invasion should not be due to reduced cell proliferation rate as FOXQ1 ablation did not change the proliferation rate of shFOXQ1-SC MDA-MB-231 cells (Figure 3.6D).

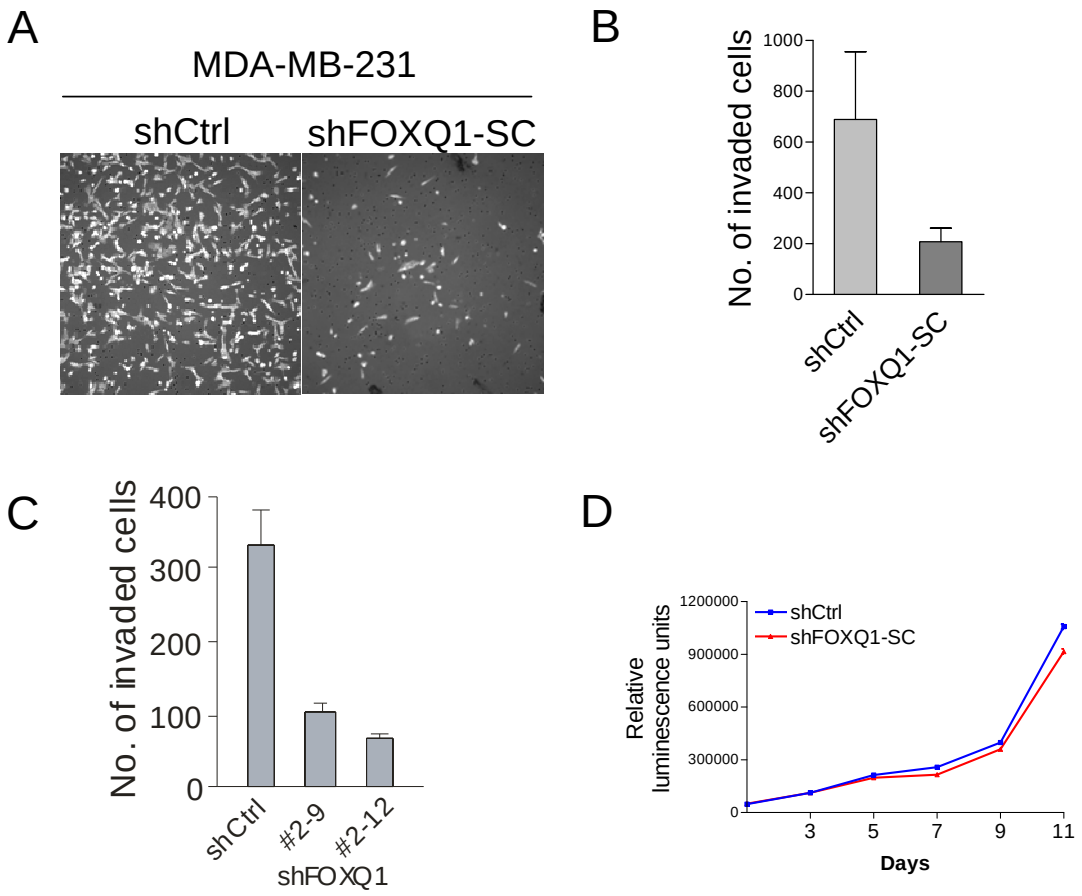

Figure 3.6 FOXQ1 depletion reduced the invasive ability of MDA-MB-231 cells in vitro.

A, Representative view of invaded cells beneath the matrigel-coated membrane for the indicated cell lines.
B, Invaded cells were quantified in FOXQ1-SC cells.
C, Invaded cells were quantified in another two FOXQ1 depleted clones.
D, Proliferation rate of FOXQ1-SC MDA-MB-231 cells.

The ability to differentiate was measured under in vitro condition of 3D matrigel culture. MCF10A, a non-cancerous human mammary epithelial cell line, was able to differentiate into spheroid structure with a lumen which mimics acinar tissue structure in vivo (Figure 3.7C). The black arrow indicates the luminal space of MCF10A tissue cells. The acinar tissue structure will be disrupted in the presence of oncogenic signals such as Ras. Figure 3.7 B shows the 3D tissue structure of MCF10A cells transformed with Ras oncogene relative to an empty vector control. Ras expressing MCF10A cells displayed a spread and aggressive morphology compared to its empty vector (pBabe) control. To assess 3D growth potential in FOXQ1 depleted cells, three different shFOXQ1 MDA-MB-231 cell lines were cultured under conditions of 3D matrigel. The control MDA-MB-231 cells displayed aggressive phenotype by showing highly disorganized structures of cell cluster lacking basal polarity (Figure 3.7A). This aggressive phenotype is similar with the Ras oncogene transformed MCF10A cells (Figure 3.7B). In contrast, MDA-MB-231 cells depleted of FOXQ1 showed more uniform and polarized acinar structures in all three cell lines (Figure 3.7A). Therefore, FOXQ1 depletion in MDA-MB-231 breast cancer cells may attenuate the aggressive phenotype associated with EMT.

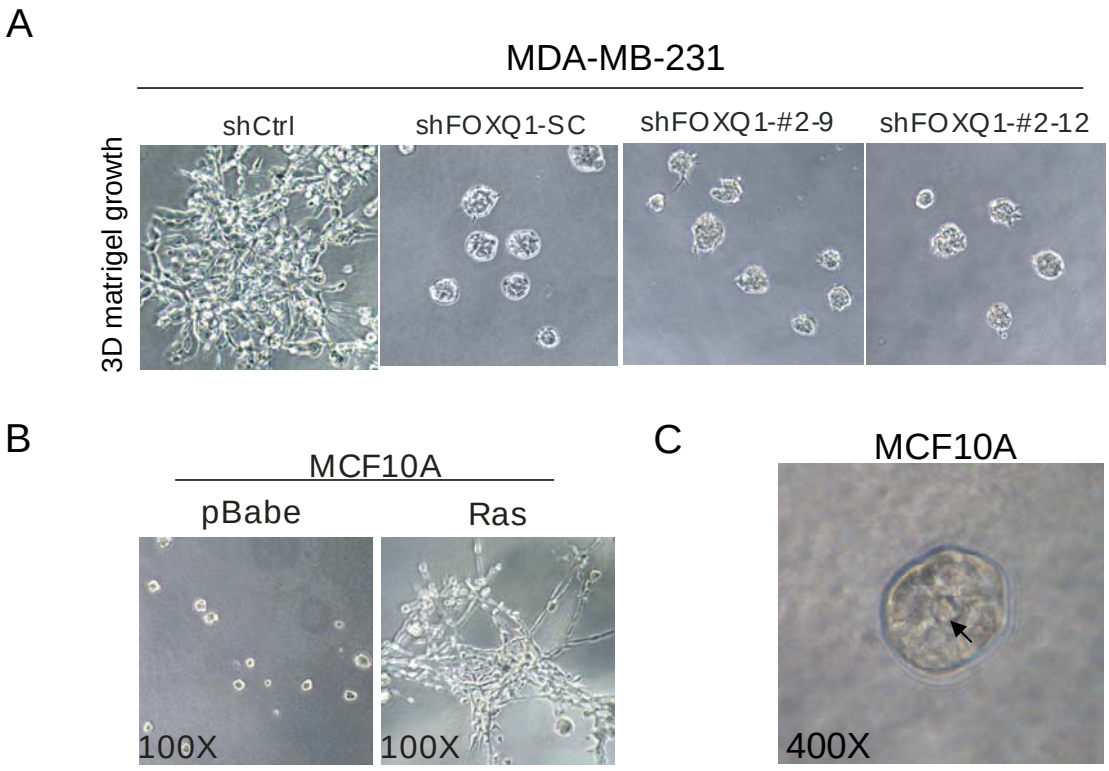

Figure 3.7 3D matrigel growth of MDA-MB-231 FOXQ1 depleted cells.

A, 3D matrigel growth of three MDA-MB-231 FOXQ1 depleted cell lines.
B, MCF10A cells transfected with vector control pBabe or Ras oncoprotein were grown on matrigel.
C, Magnified view of the luminal space enclosed in a ring of MCF10A cells.

3.3 Ectopic FOXQ1 expression in human mammary epithelial cells induces EMT and mammosphere formation

After showing that FOXQ1 has functional regulation of EMT in aggressive MDA-MB-231 cells, I next examined whether ectopic expression of FOXQ1 is able to trigger mesenchymal phenotype in immortalized human mammary epithelial cells. To achieve this, I used a semi-transformed human mammary epithelial cell line (HMLER) as a model which has been previously shown to undergo EMT upon overexpression of EMT regulator such as Snail or Twist. A stable HMLER cell line expressing FOXQ1 was established through retroviral induction (designated as HMLER-FOXQ1). The validation of FOXQ1 expression in cell lines with the appropriate matching controls is shown in Figure 3.9 by RT-PCR and quantitative PCR. While the HMLER cells expressing a control vector (HMLER-pMN) retained an epithelial morphology with tight cell-to-cell adhesion, in contrast, HMLER-FOXQ1 cells displayed an elongated morphology typically associated with mesenchymal phenotype (Figure 3.8). These morphological changes in HMLER-FOXQ1 cells were accompanied by a marked reduction of E-cadherin (CDH1) expression and increased expression of vimentin (Vim) at both mRNA and protein levels (Figure 3.10). The immunofluorescent confocal imaging showed the loss of E-cadherin at the cell boundary and gain of vimentin in HMLER-FOXQ1 cells (Figure 3.11) at single cell level. These findings suggested that ectopic expression of FOXQ1 in HMLER cells can result in induction of EMT.

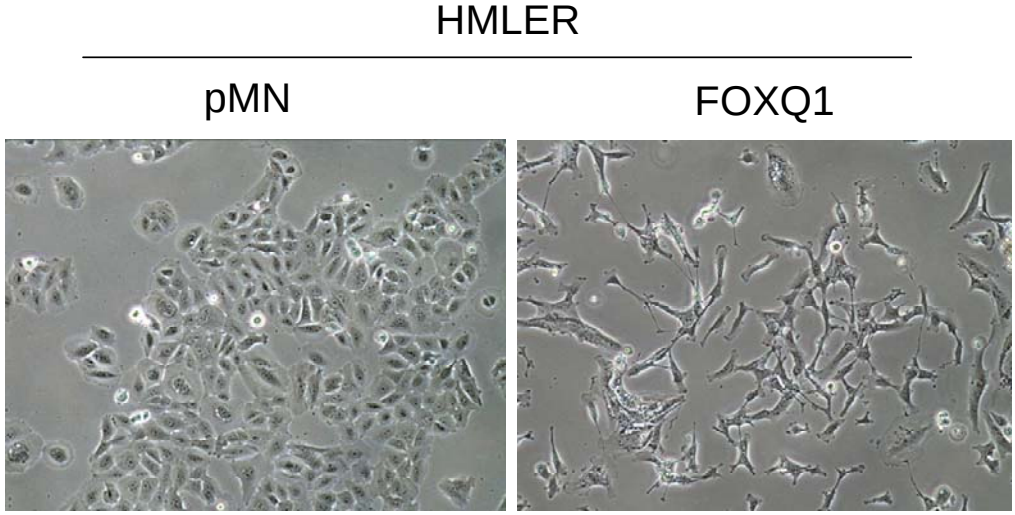

Figure 3.8 Ectopic expression of FOXQ1 in HMLER cells led to gain of mesenchymal morphology and loss of epithelial phenotype.

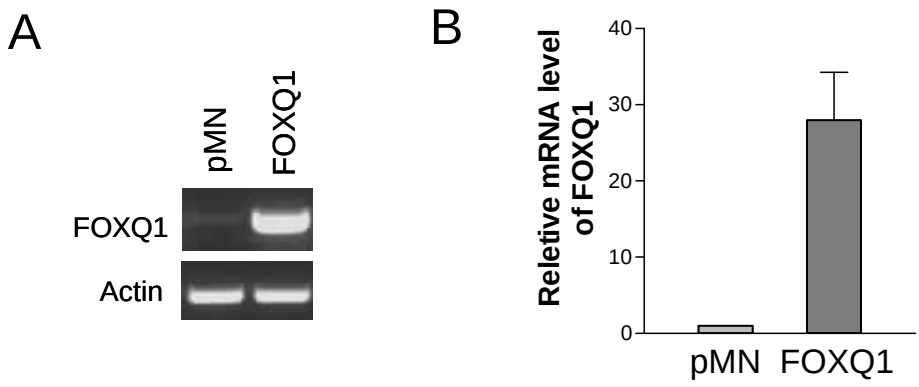

Figure 3.9 Validation of ectopic FOXQ1 expression in HMLER cells.

A, RT-PCR using FOXQ1 specific primers in vector control cells HMLER-pMN, and FOXQ1 expressing cells HMLER-FOXQ1.
B, Quantitative PCR using FOXQ1 Taqman probe for mRNA of above cell lines.

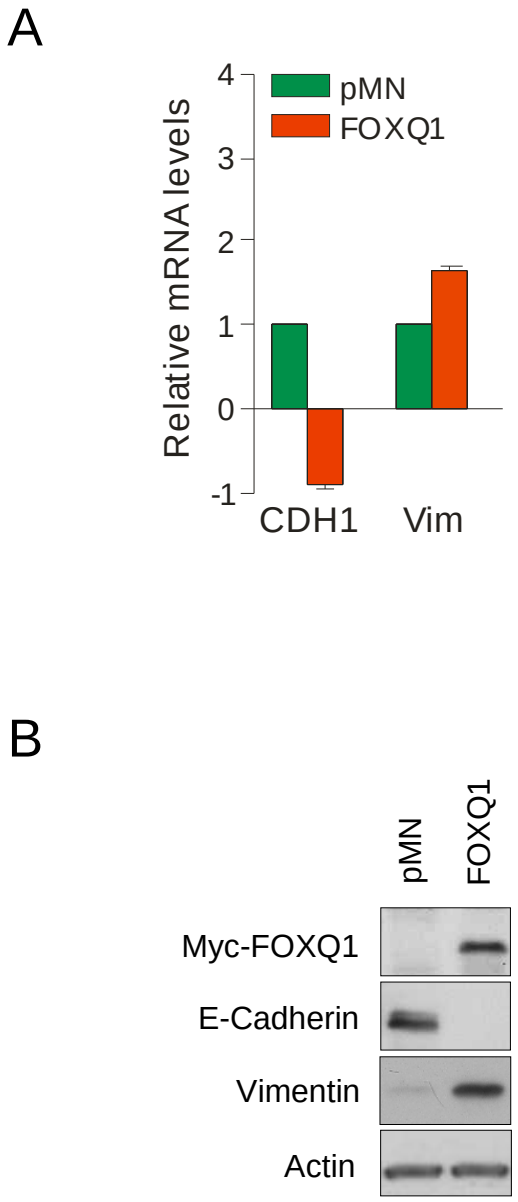

Figure 3.10 Changes in the level of EMT markers which accompanied FOXQ1-induced EMT in HMLER cells.

A, Quantitative PCR of CDH1 (E-cadherin) and Vim (vimentin) in HMLER cells, carrying empty vector pMN or FOXQ1 overexpression vector.
B, Western blot analysis showing protein levels of EMT markers in both pMN and FOXQ1 cells.

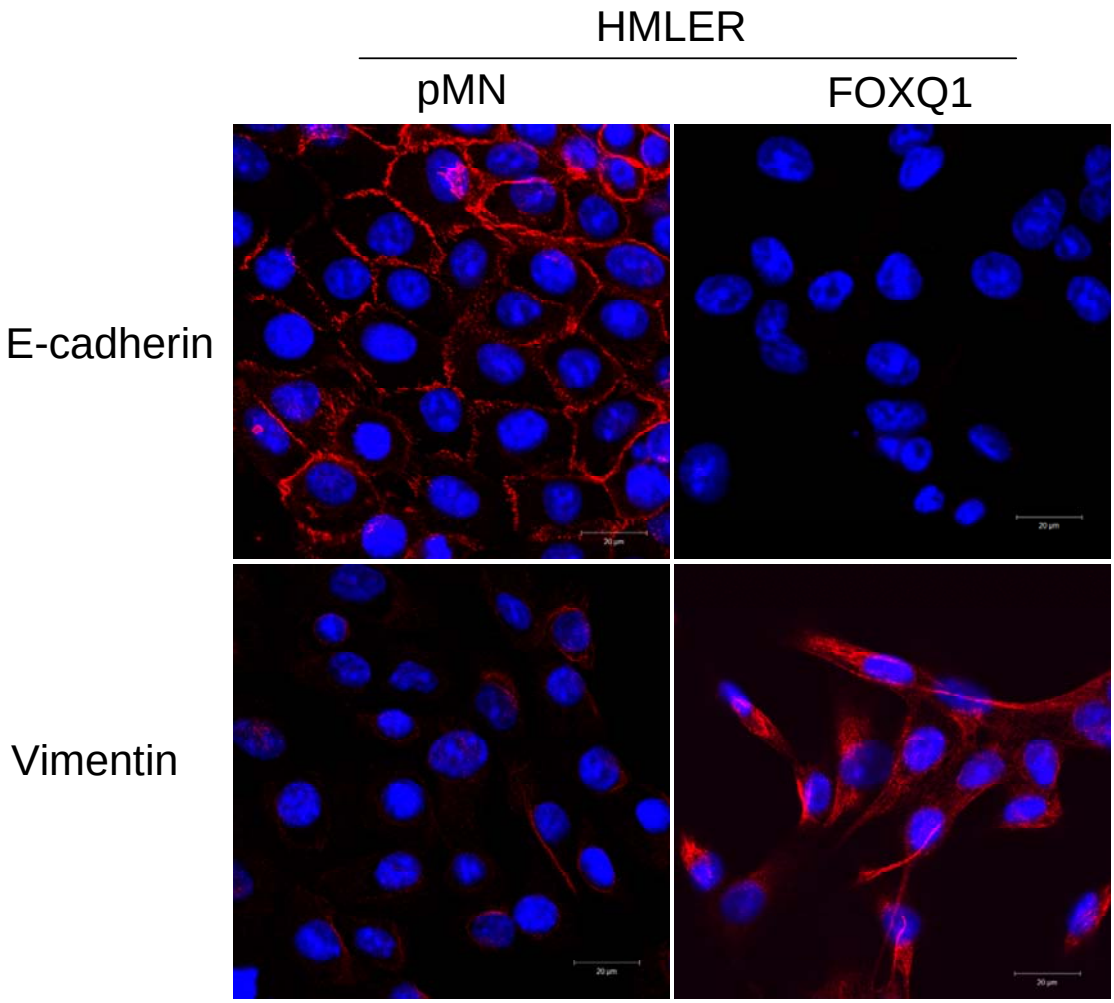

Figure 3.11 Immunofluorescent confocal images of EMT markers in HMLER cells expressing control vector or FOXQ1.

Both E-cadherin and vimentin were stained with Alexa Fluor 546 in red color, and nucleus is stained by DAPI in blue.

Recent studies have shown that human mammary epithelial cells undergoing EMT often exhibit a gain of stem cell-like characteristics, including increased expression of breast stem cell marker CD44, and reduced expression of CD24, as well as enhanced capacity to form spherical colonies in suspension cultures, termed tumor mammospheres. To test whether FOXQ1 overexpression in HMLER cells can also result in similar stem cell-like properties, I assessed the alterations in expression of CD44 and CD24 in HMLER-FOXQ1 cells as well as the cell's capacity to form mammospheres. Indeed, HMLER-FOXQ1 cells expressed increased levels of CD44 and reduced CD24 as compared to the control cells (Figure 3.12) in both mRNA and protein levels and formed significantly larger numbers of mammospheres when cultured in suspension using a mammosphere formation assay (Figure 3.13A and B). The formed mammosphere populations were found to be further enriched in protein levels of FOXQ1 as well as CD44, which supports a role of FOXQ1 in driving the formation of mammosphere (Figure 3.13C). Taken together, I propose that FOXQ1 induced EMT in HMLER cells endowed these cells with breast cancer stem cell-like characteristics. Hence, FOXQ1 is believed to be a positive regulator in breast cancer pathology.

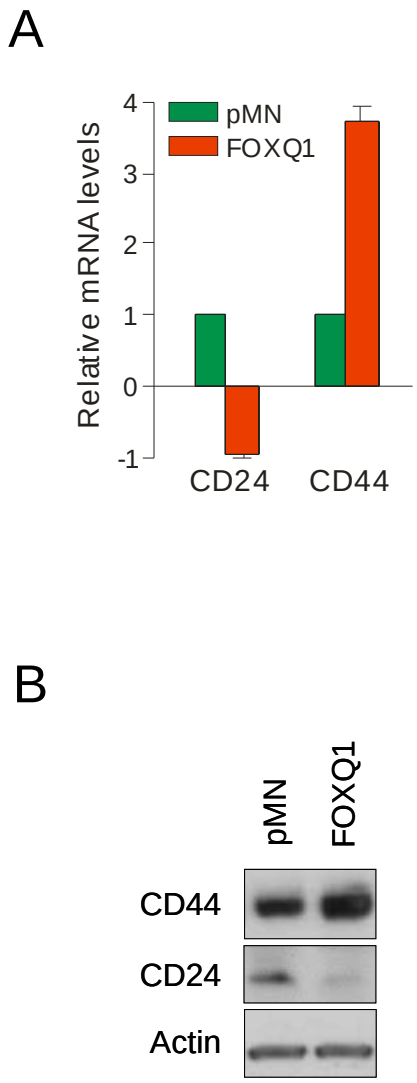

Figure 3.12 Breast cancer stem cell marker changes in HMLER cells expressing either vector control or FOXQ1.

A, Quantitative PCR measuring CD24 and CD44 mRNA levels in HMLER cells expressing either control vector or FOXQ1.
B, Western blot analysis measuring protein levels of CD24 and CD44 in indicated cells.

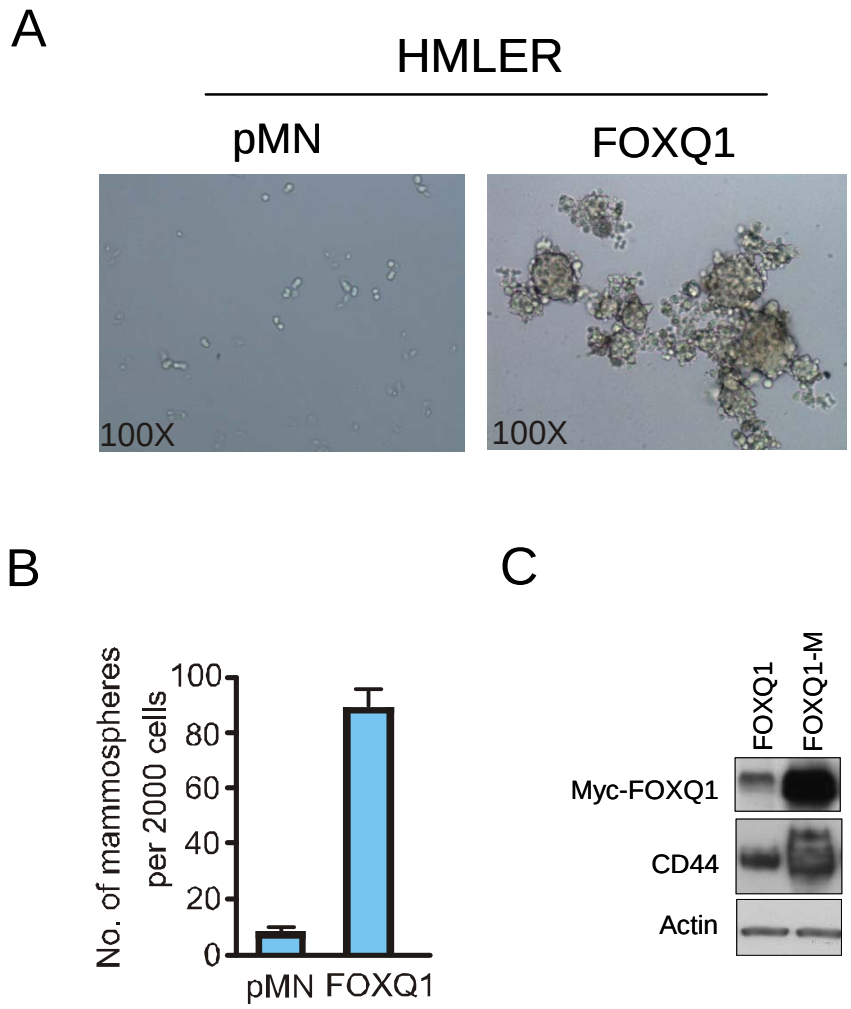

Figure 3.13 Ectopic expression of FOXQ1 in HMLER cells led to gain of stem cell-like characteristics.

A, Mammosphere formation in indicated cultured cell lines at day 7.
B, Quantification of formed mammosphere in indicated cell lines.
C, Protein levels of myc-tagged FOXQ1 and CD44 were measured in mammosphere population (FOXQ1-M).

Consistent with an established role of E-cadherin depletion in EMT induction in mammary epithelial cells, I showed that E-cadherin knockdown in HMLER cells led to the establishment of a mesenchymal-like morphology (Figure 3.14A). Depletion of E-cadherin was sufficient to induce EMT and mammosphere formation (Figure 3.14B), with corresponding changes in levels of vimentin, CD44 and CD24 (Figure 3.15B). Thus, the deletion of E-cadherin could be a functionally relevant target of FOXQ1 in EMT induction. Collectively, these findings suggested that FOXQ1 is able to induce EMT and stem cell-like characteristics, further supporting an oncogenic role for FOXQ1 in aggressive breast cancers.

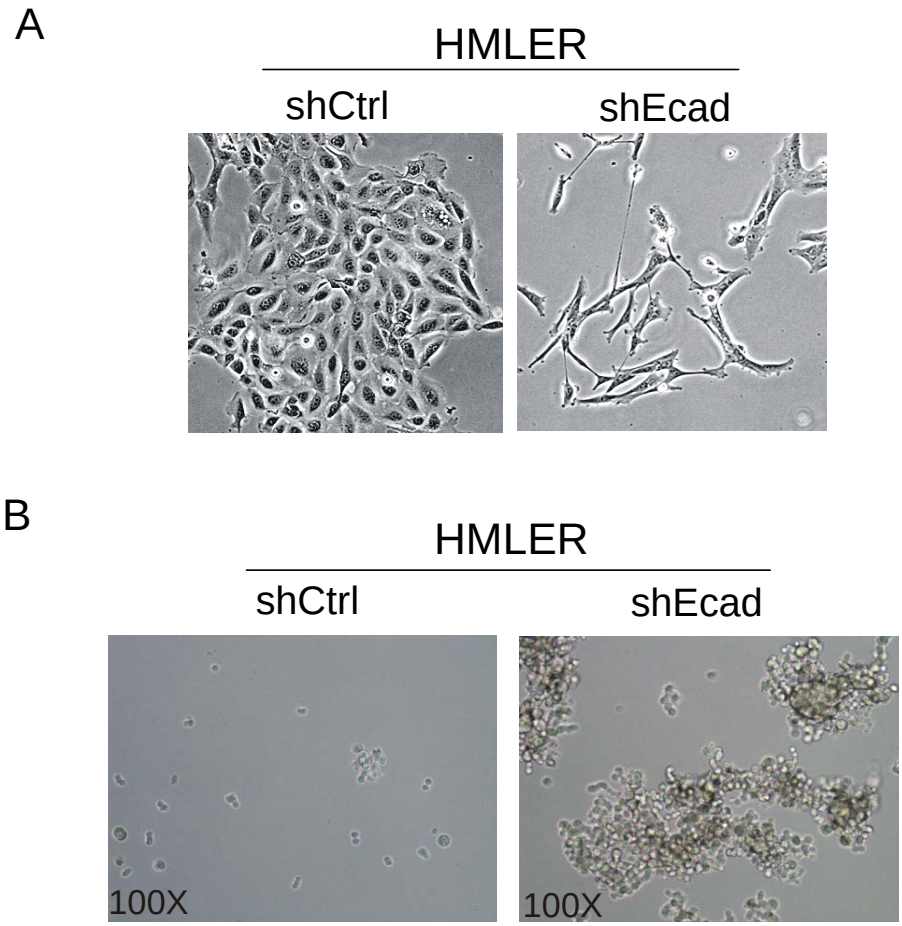

Figure 3.14 Morphology and mammosphere formation of E-cadherin knockdown HMLER cells.

A, Morphological change in control (shCtrl) and E-cadherin knockdown (shEcad) HMLER cells.
B, Mammosphere formation by the respective cells.

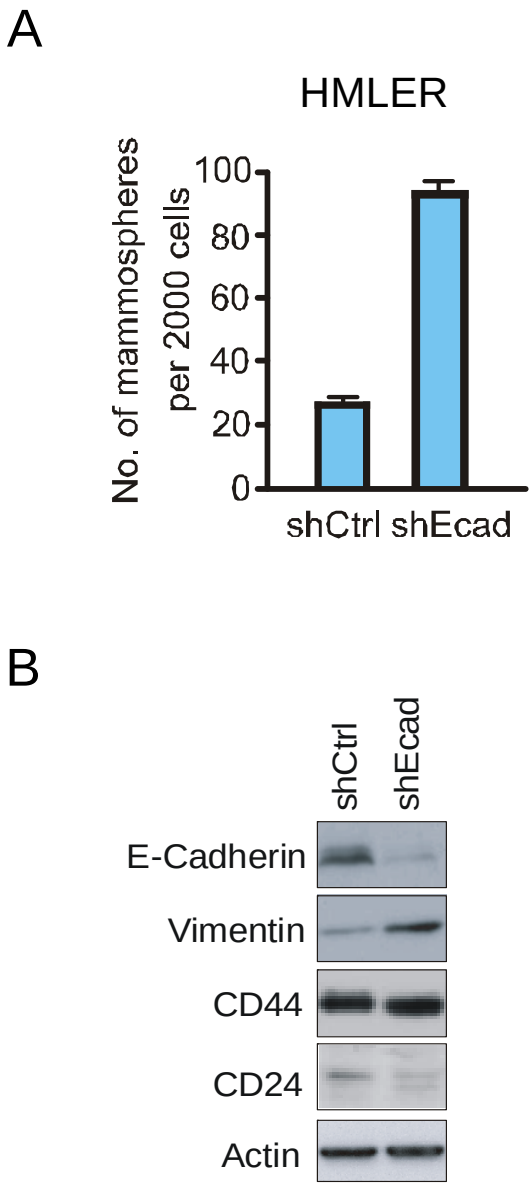

Figure 3.15 E-cadherin knockdown in HMLER cells induces EMT and stem cell-like traits.

A, Quantification of mammospheres formed in HMLER cells in vector control (shCtrl) and E-cadherin knockdown (shEcad) samples.
B, Western blot analysis of EMT and stem cell markers in the above cell lines.

3.4 Depletion of FOXQ1 expression in MDA-MB-231 cells increases sensitivity to chemotherapy-induced apoptosis

Cancer cells undergoing EMT has recently been connected to chemoresistance, which has been observed in FOXQ1 overexpressing colon cancers in Chapter 4. Hence I next investigated whether FOXQ1 has a role to play in apoptosis induced by DNA-damaging agents in shFOXQ1-SC MDA-MB-231 breast cancer cells. I found that FOXQ1 depletion in MDA-MB-231 cells resulted in increased apoptotic response (more than 50%) to a series of chemotherapeutic drugs, including 5-Flurouracil (5FU), paclitaxel (Taxol) and camptothecin (CPT) in a dose-dependant manner, as assessed by Caspase 3 activation assay through FACS analysis (Figure 3.16). Hence, these results showed that FOXQ1 deregulation not only induced EMT but also could be a potential therapeutic target to modulate resistance to drug-induced apoptosis.

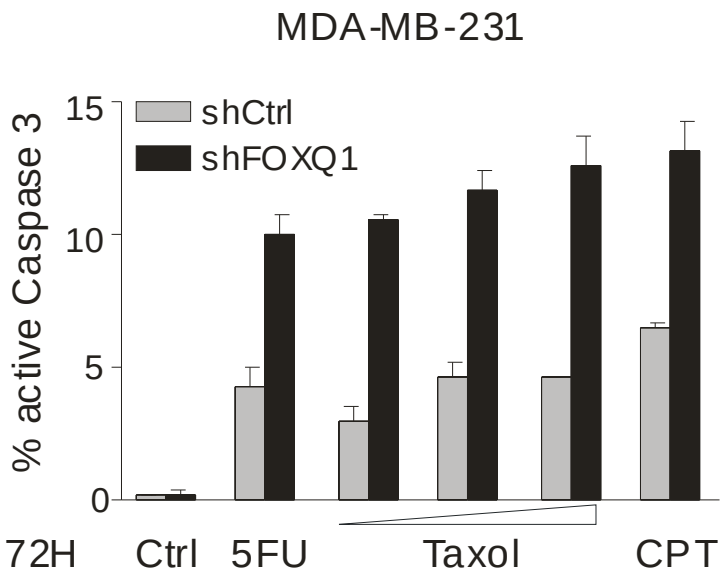

Figure 3.16 FOXQ1 depletion in MDA-MB-231 cells increases their drug sensitivity in a dose-dependent manner.

Active Caspase 3 activity was measured after treatment using 375 µM of 5FU; 0.5 µM, 1 µM and 2 µM of Taxol; and CPT for 72 hours.

3.5 FOXQ1 mediated transcription network in breast cancer cells

Since EMT regulation by transcription factor FOXQ1 has been observed in both FOXQ1 overexpression and knockdown system, therefore, I sought to identify the transcriptional network regulated by FOXQ1.

Microarray gene expression analysis was performed in both FOXQ1 overexpression (HMLER) and knockdown (MDA-MB-231) systems. I planned to identify two set of genes in which one is positively regulated by FOXQ1, and the other is negatively regulated by FOXQ1. To achieve this, genes upregulated in HMLER-FOXQ1 as compared to HMLER-pMN control were overlapped with those that were downregulated upon FOXQ1 knockdown in MDA-MB-231 cells. Using this method, I was able to identity the gene set positively regulated by FOXQ1. Conversely, those FOXQ1 negatively regulated gene set can then be obtained by using reverse analysis. The Venn Diagram in Figure 3.17A shows the gene sets upregulated and downregulated by FOXQ1 respectively. Among the genes upregulated in HMLER-FOXQ1 versus HMLER control (a) and genes downregulated in MDA-MB-231 shFOXQ1 versus MDA-MB-231 shControl (b), there are a total of 63 genes that co-presented in both parts, and these 63 genes were designated as ‘set I’ which is positively regulated by FOXQ1 (Figure 3.17A left panel). In the right panel of Figure 3.17A, the genes downregulated in HMLER-FOXQ1 versus control (c) and the genes upregulated in MDA-MB-231 shFOXQ1 versus shControl (d) (using 5-fold cut off) were over lapped and it turns out there were 206 genes that co-presented in both parts, and these 206 genes were designated as ‘set II’ which is negatively regulated by FOXQ1. Next, these two sets of genes were clustered by GeneSpring (Figure 3.17B),

and the full list of genes was subjected to pathway analysis by Ingenuity Pathway Analysis (IPA) and their top function affected by FOXQ1 is listed in the lower panel of Figure 3.17B. After comparing the two sets of genes, I found there were more FOXQ1 negatively regulated genes than positively regulated ones, suggesting that the main role of FOXQ1 in breast cancer regulation could be to repress certain gene expressions rather than to activate gene expressions. In the list of functions affected, cell morphology was at the top which is consistent with my observation of EMT phenotype induced by FOXQ1. Gene Ontology (GO) analysis revealed that genes downregulated by FOXQ1 were most enriched for gene sets related to cell morphology or migration and motility, thus supporting a functional role of FOXQ1 in regulation of EMT.

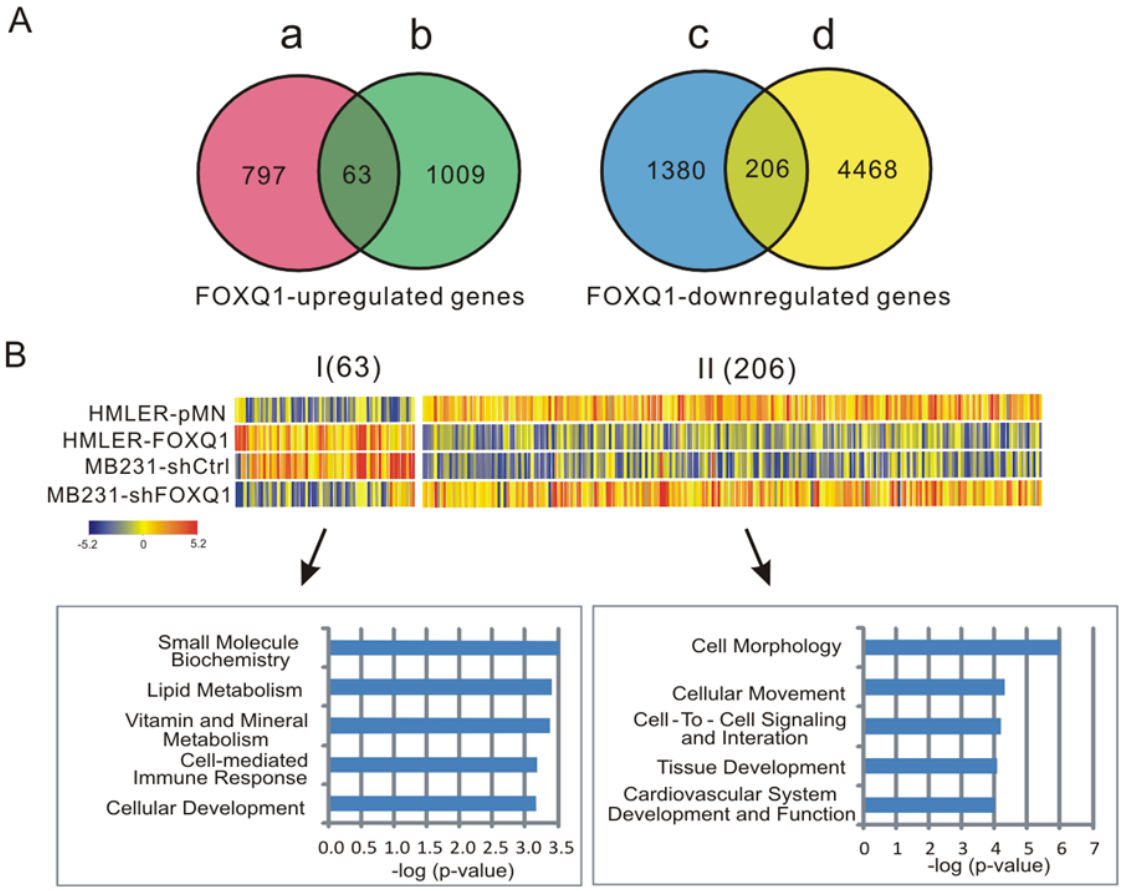

Figure 3.17 Gene expression program associated with FOXQ1 expression.

A, Venn Diagram showing the gene sets upregulated and downregulated by FOXQ1 respectively. a, genes upregulated in HMLER-FOXQ1 versus HMLER control; b, genes downregulated in MDA-MB-231 shFOXQ1 versus MDA-MB-231 shControl; c, genes downregulated in HMLER-FOXQ1 versus HMLER control; d, genes upregulated in MDA-MB-231 shFOXQ1 versus MDA-MB-231 shControl.
B, Gene clustering showing two sets of genes that are upregulated (I) and downregulated (II) by FOXQ1, respectively (upper panel). The lower panel shows the Gene Ontology (GO) analysis of the two gene sets by Ingenuity Pathway Analysis. The top five gene functions were listed.

3.6 FOXQ1 represses E-cadherin transcription in breast cancer cells

The gene network among the cell morphology subset were extracted from IPA and shown in Figure 3.18. Interestingly, the network showed that CDH1 (E-cadherin) is located in the centre. CDH1 is also found to be transcriptional regulated in FOXQ1-induced EMT, further confirming the importance of E-cadherin-associated gene expression program in FOXQ1-induced EMT.

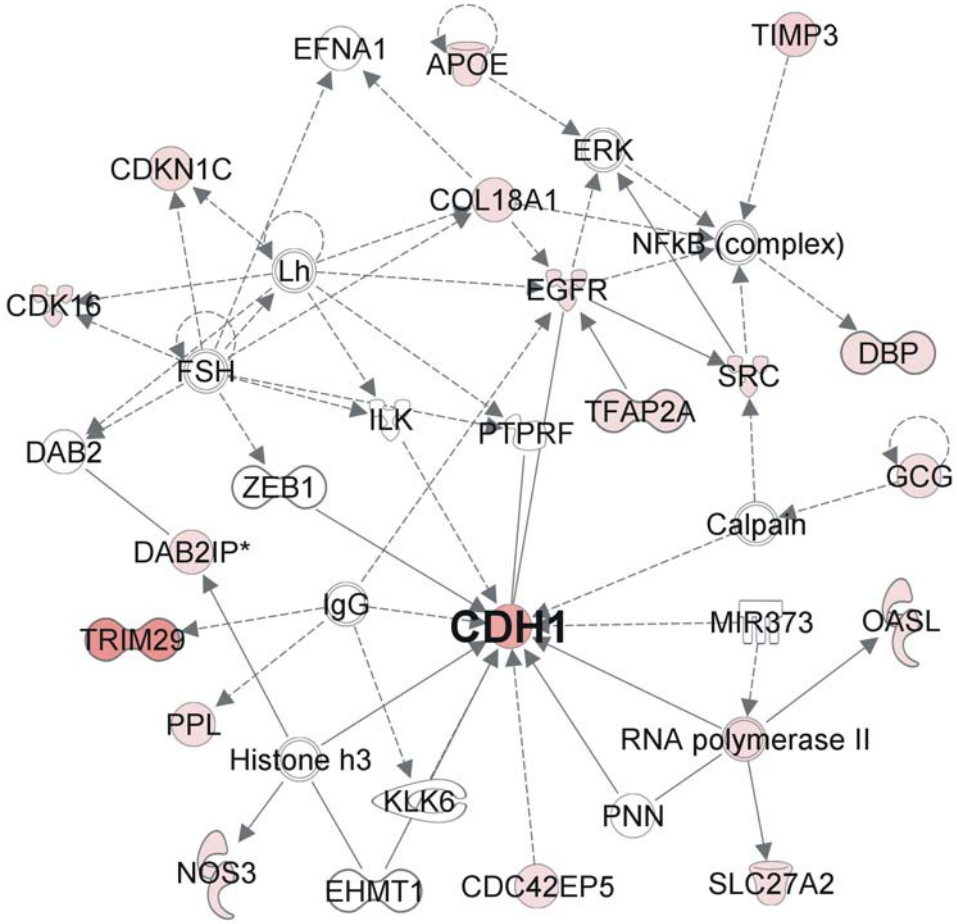

Figure 3.18 Ingenuity Pathway Analysis (IPA) showing the top network of FOXQ1-downregulated genes with CDH1 as a central node.

To determine whether FOXQ1 inhibits E-cadherin transcription, a promoter region of CDH1 (encoding E-cadherin) is cloned and reporter assays were performed (Figure 3.19A) in both HMLER overexpression and MDA-MB-231 knockdown systems. As expected, CDH1 promoter activity is repressed in HMLER-FOXQ1 cells, and increased in MDA-MB-231 FOXQ1 knockdown cells. This indicated that CDH1 transcription activity is repressed during FOXQ1-induced EMT process. However, the question of whether CDH1 is directly regulated by FOXQ1 still remains. In HMLER overexpression system, chromatin immunoprecipitation (ChIP) was preformed using anti-myc antibody to precipitate ectopically expressed myc-tag FOXQ1 protein, and its binding to different CDH1 promoter regions were examined. However, ChIP results did not show any convincing binding between FOXQ1 and CDH1 promoter (Figure 3.20). This suggested that E-cadherin is not a direct transcriptional target of FOXQ1, and the downregulation of E-cadherin in FOXQ1-induced EMT could be caused by certain intermediate player regulated by FOXQ1.

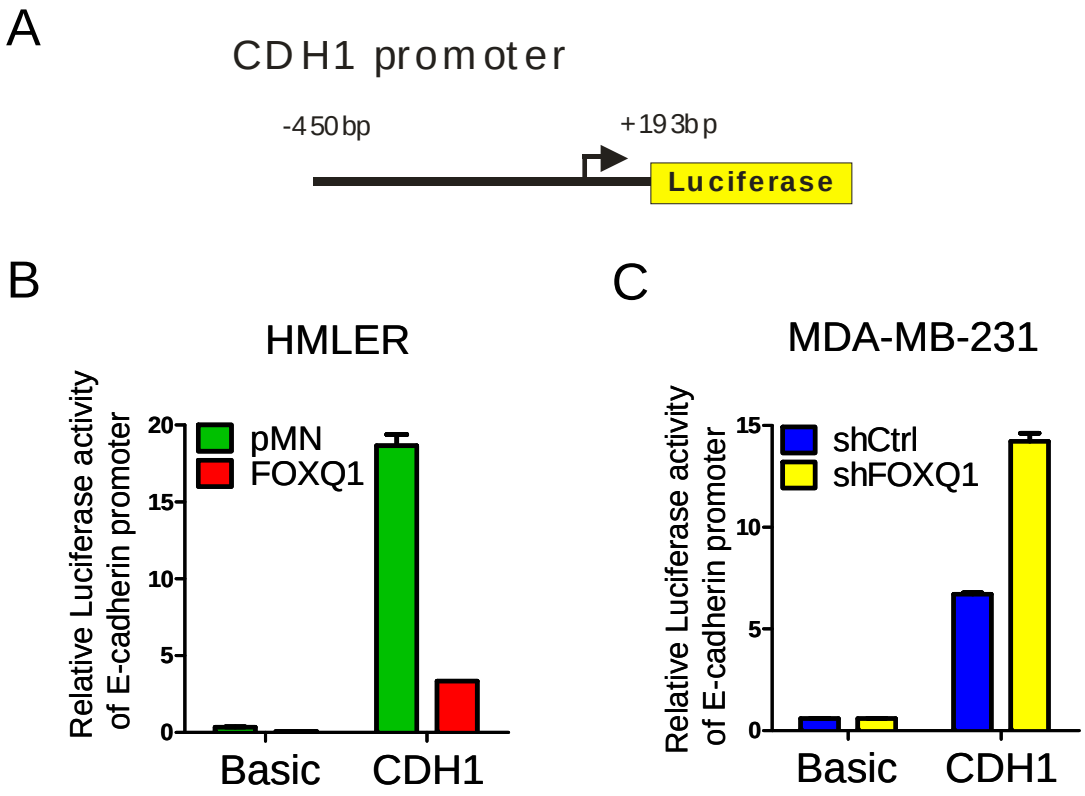

Figure 3.19 CDH1 promoter activity is negatively regulated by FOXQ1.

A, Schematic structure of CDH1 promoter region.
B, E-cadherin (CDH1) promoter reporter activities were measured in HMLER control or FOXQ1 expressing cells.
C, E-cadherin (CDH1) promoter reporter activities were measured in MDA-MB-231 control or FOXQ1 knockdown cells.

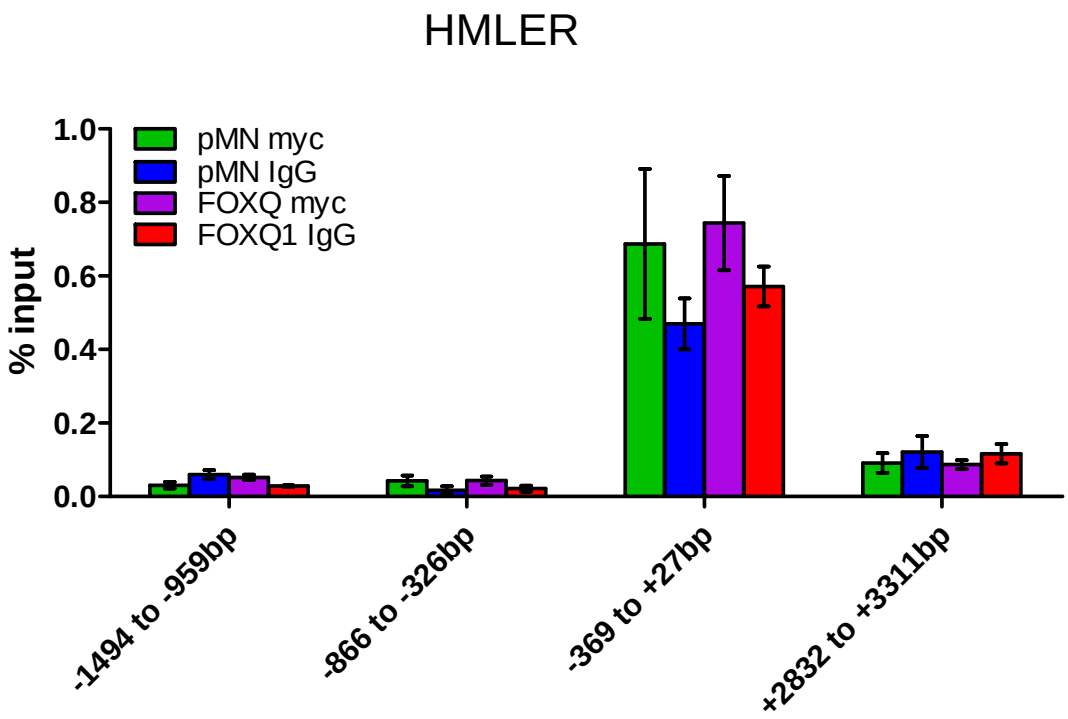

Figure 3.20 ChIP assay of FOXQ1 on the promoters of CDH1 in HMLER FOXQ1 overexpression cells.

3.7 Summary

In breast cancer, FOXQ1 is found to be correlated with its aggressive basal-like subtype. FOXQ1's expression is associated with worse tumor grade, more metastasis, and poor survival outcomes. Among various breast cancer cell lines, FOXQ1 expression is coupled with basal-like aggressive mesenchymal-like MDA-MB-231 cells. Therefore, FOXQ1 should have significant clinical relevance to aggressive basal-like subtype of breast cancers. In this study, the functional role of FOXQ1 in breast cancer was investigated in both the knockdown and overexpression system.

In MDA-MB-231 cells, depletion of FOXQ1 is able to attenuate the mesenchymal phenotype in terms of increased cell-cell connection and decreased spindle shapes. This phenotypic change results in impaired invasive ability in vitro. In addition, knockdown of FOXQ1 in MDA-MB-231 cells sensitized these cells to chemotherapeutic drug induced apoptosis. Considering the expression profile of FOXQ1 in aggressive breast cancer and the sensitization effect observed in FOXQ1 depleted cells, I propose that FOXQ1 could be a potential drug target against breast cancer, and may serve as a biomarker specifically for potentially invasive breast cancers. In the ectopic HMLER overexpression system, FOXQ1 successfully triggered the EMT phenotype in these cells. Together with EMT, HMLER-FOXQ1 cell gained the ability to form mammosphere, and also expressed breast cancer stem cell markers CD44+/CD24-. These pointed out that ectopic expression of FOXQ1 in HMLER induce these cells to de-differentiate and become breast cancer stem cells. My results are consistent with current literature on EMT induction of cancer stem cell formation. Moreover, direct E-cadherin knockdown in HMLER also showed a similar

outcome with respect to HMLER-FOXQ1 cells. Together, FOXQ1 is believed to be an important gene in regulating breast caner progression and metastases by triggering EMT process and development of gain breast cancer stem cell characteristics.

The transcriptional network mediated by FOXQ1 in breast cancer was analyzed. From gene ontology analysis, CDH1 was shown to play an important functional role in FOXQ1-induced EMT network. However, other well-known EMT inducers are not significantly affected. At the transcriptional level, CDH1 promoter activity was upregulated in HMLER-FOXQ1 cells, and downregulated in FOXQ1 depletion MDA-MB-231 cells. However, the chromatin immunoprecipitation analysis did not show pronounced binding between FOXQ1 and CDH1 promoter. Hence, whether or not CDH1 is directly transcriptional regulated via transcription by FOXQ1 or regulated via other novel intermediate players during FOXQ1-induced EMT remains to be elucidated.

However, the observed EMT phenotype and stem cell-like traits driven by FOXQ1 were not seen in other normal human mammary epithelial cell lines such as MCF10A and HMEC. In MCF10A and HMEC cells, ectopic overexpression of FOXQ1 by using the same retroviral expression system did not result in any visible mesenchymal morphology as compared with the empty vector control (Figure 3.20). Besides the absence of EMT, ectopic overexpression of FOXQ1 in MCF10A cells also did not change protein levels of epithelial marker E-cadherin and mesenchymal marker vimentin. Finally, there was no significant change observed in breast cancer stem cell markers CD44 and CD24. In HMEC cells, ectopic FOXQ1 overexpression also did not trigger EMT phenotype. In contrast, HMEC FOXQ1 overexpressing cells showed

elevated E-cadherin protein and decreased vimentin expression, both of which are enhanced epithelial traits. CD44 was found increased and CD24 decreased in HMEC. However, these changes in CD44 and CD24 were not coupled to increased mammosphere formation in vitro.

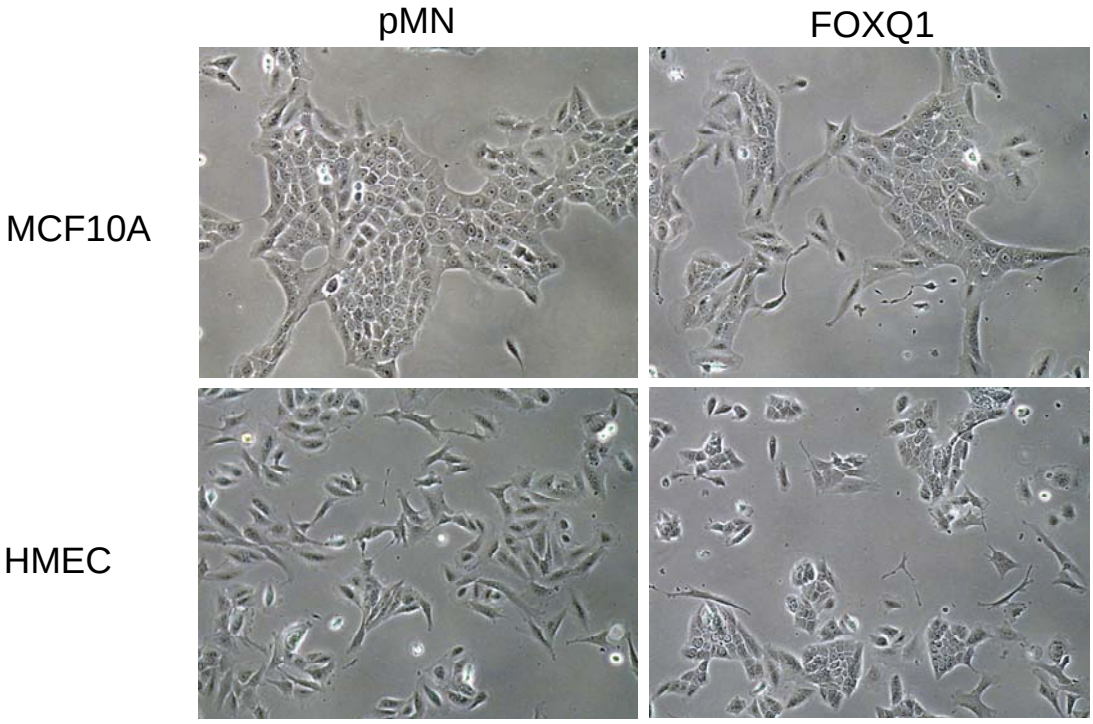

Figure 3.21 Morphology of MCF10A and HMEC cells with ectopic expressing vector pMN and FOXQ1.

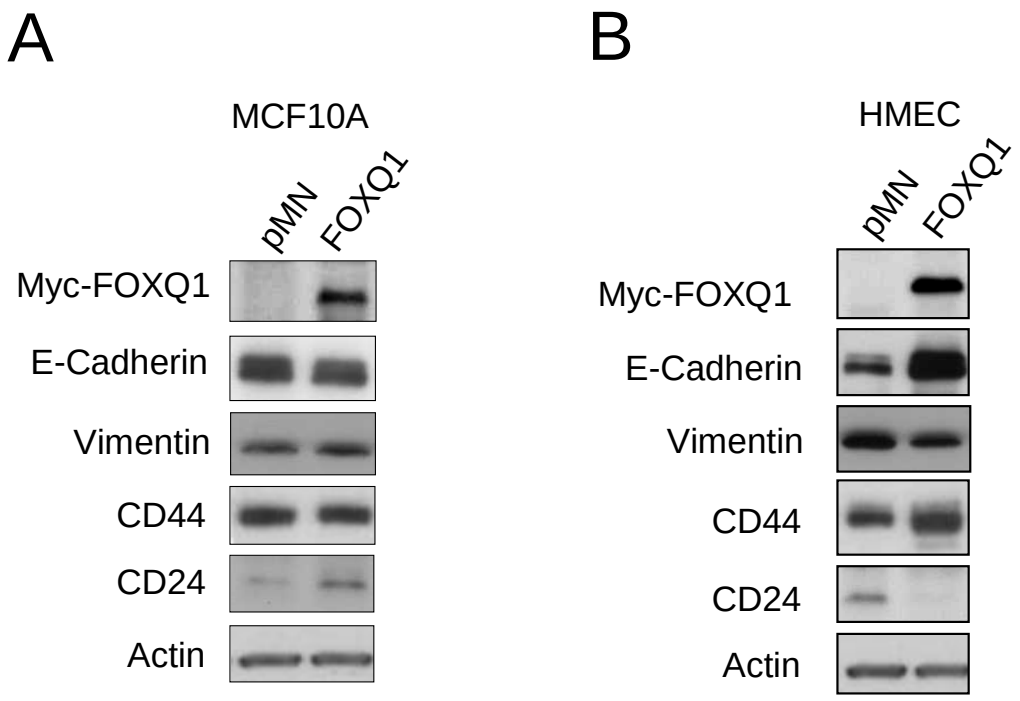

Figure 3.22 Protein levels of EMT and breast cancer stem cell markers in MCF10A and HMEC cells with ectopic expressing vector control pMN and FOXQ1.

CHAPTER 4:

FUNCTIONAL CHARACTERIZATION OF FOXQ1 IN COLON CANCER

In the previous chapter, I have shown evidence to suggest that FOXQ1 was capable of regulating human mammary epithelial cell plasticity. In addition, FOXQ1 was also required for maintenance of mesenchymal phenotype linked to MDA-MB-231 cell invasion. In the following chapter, I shall investigate the function of FOXQ1 in colorectal carcinoma cells.

4.1 FOXQ1 is overexpressed in colon cancer

Exploring our previously published data on microarray gene expression profiling of 24 pairs of clinical human colon tumor and matched normal mucosa tissue samples (Jiang, Tan et al. 2008), FOXQ1 was found to be highly expressed in colon tumors compared with paired normal tissues. As shown in gene clustering analysis of microarray data, FOXQ1 together with CCND1 and MYC were overexpressed in tumor samples compared to normal counterparts (Figure 4.1A). To further validate the array data, RT-PCR analysis was performed in 8 randomly selected pairs. The DNA agrose gel electrophoresis results in Figure 4.1B indicated that FOXQ1 gene is overexpressed in all 8 paired tumor samples. Together with microarray gene expression analysis, overall results indicated that expression of FOXQ1 in human colon tumors was elevated. The expression status of FOXQ1 in colon tumors suggests that this gene may play an oncogenic role. To further validate the expression level of FOXQ1 in colorectal cell lines, the following experiments were carried out.

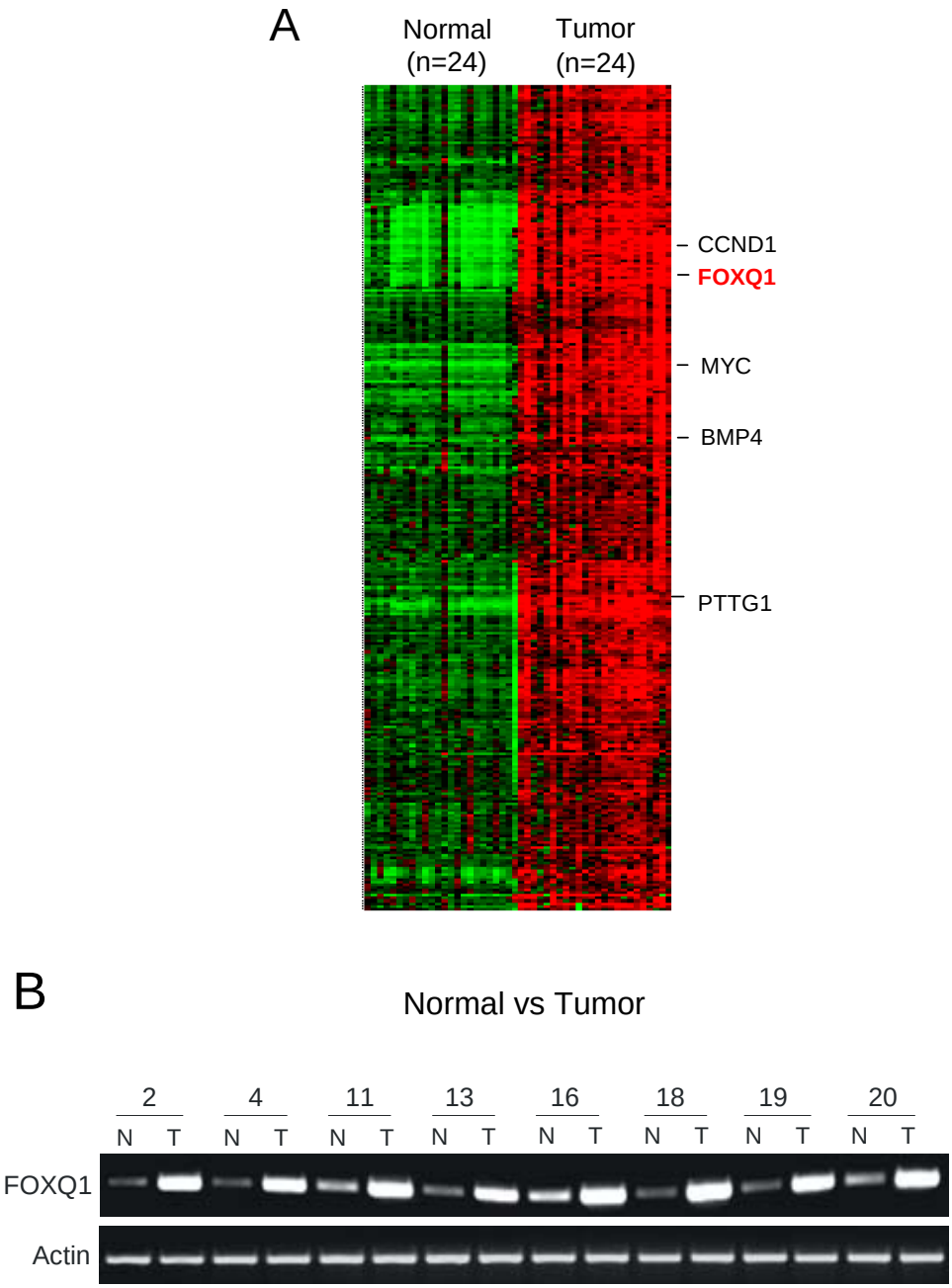

Figure 4.1 FOXQ1 gene is highly expressed in 24 pairs of clinical colon tumor samples.

A, Heatmap extracted from microarray gene expression analysis shows that FOXQ1 is the most highly expressed gene in clinical colon tumors as compared to normal controls.
B, RT-PCR performed on 8 randomly selected colon tumor RNA samples and their paired normal samples for specific FOXQ1 primers. Actin was used as internal control.

After showing FOXQ1 overexpression status in clinical samples, I proceeded to examine the FOXQ1 expression level in colon cancer cell lines including HCT116, DLD1, SW480, SW620, HT29, and HT15 cells by quantitative RT-PCR using FOXQ1 Taqman probe (Figure 4.2A). However, the protein analysis of FOXQ1 by western blot as shown in Figure 4.2B indicated that the protein levels of FOXQ1 do not always correlate with its mRNA expression amongst the various colon cancer cell lines which have been examined. One possible explanation for this inconsistency may be due to posttranslational modification which is a common feature associated with the forkhead box transcription factor family.

According to the results shown in Figure 4.2, HCT116 cell line is consistently expressing very low level of FOXQ1. After checking the promoter methylation database available in our lab, the promoter of FOXQ1 in HCT116 cells is hypermethylated which likely resulted in silencing of FOXQ1 in these cells. In view of this silencing, I opportunistically planned for ectopic overexpression of FOXQ1 in this cell line. In addition to the very low endogenous expression of FOXQ1, HCT116 cells present a typical epithelial morphology, which provided further possibility to investigate the function of FOXQ1 in regulating epithelial plasticity in colorectal cancer.

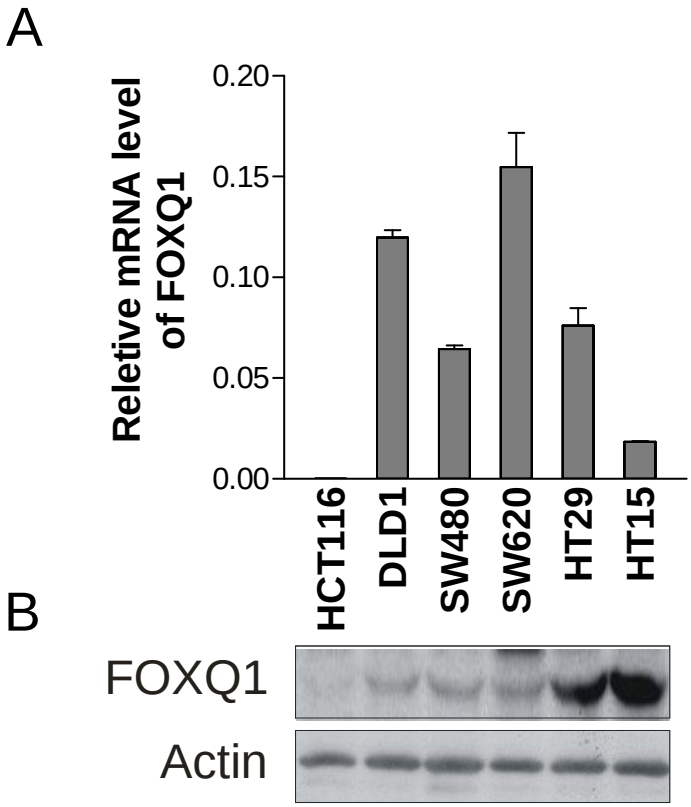

Figure 4.2 FOXQ1 expression status in various human colon cancer cell lines.

A, Quantitative real-time PCR by FOXQ1 Taqman probes in indicated colon cancer cell lines.
B, FOXQ1 protein levels were analysis by western blot among indicated colon cancer cell lines.

4.2 Generation of Tet-on inducible FOXQ1 cell line system

In order to further assess the functional role of FOXQ1, an inducible and reliable ectopic expression system, that is the Tet-on inducible system, was established in HCT116 cells. In Tet-on expression system, the expression of myc-tagged FOXQ1 depended on the presence of doxycycline (DOX) in the cell culture medium. The principle of Tet-on inducible system is described in Figure 4.3.

In order to generate an optimal and stable expression system for FOXQ1, single clones were picked after antibiotic selection. After screening a number of stable clones by western blot analysis for myc-tagged FOXQ1 expression using anti-myc antibody, clone 1 and clone 5 (designated as C1 and C5) were identified to have the desired doxycycline inducible expression of FOXQ1 (Figure 4.4A). In order to optimize the induction by doxycycline, its kinetics has to be taken into consideration. Therefore, I examined the expression pattern of FOXQ1 levels upon doxycycline treatment at different time intervals. From the results of western blot analysis in Figure 4.4B and C, the doxycycline-induced FOXQ1 expression was shown to be time dependent, reaching its peak level at 48 hours after doxycycline treatment, and returning to nearly its basal level at 72 hours. Hence, in this study, cells were treated with doxycycline for 48 hours to induce optimal FOXQ1 expression, and clone 5 was chosen for the following experiments due to its high expression levels.

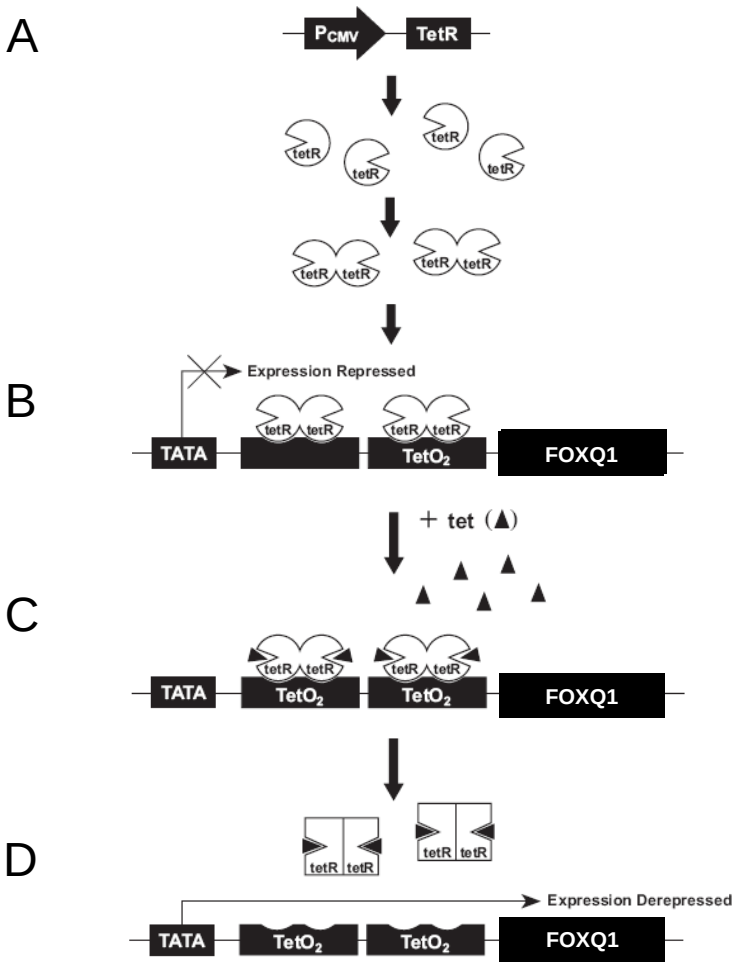

Figure 4.3 Workflow of Tet-on inducible expression system.

A, Tet repressor (tetR) protein is expressed from pcDNA6/TR in established host cells.
B, TetR homodimers bind to Tet operators ($TetO_2$) sequences in the FOXQ1 inducible expression vector which was sequentially transfected into host cells, repressing transcription of FOXQ1.
C, Addition of tetracycline (tet) that binds to tetR homodimers. Tetracycline was replaced by doxycycline to relief the tet repressor.
D, Binding of tet to tetR homodimers causes a conformational change resulting in the release of tetR from the Tet operator sequences, and induction of transcription from FOXQ1.

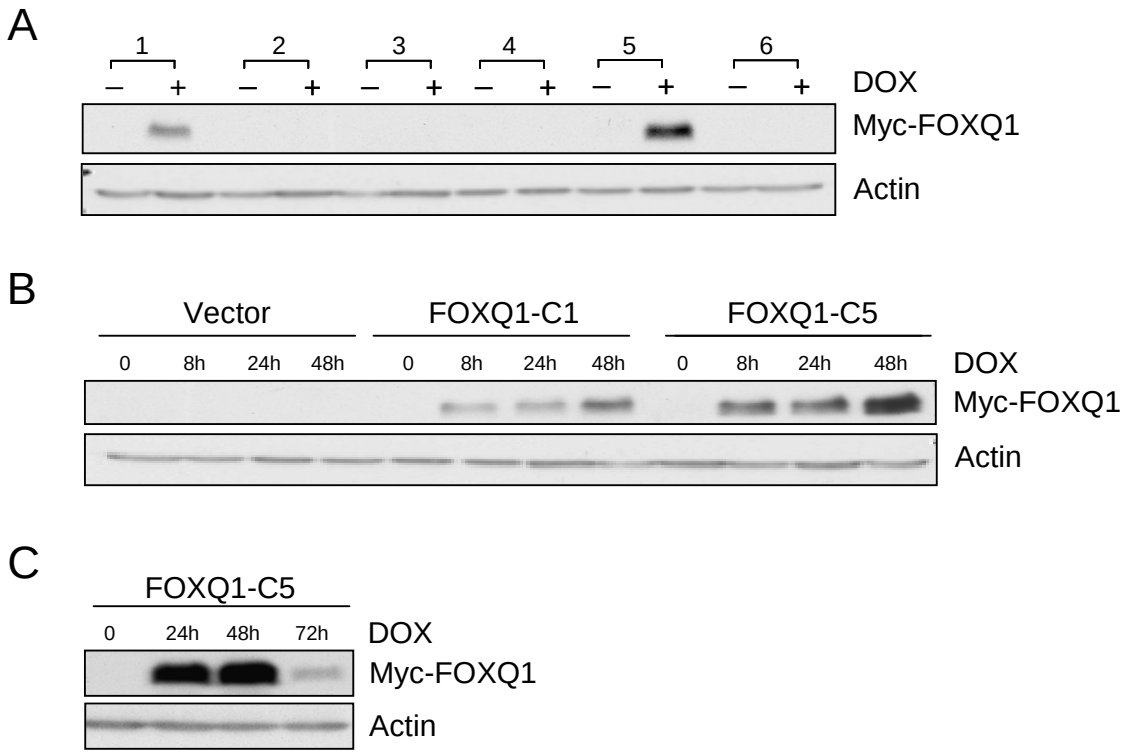

Figure 4.4 Screening for functional Tet-on inducible FOXQ1 expression in six HCT116 cell lines.

A, FOXQ1 protein levels were measured in different clones by western blot analysis upon 2μg/ml DOX (doxycycline) treatment for 24 hours. Myc-tagged FOXQ1 protein is detected by anti-myc antibody.
B, Two FOXQ1 expressing clones (FOXQ1-C1 and FOXQ1-C5) and empty vector cells were treated with DOX for indicated time points. FOXQ1 expressions were detected with anti-myc antibody.
C, FOXQ1-C5 treated with DOX for indicated time points were probed with anti-myc antibody.

As FOXQ1 belongs to the forkhead transcription factor family, it is expected to translocate into the nucleus where it exerts its effect on target gene expression. To investigate nuclear localization of full-length FOXQ1 in HCT116 Tet-on inducible cell line, the doxycycline induced FOXQ1 was visualized by confocal immunoflurorescence microscopy. The results shown in Figure 4.5 demonstrated that ectopic FOXQ1 located in the nucleus when HCT116-FOXQ1 cells were treated with doxycycline. These results not only confirmed the validity of the Tet-on FOXQ1 inducible system, but also proved that FOXQ1 localized in nucleus.

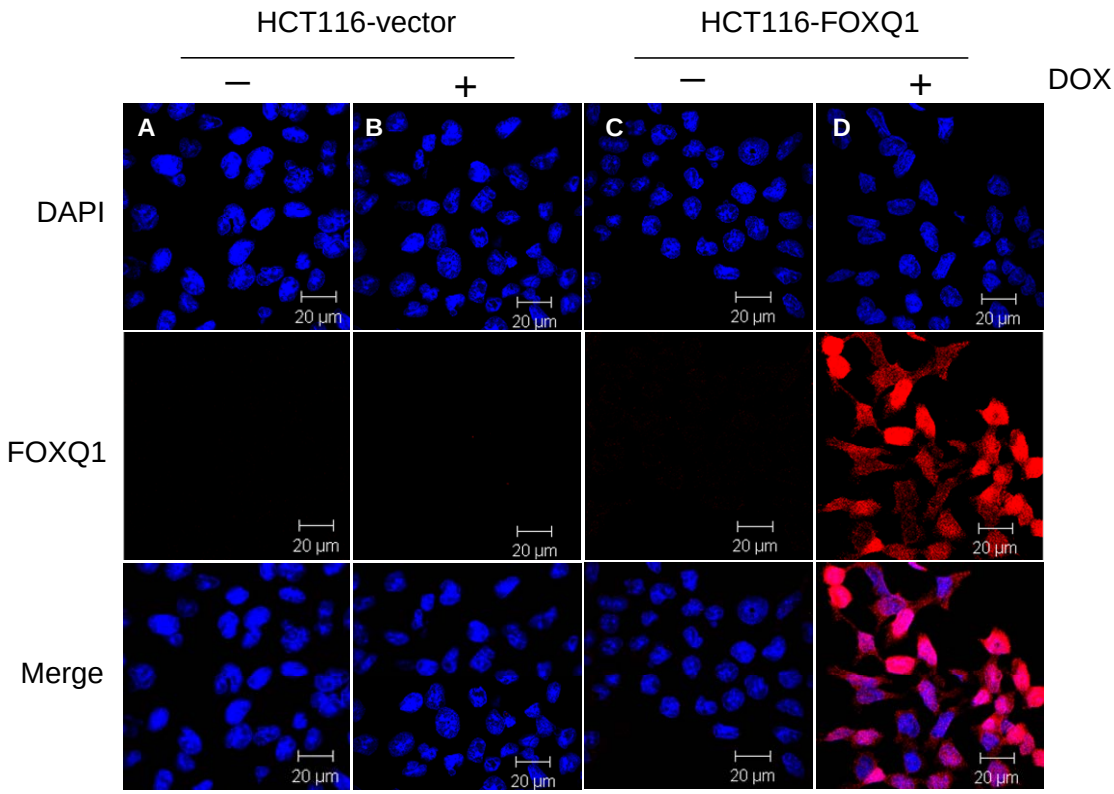

Figure 4.5 Confocal imaging of FOXQ1 expression in HCT116 Tet-on inducible cell lines.

Immunofluorescence of HCT116 vector cell line detected using an anti-myc monoclonal antibody, in the absence (A) or presence (B) of DOX (doxycycline). A selected clone of HCT116 expressing FOXQ1 (FOXQ1-C5) stained with an anti-myc monoclonal antibody for detecting ectopic myc-tagged FOXQ1, in the absence (C) or in the presence (D) of DOX. The color theme is shown below. Red color indicated the ectopic expression of myc-tagged FOXQ1 protein which is stained with anti-myc antibody, and blue color indicated the nuclei of the cells stained with DAPI.

4.3 Ectopic FOXQ1 expression induces epithelial to mesenchymal transition in epithelial-like HCT116 colon cancer cells

I made an interesting observation in HCT116-FOXQ1 inducible cells that have been subjected to long-term doxycycline treatment. The original typical cuboidal-shape epithelial morphology of HCT116 cells became elongated and spindle mesenchymal-like.

HCT116 cells are known to exhibit epithelial characteristics and carry silenced FOXQ1 expression. My results demonstrated that consistent overexpression of FOXQ1 for a period of 1-2 weeks in doxycycline-induced cells indeed caused HCT116 cells to exhibit morphological changes characteristic of epithelial to mesenchymal transition, namely the loss of cell-cell interaction and gain of spindle-like phenotype (Figure 4.6). However, this morphological transition is reversible and the cells will revert back to epithelial phenotype after doxycycline is withdrawn from cell culture to switch off FOXQ1 expression. My hypothesis is that the change from epithelial to mesenchymal-like morphology may be caused by ectopic FOXQ1 expression in HCT116 cells. The HCT116 vector control did not show any of the mentioned phenotype changes upon doxycycline treatment for the same length of time, eliminating the possibility that the morphological changes of FOXQ1 expressing cells were due to the side effect of doxycycline.

To further look into the biological function of FOXQ1 in HCT116 cells, I have generated an additional Tet-on inducible cell line using a FOXQ1 deletion mutant D6 (designated as HCT116 FOXQ1-D6). The rationale of selecting D6 is based on the

observation that D6 can not transcriptionally activate potential transcriptional target CTGF promoter activity by FOXQ1 shown in Chapter 5. D6 seems to have less transactivation ability than full-length FOXQ1 on CTGF promoter in the genomic region of upstream 874bp to downstream 195bp (CTGF-P2). I next examined the ability of inducing EMT in these FOXQ1 mutant expressing cells. By contrast, this EMT phenotype also did not occur in D6 truncated FOXQ1 mutant expressing cells (Figure 4.7) suggesting that wild type full-length FOXQ1 is a pre-requisite for such epithelial to mesenchymal transition.

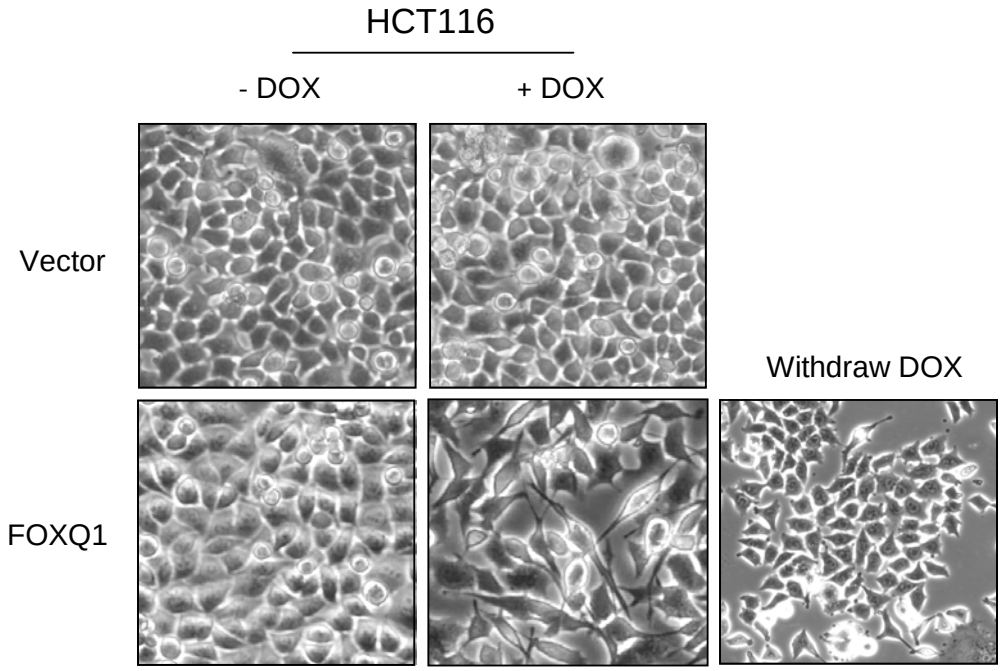

Figure 4.6 Morphologic change of HCT116-FOXQ1 cells.

Phase contrast images of HCT116 vector control and FOXQ1 cells either treated with or without DOX for over two weeks period. FOXQ1 expressing cells exhibit a phenotypic change resembling EMT. This mesenchymal morphology was reverted back to epithelial after withdrawal of DOX treatment for more than one week.

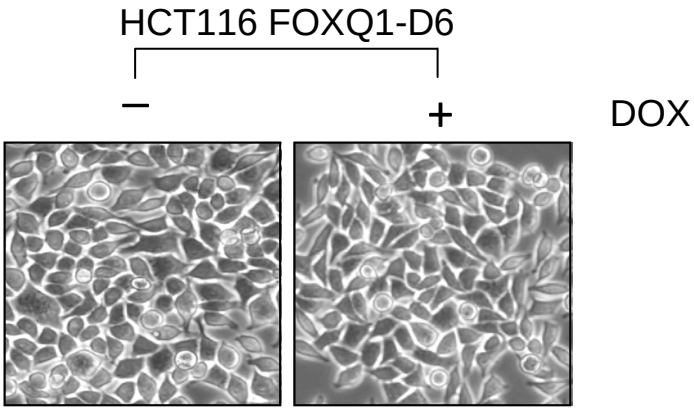

Figure 4.7 Morphology of HCT116 cells expressing indicated FOXQ1 deletion.

HCT116 cells with FOXQ1-D6 truncated deletion mutant were treated with or without DOX for a period of two weeks.

As its name suggests, EMT is a transition process that resulted not only in morphological changes in the cells but also gaining the ability of migration and invasion. In this process it is usually coupled with decreased expression of epithelial markers such as E-cadherin, and increased expression of mesenchymal markers such as vimentin. In order to confirm the morphologic changes which have occurred in FOXQ1 expressing HCT116 cells were indeed EMT related, I proceeded to test for such EMT markers.

Since EMT morphologic changes were not observed in short-term doxycycline treatment, that is to say short-term FOXQ1 induction may not be sufficient to trigger this phenotype. Hence, both long-term and short-term FOXQ1 inductions were examined for EMT markers using RT-PCR, quantitative PCR, and western blot analysis. In FOXQ1 expressing cells exposed to long-term doxycycline treatment, the mRNA and protein levels of E-cadherin were both decreased accompanied by loss of characteristic epithelial traits (Figure 4.8). The mRNA and protein levels of vimentin were both increased upon long-term FOXQ1 induction. Besides the expected changes in EMT markers, I also found that the mRNA level of the metastasis related gene CTGF was upregulated in response to long-term FOXQ1 induction, and it could be a potential FOXQ1 target (Figure 4.8A). Next, I tested two well established EMT triggers Slug and Snail. Interestingly, the mRNA level of Slug is enriched in FOXQ1 expression cells but not Snail (Figure 4.8A). In addition, the Slug protein level was also elevated as shown in Figure 4.8B. However, no changes were observed with another EMT trigger Snail. In addition, changes in these EMT markers were not seen in cells whereby FOXQ1 were overexpressed for a short period of time (Figure 4.9). Although increase in CTGF mRNA level can be detected shortly after 24 hours,

changes in Slug level was not detected (Figure 4.9A). The results demonstrated a strong correlation between long-term FOXQ1 expression and EMT induction.

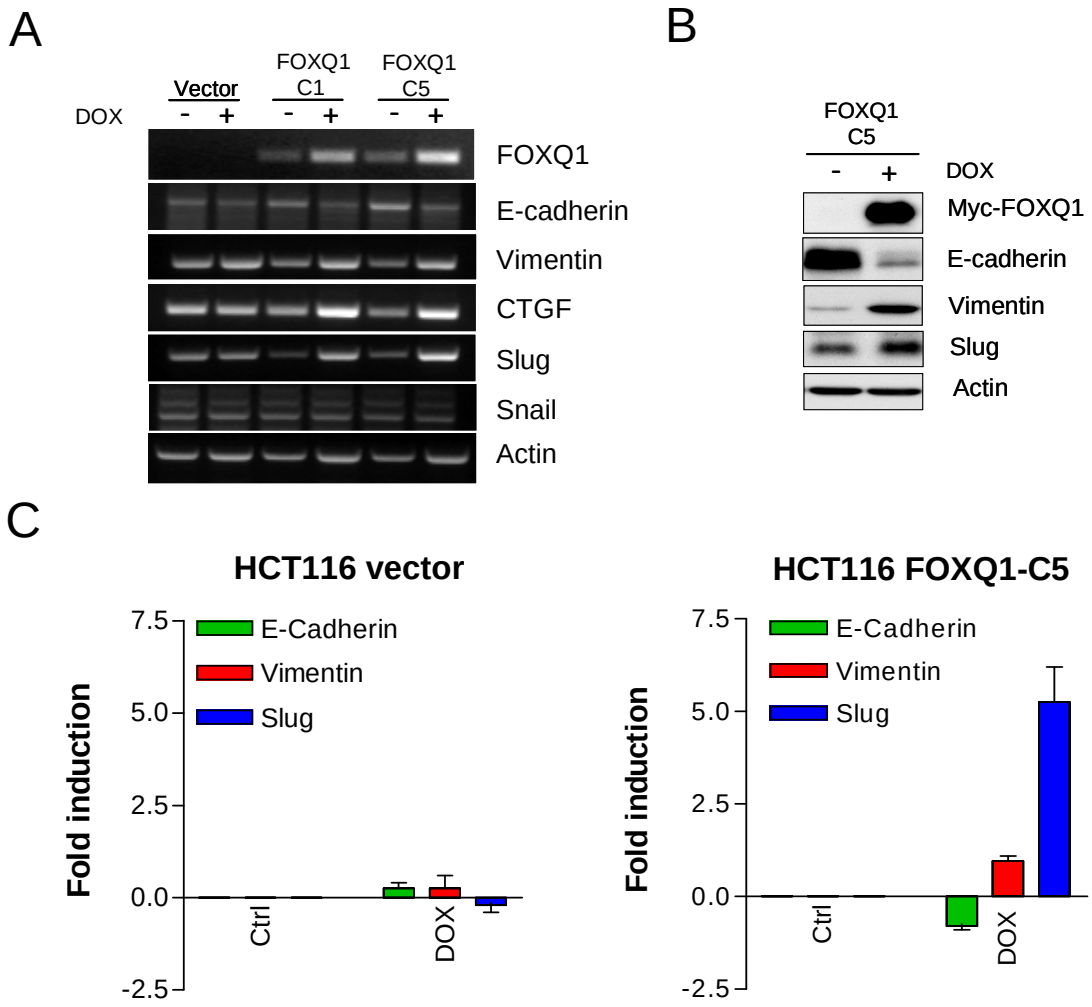

Figure 4.8 Long-term and steady FOXQ1 expression induced morphological change in HCT116 associated with EMT.

A, RT-PCR analysis of HCT116 vector cells and two clones of FOXQ1 expressing cells for epithelial marker E-cadherin, mesenchymal marker vimentin, CTGF, EMT inducers Slug and Snail. Actin was used as internal control.
B, Western blot analysis for myc-tagged FOXQ1, EMT markers (E-cadherin and vimentin) and inducer (Slug).
C, Quantitave PCR of EMT markers and inducer in HCT116 vector and FOXQ1-C5 expressing HCT116 cells, with or without DOX trigger.

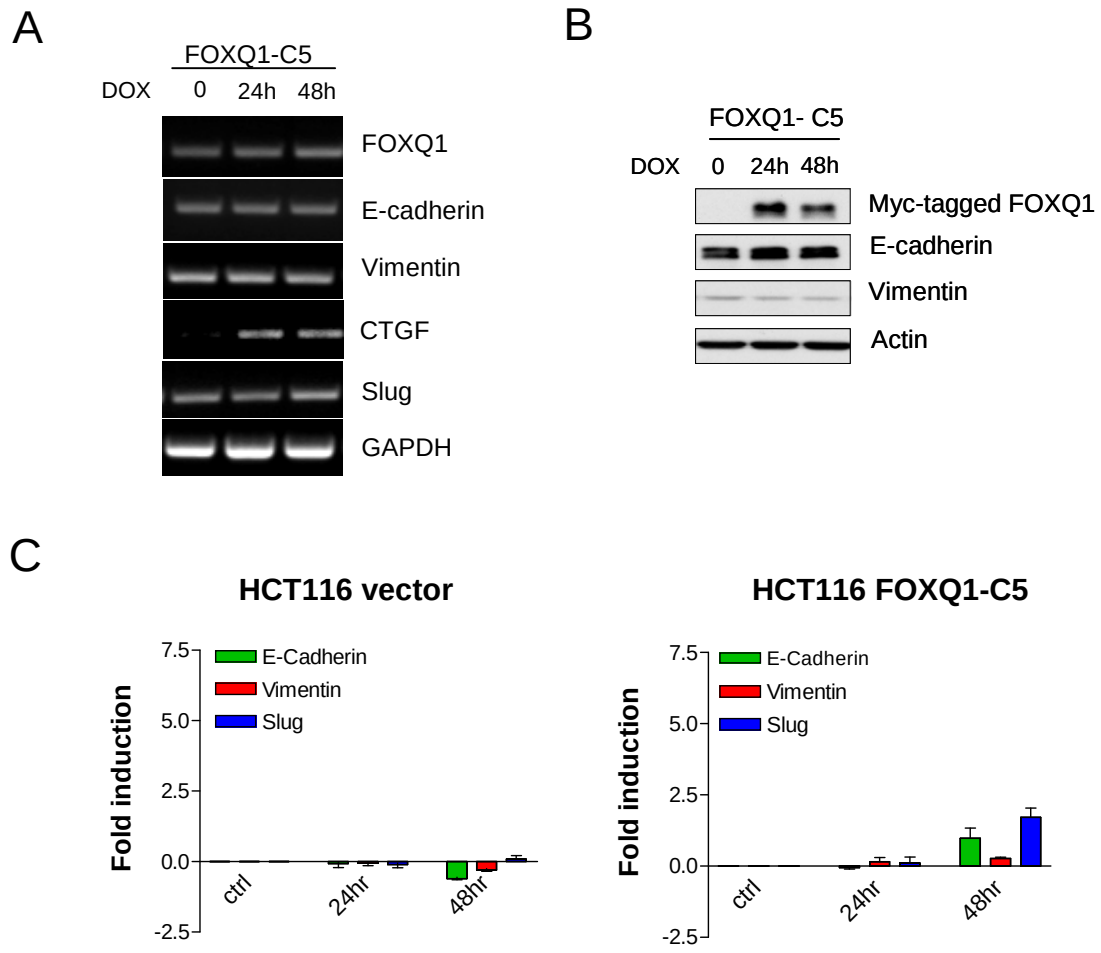

Figure 4.9 Short-term FOXQ1 expression in HCT116 is not sufficient to trigger EMT morphological change and there were no changes in EMT markers at both mRNA and protein levels.

A, RT-PCR analysis in HCT116 FOXQ1-C5 treated with DOX for indicated time duration did not induce changes in the EMT marker, and Slug expression. Nevertheless, CTGF was upregulated 24 hour after treatment with DOX.
B, Western blot analysis for the EMT markers E-cadherin and vimentin in HCT116-FOXQ1-C5 cells.
C, Quantitative PCR of EMT markers and inducer in HCT116 vector and FOXQ1-C5 expressing HCT116 cells.

Next, I checked for any alterations in levels of E-cadherin and vimentin in single cell level following long-term FOXQ1 expressions as well as cells that have FOXQ1 withdrawn. The preparations were visualized by confocal microscopy with staining of E-cadherin and vimentin expression. Figure 4.10A shows that loss of E-cadherin is only detected in doxycycline treated FOXQ1 expressing population, but not in FOXQ1 withdrawn cell population and without doxycycline treated control cells. The response of vimentin to FOXQ1 was opposite to the response of E-cadherin as shown in Figure 4.10B.

In summary, prolonged and consistent FOXQ1 overexpression in HCT116 cells seems to trigger EMT accompanied by marked loss of E-cadherin and gain of vimentin.

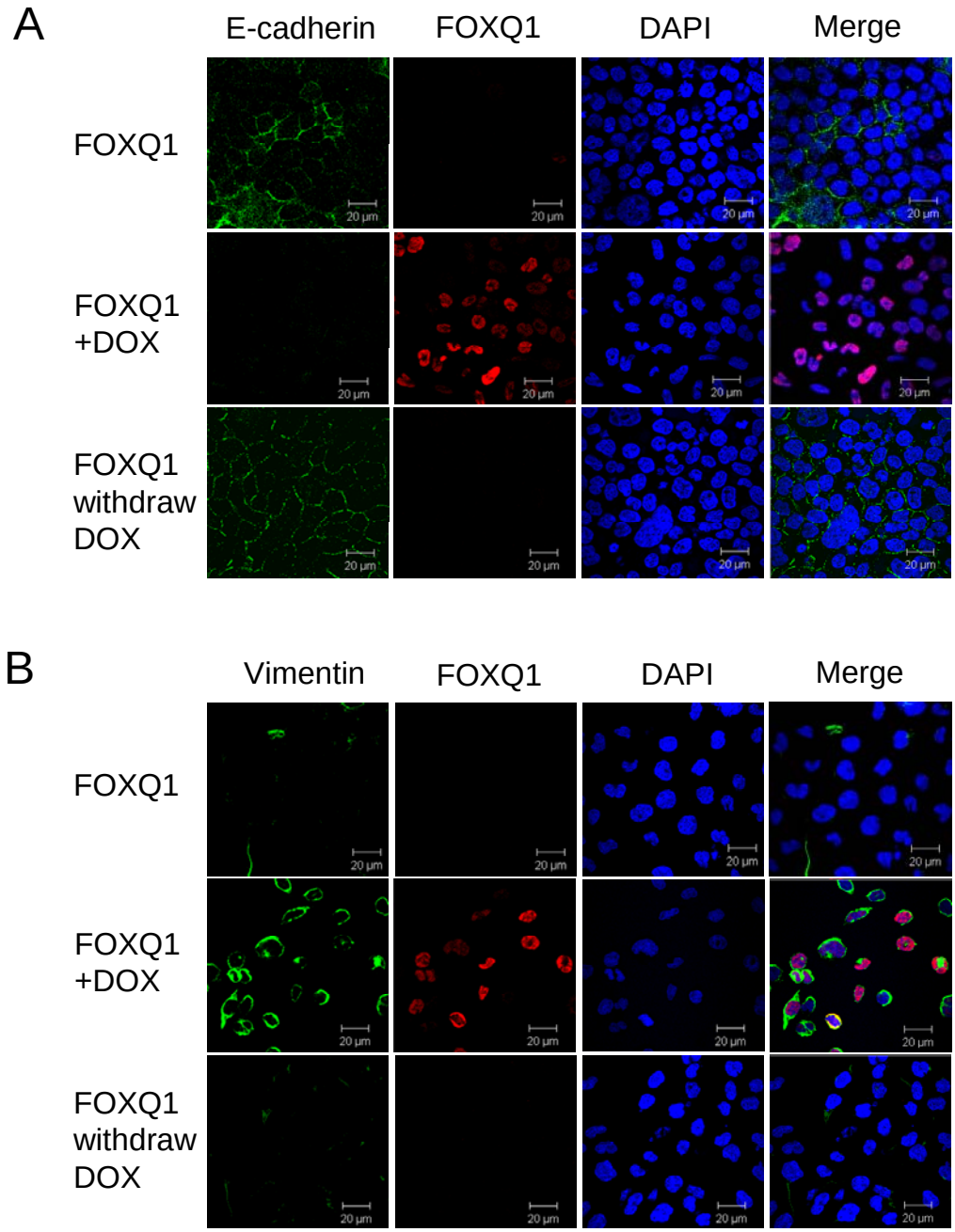

Figure 4.10 Immunofluroscent confocal images of EMT markers in HCT116-FOXQ1 cells with or without DOX and DOX withdrawn population.

A, E-cadherin is stained with Alexa Fluor 488 appearing green. Myc-tagged FOXQ1 is stained with Alexa Fluor 546 appearing red. Nucleus is stained with DAPI appearing blue.
B, Vimentin is stained with Alexa Fluor 488 appearing green. Myc-tagged FOXQ1 is stained with Alexa Fluor 546 appearing red. Nucleus is stained with DAPI appearing blue.

4.4 Effect of FOXQ1 on proliferation rate in HCT116 cells

To understand the biological function of FOXQ1, I examined the effect of FOXQ1 induction on cell proliferation. Cell growth and colony formation assay were performed in Tet-on inducible cell lines including vector control, full-length FOXQ1 and D6 deletion mutant. In addition, the inducible protein expression and subcellular localization were viewed by confocal microscopy. As expected, the wild type FOXQ1 was detected in the nucleus (Figure 4.12A), whereas the D6 was detected only in the cytoplasm (Figure 4.13A). These data are consistent with the transient transfection experiments. The growth rate was reduced only in full-length FOXQ1 cells when treated with doxycycline for 11 days. The doxycycline was replaced every two days (Figure 4.12B). However, this cell growth inhibition was not observed in cells expressing D6 mutant as well as vector control cells (Figure 4.11B, 4.13B). These findings suggested that wild type full-length FOXQ1 has the ability to reduce HCT116 cell proliferation in vitro. However truncation of FOXQ1 protein impaired its ability to retain HCT116 cancer cell growth and proliferation. In addition, colony formation assay showed that ectopic expression of FOXQ1 in HCT116 cells inhibited colony formation. This phenomenon is consistent with results obtained in cell proliferation assay. Whereas, HCT116 expressing D6 deletion mutant did not show any cell growth inhibition, neither in colony formation nor cell proliferation assay. The functional results of FOXQ1-D6 in cell proliferation and colony formation ability are correlated with the loss of transactivation ability on reporter assay of CTGF-P2. Hence, the growth arrest caused by wild type FOXQ1 might be affected through regulation of CTGF transcriptional activity.

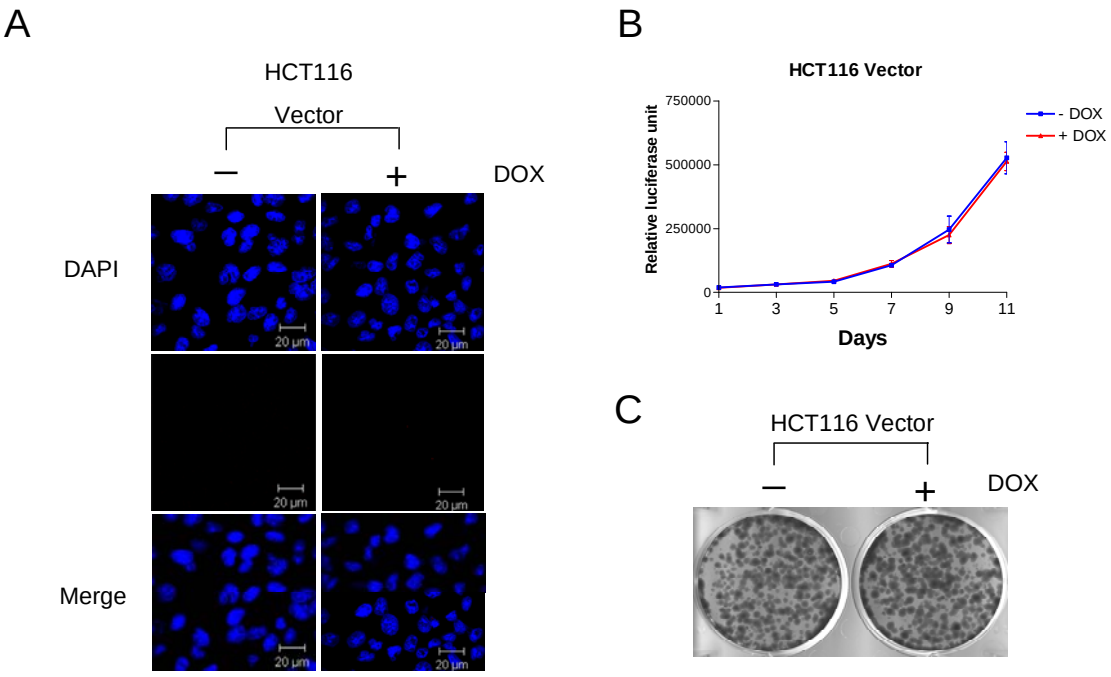

Figure 4.11 Proliferation rate of HCT116 vector control cell lines in conditions of with or without DOX (doxycycline) treatment.

A, Immunofluroscent confocal staining with anti-myc antibody in HCT116 vector control cells.
B, Proliferation rate of HCT116 vector control cells.
C, Colony formation of HCT116 vector control cells.

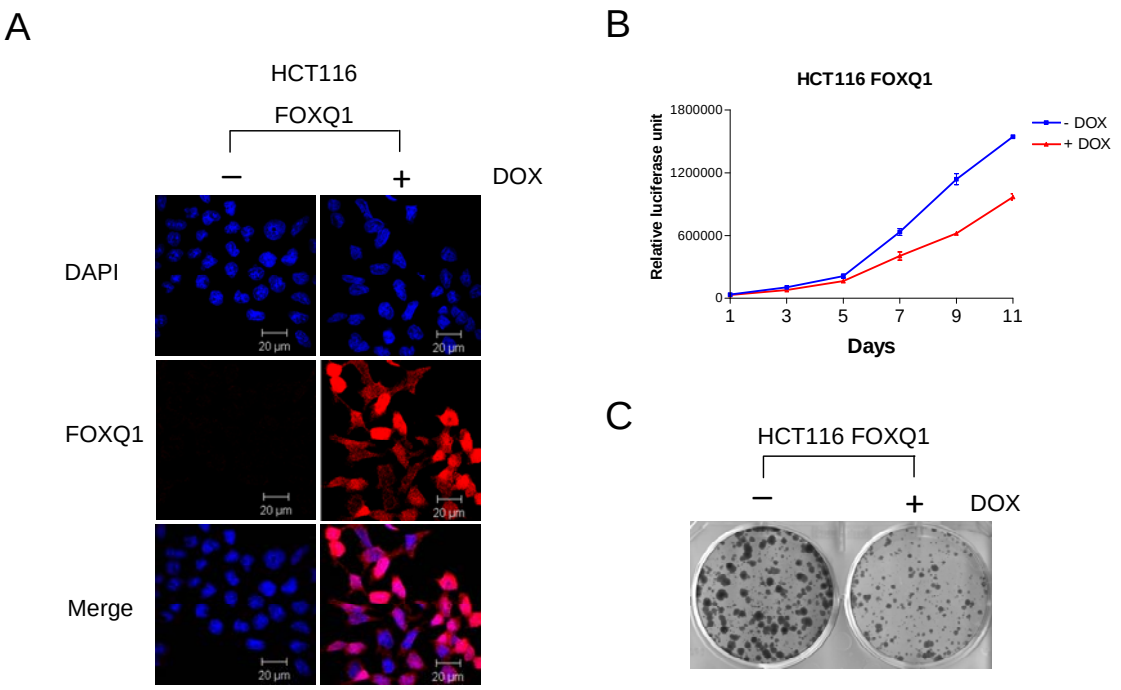

Figure 4.12 Proliferation rate of full-length FOXQ1 expressing HCT116 cell lines in conditions of with or without DOX (doxycycline) treatment.

A, Immunofluroscent confocal staining for myc-tagged FOXQ1 expressing cell line.
B, Proliferation rate of FOXQ1 expressing cell line.
C, Colony formation of FOXQ1 expressing cell line.

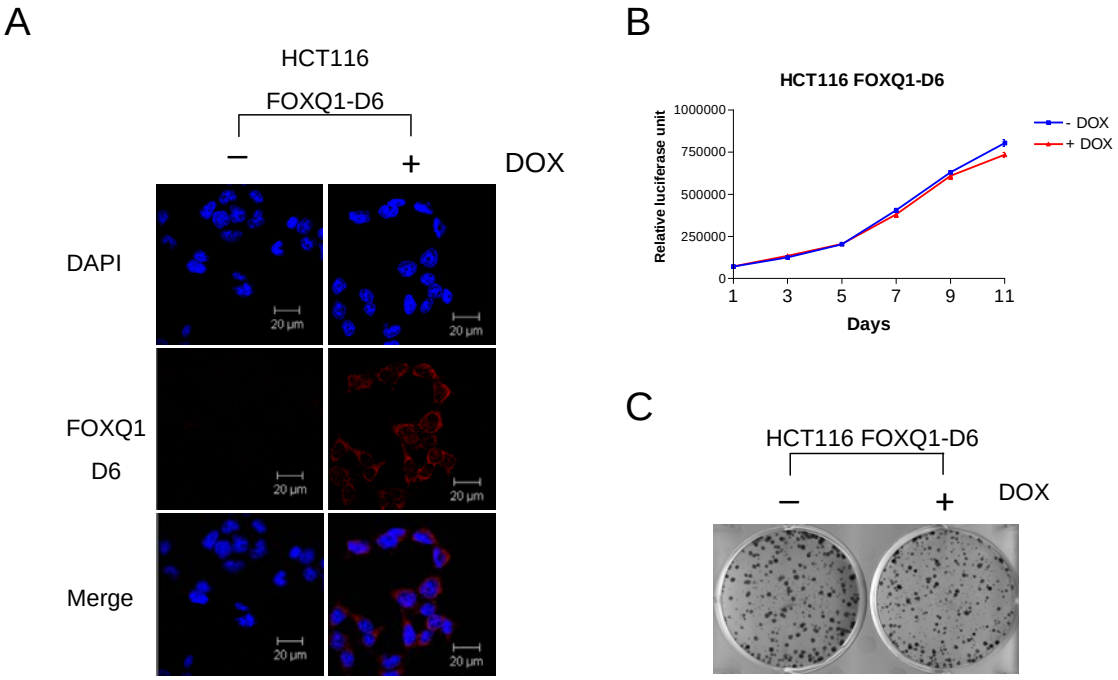

Figure 4.13 Proliferation rate of D6 truncated FOXQ1 expressing HCT116 cell lines in conditions of with or without DOX (doxycycline) treatment.

A, Immunofluroscent confocal staining for myc-tagged D6 truncated FOXQ1.
B, Proliferation rate of D6 truncated FOXQ1.
C, Colony formation of D6 truncated FOXQ1.

4.5 Identified transcriptional target of FOXQ1 that associated with epithelial to mesenchymal transition

A protein called Slug which is a known EMT trigger was strongly upregulated together with CTGF in HCT116 cells. The other known EMT triggers, namely, Twist and Snail, however, did not show any changes. Notably, Twist is known to be silenced by DNA methylation in HCT116 cells. These changes of EMT triggers have been consistently observed in two FOXQ1 clones examined. This suggested that FOXQ1-induced EMT is linked to transcriptional upregulation of CTGF and Slug as well as downregulation of E-cadherin.

To further verify CTGF as a potential target of FOXQ1, I isolated two genomic regions upstream of CTGF transcription start site (TSS). The two regions are the CTGF-P2 promoter region (-874 to +195bp) and a more distal region CTGF-P1 (-2000 to -797bp) (Figure 4.14A). The two fragments of CTGF promoter regions were subcloned into pGL3 luciferase reporter plasmid individually. Co-transfection of 100 ng of FOXQ1 and 1 μg of pGL3 reporter plasmid into HCT116 cells resulted in a strong induction of reporter activity containing the CTGF-P2 promoter region, but had no effect on reporter plasmid containing a more distal region CTGF-P1 (Figure 4.14B). These results indicated that FOXQ1 did activate CTGF promoter activity in the region of -874 to +195bp, further proof that CTGF is a potential transcriptional target of FOXQ1.

A

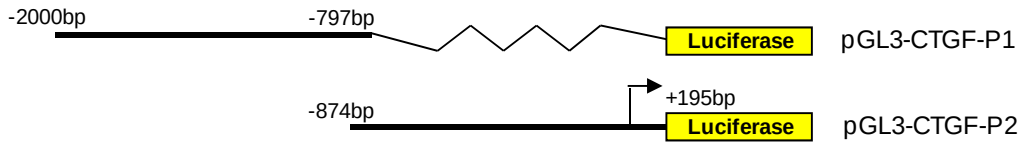

B

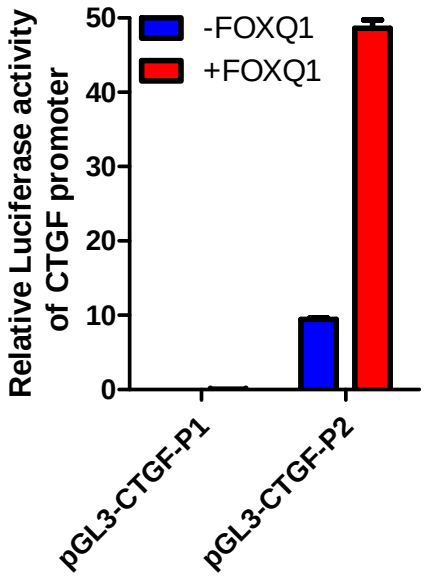

Figure 4.14 Identification of promoter region of CTGF in response to FOXQ1 in HCT116.

A, CTGF promoter construct designs. Two fragments of CTGF promoter regions: upstream 2000bp to 797bp (CTGF-P1) and upstream 874bp to downstream 195bp (CTGF-P2) were constructed into pGL3 luciferase reporter system.
B, Relative luciferase activity of CTGF promoters by transient co-transfection with or without FOXQ1.

To investigate whether Slug is transcriptionally regulated by FOXQ1, several promoter regions of Slug were cloned in to pGL3 luciferase vector including SLUG-P1 (-2000 to -800bp), SLUG-P2 (-900 to +100bp), SLUG-P3 (-400 to -50bp), SLUG-P4 (-400 to +100bp), SLUG-P5 (-900 to -400bp) (Figure 4.15A). The reporter luciferase assay was performed by co-transfection of FOXQ1 and Slug promoter plasmids. The information in Figure 4.15B indicated that SLUG-P4 is the response element to FOXQ1, and it contains the region of nt-400 to +100 of the Slug promoter. It suggested that FOXQ1 can transcriptionally activate Slug promoter activity in this specific region.

The above results demonstrated that FOXQ1 has the potential to transcriptionally activate both CTGF and Slug promoter regions. Since the different enrichment of the promoter activity of CTGF and Slug by FOXQ1 (5-fold and 2-fold respectively), it is assumed that FOXQ1 may control these two potential targets by different ways and strength. In Chapter 4.3, CTGF was shown to be upregulated by FOXQ1 in 24 hours, however, Slug enrichment can be seen only when EMT phenotype appeared. These suggested CTGF activation through FOXQ1 is faster than Slug, hence, CTGF could be used as an indicator for studying functional domain of FOXQ1 protein.

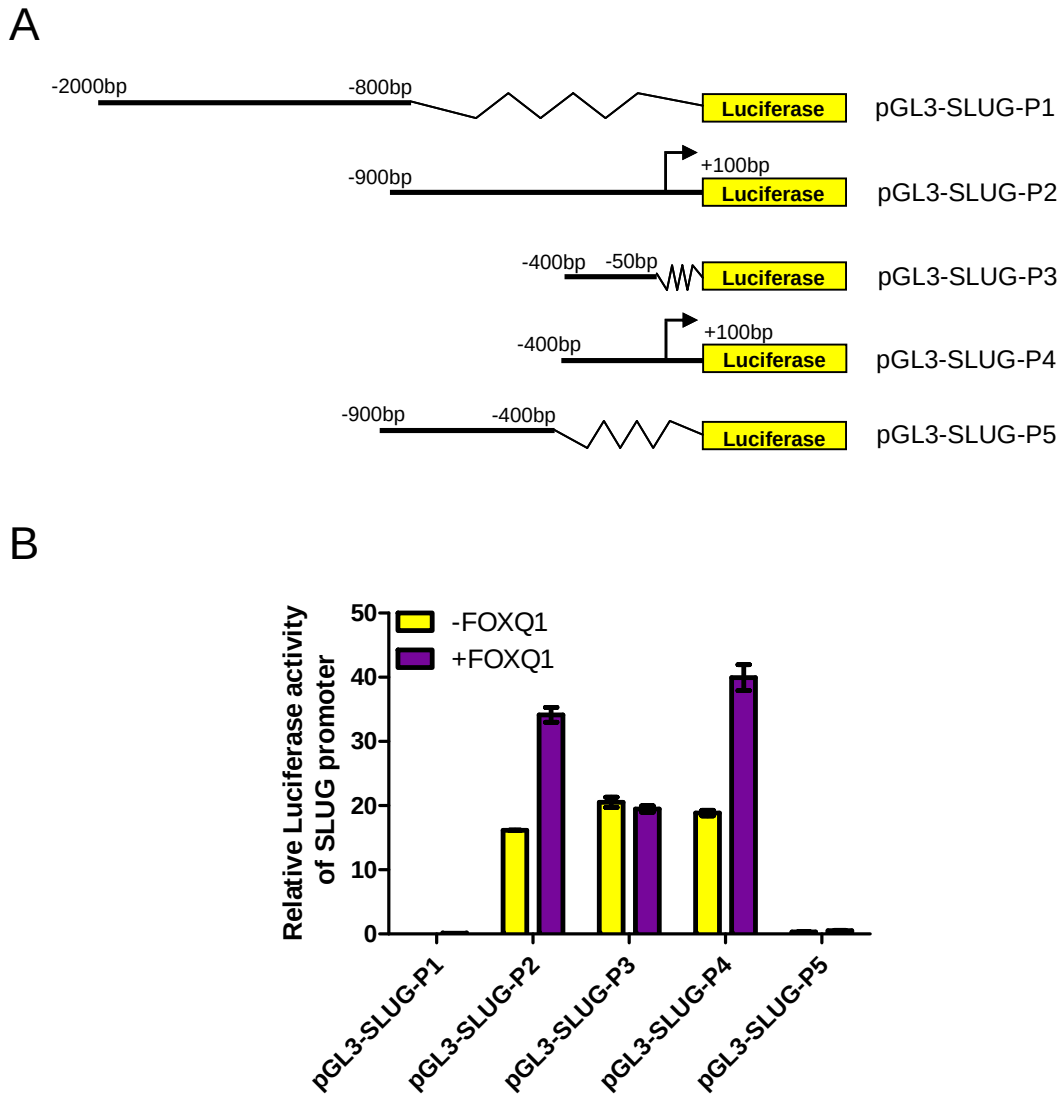

Figure 4.15 Schematic structure of Slug promoter regions and luciferase reporter activity of Slug promoter regions in response to FOXQ1.

A, View of schematic structures of 5 fragments of Slug promoter regions which were constructed in pGL3 vector.
B, Luciferase reporter activity of the 5 Slug promoters in response to FOXQ1.

4.6 FOXQ1 induced EMT in HCT116 cells is independent of TGF-β signalling pathway

TGF-β signalling pathway in colon cancers is distinct from other types of cancer. In colon cancer TGF-β receptor is mutated, hence, as a result, colon cancer cells became unresponsive to TGF-β signalling. In order to better understand the relationship between FOXQ1 and TGF-β pathway, I have chosen a non-cancerous cell line HEK-TERV in addition to HCT116 cells which have functional TGF-β receptors. Slug and CTGF were assayed after treatment with TGF-β1 for different time points, because Slug and CTGF were reported as downstream targets of TGF-β signalling pathway. Figure 4.16 demonstrated that after treatment with TGF-β1 for 4 hours, Slug and CTGF were increased and remain elevated for 72 hours in HEK-TERV cells. However, a similar response to TGF-β1 was not seen in HCT116 cells. This finding verified that TGF-β signalling in HCT116 cells was impaired.

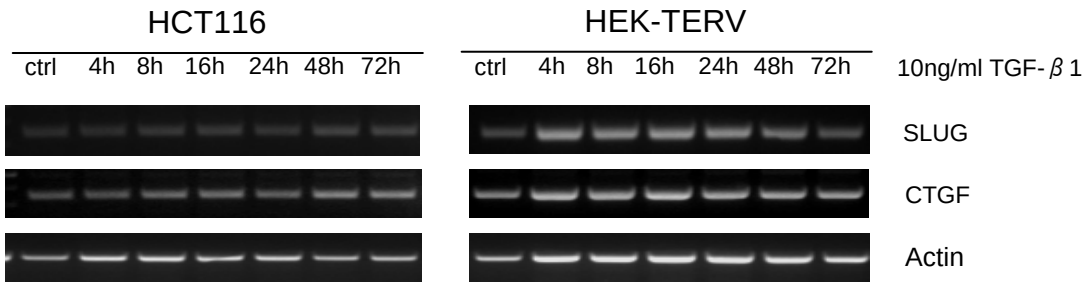

Figure 4.16 RT-PCR images of Slug, CTGF and actin after HCT116 and HEK-TERV cells treated with 10 ng/ml reconstituted TGF-β1 for indicated time points.

4.7 Ectopic FOXQ1 expression in HCT116 cells confers resistance to apoptosis induced by chemotherapeutic drugs

I further investigated whether ectopic expression of FOXQ1 in HCT116 will alter the responses to apoptosis. Two methods were used to induce stress. One method is 5-Flurouracil (5FU) treatment, because 5FU is a first line chemotherapeutic drug used in clinic for the treatment of colorectal cancers. The other method is to subject cultured cells to serum starvation.

Interestingly, both methods showed similar results. In Figure 4.17A, phase contrast images indicated that HCT116-FOXQ1 expressing cells upon doxycycline treatment have more surviving cells compared with non doxycycline condition, following 5FU treatment at a concentration of 375μM for 5 days. Similarly, under condition of serum starvation for 60 hours, HCT116-FOXQ1 expressing cells with doxycycline treatment remained intact and maintained its normal morphology, whereas, in the absence of doxycycline treatment, these cells began to exhibit signs of apoptosis (Figure 4.17B).

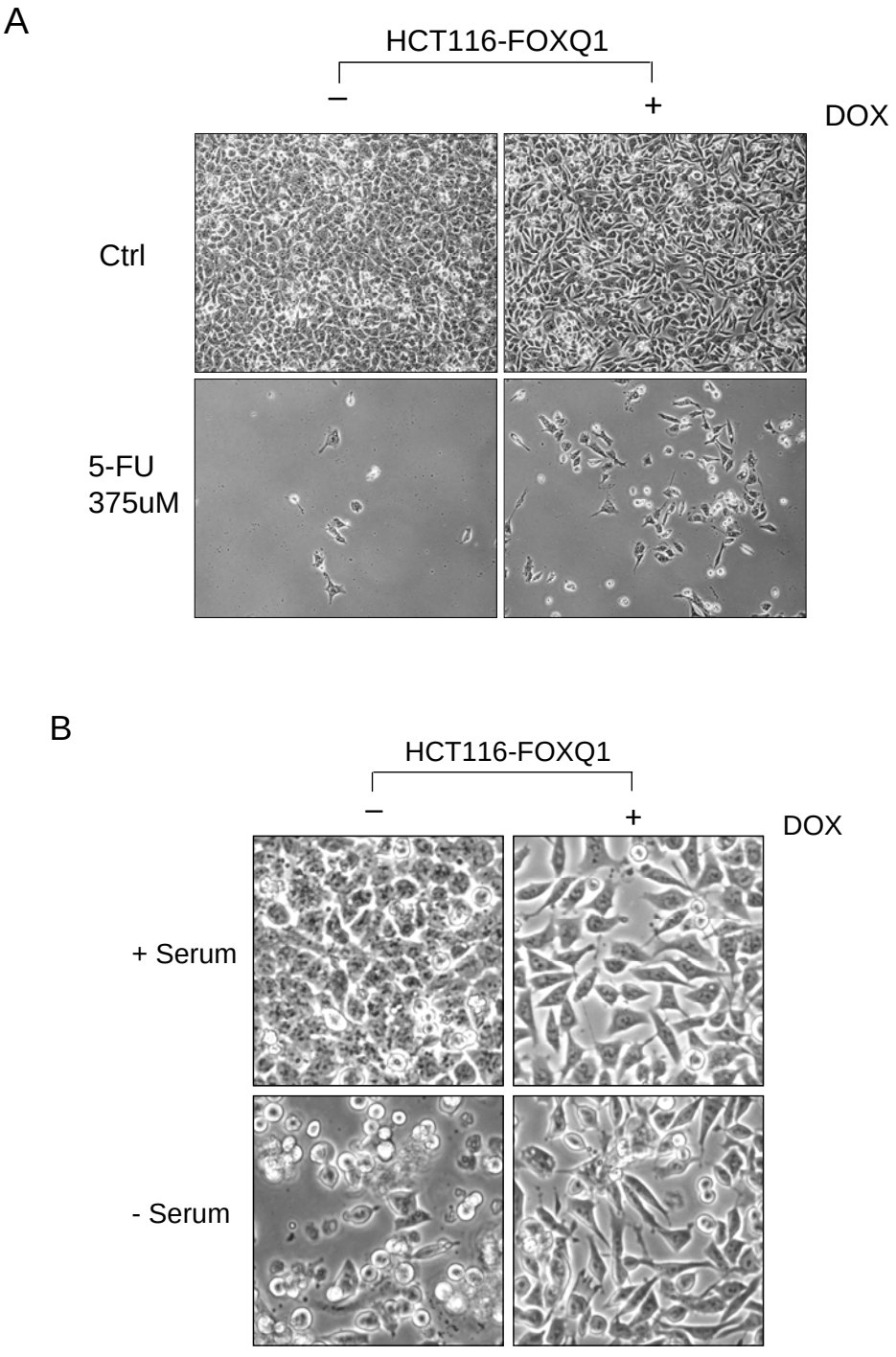

Figure 4.17 Phase contrast images of HCT116-FOXQ1 cells in response to stress under conditions with or without DOX treatments.

A, HCT116-FOXQ1 cells were treated with 375 μM of 5FU for 5 days with or without DOX treatment.
B, HCT116-FOXQ1 cells were cultured in serum starved (-Serum) or 10% serum (+Serum) condition for 60 hours with or without DOX.

The anti-apoptotic effect of FOXQ1 in HCT116 cells was further examined by measuring SubG1 DNA contents using FACS analysis following 5FU treatment at different time intervals. The results showed that HCT116-FOXQ1 cells induced to express FOXQ1 by doxycycline have reduced SubG1 phase, thus suggesting that these cells were resistant to 5FU-induced apoptosis (Figure 4.18A). Meanwhile, HCT116 FOXQ1-D6 deletion mutant cells were used to perform the same experiments, and results showed that there was no significant difference in apoptosis in conditions with or without doxycycline treatment (Figure 4.18B). Together, the observed anti-apoptotic effect is likely associated with the wild type full-length FOXQ1 but not the truncated FOXQ1 mutant.

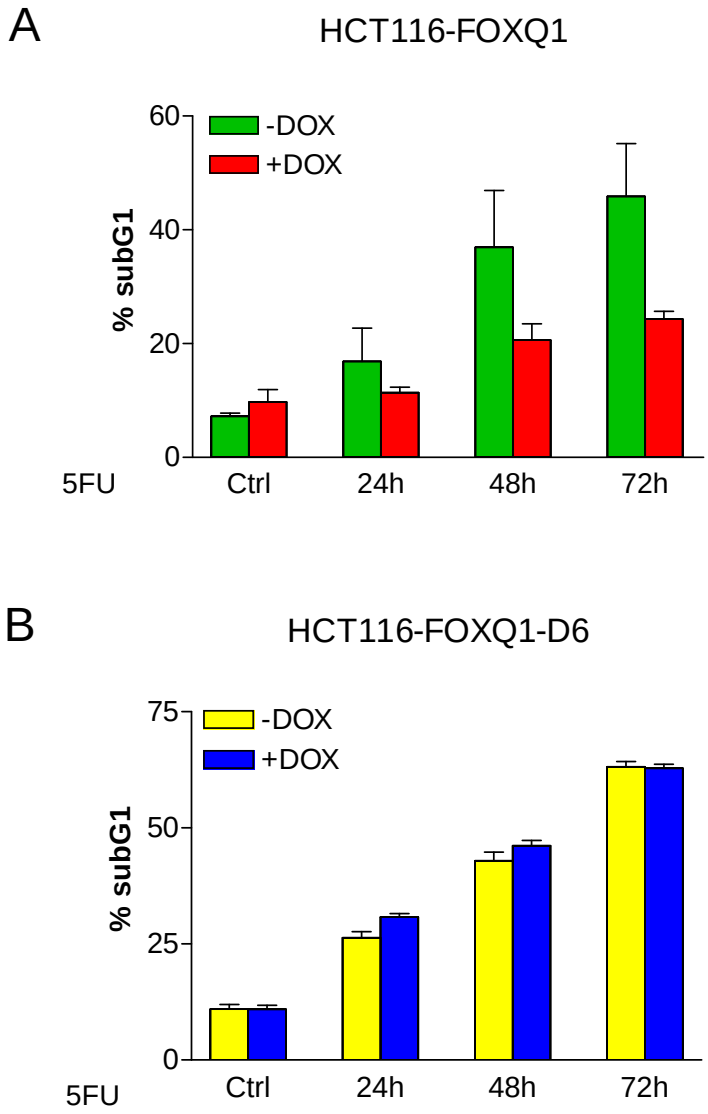

Figure 4.18 Overexpression of FOXQ1 decreased apoptotic responses to 5FU treatment (as measured by subG1 population) in HCT116 cells.

A, Apoptotic rates were measured by FACS for PI staining in HCT116 FOXQ1 full-length cells with or without DOX treatment for indicated time points in response to 375 μM of 5FU.
B, Apoptotic rates were measured by FACS for PI staining in HCT116 FOXQ1-D6 deletion mutant cells with or without DOX treatment for indicated time points in response to 375 μM of 5FU.

We know that PARP cleavage occurs downstream of Caspase 3 activation in the apoptosis cascade. In this case, I decided to use cleaved-PARP to measure the apoptotic response. Western blot analysis showed that the protein levels of cleaved-PARP decreased in HCT116-FOXQ1 expressing cells after treatment with 375μm of 5FU for the indicated time intervals (Figure 4.19A). Similar results were also observed in serum starvation condition, and the amount of cleaved-PARP was decreased in HCT116-FOXQ1 expressing cells (Figure 4.19B). However, in HCT116-FOXQ1-D6 cells, the amount of cleaved-PARP was not significantly different in 5FU or serum starved conditions following 48 hours of treatment with or without doxycycline (Figure 4.19C). In addition, FOXQ1 overexpression also confered reduced PARP cleavage by other chemotherapeutic drugs including camptothecin (CPT), adriamycin (ADR) and etoposide (VP16) (Figure 4.19D). Active Caspase 3 activity was also measured by FACS in samples treated with different dosages of drug for 48 hours (Figure 4.20). FACS data showed that FOXQ1 expression in HCT116 cells resulted in less than 50% of active Caspase 3 activities after 5FU, CPT, ADR, and SAHA treatments. Taken together, these data proved that FOXQ1 may attenuate chemotherapeutic drugs induced apoptosis in HCT116 cells.

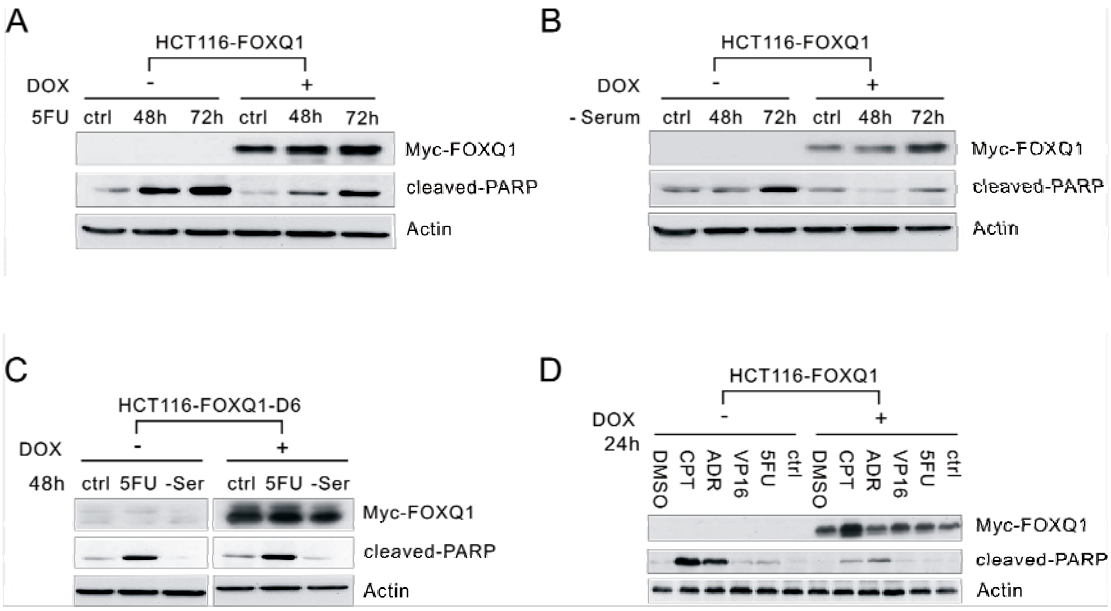

Figure 4.19 Ectopic expression of FOXQ1 in HCT116 cells confers resistance to PARP cleavage induced by chemotherapeutic drugs.

A, Western blot analysis of PARP cleavage by using antibody specific for cleaved PARP. Cells were treated with 5FU (375μM) for indicated times.
B, Protein levels of PARP cleavage were measured in HCT116 FOXQ1 cells with or without DOX after incubation under serum starved culture condition for indicated time points.
C, Protein levels of PARP cleavage were measured in HCT116-FOXQ1-D6 cells with or without DOX for 48 hours of treatment by either 375 μM 5FU or incubation under serum starved condition.
D, Protein levels of PARP cleavage were measured in HCT116 FOXQ1 cells with or without DOX in response to a series of DNA toxic drugs for 24 hours.

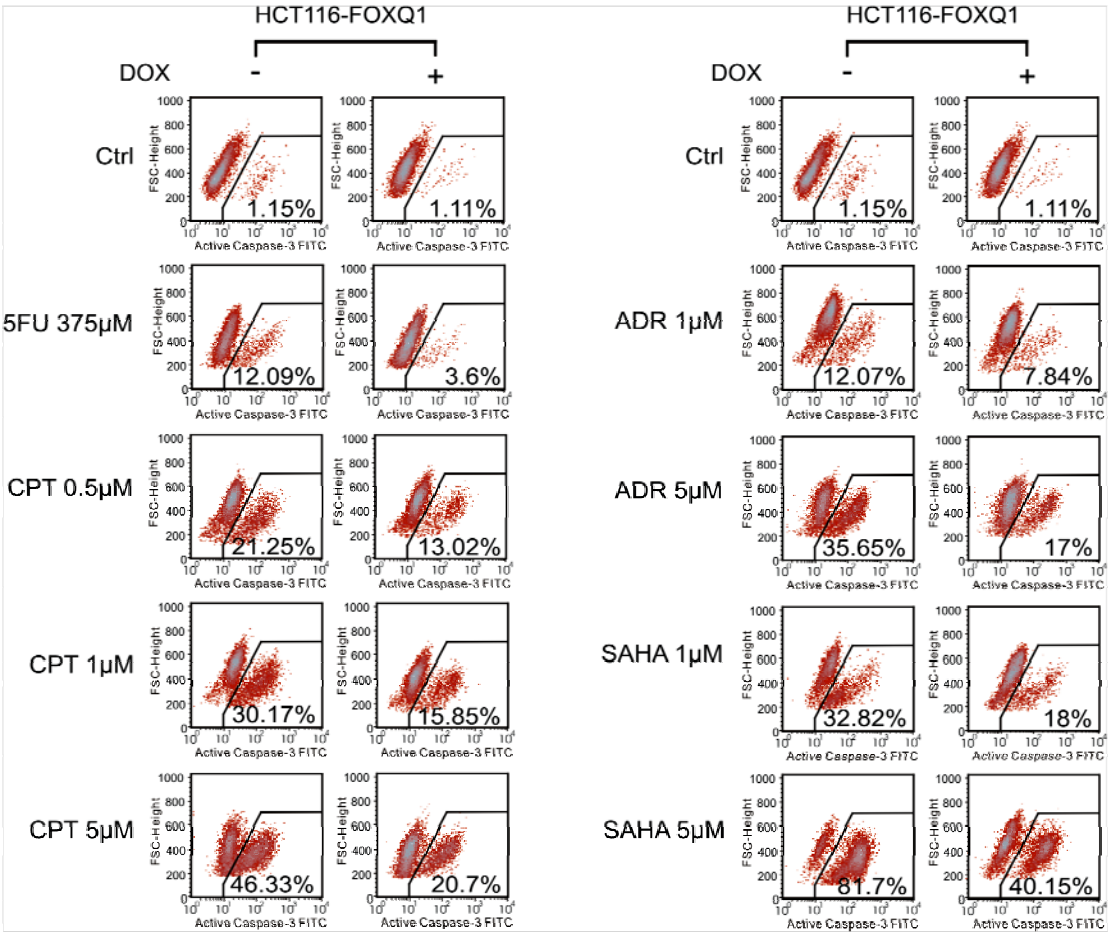

Figure 4.20 FACS analysis of Caspase 3 activity of HCT116 FOXQ1 cells treated with various drugs in the presence or absence of DOX.

Active caspase 3 activities were measured by FACS, and the percentage of active Caspase 3 is shown after treatment with various chemotherapeutic drugs at different dosages for 48 hours.

4.8 Summary

In clinical colorectal tumors, FOXQ1 expression is highly upregulated. In Tet-on FOXQ1 inducible system in HCT116, the EMT phenotype was observed in the presence of ectopic wild type full-length FOXQ1 expression, but not in cells expressing truncated FOXQ1. Moreover, this change is reversible and is coupled with biochemical changes of EMT markers including upregulation of epithelial marker E-cadherin, and downregulation of mesenchymal marker vimentin. By examining other known EMT triggers, Slug was found to be increased upon FOXQ1 expression together with CTGF. Simultaneously with the EMT phenotype triggered by FOXQ1 expression in HCT116 cells, these cells became chemoresistant to several DNA damaging drugs. Overall, FOXQ1 may contribute to colon cancer progression through protecting DNA from damages, and FOXQ1 could be a potential therapeutic target to sensitize colon cancers to current chemotherapy.

CHAPTER 5:

CHARACTERIZATION OF FUNCTIONAL DOMAINS OF FOXQ1 PROTEIN

Having demonstrated the functional role of FOXQ1 in breast and colon cancers, the functional domains of FOXQ1 protein were investigated in the following chapter through various deletion mutants of FOXQ1 summarized in Figure 5.1.

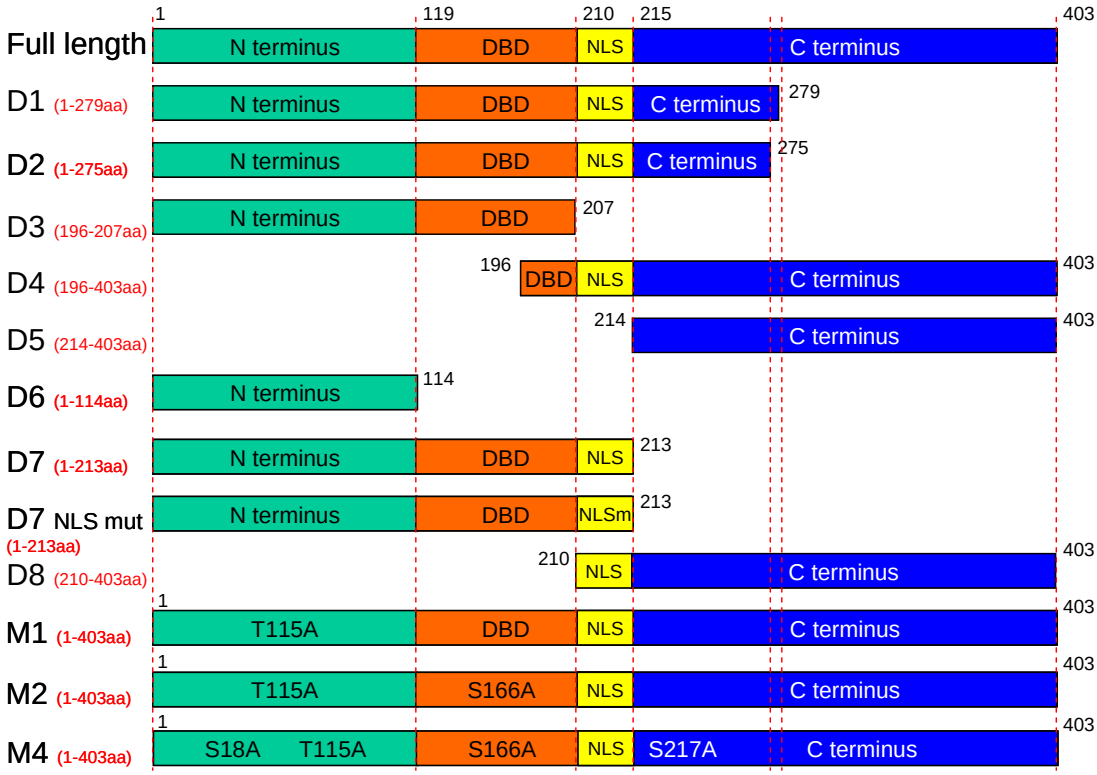

Figure 5.1 Schematic structures of a series of deletion mutants of FOXQ1 protein.

5.1 Mapping the transactivation domain of FOXQ1

The FOXQ1 protein contains a conserved DNA binding domain (DBD) and a predicted putative nuclear localization signal (NLS) as well as a predicted transactivation domain in the C-terminus. In order to map the protein sequence required for directing FOXQ1 activity, a series of myc-tagged FOXQ1 deletion mutants were generated as schematically presented in Figure 5.2A. The ability of FOXQ1 mutants to activate CTGF-P2 promoter was used as an indicator of transactivation ability of FOXQ1 measured by a luciferase reporter assay system.

As summarized in Figure 5.2B, deletion of FOXQ1's C-terminal region reduced its ability to transactivate CTGF promoter. To establish whether the drop in reporter activity reflected the removal of the transactivation domain or is simply caused by instability of truncated proteins, I performed western blot analysis for these deletion mutants. The results in Figure 5.2C showed that the expression of these FOXQ1 deletion mutants, as detected using anti-myc antibody, were expressed in similar levels, thus showing that the drop of CTGF promoter activity was due to the removal of transactivation domain of FOXQ1. D1 (1-279aa) showed an activity of approximately half the potency of the full-length FOXQ1, and additional deletions from 279 to 275aa (D2), and 275 to 213aa (D7) did not further reduce its activity. This indicated that the region from 279 to 403aa contains a transactivation domain required for a fully functional of FOXQ1. However, further removal of 213 to 207aa (D3) or 207 to 114aa (D6) resulted in a nearly complete loss of FOXQ1 activity on CTGF promoter, suggesting that the region from 114 to 213aa contain both conserved DBD and a predicted NLS that is critical for its activity. Notably, consistent with a

loss of predicted NLS from 207 to 213aa, D3 (1-207aa) completely lost its activity similar to D6 (1-114aa) although still retaining a DBD domain. This suggests that FOXQ1 without the NLS should be located in the cytoplasm and thus cannot gain access into the nucleus to exert its transcriptional function.

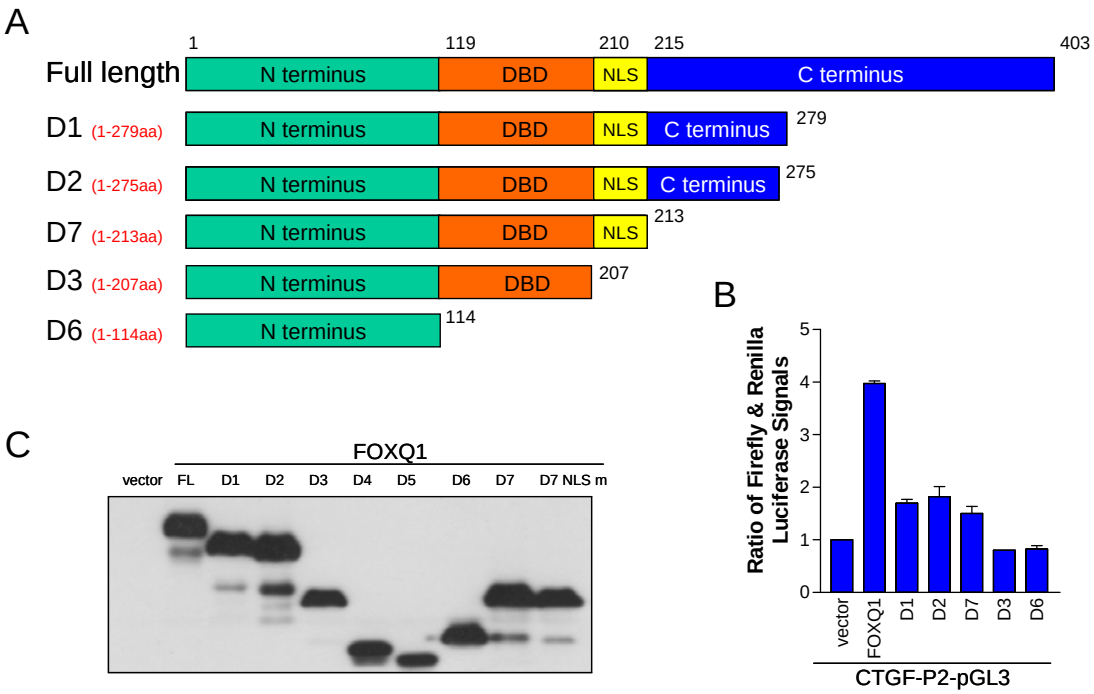

Figure 5.2 Identification of transactivation domain of FOXQ1.

A, Schematic structures of full-length FOXQ1 and a series of C-terminal deletion mutants. DBD (DNA binding domain); NLS (nuclear localization signal)
B, CTGF-P2 promoter activities responded to various deletion mutants of FOXQ1 compared with full length.
C,Western blot analysis shows myc-tagged FOXQ1 deletion mutants detected by anti-myc antibody.

5.2 Validation of nuclear localization signal of FOXQ1

The main function of nuclear localization signal is to determine the ability of the protein to translocate from cytosol to nucleus, and whether its biological function can be exerted in the nucleus. In order to do so, I used confocal immunofluorescent microscopy to visualize the cellular localization of FOXQ1 deletion mutants and also to measure its functional ability by reporter assay.

In the confocal microscopy experiment, FOXQ1 deletion mutants tagged with myc peptide were labelled red color, and the nucleus was stained blue. Hence, by judging the degree of co-localization of these two colors, I can accurately tell the distribution of the protein either in cytoplasm or nucleus or both. In the absence of any structural modification, full-length (FL) FOXQ1 is perfectly localized in the nucleus, thus reflecting the function role of FOXQ1 as a transcription factor. As expected, the D3 (1-207aa) and D6 (1-114aa) truncated proteins that do not contain the nuclear localization signal (NLS) did not locate in the nucleus (Figure 5.3), whereas D7 (1-213aa) that retains the NLS remained in the nucleus (Figure 5.4B). These results demonstrated that the amino acid region of 207 to 213aa of FOXQ1 contained a functional nuclear localization signal.

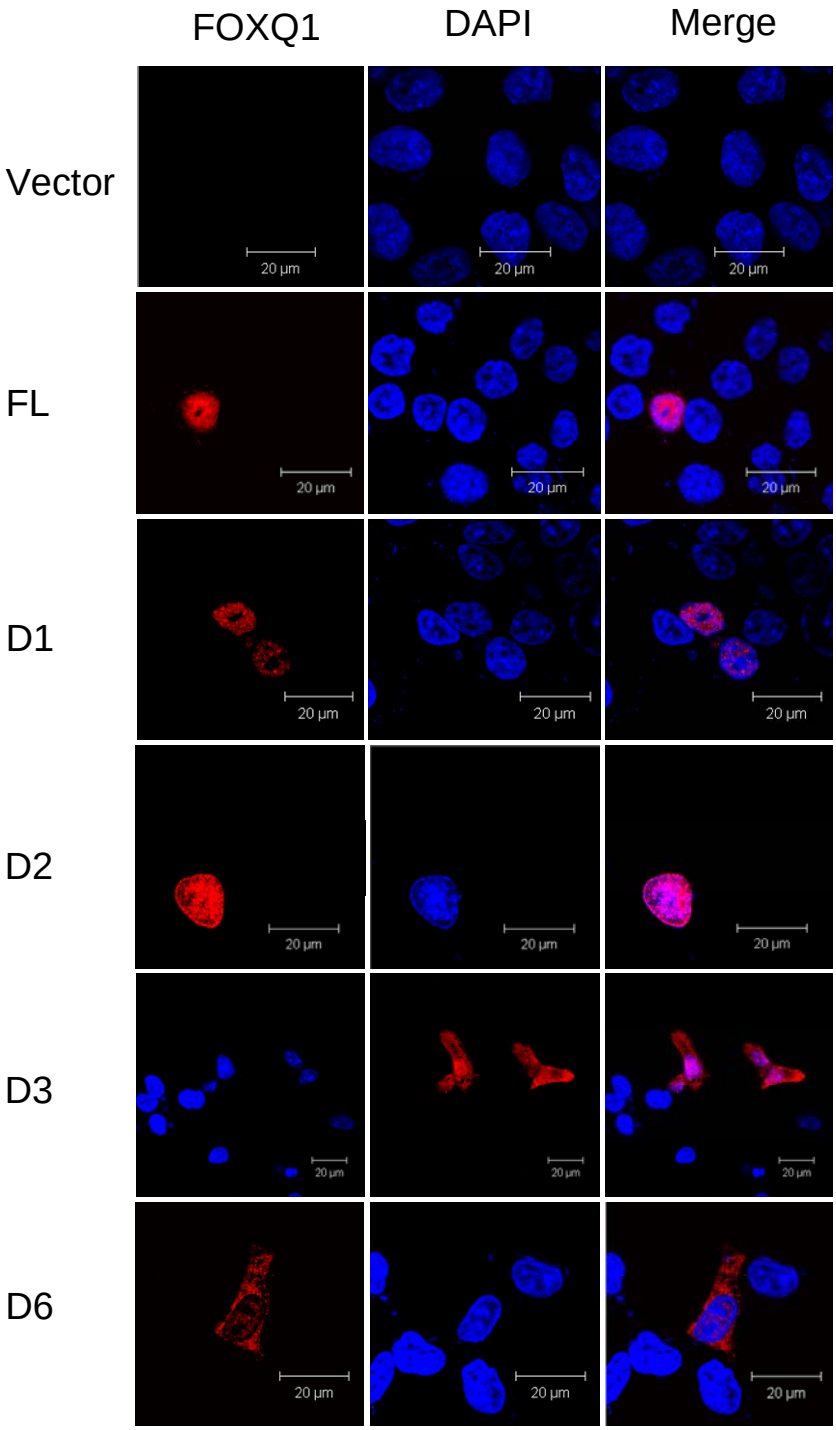

Figure 5.3 Localization of truncated FOXQ1 deletion mutants visualized by immunofluroscent confocal microscopy.

Indicated FOXQ1 deletion mutants were transiently transfected into HCT116 cells. Myc-tagged FOXQ1 proteins were detected by primarily anti-myc antibody and secondary antibody is Alexa Fluor 546 which appears red. Nucleus is stained blue with DAPI.

To further identify the crucial amino acid residues functionally required for the NLS activity in the region of 207 to 213aa, I performed the site-directed mutagenesis analysis in D7 through mutation of the amino acid sequence from RRRRRK domain to ARARAR (designated as D7 NLS mut) (Figure 5.4A). The generated D7 NLS mutant was found predominantly in the cytoplasm (Figure 5.4B) and therefore, this mutant's reporter activity to CTGF-P2 became indistinguishable from the background level as shown in Figure 5.4C. Taken together, these findings supported that the sequence of RRRRRK had a functional nuclear localization signal targeting FOXQ1 protein to enter the nucleus and exert its transcription factor function.

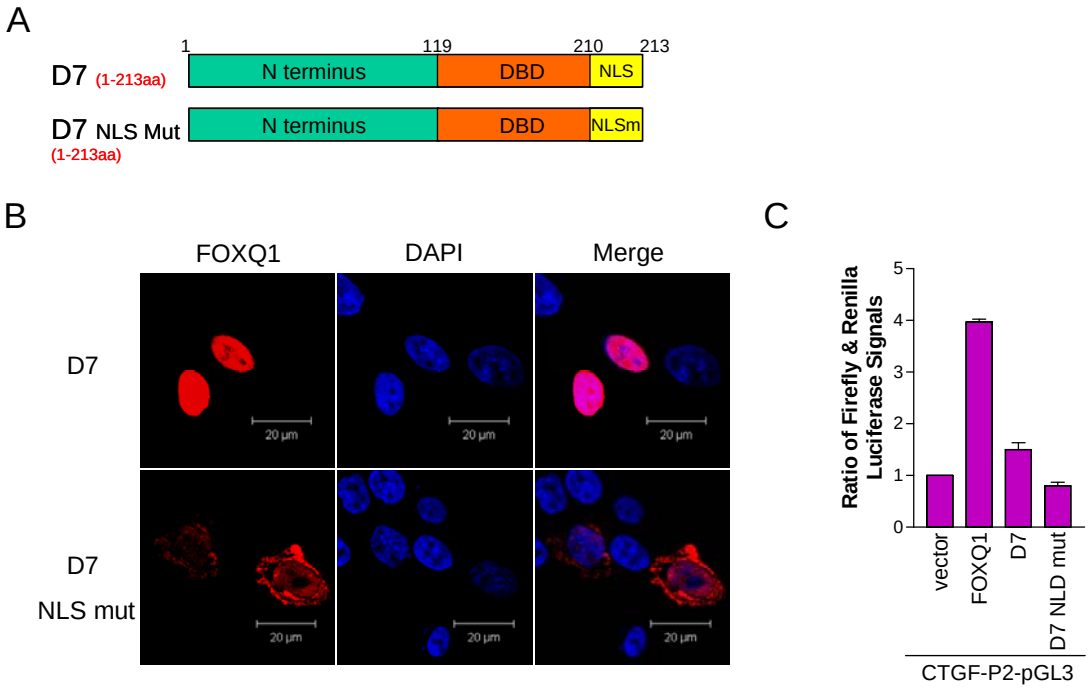

Figure 5.4 Identification of nuclear localization signal of FOXQ1.

A, Schematic structures of FOXQ1 deletion mutants D7 and D7 NLS mutant.
B, Localization of indicated FOXQ1 deletion mutants by immunofluroscent confocal microscopy. Myc-tagged FOXQ1 detected by anti-myc primary antibody and subsequently with Alexa Fluor 546 that appears red. Blue indicate nucleus stained with DAPI.
C, Luciferase reporter assay for co-transfection of CTGF-P2 and indicated FOXQ1 deletion mutants.

5.3 The N-terminal region of FOXQ1 contains an inhibitory domain

To define the functions of N-terminal region, I further constructed a series of N-terminal deletion mutants of FOXQ1 which were summarized in Figure 5.5A. Intriguingly, I found that the D4 (196-403aa) and D8 (210-403aa) exhibited a higher activity on CTGF promoter (1.5 and 1.2 fold higher respectively) than that of full-length FOXQ1. In addition, the D5 (214-403aa) had no activity due to the loss of NLS as anticipated (Figure 5.5B). The data suggested that the N-terminal region of FOXQ1 protein might contain an inhibitory domain to restrain the FOXQ1 transcription activity. The confocal microscopy images showed that D4 and D8 were located in both cytoplasm and nucleus, while the D5 only in the cytoplasm (Figure 5.5C).

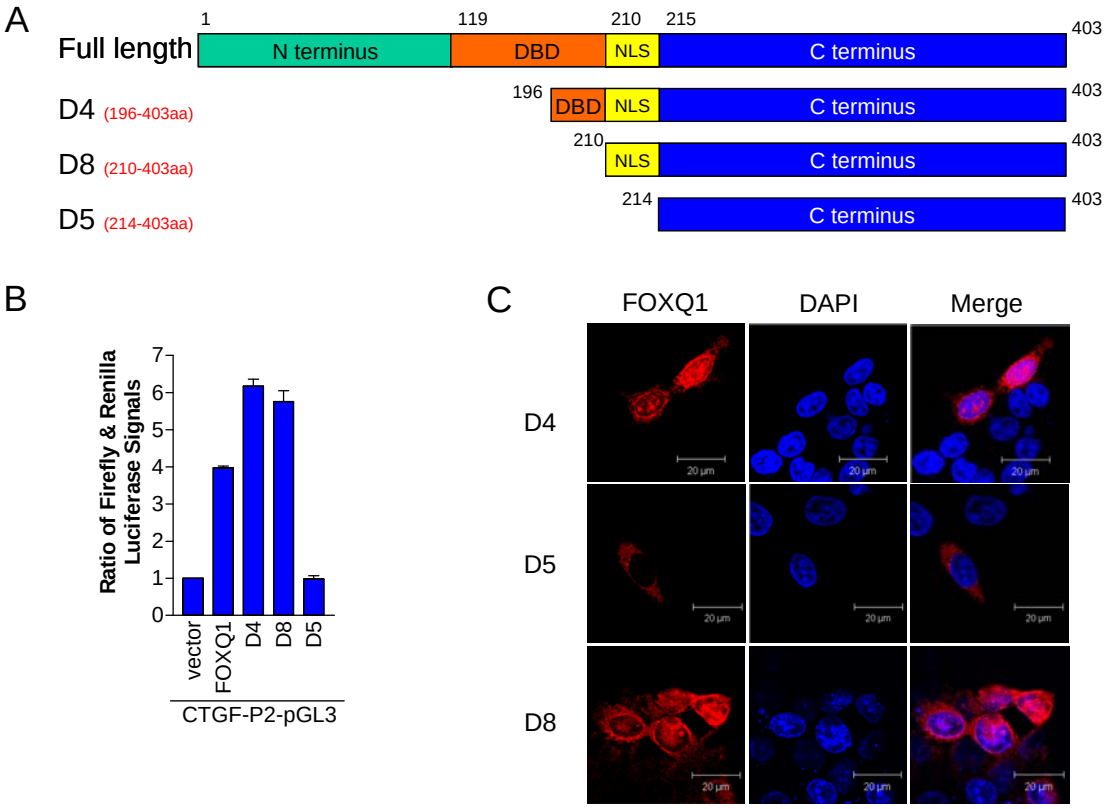

Figure 5.5 Identification of inhibitory domain of FOXQ1.

A, Schematic structures of a series of N-terminal deletion mutants of FOXQ1.
B, Luciferase reporter activity of CTGF-P2 in response to indicated FOXQ1 deletion mutants.
C, Localization of indicated FOXQ1 deletion mutants by immunofluroscent confocal microscopy. Myc-tagged FOXQ1 is detected by anti-myc primary antibody and subsequently with Alexa Fluor 546 appearing red. Blue indicate nucleus stained with DAPI.

Previous reports showed that the activity of transcription factors of FOXO family member is often regulated by phosphorylation. I hypothesized that the inhibitory activity of N-terminal region might be mediated by aberrant phosphorylation signals in colon cancer cells. Protein sequence analysis of N-terminus of FOXQ1 with Motif Scan (http://hits.isb-sib.ch/cgi-bin/index) revealed the presence of multiple consensus phosphorylation sites for several protein kinases, including PKC, PKA (CAMP-dependent) and CK2. To determine whether these phosphorylation sites are important to mediate the inhibitory activity of N-terminal region, I have conducted site-directed mutagenesis and generated several mutants to remove one or more concomitant multiple phosphorylation sites and analyzed their activity using CTGF reporter assay. These mutants include replacing PKC phosphorylation site (TRR) at Threonine-115 with Alanine, and (SVR) Serine-166 with Alanine, CAMP phosphorylation site (KRLS) Serine-217 with Alanine, and CK2 phosphorylation site (SDLE) Serine-18 with Alanine in the N-ternimus (Figure 5.6A).

I found that abrogation of either one (T115) (M1) or both (T115 and S166) (M2) of PKC sites slightly increased the transcription activity of FOXQ1 compared with the wild type counterpart. However, concomitant abrogation of all 4 phosphorylation sites of PKC, PKA, CK2 (T115, S166, S18, and S217) resulted in a marked increase in activity (Figure 5.6B). These findings suggested that phosphorylation of these sites might inhibit FOXQ1 activity in colon cancer. I therefore proposed that oncogenic kinase signaling could be responsible for this inhibitory regulation in colon cancer.

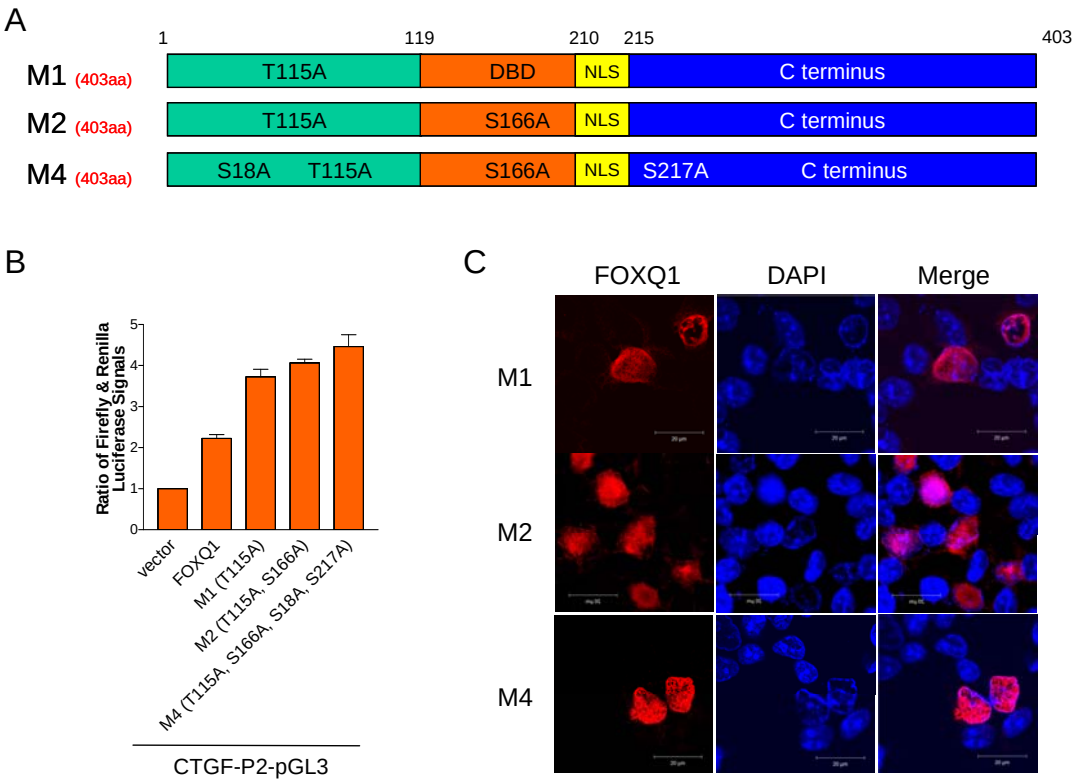

Figure 5.6 Potential phosphorylation sites of FOXQ1.

A, Structures of site-directed mutations.
B, Transcription activity of wild type and mutant FOXQ1.
C, Localization of indicated FOXQ1 deletion mutants by immunofluroscent confocal microscopy. Myc-tagged FOXQ1 is detected by anti-myc primary antibody and subsequently with Alexa Fluor 546 appearing red. Blue indicate nucleus stained with DAPI.

5.4 Summary

In this area of research, forkhead family FOXQ1 was found to be highly expressed in human clinical colon tumor samples and most of colon cancer cell lines except epithelial-like colon carcinoma cell line HCT116. Hence, HCT116 was used as a cell line model to study the functional impact of FOXQ1 in colon cancers. In ectopic FOXQ1 expression system in HCT116, I first identified CTGF as a potential transcription target of FOXQ1, and in turn used reporter luciferase assay to zoom in on the responsive region of CTGF believed to be regulated by FOXQ1. This region of CTGF was further used as an indicator for searching FOXQ1 protein functional domains in HCT116 cells. By constructing different truncated FOXQ1 deletion mutants, the transactivation domain was identified to be located in the C-terminus region of 279 to 403 amino acid (aa). The inhibitory region is contained in the N-terminal region of 1 to 196aa. In addition, located near the end of the DNA binding domain (210 to 213aa) is the nuclear localization signal which directs the FOXQ1 protein to the nucleus. These findings are based on the reporter activity of CTGF transactivated by truncated FOXQ1 mutants.

CHAPTER 6:

DISCUSSION

The present study aims to delineate the cellular functions of FOXQ1 in breast and colorectal carcinoma, including mechanisms behind the induction of mesenchymal-like phenotype by FOXQ1 in epithelial cells. The important and previously unknown role of FOXQ1 in cellular pathogenesis of invasion, migration and metastasis has been studied here. The evidence presented in this study supports a novel role of FOXQ1 as a critical participant in tumor progression through epithelial to mesenchymal transition (EMT), cancer stem cells, and anti-apoptotic ability. As a forkhead factor, FOXQ1 shares functional and structural similarities with some other forkhead family members.

6.1 The potential of FOXQ1 in modulating epithelial plasticity

Our understanding of EMT have greatly benefited from the discovery that some transcriptional factors and members of the TGF-β family can induce EMT both in vitro and in vivo which led to the establishment of cell culture models. These discoveries have generated great impetus and momentum to further dissect the signaling pathways which drive or contribute to EMT. The identification of distinct families of transcription factors, whose expression is activated during EMT, has provided greater insight into the transcription programs that are driving EMT. Interestingly, the signaling mechanisms and transcription programs that characterize EMT under physiological conditions appear to be largely recapitulated during EMT processes under pathological conditions. Although EMT has been well documented under physiological condition, there is much debate and discussion about its role and contribution under pathological conditions. The transient and reversible nature of EMT in cancer progression may contribute to some aspects of this debate, as cells that

have undergone EMT may revert to their differentiated epithelial state and are therefore not easily isolated for scrutiny. Another aspect of the debate centred around the acquisition of mesenchymal properties, especially since mesenchymal characteristics are ill-defined. Furthermore, in many cases epithelial cells lose epithelial characteristics and become migratory without acquiring mesenchymal features. These observations suggest there is a spectrum of epithelial plasticity changes that can occur, which will result in downregulation of epithelial differentiation and integrity to varying extents, and therefore in the end, may or may not qualify as EMT. By considering EMT as the most striking manifestation of epithelial plasticity, much debate on the relative contribution of EMT to cancer pathology maybe mooted in different degrees of observed epithelial plasticity. Finally, the realization that EMT provided a basis for cell invasion, leading to metastasis of carcinomas in different organs have also stimulated interest to find therapeutic modalities which will inhibit EMT, hence interfere with or prevent the progression of metastases.

In this study, I have extended our knowledge on forkhead box transcription factor family and its impact on regulating EMT. Among this family, FOXQ1 was found to be highly expressed in most of colorectal cancer, and in particular aggressive basal-like breast cancer subtype. The expression pattern of FOXQ1 suggested that it may have a potential oncogenic role to facilitate tumor progression in many types of cancers. By examining the biological role of FOXQ1 in ectopic overexpression system in both epithelial-like colon cancer HCT116 cells, and immortalized human mammary epithelial cells, prolonged and consistent FOXQ1 expression induced a phenotypic change from epithelial towards mesenchymal. Reflecting the

morphological changes are corresponding switches in markers of epithelium to mesenchyme. The results, as demonstrated in both colon and breast cancer cells, support the capability of FOXQ1 in regulation of epithelial plasticity and manifestation of EMT.

The human FOXQ1 gene was isolated almost a decade ago by a team in Göttingen university (Bieller, Pasche et al. 2001). However, the biological function of this gene in human remained elusive until now. Several discoveries about the function role of FOXQ1 only emerged recently in year 2010. When this project started, there were no literature describing the role of FOXQ1 in regulation of epithelial plasticity nor its relationship with human malignancies. In 2010, Kaneda and colleagues were the first to link the expression status of FOXQ1 with colon cancer and concluded that FOXQ1 played a positive role in colon cancer progression (Kaneda, Arao et al. 2010). Their results are consistent with my own findings in colon cancer. However, I went several steps further with my discovery that FOXQ1 has the ability to repress epithelial morphology by promoting mesenchymal-like phenotype in colon carcinoma cells. The role of FOXQ1 in regulating epithelial plasticity has also been recognised in mouse mammary gland epithelial cells by Feuerborn and team. They found that FOXQ1 is upregulated by TGF-β treatment in normal mouse mammary epithelial cell (NMuMG) and the level of FOXQ1 influenced the outcome of TGF-β signalling pathway (Feuerborn, Srivastava et al. 2010). What's more, they showed that FOXQ1 has the ability to regulate epithelial plasticity in morphologically homogenous subclone of the parental NMuMG cell line (NM18). However, there was no mention in their paper about the role of FOXQ1 in the context of cancer.

The impact of FOXQ1 in modulating epithelial plasticity is not limited only to colon cancer. Its impact also extends over breast cancer. In this study, I have shown that FOXQ1 expression level played a pivotal role in breast cancer especially the basal-like subtype. My results indicated that FOXQ1 is required to maintain the aggressive phenotype of basal-like human breast cancer cell MDA-MB-231 through promoting EMT processes, while depletion of FOXQ1 expression is sufficient to reverse the mesenchymal-like morphology of these cells, resulting in impaired ability to invade in vitro. In my ectopic expression system, FOXQ1 successfully triggered EMT in human mammary epithelial cells (HMLER). At the same time, Zhang and team have also revealed a similar finding on FOXQ1 in their experiments on mouse breast cancer cells (Zhang, Meng et al. 2011). They demonstrated that FOXQ1 contributed to the metastatic ability of 4TI mouse breast cancer cells in vivo. In FOXQ1 expressing 4TI cancer cells, FOXQ1 knockdown in these cancer cells reduced the long-distance metastasis when injected into fat pads of BALB/c mice. In their ectopic expression system, they claimed that FOXQ1 can trigger EMT morphology in human mammary epithelial cell (HMLE) and MDCK cell line. In addition, reversal of EMT due to FOXQ1 knockdown in 4TI cancer cells has also been observed. Taken together, the capability of FOXQ1 in regulating epithelial plasticity is believed to occur in a wide range of mammalian cells. FOXQ1 also played an active role in metastasis of both colon and breast carcinoma through positive regulation of EMT processes. Investigation into the role of FOXQ1 in malignancies will help us to better understand how the forkhead box family control tumor progression as well as other roles in embryonic development.

In both Feuerborn's and Zhang's publications which I have mentioned earlier, they have showed that FOXQ1 is responsive to TGF-β signalling pathway in murine mammary epithelial cell line systems, such as EpRas and NMuMG. In their experimental systems, FOXQ1 was observed to be upregulated upon TGF-β1 treatment. In contrast, there was no observable change in FOXQ1 level when I treated HCT116 cells with TGF-β1. This could be due to mutation in the TGF-β receptor which is common in colon cancer, and hence, the negative response to TGF-β1 in my setup. Despite the probable mutant status of TGF-β receptor in HCT116 colon carcinoma cell, FOXQ1 was able to successfully induce EMT in the cells and moreover, the acquired EMT morphological changes were reversible depending on the FOXQ1 levels. Therefore, FOXQ1 may have the potential to trigger EMT processes but independent of TGF-β signalling.

The induction of EMT by FOXQ1 in vitro appeared to be specific to certain cell lines. EMT is a key developmental process during cancer progression, invasion and the metastatic cascade. From my observation, ectopic FOXQ1 expression in several epithelial cell lines namely A549, SAOS2, U2OS, MCF7, MCF10A, and HMEC did not trigger the cells to exhibit EMT phenotype. However, FOXQ1 was able to induce EMT in HMLER and HCT116 cell lines. HMLER is a semi-transformed immortalized human mammary epithelial cell line and widely used as a model system to study EMT. HMLER cell line has been engineered on the basis of HMEC with the simian virus 40 large-T oncoprotein and low expression level of H-Ras oncogene. HMEC is human mammary epithelial cell which was immortalized by telomerase catalytic subunit (hTERT). The findings presented herein describes that FOXQ1 is able to promote EMT in semi-transformed HMLER cells and also enable these cells

to express stem cell-like traits. However, I failed to note a similar phenotype in non-transformed normal human mammary epithelial cells with ectopic overexpressed FOXQ1. On the other hand, FOXQ1 alone is sufficient to provoke EMT in epithelial colon cancer cells albeit over an extended period of time. The EMT induced by FOXQ1 is reversible upon withdrawn of FOXQ1 induction, which suggests that FOXQ1 could be a potential target to overcome EMT in cancer metastasis. These evidence favours a relatively weak oncogenic signalling role for FOXQ1, which is dependent on other low level oncogenic signal to exert a combined synergistic effect of inducing human mammary epithelial cells to progressively acquire mesenchymal-like phenotypes. To better understand the role of FOXQ1 in cancer, immortalized cells are increasingly used as experimental models for research (Boehm and Hahn 2004). The above-mentioned role of FOXQ1 in modulating EMT shed new light on understanding of novel functions of FOXQ1 in various human cancers.

6.2 The transcriptional network mediated by FOXQ1 during EMT

In my study, I discovered the EMT phenotypic changes induced by FOXQ1 in both colon and breast epithelial cells, but the transcriptional network governing this morphological change remain unclear. Since the forkhead family is a group of transcriptional factors, I therefore dissected the potential transcriptional network regulated by FOXQ1 in both colon and breast carcinomas. CDH1, CTGF and Slug will be discussed as potential transcriptional targets of FOXQ1 as follows.

6.2.1 CDH1

Protein E-cadherin encoded by CDH1 gene is expressed on cell junction of epithelial cells and functions as glue which holds adjacent cells together thus inhibiting individual cell movement. During EMT processes, E-cadherin plays a downstream role and its mRNA counterpart is a transcriptional target of several well-known EMT inducers. These EMT inducers regulate E-cadherin expression either by binding to E-box of CDH1 promoter region to directly repress CDH1 transcription or indirectly inhibit E-cadherin expression. As a result of EMT, E-cadherin expression is reduced at cell junctions which leads to weaken intercellular binding. Thus, the epithelial cells become freed from adjacent cells. I have observed that E-cadherin mRNA and protein expressions are inversely correlated with FOXQ1 level in both breast and colon carcinomas. However, in breast carcinoma, the well-known EMT inducers did not show any significant changes in gene expression assay using microarray analysis. Hence, the acquired EMT induced by FOXQ1 in breast epithelial cells maybe due to direct or indirect repression of CDH1 transcriptional activity. As an example of forkhead family transcription factor, FOXC2 was shown to regulate breast carcinoma EMT through indirect repression of CDH1 and resulting in the relocation of E-cadherin protein from cell junction to cytosol (Mani, Yang et al. 2007). Such translocation of E-cadherin partially releases epithelial cells to become individual units with increased mobility. In order to further understand relationship between CDH1 and FOXQ1, the promoter region of CDH1 was cloned and reporter activity was measured in stable ectopic FOXQ1 expressing HMLER cells as well as MDA-MB-231 cells with FOXQ1 knockdown. Reporter activity of CDH1 is inversely correlated with FOXQ1 levels, but the chromatin immunoprecipitation (ChIP) assay

did not detect any pronounced binding between CDH1 promoter region and FOXQ1 in vivo. Hence, FOXQ1 may regulate EMT processes by indirectly repressing CDH1 transcriptional activity. The difference between FOXQ1 and FOXC2 in regulating CDH1 is that FOXQ1 can fully repress E-cadherin protein and mRNA expression, but FOXC2 can only partially repress its expression and also result in its translocation. The gene ontology analysis revealed that CDH1 is a key player in FOXQ1 mediated EMT transcriptional network in breast carcinoma. I propose that FOXQ1 does not modulate E-cadherin directly and therefore I believe that some intermediate players exist between them.

6.2.2 CTGF

The other potential transcriptional targets of FOXQ1 identified in this study are CTGF and Slug, both established EMT inducers (Kurrey, K et al. 2005; Liu, Zhang et al. 2006). In colon carcinoma cells, CTGF and Slug were detected to be transcriptionally activated by FOXQ1. In order to identify the transcriptional target of FOXQ1 in mediating EMT process, microarray gene expression profiling was analyzed. In colon carcinoma HCT116 cells, CTGF and Slug were observed to be upregulated in response to FOXQ1 overexpression at different time points. CTGF was elevated rapidly only after 24 hours of FOXQ1 induction. However, Slug upregulation was only detected upon prolonged FOXQ1 overexpression for a period of at least two weeks. These suggest that FOXQ1 may activate CTGF and Slug expression via different mechanisms. In addition, following my observation, I decided to map out the CTGF and Slug promoter responsive region which can be activated by FOXQ1 in a

transient co-transfection system performed in HCT116 cell line. However, whether CTGF or Slug are direct transcriptional targets of FOXQ1 remain to be determined.

Because current knowledge for FOXQ1 is limited, an alternative albeit indirect way is to understand the biological function of CTGF. CTGF (connective tissue growth factor) also known as CCN2 is a member of the CCN protein family (Bork 1993). Other members of this family are cycteine-rich 61 (CYR61/CCN1), nephroblastoma overexpressed (NOV/CCN3), WISP-1/elm1 (CCN4), WISP-2/rCop1 (CCN5), and WISP-3 (CCN6) (Perbal 2004). Members of the CCN protein family are involved in various biological functions including stimulating cellular proliferation, migration, adhesion, formation of extracellular matrix, as well as regulation of angiogenesis and tumorigenesis. CTGF is a secreted growth factor that can bind to integrins on cell surface. It can also serves as an angiogenic factor in collaboration with matrix metalloproteinase (Lau and Lam 1999; Kondo, Kubota et al. 2002). Elevated CTGF expression has been observed in breast cancers, pancreatic cancers, melanomas, and chondro-sarcomas (Kubo, Kikuchi et al. 1998; Wenger, Ellenrieder et al. 1999; Shakunaga, Ozaki et al. 2000; Xie, Nakachi et al. 2001). Specifically, in breast cancers, CTGF overexpression has been linked to increase of tumor size and lymph node metastasis (Chen, Wang et al. 2007). Microarray analysis indicated that CTGF is critically involved in the formation of osteolytic bone metastasis in breast cancer (Kang, Siegel et al. 2003; Minn, Kang et al. 2005). The paper published by Min-Liang Kuo and team in 2009 showed that CTGF promote breast cancer cell metastasis through an integrin $\alpha_v\beta_3$-extracellular signal–regulated kinase (ERK)-1/2–dependent, S100A4-upregulated pathway. This group further studied the CTGF mediated chemoresponse in breast cancers, and their results showed that CTGF overexpression

resulted in greater resistance to apoptosis induced by doxorubicin (adriamycin) and paclitaxel. The resistance was believed to be due to upregulation of Bcl-xL and cellular inhibitor of apoptosis protein 1 (cIAP1). Therefore, CTGF expression conferred resistance against apoptosis induced by chemotherapeutic agents via increasing a survival pathway through ERK1/2-dependent Bcl-xL/cIAP1 up-regulation (Wang, Chen et al. 2009). On the other hand, CTGF may act in a positive way to promote invasion and metastasis in lung adenocarcinoma and colorectal cancers (Chang, Shih et al. 2004; Lin, Chang et al. 2005). Therefore, the biological function of CTGF can change depending on the cellular environment. Furthermore, CTGF is regulated by TGF-β signalling in fibroblast. CTGF was first identified in conditioned medium collected from cultured human vascular endothelial cells, whose gene expression is strongly induced by TGF-β in fibroblast. In fibroblast, CTGF is a downstream mediator of TGF-β activity. Indeed, CTGF is known to mediate key cellular events in response to TGF-β including migration, proliferation, matrix production and contraction, and differentiation of fibroblast into myofibroblasts. CTGF induction by TGF-β is not limited to connective tissue cells. During TGF-β induced EMT in epithelial cells, CTGF can also be produced and played an important role. In human corneal epithelial cells (HCEC), CTGF is required for TGF-β-stimulated epithelial cell migration. This CTGF signalling occurred through ERK-p38 MAPK pathway to induce migration in epithelial cells derived from stratified epithelium. TGF-β cannot induce epithelial cell migration in the absence of CTGF (Bradham, Igarashi et al. 1991; Brigstock 1999; Secker, Shortt et al. 2008). In my study, CTGF was found to be upregulated by FOXQ1 expression in HCT116 colon carcinoma cells, and FOXQ1 then induced EMT phenotype in these cells. It seemed that FOXQ1 induced EMT phenomenon in HCT116 cells did not involve CTGF.

6.2.3 Slug

Slug is the next potential transcriptional target of FOXQ1 identified in colon cancer. It belongs to the same family as Snail. Slug was detected to be upregulated after prolonged FOXQ1 expression in HCT116 cells. However, no significant changes were detected with other well-known EMT inducers such as Snail and Twist. Furthermore, luciferase reporter assay revealed that certain region of Slug promoter can be transactivated by full-length FOXQ1 expression. This suggested that Slug could be the FOXQ1 responsive element to induce EMT in HCT116 cells. Unfortunately, the ChIP assay did not detected any binding between FOXQ1 and Slug promoter region from 400bp upstream to 100bp downstream. Due to the absence of commercially available FOXQ1 antibody and the customized antibody was not optimal, I therefore detected FOXQ1 protein with anti-myc antibody which not only recognized the myc tag, but also endogenous Myc. Hence, the outcome of the ChIP assay should not be accurate. Notwithstanding the failure of ChIP assay to detect any direct binding between FOXQ1 and its proposed target Slug, Slug is still believed to be an effecter in FOXQ1-induced EMT. Since Twist represses E-cadherin expression indirectly which in turn facilitate EMT induction process, in colon cancer, Twist promoter is frequently hypermethylated (Okada, Suehiro et al.). In colon cancer, the TGF-β signalling pathway which is a well-known mediator of EMT, invasion and metastasis becomes malfunction due to mutation of the TGF-β receptor II (Samowitz and Slattery 1997). Hence, Slug is postulated as the effecter of FOXQ1-induced EMT in HCT116 cells.

It is believed that FOXQ1 trigged EMT in breast and colorectal carcinomas through different molecular mechanisms. There were no significant changes on CTGF and Slug mRNA levels in breast carcinoma FOXQ1 was either overexpressed or knocked down, on the other hand, significant changes were observed in colorectal carcinoma. However, in both breast and colon cancers, E-cadherin protein and mRNA levels are inversely correlated with FOXQ1 consistently. This suggests that FOXQ1 induced EMT through different mechanisms in colorectal and breast carcinomas.

6.3 FOXQ1-induced EMT in human mammary epithelial cells results in generation of cancer stem cells

Compelling evidence exists that relates EMT to the emergence of cancer stem cell (CSC)-like phenotype, which may be a prerequisite for cancer cell metastasis (Sheridan, Kishimoto et al. 2006). Experimental evidence that showed a direct connection between EMT and cancer stem cells was recently reported (Mani, Guo et al. 2008; Morel, Lievre et al. 2008). These characteristic phenotypes have also been observed through the same HMLER cell system with FOXQ1 overexpression in my research. In addition, a growing number of evidence suggested that certain subpopulation of cells in primary breast cancers maybe endowed with self-renewal ability which enabled these subpopulations to initiate metastasis of the tumor to a distant site. The subpopulation of breast cancer cells express special cell surface antigens CD44+/CD24(-/low), which distinguished breast cancer stem cells from the bulk of the breast tumor. In addition, the concept of breast cancer stem cell is also applicable to laboratory cultured breast cancer cell lines, for example, in MDA-MB-231 cells which have at least 80% of population expressing CD44+/CD24- which are

considered as breast cancer stem cells. Besides the self-renewal ability of cancer stem cells, they also possess other stem cell characteristics such as indefinite proliferation, the ability to differentiate (developing into functional cells), and resistance to chemotherapy. Others reported that surviving residual breast cancer tissue cells after conventional therapy also have cancer stem cell properties by expressing cell surface markers CD44+/CD24-. In addition to the cancer stem cell traits, the CD44+/CD24- subpopulation of breast cancer cells also exhibited unique ability to invade matrigel in vitro and expressed higher levels of proinvasive genes such as IL-1α, IL-6, and IL-8. However, CD44+/CD24- phenotype alone is not sufficient for metastasis, then followed by proliferation at distant site (Sheridan, Kishimoto et al. 2006). Moreover, consistent with the high level of expression of FOXQ1 in MDA-MB-231 cells, these cells consist a high percentage of breast cancer stem cell population displayed CD44+/CD24(-/low) phenotype. Therefore, these findings may indicate a role of FOXQ1 in cancer EMT and possible cancer stem cell regulation. The evidence provided so far suggests that FOXQ1 is a multifunctional factor with the ability to induce EMT and regulate metastatic program in breast cancers. During the EMT processes, FOXQ1 likely transformed these cells to display breast cancer stem cell properties as shown by increased population of staining with tumor surface antigens CD44+/CD24-.

Identification of cells with cancer stem cell properties or factors that promote formation of this population will help to improve therapeutic opportunity. Currently, chemotherapy and radiotherapy only kill the bulky mass of cancerous tissue, while the remaining cancerous cells may still retain the capability to form recurrent malignancy in the future and even in distant sites. The remaining cells after chemo- or

radiotherapy share similarities with cancer stem cell. They are characterized by well-known cell surface markers CD44+/CD24- in breast cancers. In ovarian cancer, EMT inducer Snail and Slug also contribute to cancer stem cell formation. Transfection with Snail and Slug led to derepression of 'stemness' genes, including Nanog and KLF4, as well as four to five-fold increases in the size of CD44+ CD117+ cancer stem cell population that was resistant to chemo- and radiotherapy. This revolutionary finding highlighted the heterogeneity of cancer cells, of which only certain subpopulation has the ability to give rise to tumor formation. Due to the heterogeneity of tumors, they likely contain a subpopulation of self-renewing and expanding stem cells, known as cancer stem cells. EMT is an increasingly recognized mechanism to further generate cancer stem cells endowed with a more invasive and metastatic phenotype (Kurrey, Jalgaonkar et al. 2009).

6.4 Chemoresistance mediated by high level of FOXQ1 in colon carcinomas

Growing evidence is showing that one of the outcomes of EMT process is acquired chemoresistance ability. In this study, FOXQ1 not only has functions in promoting EMT in breast epithelial cells but also conferring cancer stem cell properties upon them. In colon epithelial cells, FOXQ1 initiates EMT to make them more chemoresistance. In colon cancer epithelial cell line HCT116, besides the EMT morphology displayed, ectopic expressing FOXQ1 also confers chemoresistance to a panel of DNA toxic drugs. Another unrelated research group simultaneously published similar findings with regards to FOXQ1-mediated chemoresistance in colon cancer (Kaneda, Arao et al. 2010). They demonstrated that p21 is a downstream target

of FOXQ1 in colon cancer, and overexpression of FOXQ1 in H1299 (a non-small cell lung carcinoma cell line) led to reduced apoptotic signal in terms of Annexin V and PI staining in response to both doxirubicin (Adriamycin) and CPT treatments. They concluded that the acquired chemoresistance after FOXQ1 overexpression could partially be due to upregulation of p21. However, there is no evidence to show direct connection of p21 to FOXQ1 mediated anti-apoptotic effect. Similar to my own findings, FOXQ1 was shown to mediate apoptosis resistance. However, the result from Kaneda's research was achieved using ectopic overexpressing FOXQ1 in a model of non-small cell lung carcinoma cell line (H1299). Thus, even though their results can provide a clue about FOXQ1 in regulating anti-apoptotic effect, further direct demonstration on colon cancer cell lines would be useful indeed. Considering the high expression level of FOXQ1 in most colon cancers, FOXQ1 is postulated to have functions in promoting tumorigenicity and to enable cells to bypass apoptotic signals. Hence, targeting FOXQ1 could be a practical idea to increase chemo-responsiveness of cancer cells. FOXQ1 may also be useful in the future as a biomarker of colon cancers.

Cancer therapy has often been associated with acquired resistance. An increasing body of literature now suggests that acquired resistance to chemotherapy is likely to be linked to acquired EMT (Voulgari and Pintzas 2009). For instance, elevated E-cadherin expression or increased mesenchymal phenotype can result in resistance to EGFR kinase inhibitor (Cano, Perez-Moreno et al. 2000) or DNA damaging agent-induced apoptosis (Comijn, Berx et al. 2001). Moreover, chemotherapy leading to an increase in the number of CD44+/CD24(-/low) cancer stem cells (Hajra, Chen et al. 2002) may represent a potentially important mechanism of acquired drug resistance.

Therefore, in addition to gaining self-renewal ability by cancer cells undergoing EMT, they also become chemoresistant at the same time. Consistent with this reasoning, I have shown that FOXQ1 depletion in MDA-MB-231 cells can result in sensitization to a variety of chemotherapeutic agents while enforced expression of FOXQ1 in epithelial cancer cells can induce chemoresistance. Therefore, FOXQ1 may play a broader role with respect to multiple drug resistance in human cancer and this is likely to be achieved through more than one single mechanism.

Recently, accumulating evidence has implicated the close relationship between EMT, cancer stem cells and chemoresistance (Singh and Settleman 2010). From the effect of ectopic expressing FOXQ1 in colon cancer and immortalized mammary epithelial cells, FOXQ1 indeed has biological function in manipulating epithelial plasticity, gaining chemoresistant ability, and acquiring stem cell traits. Although I could not provide direct evidence for chemoresistance and stem cell-like properties, there is a growing amount of literature on this topic of cancer stem cell and its role in response to chemotherapy. Regardless of the lack of direct evidence, EMT processes still promote tumor progression, contribute to cancer relapses and chemoresistance. EMT not only contributes to tumor progression, subsequent invasion and metastasis, but also enables tumor cells to acquire chemoresistance. In ovarian cancers, overexpression of EMT inducers Slug and Snail in epithelial ovarian caner cell line triggered EMT phenotype while enabling these cells to have enhanced survival and resistance to radiotherapy. On the other hand, paclitaxel resistant ovarian cell line was established by exposure to paclitaxel for a certain period of time. These paclitaxel resistant cells acquire a spindle-like shape morphology, and both Slug and Snail expression was up-regulated. Hence, EMT is associated with chemo- and radio-

resistance in ovarian cancer. In addition, the acquired chemoresistance was also reported in EMTed epithelial breast cancer, while artificially generated chemoresistant breast cancer cells also exhibited EMT phenotypes. Hence, EMT processes contribute towards cancer recurrent and progression by promoting invasion and metastasis. Hence, I believe that intervention of EMT processes has potential clinical relevance (Kajiyama, Shibata et al. 2007; Kurrey, Jalgaonkar et al. 2009; Ahmed, Abubaker et al. 2010).

Conventional chemotherapeutic agents have acceptable ability to shrink tumor size and limit tumor cell growth, but residual tumor cells evolve to gain resistance against previously exposed chemotherapeutic drugs. These surviving cells are responsible for tumor recurrence and metastasis to distant sites. Consequently, conventional chemo- and radio-therapy actually increases the cancer stem cell population by killing off the susceptible tumor mass, and thereby increasing the risk of malignancy recurrence. Weinberg's group recently published data which demonstrated that salinomycin can effectively and selectively induce breast cancer stem cell death (Gupta, Onder et al. 2009). Therefore, investigation of selective inhibitor of cancer stem cells can have important clinical relevance, and understanding the biological outcome of FOXQ1-induced EMT and breast cancer stem cell can provide clues to future research.

6.5 Repressed cell proliferation rate by ectopic FOXQ1 expression

Besides EMT induced by FOXQ1 in colon and breast carcinomas, I also discovered another biological function of FOXQ1 which is inhibition of proliferation in both colon cancer cells HCT116 and immortalized human mammary epithelial cells

(HMLER). These two functions may appear contradictory at first impression, but this dual function is similar to TGF-β signalling in terms of regulating proliferation and EMT. Proliferation rate is an independent cell process with no ties to EMT process in promoting cancer progression. From my observation, EMTed cells showed a much slower proliferation rate. This de-differentiation process is proposed to enrich the population with cancer stem cells which is widely acknowledged in breast and colon cancer. In colorectal cancer, an inverse relationship between cancer progression and tumor proliferative activity was reported by Lin and team where primary tumor and liver metastasis of colorectal cancer were analyzed. They also found an association between more aggressive biological behavior and low proliferation in colorectal cancer by analyzing colorectal cancer liver metastases and a series of primary tumors differing in metastatic potential. Both metastasizing primaries and liver metastases are characterized by reduced proliferative activity compared to non-metastatic colorectal cancers (Lin, Chatterjee et al. 2007; Anjomshoaa, Nasri et al. 2009). These findings support the slow proliferative rate of HCT116 cells carrying ectopic FOXQ1 expression vector since ectopic FOXQ1 expression in HCT116 cells induced EMT which potentially contributed to cancer progression and metastasis. This impaired cell proliferation is only associated with wild type full-length FOXQ1 expression, but not the truncated FOXQ1 deletion mutants (D6). Since the rationale of deletion mutant design of FOXQ1 is based on the transactivation ability to certain CTGF promoter region, there is a certain degree of limitations in the functional study of FOXQ1 in the specific CTGF region. The slower proliferation together with induced EMT phenotype and acquired chemoresistance ability did not appear in HCT116 cells expressing truncated FOXQ1 D6 deletion mutant. This indicated that the decreased proliferation rate, and EMT induction by full-length FOXQ1 is not involved in

transactivating CTGF promoter, at least in certain examined region. Even though FOXQ1 can transcriptionally activate CTGF promoter in vitro, however, the biological significance remains to be determined in colon cancer.

6.6 Functional structures of FOXQ1 protein

Forkhead box family is characterized by the highly conserved DNA binding domain (DBD). In this study, I attempted to first identify the functional structure of FOXQ1 protein based on knowledge of conserved DBD in other forkhead family members. In order to do that, CTGF, the potential transcription target of FOXQ1 was used to perform this study. A certain genomic region of CTGF (CTGF-P2) was confirmed by reporter assay and the functional structure analysis was based on the transcriptional activity of truncated FOXQ1 deletion mutant to CTGF-P2 promoter activity. These truncated FOXQ1 deletion mutants were designed on the knowledge of the well-studied forkhead family member FOXO. Molecule of FOXO proteins contains 4 domains: a highly conserved DNA-binding domain, a nuclear localization signal just located downstream of DBD, a nuclear export signal, and a C-terminal transactivation domain (Obsilova, Vecer et al. 2005; Gao, Wang et al. 2010).

According to the structures of FOXO proteins, the nuclear localization signal (NLS) is right after the DBD region and share several amino acid with DBD. The core protein sequence of NLS is RRRRA. The function of FOXO is under the control of insulin/insulin-like signalling. The regulation of FOXO depends on the shuttling of this factor between nucleus and cytosol. FOXO is in charge of a multitude of biological processes including cell-cycle, cell death, DNA repair, metabolism and

protection from oxidative stress. The shuttling of FOXO requires protein phosphorylation within several domains, and associated with 14-3-3 proteins and the nuclear transport machinery (Obsil and Obsilova 2008). FOXO is the most studied forkhead family in terms of structures. On the basis of our knowledge of FOXO structure, the FOXQ1 protein was truncated from N-terminal or C-terminal region. The transactivation and inhibitory domain as well as the nuclear localization signal were identified in this study. The transactivation domain locates at the C-terminal region of FOXQ1. Similarly, the transactivation domain in FOXO is also in the C-terminal region but in different sequences. All forkhead proteins showed a high degree of amino acid identity in the region of winged helix DNA binding domain.

FOXQ1 could also involve posttranslational modification. Unfortunately, I am not able to provide detailed research on this topic. The other limitation of FOXQ1 structural study is based on the transcriptional activity to activate certain CTGF genomic region. However, wild-type FOXQ1 locates to the nucleus rather than cytosol to exert its transcriptional activity. This characterization is different from FOXO, which only travels into the nucleus when needed. When NLS of FOXQ1 is abolished, the ability to enter nucleus to exert transcriptional activity became lost. Hence, the main functional regulation of FOXQ1 is believed to be control of gene transcription.

6.7 Significance of this study

6.7.1 FOXQ1 is an important forkhead factor that regulates EMT

In this study, I have demonstrated FOXQ1 as a forkhead factor with the ability to regulate EMT, functionally similar with FOXC1 and FOXC2. Unlike FOXC1 and FOXC2, FOXQ1 regulates EMT in a much broader way, and it induced EMT in both breast and colon carcinoma cells.

In human keratinocytes, FOXQ1 has been reported to be decreased in expression in a Smad4-dependent manner in response to TGF-β treatment (Levy and Hill 2005). Other forkhead factors are also reported to regulate epithelial plasticity and dedifferentiation. FOXA1 and FOXA2 for example, are involved in maintaining the epithelial phenotype and loss of expression was sufficient to induce the dedifferentiation of pancreatic cancer cells (Song, Washington et al.). Next, FOXA2 influenced epithelial polarity and epithelialization in the endoderm germ layer of mouse embryos (Burtscher and Lickert 2009). The first identified DNA-binding partner for Smad proteins and thus functionally implicated in mediating TGF-β/activin responses was the Xenopus Forkhead-factor FAST1 (FOXH1) (Chen, Rubock et al. 1996; Attisano, Silvestri et al. 2001). Furthermore, in human keratinocytes, FOXO-factors functionally synergized with TGF-β-activated Smad factors, which is crucial for the regulation of several immediate early genes in response to TGF-β treatment (Gomis, Alarcon et al. 2006). Together, these studies demonstrated that the expression of FOX factors is regulated by TGF-β and they play important roles for the outcome of TGF-β signalling. However, in the TGF-β receptor mutated background such as colon carcinoma, FOXQ1 also retained the ability to

induce EMT. This suggested that FOXQ1 may regulate both TGF-β dependent and independent pathways.

6.7.2 FOXQ1 may be used as a diagnostic and prognostic biomarker for aggressive breast cancer and colon cancer

Cancer is considered as a chronic disease. Its development requires accumulation of genetic mutations including mutations in tumor suppressor genes. Most cancers remain silent until there is some clinical manifestations. In fact, benign tumors remain silence for years until it becomes malignant. Cancer in the benign stage usually shows no symptoms because the benign tumor has limited capability of invading surrounding tissue and organ. Clinically, symptoms may not be obvious even in the early stages before metastasis of malignant tumors to the various parts of the body. Hence, developing technology to detect cancer in early stages can greatly improve the treatment outcome and provide patients with a better quality of life. In this study, evidence was provided that FOXQ1 is clinically associated with basal-like breast cancer, which is associated with poor clinical outcome and an aggressive phenotype. This association is supported by our knowledge of FOXQ1 in nature. The treatment for cancer can start with surgical removal of solid tumor mass, followed by systematic chemotherapy and/or radiotherapy. However, different cancer types have varying responses to chemo- and radio-therapy, and sometimes the outcome is not desirable. Cancer cells have the ability to evolve in response to chemo- and radio-therapy. As a result, they can acquire resistance to previous therapeutic exposures. The status of FOXQ1 in the cells may decide the chemo-responses of these cells. FOXQ1 can promote EMT in both colon and breast cancer cells and potentially regulate cell

invasion and metastasis. It is therefore logical to decide to monitor FOXQ1 expression levels in clinical samples which could be used as a biomarker to determine disease prognosis and better propose treatment regimen.

6.7.3 FOXQ1 may be used as potential therapeutic target for breast and colon cancer

The role of epithelial to mensenchymal transition (EMT) during tumor progression, invasion and metastasis has been recently discussed and applied in anti-cancer drug discovery. Growing evidence indicates that EMT in cancer progression occurs in a wide range of malignancy and is a potential target for pharmaceutical intervention to reduce the aggressive behavior of malignancy and improve patient outcome. Hence, targeting genes driving EMT and corresponding downstream signaling pathway effectors could be a practical approach to intervene cancer progression.

The gene of FOXQ1 was analyzed by several clinical breast cancer databases on Oncomine. FOXQ1 was revealed to be highly associated with basal-like (triple negative) breast cancer subtype, high metastasis rate, and higher tumor grades. In addition, patients with high level of FOXQ1 have lower survival rate depending on presence or absence of distant metastasis (DM). The expression status of FOXQ1 in breast cancer is closely correlated with the following findings and potential applications. In aggressive basal-like breast cancer MDA-MB-231 cells, lowering FOXQ1 expression reduced the invasion ability in vitro and inhibited the mesenchymal morphology. At the same time, these FOXQ1 depleted cells exhibit more apoptotic responses to several DNA damage agents. It suggested that lowering

FOXQ1 expression is able to reduce the aggressive phenotype of MDA-MB-231 breast cancer. I have examined the capability of FOXQ1 in manipulating epithelial plasticity in human mammary epithelial cells (HMLER), EMT process triggered by ectopic expressing FOXQ1, and gain of cancer stem cell properties by expressing cell surface markers CD44+/CD24-. These phenotypes were coupled with increased capability of forming mammospheres in low adherent condition in vitro.

The expression pattern of FOXQ1 in breast cancers is highly associated with basal-like breast cancers. This type of breast cancer comprised 15% of total breast cancer population. It is extremely difficult to target and the outcomes are not desirable. The other obstacle of breast cancer treatment is relapse and metastasis to distant sites in the brain, lung, and skeleton. Hence, targeting proteins involved in EMT may provide a therapeutic strategy for eliminating residual cells to prevent recurrence and improve long-term survival in breast cancer patients. Despite advances in detection and treatment of metastatic breast cancer, mortality from this disease remains high because current therapies are limited by the emergence of therapy-resistant cancer cells, which were recently named ‘breast cancer stem cells’. The cancer stem cell concept is supported by important clinical finding that for most tumors, there is little correlation between response to therapy and long term survival. Certainly, patients who do not respond to treatment do not survive, but a large proportion of patients with cancer die of their disease despite responding well to chemotherapy. In this paper, I provide more evidence to link EMT and breast cancer stem cell. Although direct targeting of cancer stem cell is difficult because of difficulty defining what they are, targeting proteins that positively regulate EMT is more realistic. Based on this rationale, targeting FOXQ1 might therefore be a realistic approach to eliminate

formation of breast cancer stem cells and finally result in better survival outcome for patients after chemotherapy.

6.8 Conclusions

Basal-like breast cancer is an aggressive subtype of breast cancer associated with poor clinical outcome. The genetic makeup of this type of breast cancer enables them to tolerate and survive after conventional hormonal therapy. In this study, I report that forkhead factor FOXQ1 contributed to an aggressive phenotype, cancer cell invasion and metastatic ability of this subtype of breast cancer through positively regulating EMT. As a consequence of EMT, FOXQ1 triggered breast cancer stem cell phenotype in immortalized human mammary epithelial cells, which also provide evidence that FOXQ1 contributed to aggressive breast cancer phenotype. On the other hand, in colon cancer, FOXQ1 is upregulated in most of colon tumor and FOXQ1 also triggered EMT in colon carcinoma cells, enabling these cells to become chemoresistance. These EMT phenotype triggered by FOXQ1 in colon cancer may have occurred through upregulation of well-known EMT inducers such as Slug and CTGF. The above characterization of the roles of FOXQ1 in breast and colon cancer shed new light on the complex mechanisms underlying the tumorigenesis of basal-like breast cancer and colon cancer. FOXQ1 has been suggested to possibly serve as a novel biomarker for determining clinical prognosis and a potential therapeutic target to control progression and metastatic potential of human breast and colon cancer.

6.9 Future prospect

Following the recognition of EMT in cancer progression, several EMT regulators were rapidly identified which included several forkhead transcription factors. In this study, I have demonstrated the biological function of FOXQ1 and its importance in regulating cancer progression and metastasis through modulation of EMT processes in breast and colon cancers. The mechanism by which FOXQ1 regulates EMT will be the next priority in future FOXQ1 research. FOXQ1 is believed to play an oncogenic role in cancer in view of its clinical expression status. FOXQ1 is worth further research especially in the area of transcriptional network in regulating EMT, cancer stemness and chemoresistance.

References

Abell, M. R. (1966). "The nature and classification of ovarian neoplasms." Can Med Assoc J **94**(21): 1102-1124.

Adesina, A. M., Y. Nguyen, et al. (2007). "FOXG1 is overexpressed in hepatoblastoma." Hum Pathol **38**(3): 400-409.

Ahmed, N., K. Abubaker, et al. (2010). "Epithelial mesenchymal transition and cancer stem cell-like phenotypes facilitate chemoresistance in recurrent ovarian cancer." Curr Cancer Drug Targets **10**(3): 268-278.

Aigner, K., B. Dampier, et al. (2007). "The transcription factor ZEB1 (deltaEF1) promotes tumour cell dedifferentiation by repressing master regulators of epithelial polarity." Oncogene **26**(49): 6979-6988.

Ailles, L. E. and I. L. Weissman (2007). "Cancer stem cells in solid tumors." Curr Opin Biotechnol **18**(5): 460-466.

Akhurst, R. J. and R. Derynck (2001). "TGF-beta signaling in cancer--a double-edged sword." Trends Cell Biol **11**(11): S44-51.

Al-Hajj, M., M. S. Wicha, et al. (2003). "Prospective identification of tumorigenic breast cancer cells." Proc Natl Acad Sci U S A **100**(7): 3983-3988.

Albergaria, A., J. Paredes, et al. (2009). "Expression of FOXA1 and GATA-3 in breast cancer: the prognostic significance in hormone receptor-negative tumours." Breast Cancer Res **11**(3): R40.

Anjomshoaa, A., S. Nasri, et al. (2009). "Slow proliferation as a biological feature of colorectal cancer metastasis." Br J Cancer **101**(5): 822-828.

Ansieau, S., J. Bastid, et al. (2008). "Induction of EMT by twist proteins as a collateral effect of tumor-promoting inactivation of premature senescence." Cancer Cell **14**(1): 79-89.

Anton Aparicio, L. M., R. Garcia Campelo, et al. (2007). "Prostate cancer and Hedgehog signalling pathway." Clin Transl Oncol **9**(7): 420-428.

Antony, M. L., R. Nair, et al. (2010). "Changes in expression, and/or mutations in TGF-beta receptors (TGF-beta RI and TGF-beta RII) and Smad 4 in human ovarian tumors." J Cancer Res Clin Oncol **136**(3): 351-361.

Appelbaum, F. R., J. M. Rowe, et al. (2001). "Acute myeloid leukemia." Hematology Am Soc Hematol Educ Program: 62-86.

Arslan, C., O. Dizdar, et al. (2009). "Pharmacotherapy of triple-negative breast cancer." Expert Opin Pharmacother **10**(13): 2081-2093.

Attisano, L., C. Silvestri, et al. (2001). "The transcriptional role of Smads and FAST (FoxH1) in TGFbeta and activin signalling." Mol Cell Endocrinol **180**(1-2): 3-11.

Avraham, K. B., C. Fletcher, et al. (1995). "Murine chromosomal location of eight members of the hepatocyte nuclear factor 3/fork head winged helix family of transcription factors." Genomics **25**(2): 388-393.

Badve, S., D. Turbin, et al. (2007). "FOXA1 expression in breast cancer--correlation with luminal subtype A and survival." Clin Cancer Res **13**(15 Pt 1): 4415-4421.

Baker, S. J., A. C. Preisinger, et al. (1990). "p53 gene mutations occur in combination with 17p allelic deletions as late events in colorectal tumorigenesis." Cancer Res **50**(23): 7717-7722.

Batlle, E., E. Sancho, et al. (2000). "The transcription factor snail is a repressor of E-cadherin gene expression in epithelial tumour cells." Nat Cell Biol **2**(2): 84-89.

Bellam, N. and B. Pasche (2010). "Tgf-beta signaling alterations and colon cancer." Cancer Treat Res **155**: 85-103.

Ben-Porath, I., M. W. Thomson, et al. (2008). "An embryonic stem cell-like gene expression signature in poorly differentiated aggressive human tumors." Nat Genet **40**(5): 499-507.

Bernardo, G. M., K. L. Lozada, et al. (2010). "FOXA1 is an essential determinant of ERalpha expression and mammary ductal morphogenesis." Development **137**(12): 2045-2054.

Bialek, P., B. Kern, et al. (2004). "A twist code determines the onset of osteoblast differentiation." Dev Cell **6**(3): 423-435.

Bieller, A., B. Pasche, et al. (2001). "Isolation and characterization of the human forkhead gene FOXQ1." DNA Cell Biol **20**(9): 555-561.

Boehm, J. S. and W. C. Hahn (2004). "Immortalized cells as experimental models to study cancer." Cytotechnology **45**(1-2): 47-59.

Bolos, V., H. Peinado, et al. (2003). "The transcription factor Slug represses E-cadherin expression and induces epithelial to mesenchymal transitions: a comparison with Snail and E47 repressors." J Cell Sci **116**(Pt 3): 499-511.

Bonnet, D. and J. E. Dick (1997). "Human acute myeloid leukemia is organized as a hierarchy that originates from a primitive hematopoietic cell." Nat Med **3**(7): 730-737.

Bork, P. (1993). "The modular architecture of a new family of growth regulators related to connective tissue growth factor." FEBS Lett **327**(2): 125-130.

Bos, J. L., E. R. Fearon, et al. (1987). "Prevalence of ras gene mutations in human colorectal cancers." Nature **327**(6120): 293-297.

Bradham, D. M., A. Igarashi, et al. (1991). "Connective tissue growth factor: a cysteine-rich mitogen secreted by human vascular endothelial cells is related to the SRC-induced immediate early gene product CEF-10." J Cell Biol **114**(6): 1285-1294.

Braig, M., S. Lee, et al. (2005). "Oncogene-induced senescence as an initial barrier in lymphoma development." Nature **436**(7051): 660-665.

Brigstock, D. R. (1999). "The connective tissue growth factor/cysteine-rich 61/nephroblastoma overexpressed (CCN) family." Endocr Rev **20**(2): 189-206.

Burtscher, I. and H. Lickert (2009). "Foxa2 regulates polarity and epithelialization in the endoderm germ layer of the mouse embryo." Development **136**(6): 1029-1038.

Cano, A., M. A. Perez-Moreno, et al. (2000). "The transcription factor snail controls epithelial-mesenchymal transitions by repressing E-cadherin expression." Nat Cell Biol **2**(2): 76-83.

Cao, D., S. R. Hustinx, et al. (2004). "Identification of novel highly expressed genes in pancreatic ductal adenocarcinomas through a bioinformatics analysis of expressed sequence tags." Cancer Biol Ther **3**(11): 1081-1089; discussion 1090-1081.

Carey, L. A., E. C. Dees, et al. (2007). "The triple negative paradox: primary tumor chemosensitivity of breast cancer subtypes." Clin Cancer Res **13**(8): 2329-2334.

Carr, J. R., H. J. Park, et al. (2010). "FoxM1 mediates resistance to herceptin and paclitaxel." Cancer Res **70**(12): 5054-5063.

Ceder, J. A., L. Jansson, et al. (2008). "The characterization of epithelial and stromal subsets of candidate stem/progenitor cells in the human adult prostate." Eur Urol **53**(3): 524-531.

Chaffer, C. L. and R. A. Weinberg (2011). "A perspective on cancer cell metastasis." Science **331**(6024): 1559-1564.

Chan, D. W., V. W. Liu, et al. (2009). "Overexpression of FOXG1 contributes to TGF-beta resistance through inhibition of p21WAF1/CIP1 expression in ovarian cancer." Br J Cancer **101**(8): 1433-1443.

Chang, C. C., J. Y. Shih, et al. (2004). "Connective tissue growth factor and its role in lung adenocarcinoma invasion and metastasis." J Natl Cancer Inst **96**(5): 364-375.

Chen, P. S., M. Y. Wang, et al. (2007). "CTGF enhances the motility of breast cancer cells via an integrin-alphavbeta3-ERK1/2-dependent S100A4-upregulated pathway." J Cell Sci **120**(Pt 12): 2053-2065.

Chen, X., M. J. Rubock, et al. (1996). "A transcriptional partner for MAD proteins in TGF-beta signalling." Nature **383**(6602): 691-696.

Clark, K. L., E. D. Halay, et al. (1993). "Co-crystal structure of the HNF-3/fork head DNA-recognition motif resembles histone H5." Nature **364**(6436): 412-420.

Clarke, M. F. (2005). "A self-renewal assay for cancer stem cells." Cancer Chemother Pharmacol **56 Suppl 1**: 64-68.

Clarke, M. F. and M. Fuller (2006). "Stem cells and cancer: two faces of eve." Cell **124**(6): 1111-1115.

Cleator, S., W. Heller, et al. (2007). "Triple-negative breast cancer: therapeutic options." Lancet Oncol **8**(3): 235-244.

Collado, M., J. Gil, et al. (2005). "Tumour biology: senescence in premalignant tumours." Nature **436**(7051): 642.

Comijn, J., G. Berx, et al. (2001). "The two-handed E box binding zinc finger protein SIP1 downregulates E-cadherin and induces invasion." Mol Cell **7**(6): 1267-1278.

Crouch, S. P., R. Kozlowski, et al. (1993). "The use of ATP bioluminescence as a measure of cell proliferation and cytotoxicity." J Immunol Methods **160**(1): 81-88.

Dalerba, P., R. W. Cho, et al. (2007). "Cancer stem cells: models and concepts." Annu Rev Med **58**: 267-284.

Davies, H., G. R. Bignell, et al. (2002). "Mutations of the BRAF gene in human cancer." Nature **417**(6892): 949-954.

Debnath, J., S. K. Muthuswamy, et al. (2003). "Morphogenesis and oncogenesis of MCF-10A mammary epithelial acini grown in three-dimensional basement membrane cultures." Methods **30**(3): 256-268.

Dent, R., M. Trudeau, et al. (2007). "Triple-negative breast cancer: clinical features and patterns of recurrence." Clin Cancer Res **13**(15 Pt 1): 4429-4434.

Derynck, R. and Y. E. Zhang (2003). "Smad-dependent and Smad-independent pathways in TGF-beta family signalling." Nature **425**(6958): 577-584.

Dick, J. E. (2008). "Stem cell concepts renew cancer research." Blood **112**(13): 4793-4807.

Dontu, G., W. M. Abdallah, et al. (2003). "In vitro propagation and transcriptional profiling of human mammary stem/progenitor cells." Genes Dev **17**(10): 1253-1270.

Ellenberger, T., D. Fass, et al. (1994). "Crystal structure of transcription factor E47: E-box recognition by a basic region helix-loop-helix dimer." Genes Dev **8**(8): 970-980.

Eramo, A., F. Lotti, et al. (2008). "Identification and expansion of the tumorigenic lung cancer stem cell population." Cell Death Differ **15**(3): 504-514.

Fabrizi, E., S. di Martino, et al. (2010). "Therapeutic implications of colon cancer stem cells." World J Gastroenterol **16**(31): 3871-3877.

Fang, D. D., Y. J. Kim, et al. (2010). "Expansion of CD133(+) colon cancer cultures retaining stem cell properties to enable cancer stem cell target discovery." Br J Cancer **102**(8): 1265-1275.

Fearon, E. R. and B. Vogelstein (1990). "A genetic model for colorectal tumorigenesis." Cell **61**(5): 759-767.

Fendrich, V., J. Waldmann, et al. (2009). "Unique expression pattern of the EMT markers Snail, Twist and E-cadherin in benign and malignant parathyroid neoplasia." Eur J Endocrinol **160**(4): 695-703.

Ferlay J, Shin HR, et al. (2010). "GLOBOCAN 2008, Cancer Incidence and Mortality Worldwide: IARC CancerBase No. 10." Lyon, France: International Agency for Research on Cancer; 2010: Available from: http://globocan.iarc.fr.

Ferrandina, G., G. Bonanno, et al. (2008). "Expression of CD133-1 and CD133-2 in ovarian cancer." Int J Gynecol Cancer **18**(3): 506-514.

Feuerborn, A., P. K. Srivastava, et al. (2010). "The Forkhead factor FoxQ1 influences epithelial differentiation." J Cell Physiol **226**(3): 710-719.

Feuerborn, A., P. K. Srivastava, et al. (2011). "The Forkhead factor FoxQ1 influences epithelial differentiation." J Cell Physiol **226**(3): 710-719.

Fidler, I. J. (2003). "The pathogenesis of cancer metastasis: the 'seed and soil' hypothesis revisited." Nat Rev Cancer **3**(6): 453-458.

Folkman, J. (1975). "Tumor angiogenesis: a possible control point in tumor growth." Ann Intern Med **82**(1): 96-100.

Foulkes, W. D., I. E. Smith, et al. (2010). "Triple-negative breast cancer." N Engl J Med **363**(20): 1938-1948.

Franco, H. L., J. Casasnovas, et al. (2010). "Redundant or separate entities?--roles of Twist1 and Twist2 as molecular switches during gene transcription." Nucleic Acids Res **39**(4): 1177-1186.

Frank, S. and B. Zoll (1998). "Mouse HNF-3/fork head homolog-1-like gene: structure, chromosomal location, and expression in adult and embryonic kidney." DNA Cell Biol **17**(8): 679-688.

Galli, R., E. Binda, et al. (2004). "Isolation and characterization of tumorigenic, stem-like neural precursors from human glioblastoma." Cancer Res **64**(19): 7011-7021.

Gao, X., Z. Wang, et al. (2010). "Identification of hookworm DAF-16/FOXO response elements and direct gene targets." PLoS One **5**(8): e12289.

Gemenetzidis, E., D. Elena-Costea, et al. (2010). "Induction of human epithelial stem/progenitor expansion by FOXM1." Cancer Res **70**(22): 9515-9526.

Glinsky, G. V. (2007). "Stem cell origin of death-from-cancer phenotypes of human prostate and breast cancers." Stem Cell Rev **3**(1): 79-93.

Goering, W., I. M. Adham, et al. (2008). "Impairment of gastric acid secretion and increase of embryonic lethality in Foxq1-deficient mice." Cytogenet Genome Res **121**(2): 88-95.

Gold, L. I. (1999). "The role for transforming growth factor-beta (TGF-beta) in human cancer." Crit Rev Oncog **10**(4): 303-360.

Gomis, R. R., C. Alarcon, et al. (2006). "A FoxO-Smad synexpression group in human keratinocytes." Proc Natl Acad Sci U S A **103**(34): 12747-12752.

Gong, X. Q. and L. Li (2002). "Dermo-1, a multifunctional basic helix-loop-helix protein, represses MyoD transactivation via the HLH domain, MEF2 interaction, and chromatin deacetylation." J Biol Chem **277**(14): 12310-12317.

Goss, K. H. and J. Groden (2000). "Biology of the adenomatous polyposis coli tumor suppressor." J Clin Oncol **18**(9): 1967-1979.

Grady, W. and S. Markowitz (2008). "TGF-β signaling pathway and tumor suppression." Cold Spring Harbor Laboratory Press; Cold Spring Harbor: p889-938.

Grady, W. M., L. L. Myeroff, et al. (1999). "Mutational inactivation of transforming growth factor beta receptor type II in microsatellite stable colon cancers." Cancer Res **59**(2): 320-324.

Grady, W. M., A. Rajput, et al. (1998). "Mutation of the type II transforming growth factor-beta receptor is coincident with the transformation of human colon adenomas to malignant carcinomas." Cancer Res **58**(14): 3101-3104.

Guaita, S., I. Puig, et al. (2002). "Snail induction of epithelial to mesenchymal transition in tumor cells is accompanied by MUC1 repression and ZEB1 expression." J Biol Chem **277**(42): 39209-39216.

Gupta, P. B., T. T. Onder, et al. (2009). "Identification of selective inhibitors of cancer stem cells by high-throughput screening." Cell **138**(4): 645-659.

Habashy, H. O., D. G. Powe, et al. (2008). "Forkhead-box A1 (FOXA1) expression in breast cancer and its prognostic significance." Eur J Cancer **44**(11): 1541-1551.

Hader, C., A. Marlier, et al. (2009). "Mesenchymal-epithelial transition in epithelial response to injury: the role of Foxc2." Oncogene **29**(7): 1031-1040.

Hajra, K. M., D. Y. Chen, et al. (2002). "The SLUG zinc-finger protein represses E-cadherin in breast cancer." Cancer Res **62**(6): 1613-1618.

Hamamori, Y., V. Sartorelli, et al. (1999). "Regulation of histone acetyltransferases p300 and PCAF by the bHLH protein twist and adenoviral oncoprotein E1A." Cell **96**(3): 405-413.

Hartwell, K. A., B. Muir, et al. (2006). "The Spemann organizer gene, Goosecoid, promotes tumor metastasis." Proc Natl Acad Sci U S A **103**(50): 18969-18974.

Hayashi, H. and T. Kume (2008). "Forkhead transcription factors regulate expression of the chemokine receptor CXCR4 in endothelial cells and CXCL12-induced cell migration." Biochem Biophys Res Commun **367**(3): 584-589.

Heldin, C. H., K. Miyazono, et al. (1997). "TGF-beta signalling from cell membrane to nucleus through SMAD proteins." Nature **390**(6659): 465-471.

Hiscox, S., W. G. Jiang, et al. (2006). "Tamoxifen resistance in MCF7 cells promotes EMT-like behaviour and involves modulation of beta-catenin phosphorylation." Int J Cancer **118**(2): 290-301.

Hoggatt, A. M., A. M. Kriegel, et al. (2000). "Hepatocyte nuclear factor-3 homologue 1 (HFH-1) represses transcription of smooth muscle-specific genes." J Biol Chem **275**(40): 31162-31170.

Honeth, G., P. O. Bendahl, et al. (2008). "The CD44+/CD24- phenotype is enriched in basal-like breast tumors." Breast Cancer Res **10**(3): R53.

Hong, H. K., J. K. Noveroske, et al. (2001). "The winged helix/forkhead transcription factor Foxq1 regulates differentiation of hair in satin mice." Genesis **29**(4): 163-171.

Hu, D. G. and P. I. Mackenzie (2010). "Forkhead box protein A1 regulates UDP-glucuronosyltransferase 2B15 gene transcription in LNCaP prostate cancer cells." Drug Metab Dispos **38**(12): 2105-2109.

Ikenouchi, J., M. Matsuda, et al. (2003). "Regulation of tight junctions during the epithelium-mesenchyme transition: direct repression of the gene expression of claudins/occludin by Snail." J Cell Sci **116**(Pt 10): 1959-1967.

Jemal, A., R. Siegel, et al. (2008). "Cancer statistics, 2008." CA Cancer J Clin **58**(2): 71-96.

Jiang, X., J. Tan, et al. (2008). "DACT3 is an epigenetic regulator of Wnt/beta-catenin signaling in colorectal cancer and is a therapeutic target of histone modifications." Cancer Cell **13**(6): 529-541.

Ju, W., B. C. Yoo, et al. (2009). "Identification of genes with differential expression in chemoresistant epithelial ovarian cancer using high-density oligonucleotide microarrays." Oncol Res **18**(2-3): 47-56.

Kaestner, K. H., W. Knochel, et al. (2000). "Unified nomenclature for the winged helix/forkhead transcription factors." Genes Dev **14**(2): 142-146.

Kajiyama, H., K. Shibata, et al. (2007). "Chemoresistance to paclitaxel induces epithelial-mesenchymal transition and enhances metastatic potential for epithelial ovarian carcinoma cells." Int J Oncol **31**(2): 277-283.

Kalluri, R. (2009). "EMT: when epithelial cells decide to become mesenchymal-like cells." J Clin Invest **119**(6): 1417-1419.

Kalluri, R. and E. G. Neilson (2003). "Epithelial-mesenchymal transition and its implications for fibrosis." J Clin Invest **112**(12): 1776-1784.

Kalluri, R. and R. A. Weinberg (2009). "The basics of epithelial-mesenchymal transition." J Clin Invest **119**(6): 1420-1428.

Kaneda, H., T. Arao, et al. (2010). "FOXQ1 is overexpressed in colorectal cancer and enhances tumorigenicity and tumor growth." Cancer Res **70**(5): 2053-2063.

Kang, Y. and J. Massague (2004). "Epithelial-mesenchymal transitions: twist in development and metastasis." Cell **118**(3): 277-279.

Kang, Y., P. M. Siegel, et al. (2003). "A multigenic program mediating breast cancer metastasis to bone." Cancer Cell **3**(6): 537-549.

Kemper, K., C. Grandela, et al. (2010). "Molecular identification and targeting of colorectal cancer stem cells." Oncotarget **1**(6): 387-395.

Khoor, A., M. T. Stahlman, et al. (2004). "Forkhead box A2 transcription factor is expressed in all types of neuroendocrine lung tumors." Hum Pathol **35**(5): 560-564.

Kim, T. H., S. W. Jo, et al. (2009). "Forkhead box O-class 1 and forkhead box G1 as prognostic markers for bladder cancer." J Korean Med Sci **24**(3): 468-473.

Kondo, S., S. Kubota, et al. (2002). "Connective tissue growth factor increased by hypoxia may initiate angiogenesis in collaboration with matrix metalloproteinases." Carcinogenesis **23**(5): 769-776.

Koon, H. B., G. C. Ippolito, et al. (2007). "FOXP1: a potential therapeutic target in cancer." Expert Opin Ther Targets **11**(7): 955-965.

Kubo, M., K. Kikuchi, et al. (1998). "Expression of fibrogenic cytokines in desmoplastic malignant melanoma." Br J Dermatol **139**(2): 192-197.

Kume, T. (2009). "The cooperative roles of Foxc1 and Foxc2 in cardiovascular development." Adv Exp Med Biol **665**: 63-77.

Kurrey, N. K., S. P. Jalgaonkar, et al. (2009). "Snail and slug mediate radioresistance and chemoresistance by antagonizing p53-mediated apoptosis and acquiring a stem-like phenotype in ovarian cancer cells." Stem Cells **27**(9): 2059-2068.

Kurrey, N. K., A. K, et al. (2005). "Snail and Slug are major determinants of ovarian cancer invasiveness at the transcription level." Gynecol Oncol **97**(1): 155-165.

Kwok, W. K., M. T. Ling, et al. (2007). "Role of p14ARF in TWIST-mediated senescence in prostate epithelial cells." Carcinogenesis **28**(12): 2467-2475.

Lagna, G., A. Hata, et al. (1996). "Partnership between DPC4 and SMAD proteins in TGF-beta signalling pathways." Nature **383**(6603): 832-836.

Lai, E., V. R. Prezioso, et al. (1990). "HNF-3A, a hepatocyte-enriched transcription factor of novel structure is regulated transcriptionally." Genes Dev **4**(8): 1427-1436.

Lapidot, T., C. Sirard, et al. (1994). "A cell initiating human acute myeloid leukaemia after transplantation into SCID mice." Nature **367**(6464): 645-648.

Larochelle, A., J. Vormoor, et al. (1996). "Identification of primitive human hematopoietic cells capable of repopulating NOD/SCID mouse bone marrow: implications for gene therapy." Nat Med **2**(12): 1329-1337.

Lau, L. F. and S. C. Lam (1999). "The CCN family of angiogenic regulators: the integrin connection." Exp Cell Res **248**(1): 44-57.

Lavon, N., O. Yanuka, et al. (2006). "The effect of overexpression of Pdx1 and Foxa2 on the differentiation of human embryonic stem cells into pancreatic cells." Stem Cells **24**(8): 1923-1930.

Lee, Y. M., T. Park, et al. (1997). "Twist-mediated activation of the NK-4 homeobox gene in the visceral mesoderm of Drosophila requires two distinct clusters of E-box regulatory elements." J Biol Chem **272**(28): 17531-17541.

Levy, L. and C. S. Hill (2005). "Smad4 dependency defines two classes of transforming growth factor {beta} (TGF-{beta}) target genes and distinguishes TGF-{beta}-induced epithelial-mesenchymal transition from its antiproliferative and migratory responses." Mol Cell Biol **25**(18): 8108-8125.

Li, C., D. G. Heidt, et al. (2007). "Identification of pancreatic cancer stem cells." Cancer Res **67**(3): 1030-1037.

Li, L., P. Cserjesi, et al. (1995). "Dermo-1: a novel twist-related bHLH protein expressed in the developing dermis." Dev Biol **172**(1): 280-292.

Liedtke, C., C. Mazouni, et al. (2008). "Response to neoadjuvant therapy and long-term survival in patients with triple-negative breast cancer." J Clin Oncol **26**(8): 1275-1281.

Lin, B. R., C. C. Chang, et al. (2005). "Connective tissue growth factor inhibits metastasis and acts as an independent prognostic marker in colorectal cancer." Gastroenterology **128**(1): 9-23.

Lin, H. M., A. Chatterjee, et al. (2007). "Genome wide expression profiling identifies genes associated with colorectal liver metastasis." Oncol Rep **17**(6): 1541-1549.

Linderholm, B. K., H. Hellborg, et al. (2009). "Significantly higher levels of vascular endothelial growth factor (VEGF) and shorter survival times for patients with primary operable triple-negative breast cancer." Ann Oncol **20**(10): 1639-1646.

Liu, B. C., J. D. Zhang, et al. (2006). "Role of connective tissue growth factor (CTGF) module 4 in regulating epithelial mesenchymal transition (EMT) in HK-2 cells." Clin Chim Acta **373**(1-2): 144-150.

Liu, F., C. Pouponnot, et al. (1997). "Dual role of the Smad4/DPC4 tumor suppressor in TGFbeta-inducible transcriptional complexes." Genes Dev **11**(23): 3157-3167.

Liu, N., Y. Niu, et al. (2010). "[Diagnostic and prognostic significance of FOXA1 expression in molecular subtypes of breast invasive ductal carcinomas]." Zhonghua Yi Xue Za Zhi **90**(20): 1403-1407.

Lo, P. K., J. S. Lee, et al. (2010). "Epigenetic inactivation of the potential tumor suppressor gene FOXF1 in breast cancer." Cancer Res **70**(14): 6047-6058.

Lombaerts, M., T. van Wezel, et al. (2006). "E-cadherin transcriptional downregulation by promoter methylation but not mutation is related to epithelial-to-mesenchymal transition in breast cancer cell lines." Br J Cancer **94**(5): 661-671.

Lu, S. L., D. Reh, et al. (2004). "Overexpression of transforming growth factor beta1 in head and neck epithelia results in inflammation, angiogenesis, and epithelial hyperproliferation." Cancer Res **64**(13): 4405-4410.

Lynch, H. T., J. F. Lynch, et al. (2008). "Hereditary colorectal cancer syndromes: molecular genetics, genetic counseling, diagnosis and management." Fam Cancer **7**(1): 27-39.

Mani, S. A., W. Guo, et al. (2008). "The epithelial-mesenchymal transition generates cells with properties of stem cells." Cell **133**(4): 704-715.

Mani, S. A., J. Yang, et al. (2007). "Mesenchyme Forkhead 1 (FOXC2) plays a key role in metastasis and is associated with aggressive basal-like breast cancers." Proc Natl Acad Sci U S A **104**(24): 10069-10074.

Markowitz, S., J. Wang, et al. (1995). "Inactivation of the type II TGF-beta receptor in colon cancer cells with microsatellite instability." Science **268**(5215): 1336-1338.

Martin, F., S. Ladoire, et al. (2010). "Human FOXP3 and cancer." Oncogene **29**(29): 4121-4129.

Martinez-Ceballos, E., P. Chambon, et al. (2005). "Differences in gene expression between wild type and Hoxa1 knockout embryonic stem cells after retinoic acid treatment or leukemia inhibitory factor (LIF) removal." J Biol Chem **280**(16): 16484-16498.

Minn, A. J., Y. Kang, et al. (2005). "Distinct organ-specific metastatic potential of individual breast cancer cells and primary tumors." J Clin Invest **115**(1): 44-55.

Mirosevich, J., N. Gao, et al. (2006). "Expression and role of Foxa proteins in prostate cancer." Prostate **66**(10): 1013-1028.

Mirza, M. K., Y. Sun, et al. (2010). "FoxM1 regulates re-annealing of endothelial adherens junctions through transcriptional control of beta-catenin expression." J Exp Med **207**(8): 1675-1685.

Moore-Smith, L. and B. Pasche (2011). "TGFBR1 Signaling and Breast Cancer." J Mammary Gland Biol Neoplasia.

Morel, A. P., M. Lievre, et al. (2008). "Generation of breast cancer stem cells through epithelial-mesenchymal transition." PLoS One **3**(8): e2888.

Muraoka, R. S., N. Dumont, et al. (2002). "Blockade of TGF-beta inhibits mammary tumor cell viability, migration, and metastases." J Clin Invest **109**(12): 1551-1559.

Nakamura, S., I. Hirano, et al. (2010). "The FOXM1 transcriptional factor promotes the proliferation of leukemia cells through modulation of cell cycle progression in acute myeloid leukemia." Carcinogenesis **31**(11): 2012-2021.

Nakaya, K., M. Murakami, et al. (2008). "Regulatory expression of Brachyury and Goosecoid in P19 embryonal carcinoma cells." J Cell Biochem **105**(3): 801-813.

Nakshatri, H. and S. Badve (2007). "FOXA1 as a therapeutic target for breast cancer." Expert Opin Ther Targets **11**(4): 507-514.

Nam, B. H., S. Y. Kim, et al. (2008). "Breast cancer subtypes and survival in patients with brain metastases." Breast Cancer Res **10**(1): R20.

Neve, R. M., K. Chin, et al. (2006). "A collection of breast cancer cell lines for the study of functionally distinct cancer subtypes." Cancer Cell **10**(6): 515-527.

Nielsen, T. O., F. D. Hsu, et al. (2004). "Immunohistochemical and clinical characterization of the basal-like subtype of invasive breast carcinoma." Clin Cancer Res **10**(16): 5367-5374.

Nieto, M. A. (2002). "The snail superfamily of zinc-finger transcription factors." Nat Rev Mol Cell Biol **3**(3): 155-166.

Nilsson, J., K. Helou, et al. (2010). "Nuclear Janus-activated kinase 2/nuclear factor 1-C2 suppresses tumorigenesis and epithelial-to-mesenchymal transition by repressing Forkhead box F1." Cancer Res **70**(5): 2020-2029.

Nowak, K., K. Killmer, et al. (2007). "E2F-1 regulates expression of FOXO1 and FOXO3a." Biochim Biophys Acta **1769**(4): 244-252.

Nucera, C., J. Eeckhoute, et al. (2009). "FOXA1 is a potential oncogene in anaplastic thyroid carcinoma." Clin Cancer Res **15**(11): 3680-3689.

Obsil, T. and V. Obsilova (2008). "Structure/function relationships underlying regulation of FOXO transcription factors." Oncogene **27**(16): 2263-2275.

Obsilova, V., J. Vecer, et al. (2005). "14-3-3 Protein interacts with nuclear localization sequence of forkhead transcription factor FoxO4." Biochemistry **44**(34): 11608-11617.

Oka, H., H. Shiozaki, et al. (1993). "Expression of E-cadherin cell adhesion molecules in human breast cancer tissues and its relationship to metastasis." Cancer Res **53**(7): 1696-1701.

Okada, T., Y. Suehiro, et al. "TWIST1 hypermethylation is observed frequently in colorectal tumors and its overexpression is associated with unfavorable outcomes in patients with colorectal cancer." Genes Chromosomes Cancer **49**(5): 452-462.

Onder, T. T., P. B. Gupta, et al. (2008). "Loss of E-cadherin promotes metastasis via multiple downstream transcriptional pathways." Cancer Res **68**(10): 3645-3654.

Pan, D., M. Fujimoto, et al. (2009). "Twist-1 is a PPARdelta-inducible, negative-feedback regulator of PGC-1alpha in brown fat metabolism." Cell **137**(1): 73-86.

Parsons, D. W., S. Jones, et al. (2008). "An integrated genomic analysis of human glioblastoma multiforme." Science **321**(5897): 1807-1812.

Parsons, D. W., T. L. Wang, et al. (2005). "Colorectal cancer: mutations in a signalling pathway." Nature **436**(7052): 792.

Parsons, R., L. L. Myeroff, et al. (1995). "Microsatellite instability and mutations of the transforming growth factor beta type II receptor gene in colorectal cancer." Cancer Res **55**(23): 5548-5550.

Pasche, B., T. J. Knobloch, et al. (2005). "Somatic acquisition and signaling of TGFBR1*6A in cancer." JAMA **294**(13): 1634-1646.

Peinado, H., D. Olmeda, et al. (2007). "Snail, Zeb and bHLH factors in tumour progression: an alliance against the epithelial phenotype?" Nat Rev Cancer **7**(6): 415-428.

Perbal, B. (2004). "CCN proteins: multifunctional signalling regulators." Lancet **363**(9402): 62-64.

Perl, A. K., P. Wilgenbus, et al. (1998). "A causal role for E-cadherin in the transition from adenoma to carcinoma." Nature **392**(6672): 190-193.

Perou, C. M., T. Sorlie, et al. (2000). "Molecular portraits of human breast tumours." Nature **406**(6797): 747-752.

Potter, C. S., R. L. Peterson, et al. (2006). "Evidence that the satin hair mutant gene Foxq1 is among multiple and functionally diverse regulatory targets for Hoxc13 during hair follicle differentiation." J Biol Chem **281**(39): 29245-29255.

Prince, M. E., R. Sivanandan, et al. (2007). "Identification of a subpopulation of cells with cancer stem cell properties in head and neck squamous cell carcinoma." Proc Natl Acad Sci U S A **104**(3): 973-978.

Puisieux, A., S. Valsesia-Wittmann, et al. (2006). "A twist for survival and cancer progression." Br J Cancer **94**(1): 13-17.

Qi, J., K. Nakayama, et al. (2010). "Siah2-dependent concerted activity of HIF and FoxA2 regulates formation of neuroendocrine phenotype and neuroendocrine prostate tumors." Cancer Cell **18**(1): 23-38.

Rajagopalan, H., A. Bardelli, et al. (2002). "Tumorigenesis: RAF/RAS oncogenes and mismatch-repair status." Nature **418**(6901): 934.

Ray, P. S., J. Wang, et al. (2010). "FOXC1 is a potential prognostic biomarker with functional significance in basal-like breast cancer." Cancer Res **70**(10): 3870-3876.

Reya, T., S. J. Morrison, et al. (2001). "Stem cells, cancer, and cancer stem cells." Nature **414**(6859): 105-111.

Rho, J. K., Y. J. Choi, et al. (2009). "Epithelial to mesenchymal transition derived from repeated exposure to gefitinib determines the sensitivity to EGFR inhibitors in A549, a non-small cell lung cancer cell line." Lung Cancer **63**(2): 219-226.

Rhodes, D. R., J. Yu, et al. (2004). "ONCOMINE: a cancer microarray database and integrated data-mining platform." Neoplasia **6**(1): 1-6.

Ricci-Vitiani, L., E. Fabrizi, et al. (2009). "Colon cancer stem cells." J Mol Med **87**(11): 1097-1104.

Ricci-Vitiani, L., D. G. Lombardi, et al. (2007). "Identification and expansion of human colon-cancer-initiating cells." Nature **445**(7123): 111-115.

Roberts, A. B. and L. M. Wakefield (2003). "The two faces of transforming growth factor beta in carcinogenesis." Proc Natl Acad Sci U S A **100**(15): 8621-8623.

Rottenberg, S., J. E. Jaspers, et al. (2008). "High sensitivity of BRCA1-deficient mammary tumors to the PARP inhibitor AZD2281 alone and in combination with platinum drugs." Proc Natl Acad Sci U S A **105**(44): 17079-17084.

Rouzier, R., C. M. Perou, et al. (2005). "Breast cancer molecular subtypes respond differently to preoperative chemotherapy." Clin Cancer Res **11**(16): 5678-5685.

Saito, R. A., P. Micke, et al. (2010). "Forkhead box F1 regulates tumor-promoting properties of cancer-associated fibroblasts in lung cancer." Cancer Res **70**(7): 2644-2654.

Samowitz, W. S. and M. L. Slattery (1997). "Transforming growth factor-beta receptor type 2 mutations and microsatellite instability in sporadic colorectal adenomas and carcinomas." Am J Pathol **151**(1): 33-35.

Sanders, M. A. and A. P. Majumdar (2011). "Colon cancer stem cells: implications in carcinogenesis." Front Biosci **16**: 1651-1662.

Sarrio, D., S. M. Rodriguez-Pinilla, et al. (2008). "Epithelial-mesenchymal transition in breast cancer relates to the basal-like phenotype." Cancer Res **68**(4): 989-997.

Schipper, J. H., U. H. Frixen, et al. (1991). "E-cadherin expression in squamous cell carcinomas of head and neck: inverse correlation with tumor dedifferentiation and lymph node metastasis." Cancer Res **51**(23 Pt 1): 6328-6337.

Secker, G. A., A. J. Shortt, et al. (2008). "TGFbeta stimulated re-epithelialisation is regulated by CTGF and Ras/MEK/ERK signalling." Exp Cell Res **314**(1): 131-142.

Seki, K., T. Fujimori, et al. (2003). "Mouse Snail family transcription repressors regulate chondrocyte, extracellular matrix, type II collagen, and aggrecan." J Biol Chem **278**(43): 41862-41870.

Seo, D. C., J. M. Sung, et al. (2007). "Gene expression profiling of cancer stem cell in human lung adenocarcinoma A549 cells." Mol Cancer **6**: 75.

Seo, S., H. Fujita, et al. (2006). "The forkhead transcription factors, Foxc1 and Foxc2, are required for arterial specification and lymphatic sprouting during vascular development." Dev Biol **294**(2): 458-470.

Shakunaga, T., T. Ozaki, et al. (2000). "Expression of connective tissue growth factor in cartilaginous tumors." Cancer **89**(7): 1466-1473.

Sheridan, C., H. Kishimoto, et al. (2006). "CD44+/CD24- breast cancer cells exhibit enhanced invasive properties: an early step necessary for metastasis." Breast Cancer Res **8**(5): R59.

Singh, A. and J. Settleman (2010). "EMT, cancer stem cells and drug resistance: an emerging axis of evil in the war on cancer." Oncogene **29**(34): 4741-4751.

Smolak, K. (1971). "[Studies on morphologic structure of the stroma in cancer of the breasts]." Patol Pol **22**(4): 571-581.

Song, Y., M. K. Washington, et al. "Loss of FOXA1/2 is essential for the epithelial-to-mesenchymal transition in pancreatic cancer." Cancer Res **70**(5): 2115-2125.

Song, Y., M. K. Washington, et al. (2010). "Loss of FOXA1/2 is essential for the epithelial-to-mesenchymal transition in pancreatic cancer." Cancer Res **70**(5): 2115-2125.

Sorlie, T., C. M. Perou, et al. (2001). "Gene expression patterns of breast carcinomas distinguish tumor subclasses with clinical implications." Proc Natl Acad Sci U S A **98**(19): 10869-10874.

Spaderna, S., O. Schmalhofer, et al. (2008). "The transcriptional repressor ZEB1 promotes metastasis and loss of cell polarity in cancer." Cancer Res **68**(2): 537-544.

Sun, Q., X. Yu, et al. (2009). "Upstream stimulatory factor 2, a novel FoxA1-interacting protein, is involved in prostate-specific gene expression." Mol Endocrinol **23**(12): 2038-2047.

Takahashi, H., H. Ishii, et al. (2011). "Significance of Lgr5(+ve) Cancer Stem Cells in the Colon and Rectum." Ann Surg Oncol **18**(4): 1166-1174.

Tang, Y., G. Shu, et al. (2010). "FOXA2 functions as a suppressor of tumor metastasis by inhibition of epithelial-to-mesenchymal transition in human lung cancers." Cell Res **21**(2): 316-326.

Thiery, J. P. (2002). "Epithelial-mesenchymal transitions in tumour progression." Nat Rev Cancer **2**(6): 442-454.

Thiery, J. P. and J. P. Sleeman (2006). "Complex networks orchestrate epithelial-mesenchymal transitions." Nat Rev Mol Cell Biol **7**(2): 131-142.

Thorat, M. A., C. Marchio, et al. (2008). "Forkhead box A1 expression in breast cancer is associated with luminal subtype and good prognosis." J Clin Pathol **61**(3): 327-332.

Turner, N., A. Tutt, et al. (2004). "Hallmarks of 'BRCAness' in sporadic cancers." Nat Rev Cancer **4**(10): 814-819.

Umbas, R., W. B. Isaacs, et al. (1994). "Decreased E-cadherin expression is associated with poor prognosis in patients with prostate cancer." Cancer Res **54**(14): 3929-3933.

Underwood, J. C. E. (2004). "General and Systematic Pathology." Churchill Livingstone: p223-p262.

Van Calster, B., I. Vanden Bempt, et al. (2009). "Axillary lymph node status of operable breast cancers by combined steroid receptor and HER-2 status: triple positive tumours are more likely lymph node positive." Breast Cancer Res Treat **113**(1): 181-187.

van der Heul-Nieuwenhuijsen, L., N. Dits, et al. (2009). "The FOXF2 pathway in the human prostate stroma." Prostate **69**(14): 1538-1547.

Van Meter, M. E. and E. S. Kim (2010). "Bevacizumab: current updates in treatment." Curr Opin Oncol **22**(6): 586-591.

Vandewalle, C., F. Van Roy, et al. (2009). "The role of the ZEB family of transcription factors in development and disease." Cell Mol Life Sci **66**(5): 773-787.

Vazquez, A., E. E. Bond, et al. (2008). "The genetics of the p53 pathway, apoptosis and cancer therapy." Nat Rev Drug Discov **7**(12): 979-987.

Veigl, M. L., L. Kasturi, et al. (1998). "Biallelic inactivation of hMLH1 by epigenetic gene silencing, a novel mechanism causing human MSI cancers." Proc Natl Acad Sci U S A **95**(15): 8698-8702.

Verzi, M. P., A. H. Khan, et al. (2008). "Transcription factor foxq1 controls mucin gene expression and granule content in mouse stomach surface mucous cells." Gastroenterology **135**(2): 591-600.

Voulgari, A. and A. Pintzas (2009). "Epithelial-mesenchymal transition in cancer metastasis: mechanisms, markers and strategies to overcome drug resistance in the clinic." Biochim Biophys Acta **1796**(2): 75-90.

Waldmann, J., E. P. Slater, et al. (2009). "Expression of the transcription factor snail and its target gene twist are associated with malignancy in pheochromocytomas." Ann Surg Oncol **16**(7): 1997-2005.

Wang, I. C., Y. Zhang, et al. (2010). "Increased expression of FoxM1 transcription factor in respiratory epithelium inhibits lung sacculation and causes Clara cell hyperplasia." Dev Biol **347**(2): 301-314.

Wang, J. C. and J. E. Dick (2005). "Cancer stem cells: lessons from leukemia." Trends Cell Biol **15**(9): 494-501.

Wang, M. Y., P. S. Chen, et al. (2009). "Connective tissue growth factor confers drug resistance in breast cancer through concomitant up-regulation of Bcl-xL and cIAP1." Cancer Res **69**(8): 3482-3491.

Wang, Z., A. Ahmad, et al. (2009). "Forkhead box M1 transcription factor: a novel target for cancer therapy." Cancer Treat Rev **36**(2): 151-156.

Weidinger, C., K. Krause, et al. (2008). "Forkhead box-O transcription factor: critical conductors of cancer's fate." Endocr Relat Cancer **15**(4): 917-929.

Weigel, D., G. Jurgens, et al. (1989). "The homeotic gene fork head encodes a nuclear protein and is expressed in the terminal regions of the Drosophila embryo." Cell **57**(4): 645-658.

Weissman, I. L. (2000). "Translating stem and progenitor cell biology to the clinic: barriers and opportunities." Science **287**(5457): 1442-1446.

Wendling, D. S., C. Luck, et al. (2008). "Characteristic overexpression of the forkhead box transcription factor Foxf1 in Patched-associated tumors." Int J Mol Med **22**(6): 787-792.

Wenger, C., V. Ellenrieder, et al. (1999). "Expression and differential regulation of connective tissue growth factor in pancreatic cancer cells." Oncogene **18**(4): 1073-1080.

Xie, D., K. Nakachi, et al. (2001). "Elevated levels of connective tissue growth factor, WISP-1, and CYR61 in primary breast cancers associated with more advanced features." Cancer Res **61**(24): 8917-8923.

Xie, Z., G. Tan, et al. (2010). "Foxm1 transcription factor is required for maintenance of pluripotency of P19 embryonal carcinoma cells." Nucleic Acids Res **38**(22): 8027-8038.

Yamaguchi, N., E. Ito, et al. (2008). "FoxA1 as a lineage-specific oncogene in luminal type breast cancer." Biochem Biophys Res Commun **365**(4): 711-717.

Yang, A. D., F. Fan, et al. (2006). "Chronic oxaliplatin resistance induces epithelial-to-mesenchymal transition in colorectal cancer cell lines." Clin Cancer Res **12**(14 Pt 1): 4147-4153.

Yang, J., S. A. Mani, et al. (2004). "Twist, a master regulator of morphogenesis, plays an essential role in tumor metastasis." Cell **117**(7): 927-939.

Yang, J. Y. and M. C. Hung (2009). "A new fork for clinical application: targeting forkhead transcription factors in cancer." Clin Cancer Res **15**(3): 752-757.

Yin, Z., X. L. Xu, et al. (1997). "Regulation of the twist target gene tinman by modular cis-regulatory elements during early mesoderm development." Development **124**(24): 4971-4982.

Yokoyama, K., N. Kamata, et al. (2003). "Increased invasion and matrix metalloproteinase-2 expression by Snail-induced mesenchymal transition in squamous cell carcinomas." Int J Oncol **22**(4): 891-898.

Yoshida, J., A. Horiuchi, et al. (2009). "Changes in the expression of E-cadherin repressors, Snail, Slug, SIP1, and Twist, in the development and progression of ovarian carcinoma: the important role of Snail in ovarian tumorigenesis and progression." Med Mol Morphol **42**(2): 82-91.

Yoshihara, K., A. Tajima, et al. (2009). "Gene expression profiling of advanced-stage serous ovarian cancers distinguishes novel subclasses and implicates ZEB2 in tumor progression and prognosis." Cancer Sci **100**(8): 1421-1428.

Yu, M., G. A. Smolen, et al. (2009). "A developmentally regulated inducer of EMT, LBX1, contributes to breast cancer progression." Genes Dev **23**(15): 1737-1742.

Yu, X., A. Gupta, et al. (2005). "Foxa1 and Foxa2 interact with the androgen receptor to regulate prostate and epididymal genes differentially." Ann N Y Acad Sci **1061**: 77-93.

Zavadil, J. and E. P. Bottinger (2005). "TGF-beta and epithelial-to-mesenchymal transitions." Oncogene **24**(37): 5764-5774.

Zeisberg, M. and E. G. Neilson (2009). "Biomarkers for epithelial-mesenchymal transitions." J Clin Invest **119**(6): 1429-1437.

Zhang, H., F. Meng, et al. (2011). "Forkhead transcription factor foxq1 promotes epithelial-mesenchymal transition and breast cancer metastasis." Cancer Res **71**(4): 1292-1301.

Zollinger, H. U. (1968). "[Tumors between benign and malignant. Semimalignancy, questionable dignity, precancerosis]." Chirurg **39**(1): 9-13.

List of Publications

1. Qiao Yuanyuan, Jiang X, Lee ST, Karuturi RK, Hooi SC, Yu Qiang. FOXQ1 Regulates Epithelial-Mesenchymal Transition in Human Cancers. Cancer Res. 2011 Apr 15;71(8):3076-86. Epub 2011 Feb 23. PMID: 21346143

2. Wu ZL, Zheng SS, Li ZM, Qiao YY, Aau MY, Yu Q. Polycomb protein EZH2 regulates E2F1-dependent apoptosis through epigenetically modulating Bim expression. Cell Death Differ. 2010 May;17(5):801-10. Epub 2009 Nov 6. PMID: 19893569

3. Wu Zhenlong, Shuet Theng Lee, Yuanyuan Qiao, Zhimei Li, Puay Leng Lee, Yong Jing Lee, Xia Jiang, Jing Tan, Meiyee Aau, Cheryl Zhi Hui Lim, and Qiang Yu. EZH2 regulates cancer cell fate decision in response to DNA damage. Cell Death Differ. 2011 May 6. PMID: 21546904